12-7-2015 12:00 AM

Formulation and Optimization of Antimicrobial Surfaces Via Ultra-Fine Powder Coating

Rezwana Yeasmin, *The University of Western Ontario*

Supervisor: Dr. Jesse Zhu, *The University of Western Ontario*

A thesis submitted in partial fulfillment of the requirements for the Doctor of Philosophy degree in Chemical and Biochemical Engineering

FORMULATION AND OPTIMIZATION OF ANTIMICROBIAL SURFACES VIA ULTRA-FINE POWDER COATING

(Thesis format: Integrated Article)

By

REZWANA YEASMIN

Graduate Program in Engineering Science

Department of Chemical and Biochemical Engineering

A thesis submitted in partial fulfillment

of the requirements for the degree of

Doctor of Philosophy

The School of Graduate and Postdoctoral Studies

The University of Western Ontario

London, Ontario, Canada

ABSTRACT

In a health care environment, surface bio-contamination is a constant risk and contributes to outbreaks of community-acquired and nosocominal infections. Faster surface die-off of pathogens on a surface can reduce the average surface population of these pathogens. Antimicrobial ultra-fine powder coated surfaces with high antimicrobial longevity including efficiency is a good option to reduce the surface bio-contamination. Different formulations were prepared with the additives containing silver ions (Ag^{+}) and silver nano-particles (AgNP) as an active agent and copper ions (Cu^{2+}) as a protective agent incorporated into zeolites and their antimicrobial activity was analyzed against *Escherichia coli* (*E.coli).* Two natural zeolites, known as chabazites (named LBC and LBN), were accustomed to enhance their sodium content as well as ion exchange characteristics by conditioning and was functionalized by using different combinations of the Ag and Cu ions.

No significant changes were observed during XRD and TGA analysis. Elemental analysis by ICP-OES confirmed the enhancement of silver ions after functionalization due to the conditioning process. Color analysis indicated that copper helped to maintain the color of the coated surface. These coated surfaces have shown consistent antibacterial properties with excellent durability against *E.coli* for an extended longevity. Antimicrobial efficiency of that coated surface was also proven by toxicity analysis through the production of lactate dehydrogenase (LDH).

Synthetic zeolite A (LTA) was used as a carrier for active agents in different experiments in this study. Optimum concentration of these cations (Ag^{+},1.534meq/g, Cu^{2+}3.90 meq/g) were obtained by ion exchange with silver nitrate after 24 hrs followed by further ion exchange with copper nitrate for another 24 hrs with the adjustment of pH and temperatures. TGA,

XRD, XPS and FTIR analysis were used for further characterization of these additives. The reduction of Ag^{+} can be controlled by the addition of Cu^{2+} ions and that surface was found to be very efficient since the coated surface showed 100% reduction of microorganisms within 2 hrs of exposure. Auger parameter confirmed that copper prevented silver from being reduced during the curing period. The transfer efficiency of the additives in the resin system during the spraying was improved by increasing the aggregated particle size of the final powder from 20μm to 30μm using pressing, grinding and sieving processes.

The effects of low curing additives on surface properties were analyzed based on the ASTM standards for powder coating and found comparable with the surface cured at higher temperature. The release rate of the active components from the surface was further controlled by PVA encapsulation on the additive and this process was found to provide an effective antimicrobial surface for prolonged periods.

Silver nano-particles were synthesized on the synthetic zeolite surface and were used as an additive in the presence of copper ions. Uniform distribution of silver nanoparticles synthesized by the chemical reduction method on the zeolite surface played an important role in the generation of silver ions. Hydrophilic encapsulation of this additive was essential for the generation of silver ions from nanoparticles when used in the powder coating. Different water soluble hydrophilic encapsulation were used to find the best combinations for this purpose.

Glutaraldehyde was used to form chemical cross linking between the polymer chain to reduce the hydrophilicity of the polymers during encapsulation. Due to the high hydrophilicity of the encapsulation, fine cracks were found in the coated surface after several exposures to the microorganisms. This problem was resolved by an additional clear coat

underneath the active coating. Encapsulation with anionic polymers was found to be the more effective solution for releasing the silver ions from the ultrafine powder coated surface. The retaining capacity of the encapsulation within the matrix depended on the cations present in the additives, which increased with the increase in cation concentrations. Due to the formation of physical cross linking between cations and functional groups of polymer, encapsulation became insoluble, which is the reason for enhanced encapsulation retained capacity.

Non-ionic polymer encapsulation was another option, which was observed more effective than the high hydroxyl-containing polymers. A non-polymeric hydrophilic encapsulation was made by the precipitation of calcium phosphate. Although this encapsulated additive showed efficiency against microorganism but not as good as the polymer encapsulated additives.

Finally, synthetic and natural polymer blend was found to be the best combination for encapsulation. The polymer blend was prepared with Na-alginate and Na-CMC at different proportions with polyacrylamide followed by physical cross linking with cations and the functional groups in these polymers. Encapsulation of additives with increased amount of natural polymers seemed more stable and were capable of holding more moisture within the polymer matrix which was proven through antimicrobial efficiency analysis. The final formulated surface was also found to be active against microorganism after autoclave and UV treatment, this was also proved by toxicity analysis.

Keywords: Zeolite, cabazite, silver, ultrafine Powder coating, ionexchange, antimicrobial, durability, leaching, silver nano particles

CO-AUTHORSHIP

Dr. Jesse Zhu and Dr. Hui Zhang provided full supervision and guidance to this research project as supervisors.

`Title 1: Pre-treatment and conditioning of chabazites followed by functionalization for making suitable additives used in antimicrobial ultra-fine powder coated surface

Title 2: Effectivity of silver ion on enhanced durability for antimicrobial powder coated surface

Title 3: Effective use of silver nanoparticles supported on zeolite surface embedded in ultra-fine powder coated surfaces

Title 4: Encapsulation of zeolite containing nanoparticles with blended polymers and their antimicrobial efficiency in powder coated surface

Authors: Rezwana Yeasmin, Hui Zhang and Jesse Zhu

All research works were conducted by Rezwana Yeasmin under the supervision of Dr. Jesse Zhu and Dr. Hui Zhang. Modifications of the experiments and revisions of the drafts were mainly done by Rezwana Yeasmin under the supervision of Dr. Jesse Zhu and Dr. Hui Zhang. The final version of this manuscript will be sent for future publication.

ACKNOWLEDGEMENTS

First of all, I would like to express my sincere gratitude to my supervisor, Dr. Jesse Zhu for his invaluable guidance and continuous support. I am thankful for the opportunities brought by him, which greatly improved my research horizon, scientific attitude and learning skills. I believe, I shall be highly benefited from his teaching and instructions in the rest of my life.

I am also grateful to Dr. Hui Zhang for his methodical guidance and enormous encouragement for my research work in the field of powder coating technology, which was a completely new and exciting field to me.

My perpetual gratefulness goes to Dr. Peter for initializing and providing crucial elements of knowledge at the beginning and throughout this long process on the microbiology aspect of this work. His undoubted expertise in this arena greatly helped me in my journey.

In addition, I would also like to thank, Dr. Ajay Ray, Dr. Lars Rehmann, Dr. Dimitre Karamanev, Dr. Mita Ray and from whom I have obtained supports during my course works. They helped me to develop my knowledge in different aspects in my research field that ensured the success of this study.

Moreover, my thanks also go to all office staff of the department of Chemical and Biochemical Engineering, who has spent lot of time to work for my TA works and other official works. I also extend my hand in thanks to all of my great friends and colleagues throughout last four years of my research. Their moral support, friendship and fun were and would always be much appreciated and remembered.

Finally, I want to express my gratitude to all of my family members, especially my respected father Quazi Mozaher Ali and mother Rebeka Mozaher as well as my sisters Rahnuma and Shiffat for their unreserved support and love. I would like to extend the same to my beloved sons, Sharhad and Ashfar for their understandings and assistance at home during my studies and my endless thanks to my husband Bashar for his tireless support and encouragement. I would like to dedicate my thesis whole heartedly to my family.

TABLE OF CONTENTS

LIST OF TABLES

LIST OF FIGURES

LIST OF FLOW SHEETS

LIST OF ABBREVIATIONS

ASTM	American Society for Testing and Materials
CFU	Colony forming unit
DNA	Deoxyribonucleic Acid
E.coli	Escherichia coli
EDX	Energy dispersive X-Ray spectroscopy
ICP-OES	Inductively coupled plasma atomic emission spectroscopy
LB	Luria Bertani
RNA	Ribonucleic Acid
ROS	Reactive oxygen species
SARS	Severe Acute Respiratory Syndrome
SARS	Severe Acute Respiratory Syndrome
SEM	Scanning Electron Microscope
TGIC	Triglycidyl Isocyanurate
UVA	Visible ultra violet
UWO	University of Western Ontario
XRPD	X-Ray powdered Diffraction

CHAPTER 1

GENERAL INTRODUCTION

1.1 General Introduction to Ultrafine Powder Coatings Technology

Powder coatings are environment friendly surface coating method, developed since mid 1950s, well established and commonly used today [1]. These coatings are simply dry paints formulated with resins, pigments and additives similar to the solvent borne paints with the exception of no solvent present. Powder coating is environment friendly because of no VOCs emission, low cost and highly efficient with almost 98% of powder overspray recoverability when compared to traditional liquid coating methods. Thermo plastic and thermo setting are two different classes of powder coatings that are available. Thermo plastic can re-melt upon heat exposure while thermo setting polymers melt and chemically react, unable to re-melt. These two types make the majority of the powder coatings [2].

There are four different types of powder coating process that exist; among those, electrostatic spraying is the most commonly used technique [3]. In this process powder particles are electrically charged, so they repelled each other and even distribution occurs while passing through the spray nozzle. The particles are sprayed out onto a grounded target with aerodynamic and electrostatic forces. Finally these charged particles will deposit on the target and be molten and cured to form hard coatings [4].

Electrostatic powder coating technology has been developed to apply a protective and attractive finish over a broad variety of materials and products that are using in many different industrial and consumer applications. The appearance of the coating is largely dependent on the particle size. Commonly, mean particle size between 30μm to 60μm are used in traditional powder coating processes. Its inability in applying fine and ultrafine particles always limits its application to a thicker and roughened coated film represented by texture of "orange peels"[5]. However, the increased demand for ultrafine powder coating in many different areas called for finest and uniform surface appearance. Fine and ultrafine powders of mean particle size between 10μm and 30μm are capable of forming a very thin and uniform coating being used to meet the new requirements, which is comparable to liquid coatings [6]. Ultrafine powder is preferred over regular size due to augmented physical and mechanical capabilities possessed by the final coating.

1.2 Antimicrobial Activity

Bio-contamination is a constant risk in a healthcare environment. General public are worried about bacteria and a large percentage consider food contamination as a serious health risk. More illnesses are caused due to bacteria which are resistant to antibiotics. Microbes are continuously being transferred from inanimate fomitic objects to human hands and vice versa. Majority of these infections are caused when come in contact with contaminated surfaces. The importance of hygiene in the personal health care is also growing due to the increasing alertness in certain areas, for example; hospitals, residence, schools and food processing areas etc.

Antimicrobial coating is a possible solutions to make available supplemental guard against the growth of microorganisms in an extensive range of applications. Bacteria, viruses, fungi or algae carries detrimental germs that produce bad odors, discoloration, dirty surfaces and develop mildew. These lead to degradation of the base material in most of the cases. To find solutions for these issues by producing very effective and durable surfaces in certain applications is the demand of the time. Antimicrobial coated surfaces in contamination prone areas like hospitals and medical related devices, fixtures and tools could help in preventing the spread of bacteria and viruses and in turn reduce the risks of infection, disease and death. The requirement for an efficient, durable, simple and cost effective coating against this microbial contamination is highly demanding.

First of all, the production of a functional antimicrobial surface coating is very important in terms of method of coating on to the substrate and the type of active component used. Typically, most sanitary cleaning products utilize an organically based biocide agent. Continuous use of organic compounds to inactivate or kill bacteria become a serious global health threat as bacteria begin to build immunity and get resistant to that compound. For example, certain antibiotics which were once very effective and popular in the past is no longer effective now a days and as such not prescribed or administrated. Not only do organic biocides give way for possible resistance complications but also most are harmful and toxic to human beings and animals. However, microbes cannot build up resistance or immunities on antimicrobial powder coated surface with inorganic additives and gradually getting importance as a potential additive in antimicrobial surface applications. For centuries, there have been certain heavy metals in use that have shown

antimicrobial effects and due to their inorganic and non-toxic properties. Silver is known to be a safe for human uses and also efficient against a wide range of microorganisms. Silver ions and the nanoparticles are ideal for our research purposes.

1.3 Research Objectives and Overview

Surface bio-contamination is a serious concern which contributes to pandemic of nosocominal infection. An effective antimicrobial surface coating can considerably reduce the average surface population of pathogens existing for transmission to a vulnerable host. After the investigation of many research findings including customer demand, it was found that durability as well as fast on-set of action are still the two main challenges. To overcome this challenge two key issues were needed to address:

1) Maximizing the loading capacity of antimicrobial agent

2) Controlling the rate of release of that agent

However, it is needed to develop a technology for antimicrobial coating which is simple, economically feasible and environmentally friendly. In respond to these problems, functional antimicrobial surfaces with high durability have been developed using ultrafine powder coating technology. This work is arranged in three separate parts:

Part I is concentrated on the development of highly durable and functional antibacterial surfaces by using silver ions with modified chabazites.

Part II is concentrated on the development of an effective antimicrobial surfaces with additives containing silver and copper ions in synthetic zeolite A.

Part III is concentrated on the development of decisive antimicrobial surface containing silver nanoparticles as active agent.

The research works were carried out in the specific areas as listed below:

Part I

* Modification of sodium enriched two types of chabazite by pre-treatment and conditioning.
* Functionalization of modified chabazites by silver and copper ions by ionexchange process.
* Characterization of these functionalized zeolites by XRF, ICP, XRD, TGA
* Determination of Cation exchange capacity (CEC) before and after modification
* Evaluate the transfer efficiency of additives during spraying
* Evaluate the reduction of silver ions during curing process by analyzing color of the surface.
* Evaluate the durability of the coated surface by inactivation of *E.coli* and leaching of silver ion

Part II

* Incorporation of silver and copper ions in synthetic zeolite A by ion exchange process
* Characterization of additives by XRD, TGA, ICP
* Effect of copper on the reduction of silver by XPS analysis
* Effect of low curing additives on surface properties
* Investigate the effectiveness of coated chips against microorganism and the durability.

* Evaluate the effect of autoclave on surface properties in terms of color of the surface and antimicrobial efficiency

* Effect of additional coating on slow release of active agents.

Part III

* Optimize the synthesis process of nanoparticles on zeolite surface with uniform distribution.

* Effect of hydrophilic encapsulation on additives containing nanoparticles

* Optimization of encapsulation formulation for enhanced efficiency against microorganism

* Effect of autoclave and UV on the surface for inactivation of microorganism

* Leaching of silver ions during antimicrobial analysis

* Toxicity analysis during exposure to microorganism

1.4 Thesis Structure

This thesis consists of eight chapters and follows the "Integrated-Article" format outlined in the *Thesis Regulation Guide* by the School of Graduate and Postdoctoral Studies (SGPS) of the University of Western Ontario.

Chapter 1 provides a general introduction of ultrafine powder coating and antimicrobial activity with its applications. The research objectives and project overview are stated, as well as the thesis structure, major contributions from the research study.

Chapter 2 presents the literature reviews for detailed knowledge for ultrafine powder coating technique and its applications. This chapter also provides background information of current active components for antimicrobial surfaces. Moreover, this chapter introduced preliminary research work for the applications.

Chapter 3 explains the main materials and method used for this research.

Chapter 4 investigates improvement of cation exchange capacity of chabazites before and after modification by conditioning and functionalization for an antimicrobial additives used in the surfaces made by ultrafine powder coating.

Chapter 5 evaluates the ion exchange conditions for synthetic zeolite to achieve an effective coating formulation and explain its affectivity against microorganism for long period. Surface characterizations have been done by considering the transfer efficiency of additives, effect of low curing additives, autoclave, toxicity analysis and effect of polymeric coating on release rate of active agent.

Chapter 6 explains the effects of different water soluble polymers for encapsulation of additives containing silver nano particles on antimicrobial efficiency.

Chapter 7 optimizes the encapsulation formulation with blended polymers to provide the hydrophilic environment to the silver nanoparticles and check the effectivity of encapsulation. Cytotoxicity analysis during exposure to microorganism and the effect of accelerated corrosion test are also mentioned here.

Chapter 8 summarizes the findings from this research study and discuss the contributions and provide scopes for future works.

1.5 Major Achievements

Three major achievements of this study can be summarized as below:

* To overcome the surface bio-contamination problem, a functional antibacterial surface has been developed by ultrafine powder coating technology. Silver in different forms were used as additives, where two different zeolites worked as carrier for these additives. *Escherichia coli* was used as the test organism to identify the antimicrobial effectiveness of the formulated surfaces. Cation exchange capacity of the chabazites used as carrier has been improved by pretreatment and conditioning process. The additives prepared with these conditioned zeolites contained higher amount of active agent. Antimicrobial efficacy analysis proved the competence of the formulated additives as an antimicrobial surface with prolonged durability.

* Synthetic zeolite A was found as an effective carrier for silver ions in presence of copper ions. Copper ions are needed to minimize the reduction process of silver ions during curing of the powder coating. Additional coating of the additive with polymer helped to reduce the release rate of silver during exposure to microorganism.

* Hydrophilic polymer encapsulation was found to be effective for the additives containing silver nano particles to produce silver ions embedded in the antimicrobial surfaces. But the polymer blend made with synthetic and natural showed promising antimicrobial efficiency against microorganism. All formulations proved the formations of toxicity during exposure to microorganism.

References

1. Misev T.A, 1991, *Powder Coatings: Chemistry and Technology*, John Wiley and Sons, New York

2. Berins M.L,1991, SPI plastics engineering handbook of the society of the plastics Industry, *Springer Inc.* vol.5, pages 497-503.

3. Hughes J.F, 1984, Electrostatic Powder Coating, Southampton University Department of Electrical Engineering, Southampton, 84

4. Bailey A.G, 1998, The science and technology of electrostatic powder spraying, transport and coating, *Journal of Electrostatics*, vol.45, pages85-120.

5. Jing Fu, 2010 "Study on powder coating particles and development of new powder coating application methods.," in *Chemical and Biochemical Engineering*, Master of Engineering Science. London: University of Western Ontario, , pp. 122.

6. Zhu J. and Zhang H, 2004, Fluidization Additives to Fine Powders," in *U.S patant*, 6833185

CHAPTER 2

LITERATURE REVIEW

2.1 Overview

In a health care environment, surface bio-contamination is a constant risk and contributes to outbreaks of community-acquired and nosocominal infections. Faster surface die-off of pathogens on a surface can reduce the average surface population of these pathogens available for transmission to a susceptible host. However effective chemical disinfection is difficult because it must be applied precisely and in the correct amount. The total process is also time and labor consuming.

Exotic metal like silver has potential uses in biomedical purposes, food processing, air and water purification, cosmetics, garments and many other various household products. Applications have been expanded more and now silver is one of the most commonly used engineered nanomaterials in consumer products [1]. There are many diverse forms of silver nanomaterials used in products that include metallic silver nanoparticles [2-14], silver chloride particles [4], silver infused zeolite powders and activated carbon materials [15-18], dendrimer-silver complex and composites [19-27], silver titanium dioxide composite nano powders [28] and silver nanoparticles within polymers like polyurethane [29]. All of these different forms of silver confirm antimicrobial properties somewhat through the discharge of silver ions. Additional antimicrobial capacity might demonstrate by silver nanoparticles [30].

Silver nanoparticles have been proven as an efficient biocide against 1) a wide range of bacteria such as *Escherichia coli, Staphylococcuus Aureus, Staphylococcus epidermis, Leuconostoc mesenteroides, Bacillus subtilis, Klebsiella mobilis and Klebsiella pneumonia* etc. [31, 30, 32, 33, 34, 35, 6, 23, 8, 11, 36] 2) Fungi such as *Aspergillus niger, Candida albicans, Saccharomyces cerevisia, Trichophyton mentagrophytes* and *Penicillium citrium* [6, 7, 37, 23, 8, 38, 14, 39]; 3) Virii such as Hepatitis B, HIV-1 Syncytial virus [40, 41, 42,43]. Hybrid silver nanocomposites with dendrimers and polymers also found to be effective against *S. aureus, Psedomonas aeruginosa, E.coli, B. Subtilis* and *K. mobilis* [39]. Furthermore, zeolites with silver reveal antibacterial efficiency against *Pseudomonas putida, E. coli, B. subtilis, S.aureus and P. aeruginosa* [15, 44, 45].

Silver mechanisms of action for antimicrobial activity are not properly understood. For bacteria, commonly suggested mechanisms in the literature is the release of silver ions followed by generation of reactive oxygen spices [5]. Bacteria show a low tendency to develop resistance with ionic silver [46]. Silver interferes the metabolism of microorganism associated with the sulfhydryl groups of enzymes and proteins in the structure. In addition, silver inhibits duplication by denaturing bacterial DNA and RNA [47, 48]. Although silver is recognized as an effective antimicrobial element, perfect development of inactivation requires ionic form of silver with suitable concentrations. Zeolites are porous crystal-structured aluminosilicate where metal ions can incorporate into their pores by ion-exchange process and are capable of releasing those ions at a controlled rate [15].

Whenever regular environmental cations, such as sodium, calcium or potassium, are available, controlled release of silver ions take place from silver zeolite matrix. Silver release cannot occur unless another available ion takes its place in the zeolite. In the presence of moisture, silver comes out from the zeolite and only until the concentration of silver reaches an equilibrium value. This process requires silver to be in the proper range of concentrations needed to kill the bacteria. Silver does not release in dry condition and similarly microorganisms also cannot survive without moisture. So the active material is not consumed when it is not required, and thus the duration of antimicrobial efficacy is enhanced [49, 50, 51, 52, 5]. According to the FDA, silver zeolite coatings are known as safe for use in food packaging and coating for medical devices [54]. Unfortunately, very few such high efficiency antimicrobial products have so far been produced.

2.2 Antimicrobial System and Chemicals

Antimicrobial surface can be prepared in two different ways. One method includes the embedment of active agent throughout the entire work piece and the other is by doing surface coatings. The antimicrobial agent can be included into the amorphous zones of the acrylic polymer during the manufacturing process and is durable over the lifespan of the acrylic material. If the agent is removed from the surface, more of the agent will migrate to the surface until the internal vapor pressure of the agent reaches its equilibrium state [55]. When incorporating antimicrobials throughout the entire area, organic substances are most often used, since inclusion of inorganic and heavy metals alter the mechanical properties of the work piece.

Economically, surface coatings for antimicrobial parts are more feasible methods of application. Coating application can be done by dipping, spraying or various nano technological methods such as physical and chemical vapor deposition etc. Applications include any object where bio contamination may be transmitted, as for example, treatment in public places, house hold items, food industries and others. Organic and inorganic materials can be included into a surface coating without leaching or affecting the mechanical properties of the whole part. Organic materials can be effectively used, except in certain unstable situations of greatly varying temperatures and pressures. This is also true for applications for longer periods. Organic additives, such as bleach or methyl urea, are toxic to humans, animals and plants and usually added within plastic and fabric products during manufacturing stages. These organic active agents have little effect over inorganic additives related to the mechanical properties of a part, so inorganic additives are predominantly used in surface coatings. They also show immunity against microbes. We have considered the inorganic additives for our work. There are many different types of inorganic additives that may be incorporated into a powder coating which can potentially kill microbes. Microbes include bacteria, fungi, archea and protists. Bacteria are included in archea, while protists include algae, amoebas, mold and protozoa. Viruses are also a major type of microbes. All additives show immunity against microbes but may or may not be totally effective against viruses.

2.3. Ionic Metals

Silver, copper, zinc, mercury, tin, bismuth, cadmium, chromium, cobalt, nickel, iron, manganese, arsenic, antimony and barium are known as oligodynamic metal, that means

toxic metal [56]. Silver is less cytotoxic than zinc and copper [57] whereas copper has the best antifungal effect. Cadmium, mercury and arsenic are strong antimicrobial agents but they are toxic and unsafe.

Silver is one of the most efficient antimicrobial agents and has several oxidation states: zero valent Ag^{o}, monovalent Ag^{+}, divalent Ag^{2+} and trivalent Ag^{3+}. Dispersion of silver particles in water is the most used path to achieve antimicrobial characteristics. High thermal stability and continuing activity are the special characteristics of silver and is known as a versatile antimicrobial agent [58]. Silver has strong antimicrobial properties and modest toxicity to mammalian cells and tissues. Silver ion presents a possible mechanism for inactivation of viruses due to its unique action of binding to or denaturing DNA and RNA [48)].

Silver ions can enter into the microbial cell through transmembrane by active and passive transport systems. Silver ions produce most toxic effects once they enter inside a cell. Silver binds to sulphur, nitrogen or oxygen containing electron donor groups. Silver also has the ability to bind phosphates or chlorides containing negative charged groups. For biomaterials, ionic silver is especially important as an antimicrobial agent. Clinically, silver reveals low toxicity towards human body and minimum threat is expected even after longer periods of clinical exposure [59], thus making it a great antimicrobial candidate in vivo. One report shows that 100 ppm silver ions creates a significant antibacterial effect, but 1000 ppm silver shows evidence of extreme cytotoxicity [60]. However in a separate article, it is mentioned that there is excellent biocompatibility up to the concentration of 20 ppm $AgNO_3$ [61].

2.4 Mechanisms of Inactivation

The silver ion is lethal to all bacteria, including MRSA and VRE, and few incidences of resistance have ever been recorded [62]. Direct investigation has been done for clarifying the mechanism of action of silver ions on microorganisms, where gram-negative *Escherichia coli* K-12 and gram-positive *Staphylococcus aureus,* were used as the test organisms. Similar morphological changes have been observed for both types of bacteria after insertion of silver ions. In this study, the cell walls and cytoplasm membranes were detached from each other. Subsequently condensed deoxyribonucleic acid (DNA) molecules containing region appeared in the center of the cell. Many small electron-dense granules were observed inside the cells or surrounding the cell wall. Presence of elements of silver and sulphur was observed in the electron dense granules and cytoplasm through X-ray microanalysis. The author also mention that the replication ability of DNA has been lost and the protein became inactive after the treatment with Ag^{+} (63). The prime molecular target for the silver ions is the thiol (-SH) groups, which are commonly found in enzymes. A marked enhancement of pyrimidine dimerization occurs when interacting with DNA by photodynamic reactions, which may have prevented DNA replication (64).

More-over there is an growing interest for materials that has antimicrobial characteristics and strong incentive to develop new antimicrobial products. Other than the medical sector, biomaterials infused with different types of antimicrobials have been used in food industries, building materials and in many house-hold appliances. A large sequence of the public considers food contamination a serious health risk. *Escherichia coli* and *Listeria monocytogenes* are the most common food borne pathogens and are commonly targeted by antimicrobial strategies. Antimicrobial surfaces can reduce microbial load in the food

industries. Another nonmedical application area with great interest in antimicrobial materials is the construction industry. The growth of molds in building materials and in ventilation systems can cause adverse effects to health through indoor air quality. Faster surface die-off of pathogens on a surface can significantly reduce the average surface population of pathogens available for transmission to a susceptible host. It can also reduce the time that a fomitic reservoir needs to transmit disease. Effective routine chemicals used as disinfectant are toxic, time consuming and labor intensive. Because of the increasing resistance of microbial organisms to antibiotics and the permanent pressure on health care costs, low cost but highly durable antimicrobial surfaces are obviously necessary.

2.5 Carrier Materials

Ceramic crystal carriers are often used for optimizing the performance of antimicrobial additives in powder coating sample. Such carriers include zeolites, silica glass, hydroxylapatite, and zirconium phosphates. In order to overcome and provide certain properties to the coating, organic or inorganic chemicals are added to these carriers to obtain the following properties:

1) Increased surface area - The carrier may provide three dimensional release function independent of agent concentration.

2) Protection of additives - Zeolite can withstand temperatures up to 800°C and pH values between 3 to10 while keeping proper antimicrobial effectiveness.

3) Protection of substrate (powder coating) - Ceramic carriers, like zeolite, also minimize degradation of organic materials. The substrate is not necessarily in direct contact with the additives that may oxidize organic materials.

4) Increased life expectancy - Carriers create a released environment in which chemicals can work, adding to an increased life expectancy.

Zeolite is made up a three dimensional framework of silica and alumina tetra-hedra where aluminum or silicon ions are bounded by four oxygen ions in a tetra-hedra arrangement. Zeolite possess large surface areas, high chemical, mechanical, and thermal stability, bio-compatibility, with distinctive hydrophilic and electrostatic properties [65]. These properties make zeolite a favorable carrier for antimicrobial additives. This zeolite framework is negatively charged by nature but this is stabled by the cations present in the cavities. They can accommodate a wide variety of cations. Potassium (K+), calcium (Ca+) and/or sodium (Na+) ions are the exchange sites. There are different types of zeolites, all in the form of either natural or synthetic, available for different applications. However, if one needs to be chosen, natural zeolite (Chabazite) is the best option considering its physical and chemical stability, abundance and price.

Zeolite can be manufactured as a natural or a synthetic product. Depending on the application, the ratio of silica to alumina can be determined. Synthetic zeolites have a ratio of silica to alumina of 1:1 while natural zeolites have a higher ratio. Natural zeolite can withstand acid environments and create a low anionic field which shows good affinity towards cations of lower charge [66]. Zeolites can selectively absorb or release ions and act as molecular sieves with the help of water. Interconnected tunnels and

cavities of zeolites allow organic or inorganic materials to be readily encapsulated within and trapped permanently [67]. Ion-exchange is the main method of incorporation of ions into zeolites. Cationic species wanting to be absorbed into the zeolite matrix are brought in contact with an aqueous mixture. Each ionic species is generally used in the form of a salt following vigorous and longer periods of mechanical mixing [68]. Zeolites are specifically used to remove calcium ions from water. They are also used to remove strontium and caesium from radioactive waste solutions, and absorb sulphur dioxide to purify detrimental gas exhausts from power plants.

2.6 Silver ions in Zeolite

To achieve an effective result, silver ions need to be released from the carrier material to a pathogenic environment. Zeolite is used as the carrier material because it enhances the water absorption properties ensuing in an increase of silver ion release. Silver zeolites act as an ion pump, which helps the controlled release of silver ions to an aqueous environment. The release of silver ions from the silver loaded material is compiled by three steps: 1) The diffusion of water into the loaded sample, 2) ion exchange of silver ions due to the reaction between silver and water and 3) the movement of silver ions towards the aqueous environment. The carrier material plays an effective role in accelerating the water diffusion and movement of silver ions through the polymer matrix [58].

Silver ion releases in the presence of moisture whenever general environmental cations such as sodium, potassium and calcium, are readily accessible in the zeolite. This step is

thought to create a controlled release mechanism for ionic antimicrobial species in zeolite particles. The release of ionic species is dependent on the no of charges and release will happen when there are ions available to take the place of another in a zeolite matrix. The cations that favor growth and survival of microorganisms are the same cations that promote ionic exchange with a zeolite. In very dry condition microorganisms cannot grow normally and cannot survive, so ions would not be released from a zeolite particle in the absence of moisture and any such cationic species if not present. So the longevity of the product is greater [69]. Silver zeolite also produces bactericidal action from the generation of reactive oxygen species [70].

2.7. Antimicrobial Testing and Biocompatibility

The target for any antimicrobial activity is the requirement that it last for longer periods in an effective way. Due to medical requirements, different biomedical devices are implanted into a human bodies and the body immune system considers them as foreign objects. At the same time, bacteria also tries to compete with human cells to attach to the surface of that medical device. As such, an immediate antimicrobial effectiveness is required to safe guard the human body. Over 50% of biomaterial infections occur long after their implantation and even may appear after couple of years. This is known as late biomaterial centered infection [71]. Although it is difficult to determine the period of effectiveness of the coating, as a general rule it can be said to have a lasting period at least equal to the life of the biomedical device. Since antibiotic loaded implants remain effective over a certain period of time, sometimes it is enough to prevent any attachment, but it takes longer time for body tissues to cover the implant. Antibiotic drugs, namely

Rifampin (USAN) and Vancomycin (INN), a glycopeptide antibiotic loaded in silicone polymer, are able to prevent bacterial colonization for over 50 days [72]. This method is good for cases that require a shorter duration of protection.

Titanium specimens of cylindrical shape are used for hip or knee arthroplasty (surgical repair of joint) and by vapor deposition method, Ag was used to make a thin film of silver on the surface. Release of silver ions depends on the amount of silver particles on the surface and hardly decreased after six days, meaning that it should last for long periods of time [73].

2.8 Powder Coating

Powder coatings are an acceptable method that are environmental friendly and are applied as a free flowing dry powder formulated with the same resins, pigments and additives, like liquid coatings. There are two general classes of powder coatings, thermo plastic and thermo setting. Thermo plastic can re-melt upon heat exposure while thermo setting polymers melt and chemically react, unable to re-melt; these two represent the majority of powder coatings [74].

There are many advantages to powder coating over liquid coating in respect to environmental, economical, operational and finishing techniques. Powder coatings do not incorporate any solvent, so no volatile organic compounds (VOCs) are present during their application and cleanup. Thus they protect against the hazardous air pollutants (HAPs) which occur when liquid solvents vaporize naturally during drying. Other environmental benefits include reduced waste by recycling of the overspray powder,

higher efficiency during application a safer and cleaner process. Powder coating offers lower costs in labor, energy, production, waste disposal and regulation compliance, all of which make powder coatings one of the least expensive coating application methods now a days . Since no mixing of solvents with resin is required, it is the least labor intensive process and the powder may be applied as it is received from the manufacturer. Coating with better physical consistency is another big advantage that gives better mechanical properties and good resistance to corrosion. Powder coatings provide denser cross linking of the polymer due to the higher molecular weight of solid materials than liquid coatings. Thus this powder coating has a higher resistance to hydrolysis and lower oxygen transmission [75].

2.9 Manufacturing of Powder Coatings

Three different methods are used in powder coating procedures: dry blending, solution or melt mixing. Melt mixing with thermo setting polymers was utilized in this research, and therefore it will be discussed. The following sequence of events occurred during the melt mixing manufacturing process: weighing, premixing, melt mixing (extrusion), cooling, chipping, fine grinding (pulverizing), and classification/sieving. The manufacturing process began with the measuring out of raw materials, including resin, pigment, fillers and additives. The main purpose was to create a homogeneous and uniform solid blend of the materials. Mixed raw materials were transferred into the extruder to completely homogenize the materials by melting the resin and curing agent and dispersing the additives, fillers and pigments within. The materials were then passed through the chiller rollers for cooling and pressing the molten plastic into a thin work piece. The sheets of

plastic were broken down into smaller chips, and transported for further grinding. Grinding was done by air classifying mills, opposed nozzle jet mills, or simply high powered, high shear grinders. Compressed air was used in the opposed nozzle jet milling method to create gradients of high pressure to break apart particles. Particle size was affected by the change in feed rate of particles to the system. Once fine grinding was sufficient, fine powders were sieved to retain a smaller particle size distribution range. The end product was an ultrafine powder formulation ready for application.

2.10 Electrostatic Spraying

Fluidized bed, electrostatic spray, friction static spray and electrostatic fluidized bed are the four principal methods for powder coatings applied over the surface of a part. Among all these techniques, electrostatic spray will be the greater focus in this paper since only this method was extensively utilized in this research. During 1960s the principles of electrostatic methods grew in momentum to make surface coatings with powder. Most powders behave as insulators and can be subjected to accept a positive or negative charge (polarity) and are easily attracted to a work piece that is either grounded or oppositely charged. Powder spray systems basically include five main components: a powder reservoir, a feed mechanism for the reservoir, a gun designed to spray the powder, a powder generator to charge the particles and a powder recycling equipment gathering overspray. When an electric conductor carrying current is surrounded by a fluid, an electrical discharge takes place due to the ionization of the fluid is called the corona discharge. This corona discharge occurs internally at the tip of the gun or by means of an electrode at the end of the gun. The power pack produces very high voltage in kV ranges

and very low current in mill ampere (mA) ranges that produce charge to the gun. Voltage ratings can range from 35 kV to 100 kV. The thickness and quality of the powder film is dependent on many factors, like the speed of the powder cloud produced, cloud pattern created by the gun tip, feed rate, charge, type of spray gun and resistivity of the powder. Electrostatic spraying makes a better finish and uniform thin film coatings on a cold work piece. Transfer efficiency of the spray is 100% with a recovery system (74). The recycling system is usually integrated into the spray booth. After spraying to reach the desired thickness, the part is cured using a convection oven. The selection of the oven temperatures and exposure times for complete curing (cross-linking) depend on the type of resin and binder used during the finished coating.

2.11 Compositions of Powder Coating

The binder is the main component of a powder coating that comprises of the polymeric resin and the curing agent. The binder percentage plays a major role in the type of finish of the coating. When a clear powder coating is desired, the binder content should be at least 95% the total weight, but for general use 50% of the total weight is good enough. The binder is prepared by the mixing of the resin and curing agent under different thermal conditions. Four main different resins are used namely epoxy, polyester, polyester-epoxy hybrid and polyurethane. Since the polyester system was used, in this work, only polyester curing reactions will be discussed here.

Polyester paint shows high resistance to UV rays and better resistance to weathering. Thus such resins are ideal for outdoor applications. Triglycidyl Isocyanurate (TGIC) is

widely used as a curing agent with polyester resins. The carboxylic functional group of the polyester reacts with the epoxy group from the TGIC at appropriate thermal conditions. A typical ratio of polyester to TGIC is 93:7. Other components, such as β-hydroxy-alkylamide and Araldite PT 910, may also be used as curing agents.

Polyester powder coating shows excellent mechanical properties with good flexibility and toughness. Due to their low viscosity, they have a very good flow during the melting and curing process that translates into a very smooth glossy finish. A generic polyester powder coating shows excellent flexibility, good hardness, outdoor resistance, anti-corrosion properties, appreciable chemical resistance and excellence in over baking situations [76]. However polyester coatings do not show great resistance to solvents.

Powder coating is also composed of components like pigments, specific additives and fillers. Pigments give color to the paint and present an aesthetic appearance. Components of different additives in the powder include flow agents, degassing agents, matting agents, texturing agents, light stabilizers and catalysts. These ingredients are usually present at low concentrations and control different properties of the final coating. Where flow agents work to avoid surface defects, degassing agents help control gas release during curing, matting agents act to reduce gloss, texturing agents modify surface to give particular texture patterns, light stabilizers protect surface from UV rays and catalysts yield faster cure times. Fillers play a very important role in cutting manufacturing costs by reducing the amount of expensive binders, and in addition, add hardness [77]. Moreover, other additives may be incorporated to yield a specific function in the finished coating by changing properties and creating different effects as desired from application to application.

2.12 Functional Coating

In daily use, except for some raw materials, it is rare to find objects that are not coated with some kind of coating material. Coating is described as a material which is applied onto a surface and after drying it appears as either a continuous or irregular film [78]. Depending on their compositions, coatings can be classified as solvent borne, water borne and solvent free. Solvent borne paints usually include resin, additives and pigments which are dissolved in organic solvents; water borne coatings are dissolved in water and with solvent free formulations the paints neither have solvent nor water, but rather everything dispersed within the resin. Coatings occur both in organic or inorganic forms. These properties are determined by the types of binders, additives and pigments used in the formulations. The end properties of a coating depend on the substrate (pre-treatments), application technique and conditions of film development. Generally, inorganic coatings are mostly applied for protective purposes, whereas organic coatings, including powder coatings, are used for functional reasons [79].

A functional coating is a system which possesses additional critical functionality along with the traditional properties of a coating (decoration and protection). Apart from their unique functional properties, these types of coating, are expected to satisfy additional requirements, such as stability, reproducibility, application friendly, cost effectiveness, tailored surface morphology, and environmental easiness [78]. Moreover, functional coatings are classified in several categories depending on their particular characteristics. These categories include optical properties, thermal properties, physio-chemical properties, structural and mechanical properties, electrical and mechanical properties, and hygienic properties. Antimicrobial coatings included in the hygienic category perform

their actions at the air-film interface. To evaluate the degree of effectiveness for functional coated surfaces, specifically antimicrobial coated surfaces, test may be carried out using standard methods.

2.13 Standard Efficacy Testing

Many functional antimicrobial coatings are in effect now-a-days and take part in a major role in industries. Most of these coatings are proprietary and lack complete information. Powder coating technology is still not under the umbrella of a common international standard and thus the quality, effectivity and durability of coating applications on surfaces varies from country to country and largely depends on local regulations. Thus it is always difficult to make comparisons and correlations. Most claims made by different institutions are handled using inapplicable test methods due to the absence of internationally recognized standards for testing. Different antimicrobial surface tests include:

• ASTM E2149-10: Standard Test Method for Determining the Antimicrobial Activity of Immobilized Antimicrobial Agents under Dynamic Contact Conditions

• ASTM E 2180-07: Standard Test Method for Determining the Activity of Incorporated Antimicrobial Agent(s) in Polymeric or Hydrophobic Materials

• JIS Z 2801: Japanese Standard Test for Antimicrobial Product Activity and Efficacy

• Kirby-Bauer: Zone of Inhibition (ZOI) Testing

• Minimum Inhibitory Concentration test (MIC Test)

The antimicrobial fabric tests include:

• AATCC 100: Assessment of Antibacterial Finishes on Textile Materials

• AATCC 147: Antimicrobial Fabric Test (Parallel Streak Method for Antibacterial Activity Assessment of Textile Materials)

MIC values are obtained by bulk dispersion of an antimicrobial agent in liquid media where many different types of bacteria may be used. This procedure undermines the real world effectiveness of the same substance used as an antimicrobial surface. This is because ion concentrations achieve increased levels more quickly in thin film environments on a treated surface than in a bulk dispersion analysis [68]. ASTM E2180-07 was used in the present research. This method is used to assess quantitatively the antimicrobial efficacy of active agents incorporated into or onto hydrophilic or polymeric surfaces. Mainly antibacterial activity is assessed but other activities may also be used. Bacteria are applied to surfaces by agar slurry which reduces surface tension and allows a pseudo biofilm to form providing uniform contact for the inoculums bacteria with the affected surface.

Quantitative analyses can be made between control and treated surfaces and durability can also be determined through testing washed surfaces over time. In the real world, bacteria on controlled surfaces usually die off over time due to environmental conditions. It should also be noted that the killing times and rates noticed within this research would

occur much faster in the real world, again as conditions would not be as positive for bacteria to subsist. Although there are particular testing standards in place for antimicrobial surfaces and fabrics, comparison is nearly impossible. The standards may be accurate in determining one time efficacy but there is no standard for surface soiling testing or durability tests and how long the surface or part may keep its antimicrobial properties.

Suggestions are included with some standards but they are very elemental and not detailed. Using ASTM E2180-07 standards, antimicrobial powders could be developed and tested by targeting the main goals of a functional, simple, highly durable antimicrobial surface.

References:

1. Rejeski D, 2009, Nanotechnology and consumer products. http:// www.nanotechproject.org/publications/archive/nanotechnology_consumer_products/. Accessed 22, February 2010

2. Arora S, Jain J, Rajwade J, Paknikar K, 2008, Cellular responses,induced by silver nanoparticles: in vitro studies. *Toxicol, Lett* vol.179, pages93–100.

3. Chi Z, Liu R, Zhao L, Qin P, Pan X, Sun F, Hao X, 2009, A,new strategy to probe the genotoxicity of silver nanoparticles combined with cetylpyridine bromide. *Spectrochimacta A* vol.72, pages577–581.

4. Choi O, Hu Z, 2008, Size dependent and reactive oxygen species,related nanosilver toxicity to nitrifying bacteria. *Environ,Sci Technol*, vol. 42, pages4583–4588.

5. Hwang E, Lee J, Chae Y, Kim Y, Kim B, Sang B, Gu M, 2008, Analysis of the toxic mode of action of silver nanoparticles using stress-specific bioluminescent bacteria. *Small* vol.4, pages746–750.

6. Kim J, 2007, Antibacterial activity of Ag? ion-containing,silver nanoparticles prepared using the alcohol reduction method, *J Ind Eng Chem*, vol. 13, pages718–722.

7. Kim K, Sung W, Moon S, Choi J, Kim J, Lee D, 2008a, Antifungal effect of silver nanoparticles on dermatophytes, *J Microbiol Biotechnol* , vol.18, pages1482–1484.

8. Kim K, Sung W, Suh B, Moon S, Choi J, Kim J, Lee D, 2009b, Antifungal activity and mode of action of silver nanoparticles on Candida albicans. *Biometals*, vol.22, pages235–242.

9. L, Panacek A, Soukupova J, Kolar M, Vecerova R,,Prucek R, Holecova M, Zboril R, 2008, Effect of surfactants,and polymers on stability and antibacterial,activity of silver nanoparticles (NPs). *J Phys Chem*, vol.112,pages 5825–5834.

10. Lok C, Ho C, Chen R, He Q, Yu W, Sun H, Tam P, Chiu J, Che C, 2006, Proteomic analysis of the mode of antibacterial,action of silver nanoparticles, *J Proteome Res* vol.5, pages916–924.

11. Raffi M, Hussain F, Bhatti T, Akhter J, Hameed A, Hasan M, 2008, Antibacterial characterization of silver nanoparticlesmagainst E. coli ATCC-15224, *J Mater Sci Technol*Vol.24, pages 192–196.

12. Schrand A, Braydich-Stolle L, Schlager J, Dai L, Hussain S, 2008, Can silver nanoparticles be useful as potential,biological labels? *Nanotechnology* 19.

13. Sondi I, Salopek-Sondi B, 2004, Silver nanoparticles as antimicrobialmagent: a case study on E. coli as a model formGram-negative bacteria, *J Colloid Interface Sci*, vol.275, pages177–182.

14. Vertelov G, Krutyakov Y, Efremenkova O, Olenin A, Lisichkin G, 2008, A versatile synthesis of highly bactericidal Myramistin stabilized silver nanoparticles, *Nanotechnology*

15. Cowan M, Abshire K, Houk S, Evans S, 2003, Antimicrobial efficacy of a silver-zeolite matrix coating on stainless steel. *J Ind Microbiol Biotechnol* vol.30, pages102–106.

16. Inoue Y, Hoshino M, Takahashi H, Noguchi T, Murata T, Kanzaki Y, Hamashima H, Sasatsu M, 2002, Bactericidal activity of Ag-zeolite mediated by reactive oxygen species,under aerated conditions. *J Inorg Biochem* vol 92, pages37–42.

17. Yoon K, Byeon J, Park C, Hwang J, 2008a, Antimicrobial effect of silver particles on bacterial contamination of activated carbon fibers, *Environ Sci Technol*, vol.42, pages1251–1255.

18. Yoon K, Byeon J, Park J, Ji J, Bae G, Hwang J, 2008b, Antimicrobial characteristics of silver aerosol nanoparticles against Bacillus subtilis bioaerosols. *Environ Eng Sci*, vol.25, pages 289–293.

19. Bajpai S, Mohan Y, Bajpai M, Tankhiwale R, Thomas V, 2007, Synthesis of polymer stabilized silver and gold nanostructures. *J Nanosci Nanotechnol*, vol.7, pages2994–3010.

20. Damm C, Munstedt H, 2008, Kinetic aspects of the silver ion release from antimicrobial polyamide/silver nanocomposites. *Appl Phys A* vol.91,pages 479–486.

21. Hlidek P, Biederman H, Choukourov A, Slavinska D, 2008, Behavior of polymeric matrices containing silver inclusions.1—Review of adsorption and oxidation of hydrocarbons on silver surfaces/interfaces as witnessed by FTIR spectroscopy. *Plasma Process Polym* vol.5, pages807–824.

22. JinW, JeonH,KimJ, Youk J, 2007, A study on the preparation of poly(vinyl alcohol) nanofibers containing silver nanoparticles. *Synthetic Met* vol.157,pages 454–459.

23. Kim J, Lee J, Kwon S, Jeong S, 2009a, Preparation of biodegradable polymer/silver nanoparticles composite and its antibacterial efficacy. *J Nanosci Nanotechnol* vol.9,pages 1098–1102.

24. Navarro E, Piccapietra F, Wagner B, Marconi F, Kaegi R,,Odzak N, Sigg L, Behra R, 2008, Toxicity of Silver Nanoparticles to Chlamydomonas reinhardtii, *Environ Sci Technol*, vol.42, pages8959–8964.

25. Nita T, 2008, Synthesis of antimicrobial polymer composition and in vitro drugs release study. *Chim Oggi*, vol.26, pages16–18.

26. Naidu B, Park J, Kim S, Park S, Lee E, Yoon K, Lee S, Lee J,Gal Y, Jin S, 2008, Novel hybrid polymer photovoltaics made by generating silver nanoparticles in polymer: fullerene bulk-heterojunction structures. *Sol Energy Mater Sol Cells*, vol.92, pages397–401.

27. Varun Sambhy, Blake R. Peterson, Ayusman Sen, 2008, Antibacterial and Hemolytic Activities of Pyridinium Polymers as a Function of the Spatial Relationship between the Positive Charge and the Pendant Alkyl Tail, *Angewandte Chemie,* vol. 120, no.7, pages 1270-1274.

28. Yeo M, Kang M, 2008, Effects of nanometer sized silvermaterials on biological toxicity during zebrafish embryogenesis, *Bull Korean Chem Soc*, vol.29, pages1179–1184.

29. Jain P, Pradeep T, 2005, Potential of silver nanoparticle-coatedpolyurethane foam as an antibacterial water filter. *Biotechnol, Bioeng* vol.90, pages 59–63.

30. Chen C, Chiang C,2008, Preparation of cotton fibers with antibacterial silver nanoparticles. *Mater Lett* , vol.62, pages3607–3609.

31. Benn T, Westerhoff P, 2008, Nanoparticle silver released into water from commercially available sock fabrics. *Environ Sci Technol* , vol.42, pages4133–4139.

32. Falletta E, Bonini M, Fratini E, Lo Nostro A, Pesavento G, Becheri A, Lo Nostro P, Canton P, Baglioni P, 2008, Clusters of poly(acrylates) and silver nanoparticles: structure and applications for antimicrobial fabrics. *J Phys Chem,* vol.112, pages 11758-11766.

33. Hernandez-Sierra J, Ruiz F, Pena D, Martinez-Gutierrez F, Martinez A, Guillen A, Tapia-Perez H, Castanon G, 2008, The antimicrobial sensitivity of Streptococcus mutants to nanoparticles of silver, zinc oxide, and gold. *Nanomed Nanotechnol* vol.4, pages237–240.

34. Ingle A, Gade A, Pierrat S, Sonnichsen C, Rai M, 2008, Mycosynthesis of silver nanoparticles using the fungus Fusarium acuminatum and its activity against some human pathogenic bacteria. *Curr Nanosci* vol.4, pages141–144.

35. Jung R, Kim Y, Kim H, Jin H, 2009, Antimicrobial properties of hydrated cellulose membranes with silver nanoparticles. *J Biomater Sci Polym*, vol.20, pages311–324.

36. Yang W, Shen C, Ji Q, An H, Wang J, Liu Q, Zhang Z, 2009, Food storage material silver nanoparticles interfere with DNA replication fidelity and bind with DNA, *Nanotechnology* 20.

37. Kim Y, Kim J, Cho H, Rha D, Kim J, Park J, Choi B, Lim R,Chang H, Chung Y, Kwon I, Jeong J, Han B, Yu I, 2008b, Twenty-eight-day oral toxicity, genotoxicity, and genderrelated,tissue distribution of silver nanoparticles in Sprague-Dawley rats. *Inhal Toxicol*, vol.20,pages 575–583.

38. Roe D, Karandikar B, Bonn-Savage N, Gibbins B, Roullet J, 2008, Antimicrobial surface functionalization of plastic catheters by silver nanoparticles. *J Antimicrob Chemother* vol.61, pages869–876.

39. Zhang Y, Peng H, Huang W, Zhou Y, Yan D, 2008, Facile preparation and characterization of highly antimicrobial colloid Ag or Au nanoparticles. *J Colloid Interface Sci* , vol.325, pages371–376.

40. Elechiguerra J, Burt J, Morones J, Camacho-Bragado A, Gao X, Lara H, Yacaman M, 2005, Interaction of silver nanoparticles with HIV-1. *J Nano*biotechnol , vol.3, page6.

41. Lu L, Sun R, Chen R, Hui C, Ho C, Luk J, Lau G, Che C, 2008, Silver nanoparticles inhibit hepatitis B virus replication, *Antivir Ther*, vol.13, pages253–262.

42. Sun L, Singh A, Vig K, Pillai S, Singh S, 2008, Silver nanoparticles inhibit replication of respiratory syncytial virus. *J Biomed Nanotechnol*, vol. 4, pages149–158.

43. Zodrow K, Brunet L, Mahendra S, Li D, Zhang A, Li QL, Alvarez PJ, 2009, Polysulfone ultrafiltration membranes impregnated with silver nanoparticles show improved biofouling resistance and virus removal, *Water Res*, vol.43, pages715–723.

44. Lind ML, Jeong BH, Subramani A, Huang XF, Hoek EMV, 2009, Effect of mobile cation on zeolite-polyamide thin film nanocomposite membranes, *J Mater Res* vol.24, pages 1624–1631.

45. McDonnell AMP, Beving D, Wang AJ, Chen W, Yan YS, 2005, Hydrophilic and antimicrobial zeolite coatings for gravity-independent water separation, *Adv Funct Mater*, vol.15, pages336–340.

46.Schoenbaum MA, Freund JD,Beran GW, 1994, Survival of pseudorabies virus in the presence of selected diluents and fomites. *J Am Vet Med Assoc*, vol.8, pages1393-1397.

47. Wysor MS, and Zollinhofer, RE, 1972, On the mode of action of silver sulphadiazine, *Path Microbiol*, vol.38, pages296-308.

48. Modak, SM, 1973, Binding of silver sulfadiazine to the cellular components of Pseudomonas aeruginosa, *Biochemical Pharmacology*, vol.22, pages2391-2404.

49. Galeano B, Korff E, Nicholson WL,2003, Inactivation of vegetative cells, but not spores, of Bacillus anthracis, B.cereus, and B. subtilis on stainless steel surfaces coated with an antimicrobial silver- and zinc-containing zeolite formulation, *Appl Environ Microbiol*, vol. 7, pages 4329-31.

50. Rusin P, Bright K, Gerba C, 2003, Rapid reduction of Legionella pneumophila on stainless steel with zeolite coatings containing silver and zinc ions. *Lett Appl Microbiol*, vol.36, no.2, pages 69-72.

51. Takai K, Ohtsuka T, Senda Y, Nakao M, Yamamoto K, Matsuoka J, Hirai Y, 2002, Antibacterial properties of antimicrobial-finished textile products. *Microbiol Immunol*, vol.46, no.2, pages75-81.

52. Kawahara K, Tsuruda K, Morishita M, Uchida M, 2000, Antibacterial effect of silver-zeolite on oral bacteria under anaerobic conditions. *Dent Mater*. Vol. 6,pages 452-455.

53. Morishita, M, et al., 1998, Pilot Study on the Effects of a Mouthrinse containing Silver Zeolite on Plaque Formation, *J Clinical Dentistry*, vol.9, pages94-96.

54. AgION Technologies website, September 27, 2004, http:// www.agiontech.com / applications.html

55. Watterson RS and Hanrahan WD, 2002, Antimicrobial Acrylic Material. USPTO full text and image Database , U.S. Patent 6448305

56. Mawatari M, Hamazaki C, Furuyama T, 1997, Antibacterial Resin Composition. USPTO Full text and image Database. United States Patent 5614568, March 25

57. Williams RL, Doherty PJ, Vince DG, Grashoff GJ, and williams DF, 1989, The biocompatibility of silver, *Critical Reviews in Biocompatibility*, vol.5, page221.

58. Radheshkumar C, and Munstedt H, 2007, Antimicrobial Ploymers from Polypropylene / Silver Composites Ag+ Release Measured by anode Srtipping Voltammetry, *Reactive and Functional Polymers*, vol.66, pages780-788.

59. Lansdown A, 2006, Silver in Health Care: Antimicrobial Effects and Safety in use.Karger Journals - *Biofunctional Textiles and the Skin*, vol.33, pages17–34.

60. Chung RJ, Hsieh M, Huang CW, Perng LH, Wen HW, Chin TS, 2005, Antimicrobial Effects and Human Gingival Biocompatibility of Hydroxyapatite Sol–Gel Coatings.

61. Feng QL, Cui FZ, 1999, Ag-substituted hydroxyapatite coatings with both antimicrobial effects and biocompatibility, *Journal of Materials Science Letters*. vol.18, pages 559-561.

62. Baranoski S, Ayello E. 2007, *Wound Care Essentials: Practice Principles*. Lippincott*Williams & Wilkins*, vol.2, page358.

63. Feng QL, Wu J, Chen GQ, Cui FZ, Kim TN, Kim JQ, 2000, A Mechanistic Study of theAntibacterial effect of Silver Ions on Escherichia coli and Staphylococcus aureus, Journal *Biomed Mater Res*, vol.52, no.4, pages662-668.

64. Matsumura Y, Yoshikata K, Kunisaki S, Tsuchido T, 2003, Mode of Bactericidal Action of Silver Zeolite and Its Comparison with That of Silver Nitrate. *Appl Environ Microbiol*, vol.69,no7, pages4278–4281.

65. Xie Y, Liu H, Hu N, 2007, Layer-by-layer films of hemoglobin or myoglobin assembled with zeolite particles: Electrochemistry and electrocatalysis, *Bioelectrochemistry*, vol.70, no.2, pages311- 319.

66. Langella A, Pansini M, Cappelletti P, de Gennaro B, de Gennaro M, Colella C, 2000, NH^{4+}, Cu^{2+}, Zn^{2+}, Cd^{2+}, and Pb^{2+}exchange for Na^{+} in a sedimentary clinoptilolite, North Sardinia, Italy. *Microporous and Mesoporous Materials*, vol.37, pages337–343.

67. Shen B, Scaiano JC, English AM, 2006, Zeolite Excapsulation Decreases TiO_2 photosensitizedROS Generation in Cultured Human Skin Fibroblasts. *Photochemistry and Photobiology*, vol.82, no.1, pages5-12.

68. Niira R, Niira Y, Yamamato T, Uchida M, 1990, Antibiotic Resin Composition. USPTO Full text and Image Database. United States Patent 4938955

69. Feied, Craig. (2004). Novel Antimicrobial Surface Coatings and the Potential for Reduced Fomite Transmission of SARS and Other Pathogens. *MD*. Vol.1, page1-22.

70. Kourai H, Manabe Y, Yamada Y, 1994, Mode of bactericidal action of zirconium phosphate ceramics containing silver ions in the crystal structure. *Journal of Antibacterial Antifungal Agents*, vol.22**,** pages595-601.

71. Gottenbos B, Grijpma DW, van der Mei HC, Feijen J, Busscher HJ,2001, Antimicrobial effects of positively charged surfaces on adhering Gram-positive and Gram negative bacteria. *Journal of Antimicrobial Chemotherapy*, vol.48, pages7-13.

72. Bayston R, Ashraf W, Bhundia C, 2004, Mode of action of an antimicrobial biomaterial for use in hydrocephalus shunts. *Journal of Antimicrobial Chemotherapy*, vol.53, pages778–782.

73. Ewald A, Gluckermann SK, Thull R, Gbureck U. (2006). Antimicrobial titanium/silver PVD coatings on titanium. *BioMedical Engineering* vol.5, page 22.

74. Berins ML, 1991, SPI plastics engineering handbook of the Society of the Plastics Industry. *Springer Inc*.vol.5, pages 497-503.

75. Liberto N, 2003, *User's Guide to Powder Coating*. 4th Edition, Michigan, USA: Association for Finishing Processes and Society of Manufacturing Engineers Lehr W, 1991, Powder Coating Systems. New York, USA: McGraw-Hill Inc.148

76. Lehr W. 1991. *Powder Coating Systems*. New York, USA: McGraw-Hill Inc.

77. Howell D. 2000. *Powder Coatings: The Technology, Formulation and Application of Powder Coatings.* vol 1. West Sussex, England: John Wiley and Sons Ltd.

78. Ghosh SK. 2006, Functional coatings: by polymer microencapsulation. Wiley-VCH.357: pages 1-25.

79. Wilson AD, Nicholson JW, Prosser HJ. 1987. *Surface Coatings-1*. London: Elsevier Science & Technology, (1), Chapter 1.

CHAPTER 3

EXPERIMENTAL FORMULATIONS AND TEST PROCEDURES

3.1 Antimicrobial Additive Powder Production

3.1.1 Zeolite

Two natural zeolites and one synthetic zeolite were used for this experiment. Synthetic zeolite was obtained from PQ Corporation. This synthetic zeolite was designated as type A (particle size, 2-3 micron) and contained only sodium cations for exchange. Two natural zeolites, LBN and LBC, were obtained from Zeox Corporation, Cortaro, AZ (particle size, around 10 micron).

3.1.2 Functionalization of zeolite

Silver Nitrate, $AgNO_{3,}$ was used to exchange ions into zeolite. Ion exchange was carried out in a dark environment in order to avoid any chance of photo-oxidation [1]. The following steps were carried out to deposit metallic ions into zeolite:

1). 25 g Zeolite was brought into contact with aqueous mixed suspensions (500 ml) of 0.001M, 0.01M, 0.03M or 0.05M silver nitrate solution to find the effect of concentration during ion-exchange. Ion-exchange was carried out by vigorous magnetic stirring at 500 rpm in 1000 mL glass beakers for 24 hours at room temperature.

2). After ion exchange, solid and liquid phases were separated by centrifugation at 3500 rpm for 25 minutes. Solid phase samples were washed extensively with deionized water

several times followed by repeated centrifugation to ensure chemisorbed ions only within the zeolite particles. NaCl suspension in water at 0.1 M was used to identify any ionic silver species in supernatant fluid after centrifugation and washing. If silver ion were present after washing, a perceived cloudy mixture with the supernatant would have formed.

3). The zeolite particles were then dried in an oven at 80^0C for 5-6 hrs. to maintain the dark condition, under normal pressure.

4). After sufficient drying, the particles were easily broken down into their initial respective particle sizes by a small grinder.

The same procedures were followed for all ion exchange processes by adjusting the pH of the solution below 5.0. This pH adjustment was done to keep the silver in its monovalent form, which was the maximum natural precipitation limit. This also prevented silver from forming or depositing on the surface or in the pores of the zeolite [2].

Copper nitrate solution was incorporated into the silver ion-exchanged sample during functionalization.

3.2 Powder Coating Procedure

3.2.1 Resin System

This binder resin has all the qualities to produce a good powder coating that includes free flowing capability, high flexibility, excellent smoothness, very low reactivity and a clear appearance. Triglycidyl Isocyanurate (TGIC), manufactured by Huntsman Advanced

Materials with the trade name Araldite® PT 810, was selected as the curing agent. It has a melting temperature between 86-96°C. A free flowing and degassing agent was required for the polyester powder paint. The mix formulation sheet of ingredients is shown below:

Table 3.1: Mix Formulation Sheet yielding Polyester TGIC Clear Coat before extrusion

Class	Sub Classes	Name	Weight in gm	Total (Wt %)
Binder	Resin		917.90	91.79
	Curing Agent	TGIC	69.10	6.91
Additives	Flow Agent	P10	10.00	1.00
	Degassing	BEN	3.00	0.30
Total Binder			987.00	98.70
Total Additives			13.00	1.30
Total Weight			1000.00	100.00

From the above Table 3.1, it is shown that 1000 grams was produced from the mixture. Clear polyester powder paint is the main component in all antimicrobial coatings.

Premixing

As per the formulation sheet shown above, the components were weighed and shaken in a plastic bag. This mixture was introduced into a shear grinder for about 10 seconds and produced a homogeneous dispersion with smaller particle size. Once all raw material components had been mixed and sheared together, they were then ready for extrusion.

Extrusion

Premixed raw materials were further processed using a twin screw extruder (Dong Hui Powder Coating Equipment, East Sun). At the beginning, the equipment was preheated to 80°C to ensure the previous materials in the screws were melted and then the rotation of the screws was set at 500 rpm. Later, the premixed raw materials were slowly poured into the hopper. The mixture was then passed into the extruder through the hopper with the help of the rotating movement of the twin screws. This mixture was further dripped down onto a double chiller rollers, refrigerated and rotated inwards, and this forced the extrudate to flatten through the centrifugal force of rotation. The thin extrudate was cooled while it moved along the cooling conveyer belt. The extrudate pieces were then collected from the belt and broken down into smaller pieces and thus ready for further processing.

Ultrafine Grinding

The paint chips obtained from the extruder were broken down by a high shear grinder. Paint chips that were input into the high shear grinder were allowed to grind in increments of 10 seconds and then paused for a few minutes before restarting the grinder. If longer grinding times were applied, would cause a buildup of high temperature inside the chamber and this would make the paint cure. Finally, the powder was transferred to a mechanical sieve for further processing after grinding. This grinding process was repeated several times until the desired level was reached.

Ultrafine Sieve Screening

After grinding, the powder was transferred to a sieve (Vorti-Siv, MiMi Industries Inc.) using a 325 mesh (45 micron) insert. The sieve vibrated with the help of an ultrasonic pulse and approximately 1 g/min powder was transferred slowly through the screen. Steel washers added into the sieve chamber helped the powder to pass through the screen. Once through the screen, the ultrafine paint powder was collected in a plastic bag. Occasionally, the screen would need to be cleaned of oversized clogged particles and the portion of the powder unable to pass through the screen would be sent back to the high shear grinding stage.

3.2.2 Additive incorporation to resin system

Dry Blending

Once the processing of the resin system was completed, antimicrobial additives could be incorporated. Powder coating and dry blending functional additives is a unique step that is yet to be recorded in the literature. All antimicrobial additives produced in powder form were dry blended with the polyester. The dry blending process initially involved weighing of additive powders and polyester resin using OHAUS Analytical Plus Balance (0.00000g). Polyester and each antimicrobial additive were then added into a small grinder and mixed for approximately 15 seconds while shaking. The goal of dry blending was to homogeneously disperse the smaller additives throughout the resin and in turn the functional particles would cover the surface of each polyester particle.

3.3 Powder Application

Specimen/Substrate Preparation

Approximately 2.5 grams of powder was sprayed using a Nordson Surecoat corona spray gun (Nordson Corp, TWGEMA) in order to fully coat the aluminum sheet (6.0 cm x 7.5 cm). Electrostatic field lines helped to determine the completion of powder coating on the substrate. The sheets were then hung and cured according to the specifications of the base resin in the oven.

For each antimicrobial powder sample that was prepared and tested, six aluminum substrate pieces were made. In order to replicate the same coating conditions and produce identical coating results for each aluminum substrate (for each powder sample sprayed), a unique setup was configured and used throughout the entire work. After every spraying, the weight of the surface was recorded to check the transfer efficiency of the powder.

Electrostatic Spraying

Each powder sample was electrostatically sprayed in a 14.6 cm (H) x 9.0 cm (D) x 7.5 cm (W) acrylic spray booth over the specimens. It was then hung inside the booth and grounded appropriately. A Nordson Surecoat corona spray gun (Nordson Corp, USA) was used to manually coat the prepared specimens directly. The mixed powders were also manually deposited into the gun during the process. A cone deflector tip was used at the end of the corona spray gun. Powder spray was controlled by air the pressure of the fluidizing and atomizing air sent through the gun. The corona charge generator had

constant settings for each spraying: 30 kV operating voltage, 8 uA current, and 55 air pressure strength. Only the front side of the substrate sheet was sprayed.

3.4 Curing

Once the specimens were sufficiently coated with antimicrobial powder paint, they were taken to the convection oven. All samples were hung inside and cured at 200°C for 10 minutes, which guarantees a fully cured coating as recommended by the manufacturer of the resin system. The powder with additives was melted, flowed and cured, and as such also guaranteed a fully continuous coated film as recommended by the manufacturer of the resin system. The control coated surfaces were made using the same resin powder containing raw zeolites with the same proportions and procedures.

3.5 Antimicrobial Efficacy Testing Procedure

3.5.1 Test Microorganism Used

Escherichia coli strain ATCC 35339 was purchased from the American Type Culture Collection (ATCC). This strain of bacteria was used for all antimicrobial testing purposes throughout the research. *Escherichia coli* are gram negative, rod shaped, and facultative anaerobic bacterium. *E. Coli* are predominantly used as test microorganisms for most disinfection studies as noted in the literature. According to the enclosed instructions (aseptic environment) the vial containing the bacterium in this freeze dried form was opened. To cover and rehydrate the entire pellet, 1 mL of broth (tryptone and sodium

chloride) was used and 1 mL of rehydrated pellets was then transferred from the vial into a 500 mL flask containing 50 mL recommended broth. The flask was then incubated for 24 hours, at 37°C. After incubation, two different actions were then performed with the cultured flask:

Revival

The *Escherichia coli* strain was received in frozen pellet form and was revived immediately. The propagation procedure used to revive the bacteria from this form into usable and sustainable colonies is outlined below.

i) The 50 mL cultured bacteria flask was then mixed with 50 mL glycerol, which was transferred into 50 vials for storage in the freezer until needed. The frozen vials were propagated every few months to ensure the viability of the bacteria. The contents of the frozen vials, once rehydrated, were transferred in to the 20-30 mL recommended broth and inoculated.

ii) Several drops of the inoculation from the flask were used to inoculate the agar plates. The plates were inoculated for 24 hours at 37°C. The initial plates were then streaked onto new plates using standard microbiological practices to achieve dilution of *E. coli* and essentially achieve healthy individual colonies for storage. New plates were streaked at least once a month to guarantee a viable working strain of bacteria free of contamination.

Growth Pattern

The growth pattern of *E. coli* has four phases: 1) the Lag phase occurred directly after inoculation when the bacteria were not growing, 2) during the Logarithmic (log) phase, exponential growth and cell division occurred rapidly, 3) in the Stationary phase the growth slowed and remained constant due to the limited nutrients available, and lastly 4) during the Death phase, nutrients were completely depleted and death occurred. The late log phase was the targeted time period for growth of the test microorganisms, the reason being that this stage occurred at the end of the log phase where exponential growth was completed approximately at 14 to 16 hours. A liquid medium of Luria Bertani (LB) broth was inoculated in a sterile 250 mL flask with a loop full of bacteria and placed into a Stuart Orbital Incubator 3150 at 37°C. Every hour, a sample of the medium was withdrawn into a cuvette and placed in the spectrophotometer. The emitting light source from the spectrophotometer would pass through the cuvette, and the number of photons scattered by the light (absorbance at 600nm) was proportional to the mass of cells in the sample. The resulting growth curve indicated that the inoculation of the test microorganism took place at around 16 hours before starting any inactivation experiments with powder coatings. Similar experimentation in the literature also uses the 16 hour inoculation period for *E. coli* [3].

3.5.2 Experimentation

ASTM E 2180-01

The American Society for Testing and Materials (ASTM) E2180-07 Standard test method was used to determine the efficiency of incorporated antimicrobial agent in hydrophobic or polymeric materials. Days before the experiment, all required materials and equipment used were prepared and sterilized using an AMSCO 2041 Autoclave. All related procedures and methods dealing with the inactivation of *E. coli* were carried out in a SterilGARD Biological Safety Cabinet (Baker Company Inc). This was considered a class II cabinet because it used re-circulated HEPA filtered vertical laminar air flow within. The glass sash was kept open 20-25 cm during the experiment. Part of the air flow exhausted through the HEPA filters was re-circulated inside the room. The detailed antimicrobial efficacy testing procedures and all relevant materials used are described below:

1). A loop full of bacteria was added from the LB agar stock culture plates to a 10 mL test tube containing sterile LB medium broth. The test tube was covered with a sterile foam stopper and was then inoculated for 16 hours in the Stuart Orbital Incubator at 37°C. This step was done the day before every experiment was scheduled and methods were adjusted to obtain the required amount of cells/mL of broth for each inoculation (10^7 cells/mL). The no of cells was confirmed through the growth curve of that organism.

2). Augar slurry was made from 0.85 g NaCl and 0.3 g granulated dry agar (agar-agar) were dissolved in 100 mL of deionized water, and this was called the agar slurry. After sterilization for 15 minutes, the agar slurry was kept on a hot plate at 40 +/-2°C.

3). Specimens of the coated surfaces measuring 3 cm x 3cm were placed into the sterile petri dishes. Three coated surfaces per petri dish and six petri dishes in total 18 surfaces per sample. A sterile cotton swab was then dipped into sterile 0.85% saline solution to pre wet each test sample (powder coated chip). This aided in dispersing the agar slurry evenly on the coated surface. A set of control coated surfaces were also run with every experiment.

4). 1.0 ml of the inoculated culture, from step 1, was placed into the 99 mL agar slurry, and equilibrated at 40 +/- 2°C.

5). 1.0 ml of inoculated agar slurry was pipetted evenly onto each chip sample.

6). The petri dishes were then covered with their lid and edges closed with strands of pre-cut parafilm pieces. All samples except for one petri dish - "0 hour" (3 coated surfaces), were placed into the incubator at 37°C. Open reservoirs of salt water were placed inside the incubator during the experiment to avoid the drying out of the agar slurry due to low humidity.

7). The samples were removed from the incubator at the specific pre-determined contact times, and aseptically transferred from the petri dishes into the sterile 120 ml specimen cups (1 chip per cup). Each cup contained sufficient volume of Dey/Engley (D/E) neutralizing broth to form an initial 1:10 dilution of the original inoculums slurry from each coated surface. The D/E neutralization broth was used because it had the ability to neutralize antimicrobial chemicals.

8). Specimen cups containing the recovered test samples were then placed into a sonic bath and sonicated for 1 minute. Sonication was followed by 1 minute of vigorous mechanical vortexing. This step facilitated the complete release of the agar slurry from the sample.

9). Serial dilutions were made from each specimen cup with a sterile solution of 0.85% NaCl. Vortexing was done to homogenously disperse the cells before each dilution.

10). 0.1 ml was pipetted from each dilution and spread onto the agar plates.

11). The agar plates were then covered with their lids, edges wrapped with parafilm strips and placed into the incubator at 37°C for 24 hours.

12). Colony forming units on the plates were studied, counted and recorded on the following day.

References

1. Li Z, Flytzani-Stephanopoulos M, 1997, Selective catalytic reduction of nitric oxide by methane over cerium and silver ion-exchanged ZSM-5 zeolites. *Applied Catalysis A: General*,v ol.165,no1-2, pages15-34.

2. Niira R, Niira Y, Yamamato T, Uchida M, 1990, Antibiotic Resin Composition, USPTO Full text and Image Database. United States Patent 4938955

3. Pal A, Min X, Yu LE, Pehkonen SO, Ray MB, 2005, Photocatalytic inactivation of bioaerosols by TiO2 coated membranes, International *Journal of Chemical reactor Engineering*, vol.3, noA45, pages1-11

CHAPTER 4

Pre-treatment and Conditioning of Chabazites Followed by Functionalization for Making Suitable Additives used in Antimicrobial Ultra-fine Powder Coated Surface

4.1 Abstract

Silver-copper functionalized chabazites were used to develop the antimicrobial powder coated surface. Two chabazites (named as LBC and LBN) were modified to enhance their sodium content as well as ion exchange properties by conditioning with sodium nitrate. The cation exchange capacity (CEC) of the sodium-enriched LBC and LBN was improved from 3.31meq/g and 3.46meq/g for the parent zeolites to 3.77 meq/g and 4.09 meq/g, respectively. These sodium-form zeolites were used to produce silver-copper modified zeolites. The process was optimized using different combinations of the Ag and Cu ions by varying reaction time in order to achieve durable, and efficient antimicrobial additives. These additives were used in combination with a polyester resin system to produce ultrafine powder coated surfaces. Silver was utilized as an antimicrobial agent, whereas copper was used to slowdown the reduction rate of silver ion during curing process. All materials including the raw, modified and functionalized zeolites were characterized using XRD and TGA to observe the effect of treatment. ICP-OES was used for elemental analysis at every experimental stage. Color analysis proved that copper prevents silver from reduction during the curing process and maintains the color of the coated surface, which is comparable to the control surface. These coated surfaces have shown homogeneous antibacterial properties with excellent durability against *E.coli* for

extended periods. Cell toxicity was evident from the LDH analysis of the fresh and used antimicrobial surfaces. The controlled silver release capability of the formulated surface with high concentration of silver is promising for use in different food industry and in medical facilities.

Keywords: Zeolite, chabazite, silver, ultrafine powder coating, ion-exchange, antimicrobial, durability

4.2 Introduction

Natural zeolites exhibit high cation exchange capacity (CEC), selectivity and compatibility for different industrial applications as one of the most important inorganic cation exchangers. Chabazite is a naturally occurring aluminosilicate zeolite, consists of aluminum ions in a primarily silicon framework with uniform molecular sieve pores. The substitution of aluminum atoms for silicon provide a charge imbalance, which is neutralized by different alkali (e.g., Na and K) and alkaline earth (e.g., Ca and Mg) ions, thus the cation content of a zeolite is directly related to its Si/Al ratio. Because of different sources, natural zeolites from the same type might have different Si/Al ratios and therefore, they have different proportions of exchangeable ions and water content. The framework of an aluminosilicate zeolite consists of a 3-dimensional structure of $[SiO_4]^-$ and $[AlO_4]^-$ tetrahedral linked with shared oxygen atoms. Cations do not occupy a permanent position and are free to move in the channels of the zeolite frame and can easily replace and exchange with those cations in the surrounding medium. Zeolites exhibit reversible hydration-dehydration capability without significant structural changes [1]. Cations are bonded with the zeolite framework by electrostatic forces and occur in

the open channels of the zeolites, which are potentially exchangeable through diffusion in a medium containing another cation. A diffusion process can be established between the two phases, where some cations come out from zeolite and other cations diffuse into the solid structure from the liquid phase. Considerable cation concentration difference leads to this diffusion process. Electro-negativity of the frame reduces with the addition of extra cations, so the attraction between the cations present in the zeolite reduces and the cations are loosely bonded in the lattice. It is stated that a non-localized electric field is created due to the diffusion process and influences the exchange process in spite of a partial or complete exchange of cations [2]. Cation selectivity and ion-exchange capacity are varied for different zeolite because of their structural chemistry and cation content. Natural zeolites, such as chabazite can lose or gain water in a reversible manner and can exchange their framework's cations with the cations present in the surrounding solution. Zeolites pores are of molecular dimensions which provide shape and size selectivity for outside molecules [3].

Actual CEC is different from theoretical CEC due to the position of the cations, the size of hydrated cations with their movement through the zeolite channels and cages, the ionic strength, and cation composition of the external medium. Pure natural zeolites are hardly ever found in nature and generally, several active or inactive impurities in respect to ion exchange are present. The performance of natural zeolites can be improved by pre-treatment and chemical conditioning, which are the processes applied with the aim of replacing certain cations in the zeolite with other cations for various industrial applications [4]. This treatment can also remove impurities that may hinder ion exchange while exposing the easily exchangeable ones compared to the raw zeolites. Variations in

the purity and composition, and the existence of some unwanted impurities in the natural zeolites are directly related to their cation exchange behavior and other cation exchange related properties. The conditioned zeolites should have improved effective ion exchange capability by making the exchangeable ions, that are already present within the zeolite, more accessible [1,5,6].

Literature shows that sodium–form of natural zeolite favors the exchange of Cu^{2+} over Co^{2+} [7, 8]. Ion exchanges of Cu^{2+} with chabazite and clinoptilolite, Zn^{2+} with clinoptilolite, Co^{2+} with clinoptilolite, and Cr^{3+} with chabazite and phillipsite have been reported [9,10,11] for different applications. Ion exchange and adsorption behavior of different zeolites and their modified forms for removing heavy metal cations such as cadmium, lead, nickel, and manganese [12, 13, 14, 15, 16, 17, 18] anionic species such as chromate and arsenate [19, 20] and organic pollutants such as benzene, toluene, ethyl benzene and xylene (BTEX) including the volatile organic compounds (VOCs) [21, 22, 23, 24], are studied. The Na^{+} ion is the most weakly bonded cation in natural zeolite, which can be easily replaced with other cations. Cuban clinoptilolite has been conditioned with Na^{+}, K^{+}, Ca^{2+} and Mg^{2+} for the removal of NH_4^{+} from aqueous solution [25, 26]. Na^{+} clinoptilolite shows the most improved performance among other conditioned clinoptilolite. Different sodium precursors can be used for conditioning the natural zeolites. Bulgarian clinoptilolite was conditioned by NaOH and NaCl, for the removal of Cu^{2+} from solution, but conditioning with NaCl showed better Cu^{2+} uptake compared to NaOH treatment [27]. Chabazite was conditioned with NH_4^{+} for the formation of silver nano particles on the surface of the zeolites [28].

To work with the ion exchange properties of natural zeolite it is wanted that the cationic form of the ion exchanger be near homo-ionic. Different researchers have reported different conditioning procedures to replace exchangeable cations from zeolite with a desirable cation in order to make it as a near homo-ionic form for particular applications. However, it is very difficult to convert natural zeolites into a complete homo-ionic form. Making natural zeolite into a complete homo- ionic form is not possible due to the presence of several types of cation with different electrostatic force within the solid phase as well as the presence of different mineral impurities. Based on the end use of these zeolites, one can modify the cationic configuration including their cation exchange capacity by pre-treatment and conditioning processes. Pre-treatment process helps to remove the unwanted impurities and consequently the conditioning process with strong ionic solution can also remove some detrimental exchangeable cations from the natural zeolites. These processes make the zeolite into a near homo-ionic form with significant improvement of their ion exchange capacity.

It is well known that the ion exchange properties of natural zeolites are influenced by the particular cation present in their framework, which is essential to balance the negative framework charge. Chabazite is a natural zeolite composed of different cations available for ion exchange including sodium, calcium, iron, potassium and magnesium. These native cations can be replaced by silver and copper ions via the ion exchange mechanism. Since the sodium ion is the most weakly bonded cation in chabazite, it can easily be exchanged with the cations present in the surrounding medium. Thus, by applying suitable conditions for ion exchange and cationic modification, these zeolites can be tailored into suitable carriers for some important antimicrobial industrial applications.

Nowadays, different forms of silver in zeolites are proven as effective biocides against a wide range of microorganisms and are employed in many anti-microbial products. For increasing the capacity of the carrier to hold more silver ion, pre-treatment and conditioning with sodium ion can help by improving the ion exchange efficiency. An investigation showed that the Ag^+ ions probably occupy similar positions in the frame-work to those determined for the Na^+ ions [29]. For the enhancement of ion exchange capability of chabazite with Ag^+ ion, a particular sodium salt needs to be used for particular end applications. The main objective of this study was to identify the conditioning effects with compositional changes of chabazite, which will create enhanced activity and will be an important carrier for antimicrobial additives used in ultrafine powder coating surfaces. In this study, the exploitation of the ion exchange potential of chabazite was investigated using pre-treatment and chemical conditioning. Zeolites have been tailored into suitable carrier for important antimicrobial application by applying suitable combinations of ion exchange, and chemical modification with thermal and mechanical treatments. The present work provides basic information about chabazite, which includes chemical composition, the effect of different factors on ion exchange during conditioning and the thermal stability including their uses as an antimicrobial additive.

4.3 Materials and Reagents

Two natural zeolites used in this study, named as LBN and LBC were obtained from Zeox Corporation, Cortaro, AZ (particle size, around 10 micron). Among them, LBN was a Na^+ enriched natural zeolite and LBC was a combination of Na^+ and Ca^+ ions with other

cations. All chemicals used in this study were analytical grade reagents. Deionized (DI) water was used in all experiments.

Test microorganism: *Escherichia coli* strain, ATCC 35339 was purchased from the American Type Culture Collection (ATCC). This strain of bacteria was used for all antimicrobial testing purposes throughout the research. *Escherichia coli* are gram negative, rod shaped, and facultative anaerobic bacterium. *E. coli* are predominantly used as test microorganisms for most disinfection studies.

Revival: The *Escherichia coli* strain was received in frozen pellet form and was revived immediately. The propagation procedure used to revive the bacteria from the frozen pellet form into usable and sustainable colonies is outlined in chapter 3.

4.4 Methods

4.4.1 Pre-treatment and conditioning:

An experimental approach was developed for the pre-treatment and conditioning process of chabazite for enhancing ion-exchange capacity and selectivity for certain cations.

A. Pre-treatment process:

An experimental approach was developed for the pre-treatment and conditioning process of chabazite for enhancing ion-exchange capacity and selectivity for certain cations. Purpose of pre-treatment was to remove impurities and some undesirable cations from natural zeolite to make it easily accessible for desired cation. Removal of impurities from natural zeolites by washing with DI water with sonication and continuous magnetic

stirring at 60^{o}C was the main step for pre-treatment process. Magnetic stirring and sonication helped to break the agglomerate of zeolite and promoted the water penetration into the pores of the zeolite.

25 g of each zeolite was soaked with 500 ml of DI water and stirred for 1 hr at 400 rpm at 60^{0}C and then sonicated for 1 hr followed by 1 hr of stirring at 400 rpm at 60^{0}C followed by 1 hr of sonication again. Finally the mixture was stirred for 24 hrs at the same conditions. The mixture was centrifuged for 25 min at 3500 rpm and was again washed following the same procedure as before, but this time with only 1 hr of sonication.

B. Conditioning of pre-treated chabazite with $NaNO_3$ or NaCl:

Conditioning of the samples is necessary to make the particular zeolite compatible for particular application. It was done to enhance the ion exchange capacity of the material by replacing exchangeable cations in chabazite with a single cation (sodium). Sodium chloride and sodium nitrate were selected as a source of sodium for the conditioning treatment. 1M of 500 ml solution of each sodium salt, made up from analytical grade chloride and nitrate salts of sodium that were dissolved into deionized water, was used for conditioning the zeolite. Constant magnetic stirring up to 24 hrs with 1 hr sonication and 60^{o}C were the selected parameter for this process. Sodium hydroxides were added in dilute form to raise the solution pH 11 to expedite conversion of the zeolite to the particular cationic form. The mixture was centrifuged for 25 min at 3500 rpm and followed by treating the mixture in the same procedure as before. At every step pH was measured to check the changes in its values in the mixture.

C. Washing with DI water

Excess sodium cations and nitrate or chloride ions were removed by washing the zeolites with DI water followed by the confirmation test. Presence of chloride ions was checked by the precipitation method with silver nitrate in presence of nitric acid. Nitrate ions were checked by the brown ring test, which was done by the addition of iron (ii) sulfate followed by the addition of concentrate sulfuric acid. A brown ring will form between the two layers and will confirm the presence of nitrate.

4.4.2 Functionalization of conditioned chabazite

Silver nitrate and copper nitrate salts were used to functionalize the conditioned zeolite samples. Silver loading of the zeolite was conducted in dark to avoid the photo-oxidation of silver [30]. A series of conditioned zeolite samples were stirred at 500 rpm in 500 ml of 0.05M $AgNO_3$ solution covered with aluminum foil, at a constant temperature of 60^oC for 24 to 48 hours. The pH of each solution was adjusted to 4-4.5 with the addition of HNO_3. Solid and liquid phases were separated by centrifuging at 3500 rpm for 25 min. Solid phase samples were washed several times with deionized water to ensure presence of chemisorbed ions only within the zeolite particles. 0.1M NaCl suspension in water was used to identify any ionic silver species in the supernatant fluid after centrifuging and washing. During functionalization, 0.05M $Cu(NO_3)_2$ solution was also mixed with the conditioned zeolites at different time for optimizing the maximum amount of silver and copper in zeolite. All functionalized samples were dried at 80^oC for 5-6 hrs in the dark condition. After sufficient drying, the particles which was called as additive were easily

broken down into their initial respective particle sizes by a small grinder and preserve in the dark container to avoid oxidation.

4.4.3 Surface preparation

A. Powder preparation

Antimicrobial additives could be incorporated to the polyester resin system by dry blending at different ratio. The detailed method was described in chapter 3.

B. Powder Application

Equal amount of powder was applied on the substrate to have uniform thickness of coating after the curing process for maintaining the constant thickness (45-55 micron) of the coating. Detail powder application procedure was mentioned in chapter 3.

4.5 Analysis

XRF: The elemental composition of zeolites used in this work was determined by X-ray fluorescence technique (XRF) using a PANalytical PW-2400 Wavelength Dispersive X-ray Spectrometer. The samples went under a Borate fusion process prior to analysis and the chemical compositions are reported as weight percentages.

Particle size analyzer: The particle sizes of the processed resin powder and functionalized zeolites were measured with (BT-9300S, Better Baite Instruments) Laser Particle Size Analyzer as per the ASTM Standard D5861.

ICP-OES: Elemental analysis of the zeolite samples was performed before and after conditioning to verify the effect of conditioning and to find out the possibilities for further improvement of conditioning steps by using ICP-OES (Varian Vista Pro Axial ICP). Digestion of zeolites was done according to the ASTM standard D7442-08a. All experiments were performed in triplicate and the mean value is reported as final results.

Cation exchange capacity: The cation exchange capacity (CEC) is an important parameter for zeolite to determine its efficiency for different applications. The amount of loosely bonded cations of alkali and alkaline earth metals are known as exchangeable cations in zeolites. Due to the concentration gradient these cations are easily exchanged when zeolites are kept in contact with saturated solution. The method of ammonium acetate saturation is commonly used to determine the CEC of finely grounded materials [31]. This analysis consists of four major steps: (1) sample preparation, (2) saturation of zeolite with 1 N NH_4AOc neutral solution, (3) release of NH_4^+ ions through washing with NaCl solution, which converts the NH_4^+ into NH_3 and (4) measurement of NH_3 produced in Kjeldahl apparatus. CECs of raw and conditioned chabazites were determined to evaluate the conditioning treatment.

XRD: X-ray powdered diffraction was conducted using a MiniFlex (Rigaku Corporation, Japan) to confirm the crystallinity of zeolite before and after the ion exchange process. The XRD spectra were collected on a powder diffractometer using radiation at 30 kV and 15 mA. The scans were run from 5°-60° (2θ degree), increasing at a step size of 0.05° and maintaining a counting time of 2 sec. Data were processed using the MDI-jade version 7.0 software for the calculation of crystallinity.

Thermo gravimetric analysis (TGA): To know the degradation characteristics of chabazite at their natural form and after functionalization as well as after inclusion within the resin system, thermo gravimetric analysis (TGA) of the samples was performed at a heating rate of 10^0C/min interval from 0 to 600^{o}C under nitrogen purge (40ml/min) using a Mettler Toledo instrument (Switzerland). Thermo Gravimetric and derivative of thermo gravimetric (DTGA) curves of the chabazite showed the weight loss during heating. DTGA curve was used to detect inflection point of the thermal event and the correct temperature, at which the water evaporation took place.

Transfer efficiency of additive: Additives, which are added to the resin system, may change in concentration during electrostatic spraying due to variations in the charge distribution. Additive concentration was determined using the ASTM D5630-06 Standard Test Method [32]. Powder was collected from the panel after spraying the antimicrobial powder on the panel, which is called as the transferred powder. This powder was heated at 550°C in a ceramic crucible for 90 minutes to remove all combustible materials from the powder, leaving behind the non-combustible material as a form of ash. The amount of ash was then used to calculate the actual additive concentration on the panel.

Color determination: Colorimeter readings were measured with Datacolor 110 for color determination of all panels made for the antimicrobial analysis. The color of the coated surface is expressed in terms of brightness DL, redness Da, yellowness Db and the overall difference DE from the control surface.

Leaching test: Coated surfaces were immersed in DI water for 8 weeks in the individual closed container with occasional mild oscillation for measuring the readily leached out silver ion concentration. Three samples were collected every week. Panels were washed with fresh DI water, dried and then stored for antimicrobial analysis and the solutions were analyzed by ICP-OES for the detection of silver ion concentration. Another set of coated surfaces was immersed into 0.01M $NaNO_3$ solution for 7 days to check the leaching rate of silver ions in presence of counter ions. In order to have uniform concentration and to prevent silver ion agglomeration in the panel, the solutions were homogenized by shaking the container before the withdrawal of the analyte and the surfaces.

Anti-microbial analysis: American Society for Testing and Materials (ASTM) E2180-07 standard test method was used to determine the activity of incorporated antimicrobial agent(s) against microorganism in powder coated surfaces. Antimicrobial efficacy tests were conducted by coated surface with polyester resin containing functionalized zeolite (ion exchanged by 0.05M silver nitrate and 0.05 M copper nitrate for 24 hrs). Repeated tests were conducted with the same coated surface after washing with liquid soap and water. Chips were cleaned by ethyl alcohol before exposure with microorganism. A control sample was used for the efficacy tests. All experiments were run 3 times and mean values are reported.

Bactericidal effect (Membrane Integrity/LDH Leakage): To evaluate the toxicity produced from the coated surfaces against microorganism, measurements of lactate dehydrogenase (LDH), released from damaged or destroyed cells in the surrounding

medium at different times and trials were measured by using the CytoTox-ONE^{TM} assay. Membrane Integrity was evaluated by measuring the extracellular lactate dehydrogenase (LDH) according to the procedures mentioned in the CytoTox-ONE Homogenous Assay kit. It is a fluorometric method for estimating the nonviable cells remain depend on the amount of released LDH. Amount of fluorescence produced is proportional to the number of lysed cells using a 96-well format. Excitation and emission wavelengths of 560 and 590 nm, respectively were used to measure the fluorescence with an Epoch, BioTek fluorescent microplate reader (Software is GEN2.0). Toxicity values of the control coated surfaces (additive without active agents, Ag^{+}/ AgNP/ Cu^{2+}) were considered as 100% and toxicity of the antimicrobial coated surfaces (additive with Ag^{+}/ AgNP/ Cu^{2+}) were measured as percentages of the control at different exposure of time. The expressed data are the mean values from three independent experimental results. Finally LDH was measured for the 15 times used coated surfaces after 24 hrs. of exposure time.

The same coated surface was used repeatedly called as 'trial' to check the efficiency against microorganisms. It is to be noted that the aforesaid coated surface was cleaned with soap and water and dried before every use.

4.6 Results and Discussion

4.6.1 Elemental analysis of two natural zeolites (chabazite) by x-ray fluorescence (XRF)

Chemical composition of raw zeolite and its conversion rate to a homo-ionic form are the two important parameters for evaluating the ion-exchange behavior of any natural zeolite.

The results of XRF analysis of the natural zeolites are shown in Table 1. XRF analysis was conducted to determine the Si content, which is difficult to determine by ICP-OES. Alumina content is the active negative charge of the zeolite structure, which is the indicator for total charge of the exchangeable cations. Chabazite has a low alkali content as shown in Table 1 on a wt. % basis in terms of respective oxides of sodium, potassium, calcium, magnesium and others cations present in the zeolite. The structure with high Si/Al ratio (>4) is more stable in low pH environments but in contrast, low Si/Al ratio has better hydrophilic properties [33], which is the required property for antimicrobial application. The chemical composition of LBC and LBN reveals that although both have good ion exchange capability, pre-treatment and chemical conditioning can improve their ion exchange property to some extent by replacing other monovalent and divalent cations present in the structure with easily exchangeable one from the surrounding medium. LBN contains more Na^+ in its natural state, so it has a better ion exchange capacity than LBC and its Si/Al ratio is less than LBC, which is also another indication for ion exchange capacity. More Na^+ can be accommodated easily within the zeolite by replacing the other monovalent and divalent cations through the conditioning process from the liquid media

Table 4.1: The main mineral constituents of two natural zeolites (chabazite) according to the XRF analysis, shown as % w/w content of mineral oxides and the corresponding bulk Si/Al ratios

Samples	SiO_2	TiO_2	Al_2O_3	Fe_2O_3	MgO	CaO	K_2O	Na_2O	SiO_2/Al_2O_3 ratio
LBC	54.24	0.27	12.9	3.76	1.56	1.65	1.13	5.02	4.20
LBN	52.79	0.12	13.4	2.98	0.828	0.959	1.15	7.69	3.94

which is rich in sodium cation. The XRF results shown in Table 4.1, indicate that Si/Al ratio of LBN (3.94) is lower than LBC (4.20), so LBN has a better ion exchange capability than LBC. As well, the sodium content of LBN is higher (i.e., 7.69) than LBC (i.e. 5.02). Cation content of zeolite depends on the electro negativity of the zeolite structure, which is related to the alumina content. High alumina content indicates high cations content as well as high ion exchange capacity. There are some other cations present in both zeolites, which can be replaced to some extent by sodium cations. Sodium is the most easily exchangeable cation, so after making zeolite into a near homo-ionic form, these zeolites can be used for further intended applications after making required changes.

4.6.2 Elemental analysis of two natural chabazites by Inductively Coupled Plasma Optical Emission Spectrometry (ICP-OES)

These two chabazites were ion exchanged with silver nitrate to make them silver-modified zeolites, which become a potential antimicrobial additive used for many different antimicrobial formulations. ICP-OES elemental analysis of these two zeolites before and after ion exchange with 0.05M silver nitrate is shown in Table 4.2. After the ion exchange with silver nitrate, LBN shows higher silver content than LBC as shown in Table 4.2. The presence of high alumina in LBN (from XRF analysis, Table 4.1) indicates the higher ion exchange capability which is also evident from the data.

Both analyses showed that the LBN zeolite contains more sodium cation, which can be replaced easily with any other cations having the same charge as well as any other divalent or trivalent cations during the ion exchange process. The balancing cations do

not occupy fixed positions and move within the channels of the lattice. Thus the framework charge of zeolites is not localized, which forms an electric field [37]. This electric field influences the exchange process despite partial or complete exchange of its balancing cations. The total charge of the removable cations is equivalent to the active charge of the frame work or the zeolite lattice.

Table 4.2: Elemental analysis (milli equivalent) of natural zeolites (LBC, LBN) before and after ion- exchange with 0.05M $AgNO_3$ and 0.05M $Cu(NO_3)_2$ according to ICP-OES analysis

Samples	Ag	Na	Ca	Fe	K	Mg	Pb	Cu
LBC[a]	0.00	1.988	0.40	1.81	0.188	0.92	0.0113	0.001
LBC[b]	0.82	0.591	0.29	1.80	0.186	0.69	0.0003	0.0007
LBC[c]	0.79	0.334	0.21	1.77	0.179	0.51	0.0001	0.681
LBN[d]	0.00	2.83	0.205	1.50	0.205	0.26	0.0115	0.00016
LBN[e]	1.03	1.10	0.183	1.50	0.198	0.09	0.0003	0.00018
LBN[f]	0.97	0.62	0.132	1.40	0.176	0.08	0.0003	0.733

[a]Raw LBC, [b]Ion exchanged LBC with 0.05M $AgNO_3$ for 24 hrs [c]Ion exchanged LBC with 0.05M $AgNO_3$ (24hrs) then 0.05M $Cu(NO_3)_2$(24hrs) [d]Raw LBN [e]Ion exchanged LBN with 0.05M $AgNO_3$ for 24 hrs. [f]Ion exchanged LBN with 0.05M $AgNO_3$(24 hrs) then 0.05M $Cu(NO_3)_2$(24 hrs)

Cations present within the zeolite are bonded with oxygen by electrostatic interaction and the strength of interaction depends on solvation sphere [34]. Electrostatic attraction of sodium ion is far less than any other cations present in the zeolite. Due to the concentration gradient, silver from the surrounding medium can easily replace the sodium cation in the frame through diffusion process. As a result, the silver present after the ion

exchange in LBN is higher than LBC, the most desirable parameter for making the antimicrobial additives.

ICP-OES analysis showed that both zeolites have potential ion exchange capability, which can be improved by converting those into near a homo-ionic form. Chemical conditioning is the only process to make the natural zeolite more compatible for enhanced ion exchange with desirable cations by replacing the exchangeable cations for particular end use. Among the other alkaline cations, sodium is the most weekly bonded cation which can easily be replaced [36]. A pre exchange process with high Na^+ content solution can remove some other exchangeable cations from the natural zeolites, hence helping them to improve their cation exchange capacity to some extent. An experimental approach was developed to evaluate the pre-treatment process upon the exchange capacity and selectivity for certain cations. This pre-treatment process can remove certain cations (impurities) from zeolites that may have slowed down the ion exchange process while exposing the most exchangeable ones. Water washing is the most effective way to remove the impurities present in the zeolite. Different forms of sodium salt is the best option for this conditioning process, but based upon the end use of zeolites as additives, we need to select the salt of sodium. If sodium chloride is used during conditioning, the complete removal of chloride ion from zeolite after this conditioning process is very difficult as the residue can precipitate as silver chloride during ion exchange.

Change of sodium content during treatment and conditioning of zeolite LBC and zeolite LBN at every step is shown in Table 3. Although the change of sodium content in LBC (1.15 milli eq.) is higher than LBN (0.912 milli eq.), the ultimate amount of sodium is

Table 4.3: Change of sodium content during different steps of pre-treatment and conditioning of chabazites with sodium nitrate.

Treatment	Chabazite, LBC		Chabazite, LBN	
	Sodium, milli eq	% RSD	Sodium, milli eq	% RSD
Raw Chabazite	1.99±0.043	2.14	2.83±0.075	2.67
Water washed	2.11±0.023	1.11	3.09±0.032	1.04
Conditioned with 1M $NaNO_3$	3.14±0.064	2.04	3.78±0.036	0.95
1st Water washed	2.95±0.070	2.38	3.46±0.040	1.17
2nd Water washed	2.67±0.100	3.75	3.17±0.089	2.83
3rd Water washed	2.56±0.125	4.88	3.12±0.055	1.78
2nd conditioned with 1M $NaNO_3$	4.10±0.090	2.20	4.39±0.040	0.91
1st Water washed	3.42±0.186	5.46	4.06±0.050	1.24
2nd Water washed	3.25±0.140	4.31	3.84±0.040	1.04
3rd Water washed	3.15±0.105	3.35	3.81±0.072	1.92

higher in LBN. As such, these cations (Na^+) are better available in LBN for exchange with other external cations, which is the desirable characteristic for this conditioning process and is the important pathway to obtain more efficient additive for the intended use of zeolites. It should be noted that sodium content after conditioning with sodium chloride or with sodium nitrate used for this process is almost the same for both zeolites. There is also an increase in sodium content after 2nd conditioning with $NaNO_3$.

Mechanical treatments applied during this process also helped to accelerate the ion exchange process, which was observed at the cation exchange capacity determination.

Change of molar ratio after conditioning between sodium and aluminium in these two natural zeolites is another indicator for the improvement of ion exchange capacity as shown in Figure 1. Cation holding capacity of zeolite depends on alumina content. Although the conditioning process applied for these zeolites has enhanced the molar ratio of these elements, the results show that there is further possibility to enhance the sodium content. The molar ratio of Na/Al in LBC and LBN after conditioning reached approximately 0.71 and 0.8 respectively as shown in Figure 4.1. Molar ratio of Na/Al for LBN is comparatively higher than LBC after conditioning, but the change of molar ratio is greater for LBC after conditioning. There is a possibility of increasing the molar ratio further, but the remaining cations present in the zeolite are strongly electro statically bonded within the structure of the material, which would require some stronger treatment to detach the cation from the zeolite [6]. The theoretical ion exchange capacity is always higher than the real exchange capacity, which is another reason for not obtaining Na/Al molar ratio near to 1. Strongly bonded cations are part of the material's impurities, as such, these are not exchangeable cations [37]. Paired t-test analysis showed that there is a significant difference between raw and conditioned chabazite (Appendix, table 4).

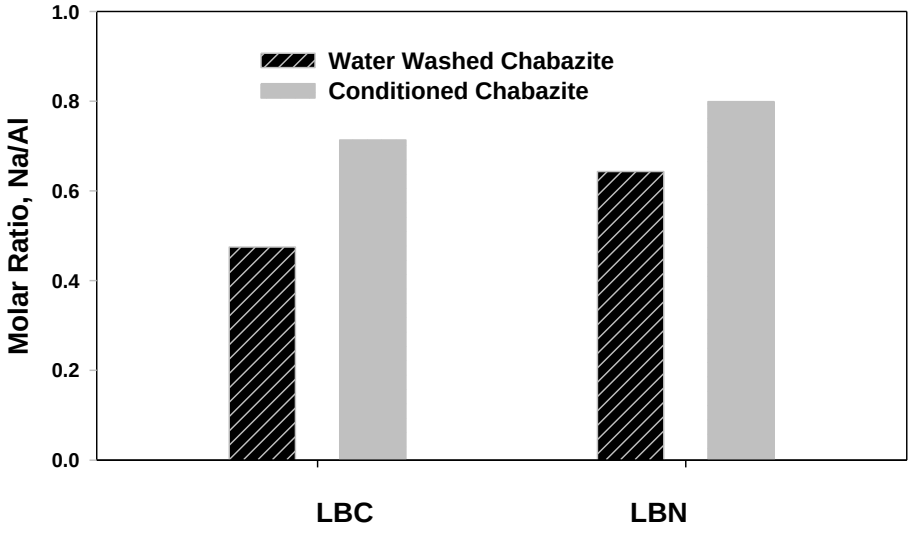

Figure 4.1: Change of Na/Al molar ratio after conditioning

4.6.3 Cation exchange capacity (CEC)

CEC of the raw and conditioned zeolites were determined to evaluate the effect of the treatment. Figure 4.2 shows CEC values for two zeolites at different steps during conditioning. Zeolites are rarely found in nature in pure form. Different frameworks cation compositions and associated minerals of different natural zeolites have diverse CEC. Naturally occurring zeolites are contaminated by different levels of other minerals, such as metals, quartz, clays and also by other zeolites. Removal or lowering of impurity content helps to improve the CEC of the zeolites. Probably, exchangeable ions in such unwanted materials do not necessarily participate in the ion exchange process; rather they may additionally block the active sites. Water washing is the best and easiest method to remove the impurities from natural zeolites. In our analysis we also found better CEC from the washed chabazites than their raw forms.

The intention was to replace some cations by a certain cation from these chabazites to make a near homo--ionic form. A pre-exchange process with solutions containing sodium ions can remove detrimental exchangeable cations from the chabazite and can improve its CEC significantly. Conditioning with sodium chloride or sodium nitrate with the help of some mechanical treatment, such as elevated temperature (60^{o}C) and sonication (2 hrs), as well as lowering pH, helps zeolites to convert into a near homo-ionic form. pH and temperature are critical parameters for natural zeolite during the ion exchange process. Low pH (~5) helps to avoid the precipitation of silver, but too low pH would

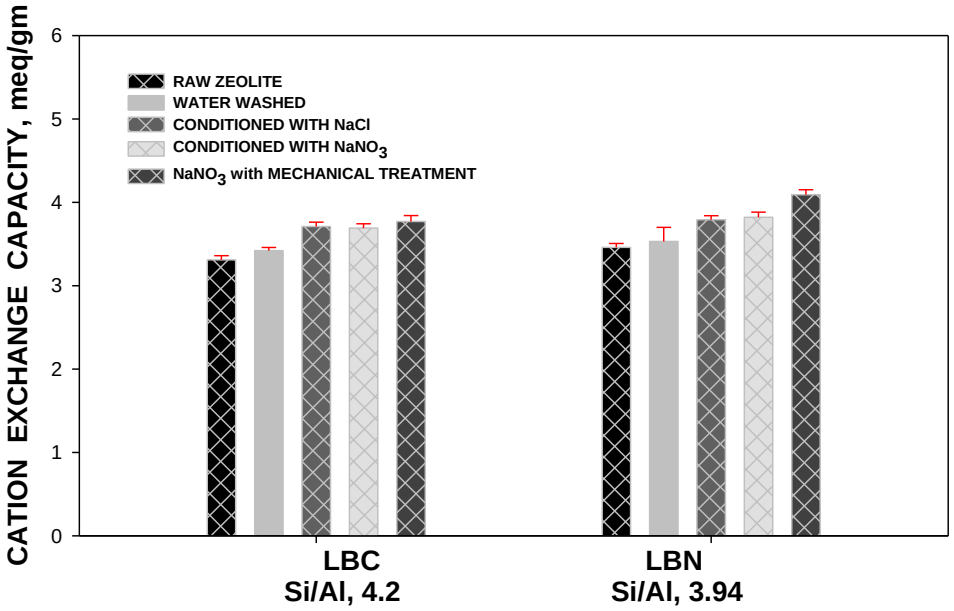

Figure 4.2: Cation exchange capacity of two raw natural chabazite (LBC, LBN) in comparison to the different conditioned samples

increase the H^{+} and H^{+} will compete with other cations. Elevated temperature helps the cations to move through the diffusion process which is present inside the zeolites and the medium. Diffusion process is the result of the concentration gradient of cations present

between phases. The existing concentration differences were balanced through ion exchange and gradually the equilibrium is established. During the diffusion process, a non-localized electric field is formed in the frame work, which influences the exchanging process [37]. There was a decrease in hydration of exchangeable cations, which eased the movement within the pore of the zeolites at elevated temperature. Sonication and elevated temperature helped to disperse the zeolite within the solution properly and improved the mobility of the cations respectively. Change of CEC for high sodium containing zeolite (LBN) was higher than the low sodium containing zeolite (LBC) and the difference of CEC between these two were 0.17 meq/g (Figure 4.2). Elemental analysis was conducted done with ICP-OES (Tables 4.4 and 4.5) of these conditioned zeolites, these were also related with their higher CEC. However determination of the real exchange capacity is difficult as the natural zeolites contain several impurities contributing to high experimental error and causing low accuracy. In few cases, some metals are reported to have adsorbed or precipitated on the surface [37].

4.6.4 Functionalization of conditioned zeolites

The main objective of functionalizing with silver and copper was to develop a durable additive for antimicrobial applications. Functionalization was conducted with 0.05M $AgNO_3$, followed by 0.05M $Cu(NO_3)_2$ mainly by the replacement of sodium ions from conditioned zeolites. Different mechanical and chemical properties, such as solid/liquid ratio, pH and temperature, agitation and magnetic stirring, can influence the ion exchange equilibrium and the cationic concentration. Sorption of different cations occurs through surface precipitation, ion exchange on internal and external surfaces and also by

molecular sieve processes [38]. Tables 4.4 and 4.5 show the different cation contents of chabazite before and after the treatment with $AgNO_3$ and $Cu(NO_3)_2$. Sodium cation plays an important role during functionalization. It helps these incoming cations (i.e. Ag, Cu) to settle down within the zeolite frame work as a guest. The highest decline of sodium content from the raw zeolite was observed in case of both the zeolites. But on the other hand, the silver and copper ion content increased during the ion exchange process marking them the main notable exchanges. Nevertheless, in the case of calcium-enriched zeolite LBC, the change in calcium ions was observed during functionalization. This suggests that the calcium is a potential exchangeable cation in chabazite too.

Table 4.4: Elemental analysis (milli eq) of LBC during pre-treatment and conditioning process with different orders of addition of silver (Ag) and copper (Cu)

Samples	Ag	Na	Ca	Fe	K	Mg	Pb	Cu
Raw LBC [a]	0.00	1.99	0.40	1.81	0.19	0.92	0.011	0.001
Washed LBC [b]	0.00	2.11	0.46	2.19	0.24	1.09	0.012	0.002
Conditioned LBC [c]	0.00	3.15	0.09	1.55	0.12	0.75	0.003	0.001
Functionalized LBC [d]	1.14	1.36	0.09	1.39	0.11	0.65	0.003	0.001
Functionalized LBC [e]	1.12	0.89	0.06	1.39	0.10	0.49	0.002	0.95
Functionalized LBC [f]	0.93	0.82	0.09	1.43	0.11	0.53	0.002	1.010
Functionalized LBC [g]	1.07	0.71	0.07	1.30	0.10	0.49	0.002	1.180

[a] Raw LBC, [b] 2 times water washed LBC, [c] Washed LBC conditioned 2 times with $NaNO_3$, [d] Conditioned LBC functionalized with 0.05M $AgNO_3$, 24 hrs [e] Functionalized conditioned LBC with 0.05M $AgNO_3$, 24 hrs 0.05M $Cu(NO_3)_2$ for another 24 hrs, [f] Functionalized conditioned LBC with 0.05M$AgNO_3$, 0.05M $Cu(NO_3)_2$ together, 24 hrs, [g] Functionalized conditioned LBC with 0.05M$AgNO_3$, 0.05M $Cu(NO_3)_2$ together, 48 hrs

Based upon the composition of silver and copper along with ion exchange time the functionalization parameters were optimized. Chabazite has low Si/Al ratio, that means a high anionic field, which showed good selectivity towards cations with higher charge density (e.g., copper) and poor selectivity towards lower charge cations (e.g., silver). Silver has a higher ionic radius (1.13 Å) than sodium (0.98Å) which has some effect for selectivity towards zeolite [39].

Table 4.5: Elemental analysis (milli eq) of LBN during conditioning with different orders of addition of silver (Ag) and copper (Cu)

Samples	Ag	Na	Ca	Fe	K	Mg	Pb	Cu
Raw LBN [a]	0.00	2.83	0.205	1.50	0.205	0.26	0.011	0.0002
Washed LBN [b]	0.00	3.09	0.30	1.53	0.25	0.3	0.012	0.0002
Conditioned LBN [c]	0.00	3.81	0.1	1.89	0.12	0.29	0.007	0.0006
Functionalized LBN [d]	1.144	1.86	0.07	1.55	0.10	0.27	0.004	0.0005
Functionalized LBN [e]	1.130	0.99	0.04	1.00	0.09	0.26	0.003	1.090
Functionalized LBN [f]	1.116	1.42	0.04	1.09	0.01	0.27	0.003	0.980
Functionalized LBN [g]	1.097	1.04	0.035	1.002	0.09	0.26	0.003	1.280

[a] Raw LBN, [b] 2 times water washed LBN, [c] Washed LBN conditioned 2 times with $NaNO_3$, [d] Conditioned LBN functionalized with 0.05M $AgNO_3$, 24 hrs [e] Functionalized conditioned LBN with 0.05M $AgNO_3$, 24 hrs 0.05M $Cu(NO_3)_2$ for another 24 hrs, [f] Functionalized conditioned LBN with 0.05M$AgNO_3$, 0.05M $Cu(NO_3)_2$ together, 24 hrs, [g] Functionalized conditioned LBN with 0.05M$AgNO_3$, 0.05M $Cu(NO_3)_2$ together, 48 hrs

Higher amount of copper compared to silver was found in both chabazites after ion exchange with silver nitrate and copper nitrate combined, for 24 and 48 hrs. As the number of cations integrated within the zeolite increased, stability of the cation was

weakened due to the change of inter cationic repulsion and possibly a reduction of hosting cations. Selectivity of divalent cations decreased due to the Coulombic force, which is also proportional to the charge of the cation [38].

4.6.5 X-ray Powdered Diffraction (XRD)

XRD is one of the appropriate analyzing tools to detect internal change in zeolite lattice after any treatment. No significant alterations in the crystalline phase occurred when compared with the XRD patterns of original or raw chabazite. Peak intensity emerged without any shift from the standard chabazite for both cases. As shown in Figure 4.3 and 4.4, some of the XRD peak intensities of functionalized zeolites have decreased slightly relatively to the raw zeolites. This is due to the change in different charge distribution among the conditioned zeolites and the electrostatic fields that occurred when sodium ions were replaced by silver and copper ions. Some researchers reported that replacement of sodium ions (ionic radius 0.98Å) from Na-zeolite Y with higher ionic radius (1.13Å) silver ions changes the (311) surface of the lattice [40].

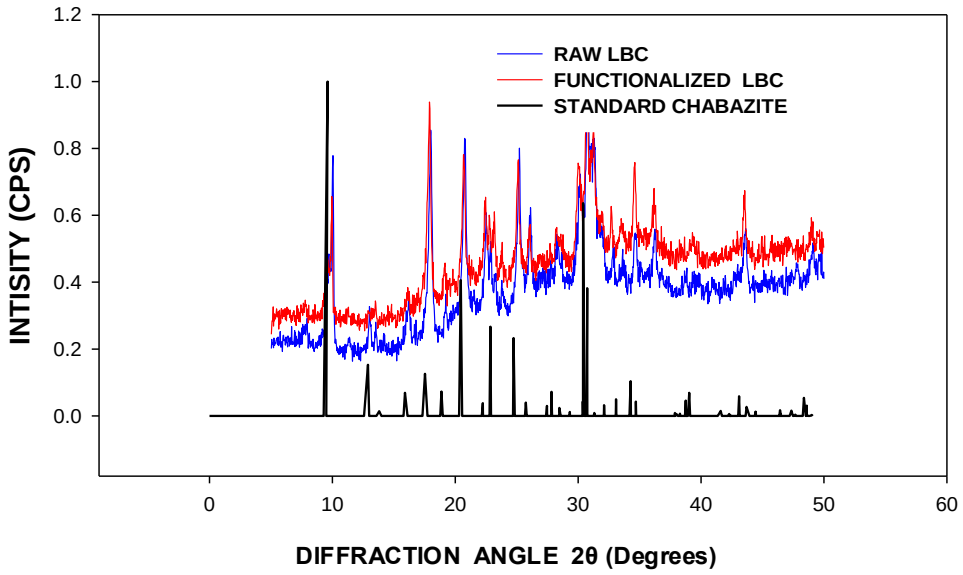

Figure 4.3: XRD patterns of Chabazite, LBC before and after functionalization

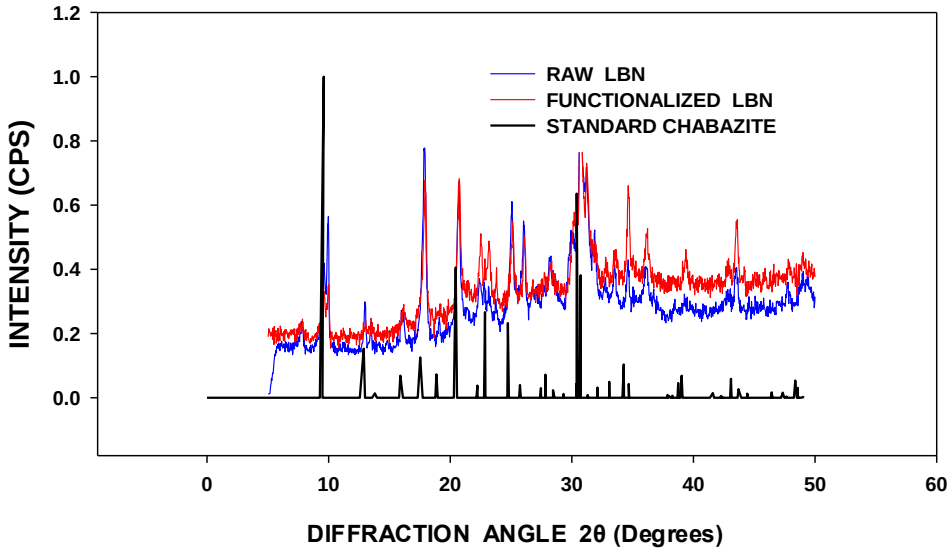

Figure 4.4: XRD patterns of Chabazite, LBN before and after functionalization

Sodium enriched conditioned chabazites were used for ion exchange with silver and copper ions (ionic radius 0.78Å) causing some internal changes in the zeolite, hence the intensity. But no remarkable changes were observed in the XRD of functionalized chabazites from the raw zeolites.

4.6.6 TGA and DTGA

The thermos-gravimetric analysis of the raw and functionalized chabazites is illustrated in Figures 4.5 and 4.6, respectively. The TGA curves of all samples presented in Figure 4.5 shows that, depending on the chemical composition of the chabazite sample, continuous and smooth dehydration started approximately at 36^{o}C and the maximum weight loss (15.5-17.2%) occurred between 280-350^{o}C followed by complete dehydration at about 480-500^{o}C [41]. The relative data of thermal analysis are shown in Table 4.6. Continuous loss of water with increasing temperature was observed in the thermos-grams. Water content under any static condition, depends on temperature and dehydration is reversible. Exchangeable cations present in the channels coordinated with water may move to different sites or other positions of coordination during dehydration process.

Channels and interconnected voids in the zeolite framework are occupied by cations and water. The net negative charge of the zeolite framework is due to the presence of Al^{3+} ions, which is balanced by cations. Higher negative charge density of the frame tends to produce stronger interactions with the dipoles of water molecules. Accordingly, loss of water from raw LBN (13.4% Al) seemed to be lower than raw LBC (12.9% Al). As such,

according to the TGA analysis, the weight loss for raw LBN was 15.64% and for raw LBC it was 17.17%, respectively. Raw chabazite (especially LBC) showed higher weight loss compared to the functionalized chabazite due to the presence of higher water content.

It is known that the acidity increases with the decrease of Si/Al ratio. The increased acidity is the result of higher aluminum present in the zeolite framework. The higher the ratio of Si/Al, the more the cluster is destabilized. If the sample shows more weight loss then it is considered more sensitive to desorption [42]. The Si/Al ratio of LBC (4.2) was slightly higher than LBN (3.9) according to the XRF analysis which was also mentioned in Table 4.1.

However, conditioning and functionalization are anticipated to improve the desorption level, which was found in this study by the TGA analysis as shown in Table 4.6. Functionalization of chabazite was conducted by the ion exchange of silver and copper cations by mainly replacing the sodium cation in conditioned chabazite. Of these two cations, this functionalized chabazite contains higher charged cations (Cu^{2+}) and higher ionic radius containing cation (Ag^{+}). After the cation replacement, the void space of functionalized chabazite was lower than the raw chabazite. Small divalent cations are more hydrated to displace the Na^{+} ions in conditioned chabazite. Literature shows that zeolitic water increases with the decrease of cationic radius in addition to increasing, the degree of exchange. The conditioning and functionalization process did not produce any substantial change in the topography of the framework structure of chabazite confirmed from XRD analysis shown in Figures 4.3 and 4.4. This process can undergo dehydration reversibly and continuously [41]. TGA curves for raw and functionalized zeolites were

similar and their water loss occurred at a wide range of temperatures as shown in Table 4.6. Substitution of sodium ions by silver and copper ions during functionalization

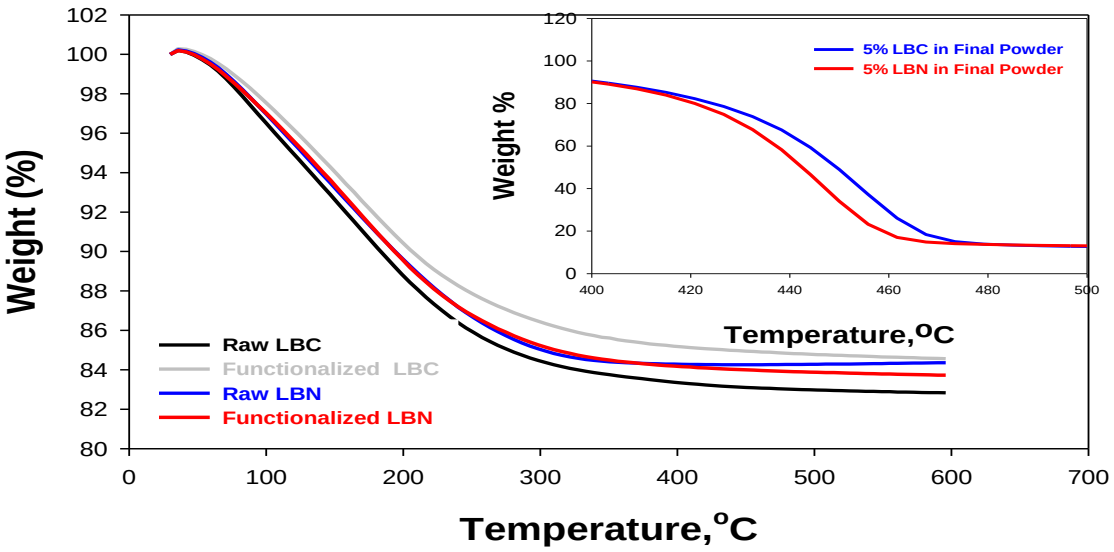

Figure 4.5: Thermo-gravimetric analysis of raw and functionalized zeolite

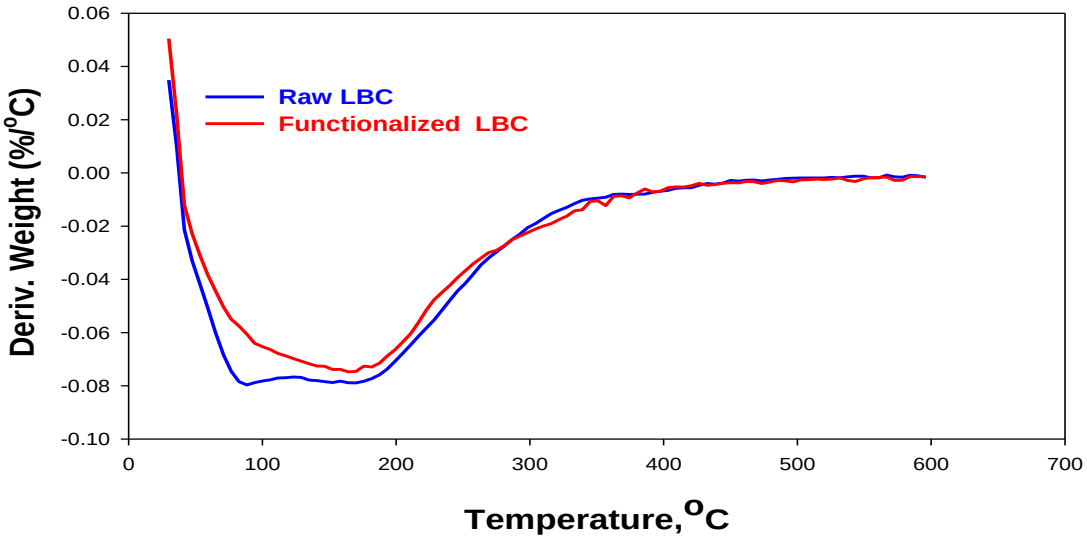

Figure 4.6: Derivatives of thermos-gravimetric analysis of raw and functionalized LBC

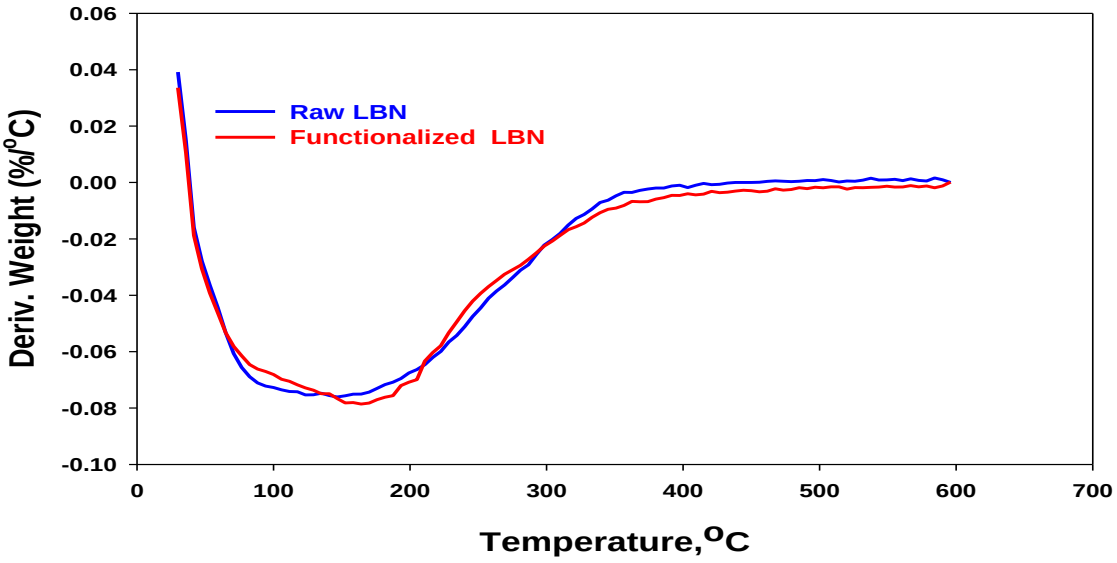

Figure 4.7: Derivatives of thermos-gravimetric analysis of raw and functionalized LBN

caused the energy homogenization of adsorption centers and smoothed out the differential curves. Hydroxyl groups coming from the water molecules are bonded with the strongly polarized cations. But simultaneously when the temperature was increased, the hydroxyls were destroyed and formed water, which in turn resulted in a very small change in weight loss at higher temperature. The dehydroxylation of zeolite was slowed and occurred around this temperature. It did not show a distinct weight loss in the TGA curve (only up to 1%).

Table 4.6: Weight loss (%) in TGA analysis for Chabazite

Sample	Peak Area	Dehydration Temperature range ,^{o}C	Optimum Dehydration Temperature, ^{o}C	Weight loss (%)
Raw LBC	17.51	36-298	152.5	17.17
Functionalized LBC	18.28	36-310	164.16	15.44
5% LBC in Final powder	81.04	339-514	455.83	88.24
Raw LBN	17.81	36-292	146.66	15.64
Functionalized LBN	17.14	36-310	164.16	16.28
5% LBN in Final powder	79.62	339-491	444.16	87.77

The TGA curves in Figure 4.5 correlated well with the DTGA profile shown in Figure 4.6 and 4.7. Maximum weight losses occurred at 280^{o}C for raw chabazites and at 280-350^{o}C for functionalized chabazites depending on the % of exchange of sodium ions during the treatment. Again, a slight weight loss occurred after 450^{o}C probably due to the dehydroxylation. The final powder containing 5% functionalized chabazite in polyester resin showed sudden weight loss (88%) at temperature 340-510^{o}C due to the decomposition of resin.

4.6.7 Transfer efficiency of additives

Transfer efficiency of additives, is the ratio of the additives deposited on the substrate to the quantity of the additives added to the final formulation. To maximize the efficiency of

the coating performance, improve productivity and to minimize the cost, the desired transfer efficiency should be as high as possible. The main parameter for effective transfer efficiency in electrostatic powder coating is the powder flow, which is heavily influenced by the airflow within the spray booth. Air flow can cause very fine particles to miss the target as well as decreasing the transfer efficiency. The air stream carries the particles from the gun, while the electric force pushes the particles on the substrate. Applied voltage controls the particle charge and their combination create the electric force, which needs to be stronger than the aerodynamic and gravitational force exerted on the particles [42]. Particle size is also another considering factor, higher particle size posses lower drag force. Drag force acts opposite motion relative to any surrounding moving object. The additives used in this formulation contain functionalized chabazites with average particle size 10 μm. Particle size helped to increase the transfer efficiency of the additive almost 85-87%.

4.6.8 Color analysis

The color of the surface is one of the most important parameter to determine the state of silver being present in the coating. Due to the reduction of silver ion to atomic silver, the color of the coating turns yellow. It is always desired that the silver present within the coated surface is in an ionic form, which can start functioning immediately against microorganism when needed. After functionalization, chabazites contains different cations such as sodium, calcium, silver, copper, iron, potassium, magnesium, etc. Transition metals like gold, silver, and copper are more electronegative than alkali metals

such as sodium, calcium, magnesium etc. Thus, these transition metals having high reduction potential can attract electrons easily compared to alkali metal ions. Due to the higher redox potential of silver ($Ag^{+} + e^{-} \rightarrow Ag$, 0.8) than copper ($Cu^{+2} + 2e^{-} \rightarrow Cu$, 0.34), copper can be reduced prior to silver and with ease. These two cations mainly occupy the surface of chabazites after functionalization, when the higher concentrations of corresponding salts were used during ion exchange. Copper reduces before silver and thereby prevents silver from reduction during curing at high temperature. This causes the color of the coated surface changed between yellow to transparent depending on the amount of copper present in the formulation. Other cations within chabazites also play

Table 4.7: Color analysis of the coated surface made with LBC containing additive

Parameters	Ion-exchange of Raw LBC with 0.05M $AgNO_3$	Ion-exchange of Raw LBC with 0.05M $AgNO_3$ and 0.05M $Cu(NO_3)_2$	Ion-exchange of conditioned LBC with 0.05M $AgNO_3$	Ion-exchange of conditioned LBC with 0.05M$AgNO_3$, 0.05M$Cu(NO_3)_2$
CIE DL	-3.54	-1.09	-8.63	-5.29
CIE Da	-0.56	-0.29	-2.1	-1.95
CIE Db	6.27	4.05	10.44	6.12
CIE DE	7.22	3.51	11.28	9.12

*Db= Yellowness, DE=Overall difference

certain role to prevent silver from reducing during the curing process. Tables 4.7 and 4.8 present the color of the surface made from LBC and LBN containing additives for different formulations. Values in Tables 4.7 and 4.8 represent the difference between the

sample and the standard for each of the three dimensions or axes and are expressed as negative or positive distances from the sample to the standard. Recall that the three colorimeter values 'DL', 'Da' and 'Db' those represent brightness, redness and yellowness respectively are all interrelated. The 'Db' values are more useful in terms of determining the reduction of silver in the coated surface.

These 'Db' values increased with the concentration of silver in zeolite after ion exchange because 'Db' has a tendency of changing color from yellow to blue and from light to dark with the increase of the concentration. Higher 'DL' values indicated the brightness of the sample and DE represented the overall difference from the standard. The sample which

Table 4.8: Color analysis of the coated surface made with LBN containing additive

Parameters	Ion-exchange of Raw LBN with 0.05M $AgNO_3$	Ion-exchange of Raw LBN with 0.05M $AgNO_3$ and 0.05M $Cu(NO_3)_2$	Ion-exchange of conditioned LBN with 0.05M $AgNO_3$	Ion-exchange of conditioned LBN with 0.05M $AgNO_3$ 0.05M$Cu(NO_3)_2$
CIE DL	-4.42	-1.27	-10.82	-6.34
CIE Da	-0.39	-0.23	-1.28	-0.09
CIE Db	7.80	4.93	10.39	5.28
CIE DE	7.61	3.09	10.74	8.08

*Db= Yellowness, DE=Overall difference

contains more silver (functionalized zeolites, shown in Table 4.4 and 4.5) showed more yellowness represented by 'Db' values than the raw zeolites containing additives. Copper helps to reduce the difference of yellowness as well as the overall difference from the standard surface in both cases.

4.6.9 Leaching Test

The silver ion concentration within the coated surface as well as its leaching rate determines its durability as an antimicrobial product. As the silver ion was introduced by ion exchange process into the zeolite, it would also come out from the zeolite by ion exchange process depending on the ionic strength of the media. Leaching would limit the durability of the coating's antimicrobial properties [43]. An amount of silver leached out into the $NaNO_3$ solution from the coated surface comprising LBN additives and was analyzed by ICP-OES shown in Figure 4.8. The leaching rate for the first 2 days was very high compared to the rate during the following 5 days. The higher rate at the earlier stage could be probably because of the abundant availability of the surface ions. It is known, that the zeolite with a low Si/Al ratio has a good hydrophilic property, thus more moisture could penetrate within the zeolite, and as such the cations migration becomes

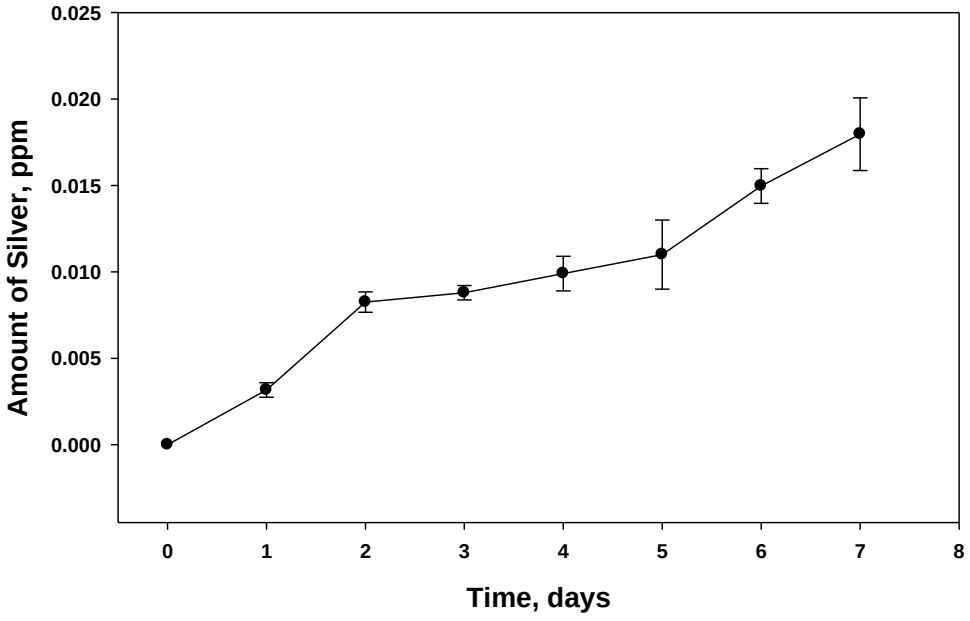

Figure 4.8: Leaching test of silver ion from the coated surfaces in presence of 0.01 M $NaNO_3$

more easier and faster in that condition. The reason behind the higher trend of silver leaching out from the coated surface at the end of the analysis (7th day) is most likely due to the hydrophilic characteristic of the zeolite. Tested surfaces were taken out from the leaching test chamber after a 7 day observation period and later used for the antimicrobial efficiency test. Figure 4.9 shows the analysis of the antimicrobial efficiency of the coated surface before and after the leaching test. It took 3 hrs to kill all the microorganisms in contrast to 2 hrs required for the un-leached surface. No remarkable difference between leached and un-leached coated surface was observed from the analysis. Another study showed that the amount of silver that leached out was around 20 ppm from silver nano

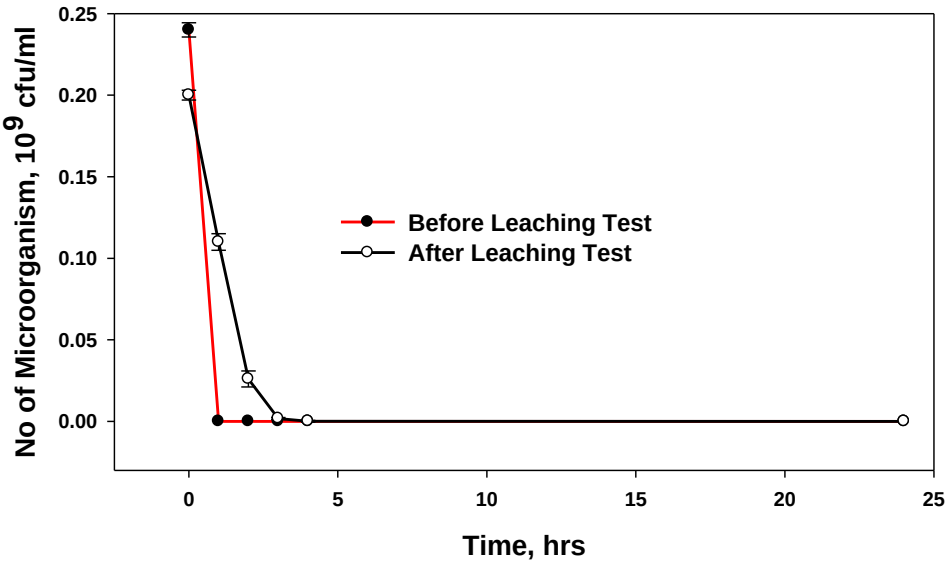

Figure 4.9: Antimicrobial efficiency before and after the Leaching test

particles containing the membrane exposed to the LB broth (which usually contains higher amount of minerals) for 48 hours under moderate shaking. When the same sample was exposed for 30 min for the second time, the amount of silver that leached out was 5.7ppm [44]. But these nanoparticles were not incorporated within any resin system. The main intention of the leaching test was to evaluate the upper limit of silver migration, measured in ppm level, upon exposure for a long time with cationic medium. From this analysis it can be concluded that the coated surface can act as a huge reservoir of silver.

4.6.10 Durability of coated surface against *E.coli*

The antimicrobial efficiency is dependent on the silver ion concentration, and the release of silver ion primarily depends on the ionic strength of the medium, which is again a media dependent ion exchange process [45, 41]. The continuous and controlled release of active component (silver ion) from the coated surface in the pathogenic environment is a critical factor for an antimicrobial product. To get an effective result, silver ions need to be released from the carrier material into an effected environment. Zeolite, used as the carrier material, enhances the water uptake properties resulting in the increased release of silver ion.

Whenever common environmental cations such as sodium, calcium or potassium are available in the effected environment, control release of silver ions from silver zeolite takes place. Silver release cannot commence unless another ion takes its place in the zeolite. Silver elutes from the zeolite in the presence of moisture, and until only the silver concentration reaches an equilibrium value. Silver does not release in dry condition and

similarly microorganism cannot survive without moisture. So the active material is not consumed when it is not required, thus the duration of antimicrobial efficacy is enhanced. Some research revealed that the silver ion can penetrate into the cells through ion channels of the cell membranes. The mechanism of action depends on their specific binding with the surface and electron donor groups or negatively charged components in protein and nucleic acids of biological molecules [46].

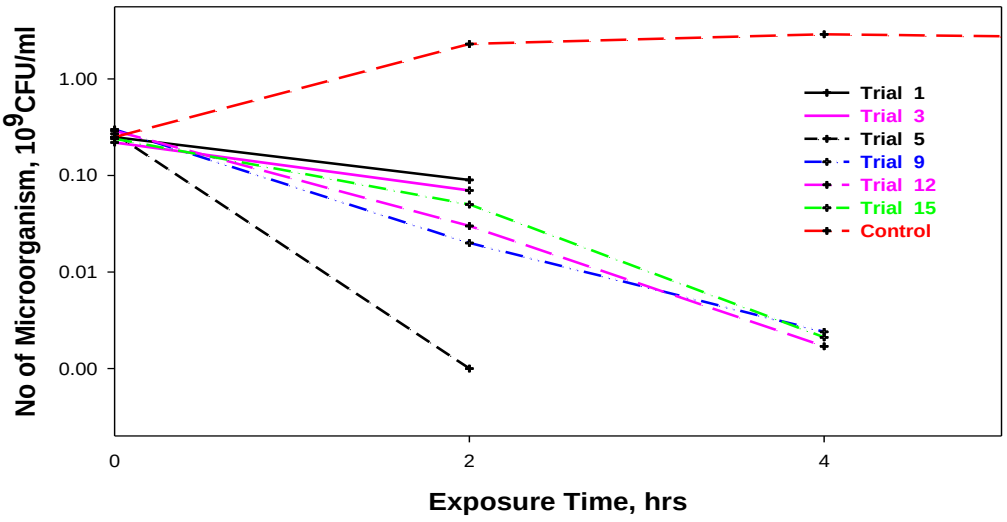

Figure 4.10: Consecutive use of antimicrobial surfaces prepared with 5% additives (Raw LBC ion-exchanged with 0.05M $AgNO_3$ and 0.05M $Cu(NO_3)_2$)

Antimicrobial efficiency was performed against Gram-negative bacteria, *E.coli*. All four samples showed excellent reduction of microorganism when compared with the control surfaces. Samples containing raw chabazite (LBC, LBN) with copper nitrate embedded showed 100% reduction approximately at 2 hrs until the 8th trial shown in Figure 10 and Table 9. This is due to the availability of silver at the coated surfaces. One previous study showed that silver and zinc containing a zeolite matrix coating on stainless steel

enhanced antimicrobial properties. The powder coating process was found to be highly durable and active with matrix containing silver (2.5% w/w) and zinc (14% w/w) as opposed to the wet coating process [47]. On the contrary, both samples showed 100% reduction of microorganism after 4 hrs of exposure after the 8th trial.

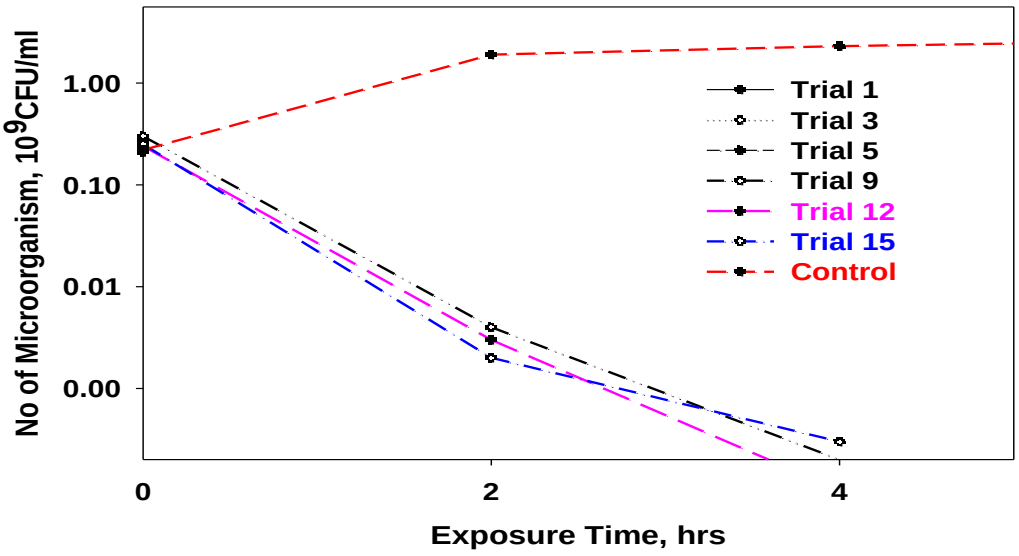

Figure 4.11: Consecutive use of antimicrobial surfaces prepared with 5% additive (Conditioned LBC ion-exchanged with 0.05M $AgNO_3$ and 0.05M $Cu(NO_3)_2$)

But the efficiency of conditioned zeolites after functionalization with silver and copper nitrate is quite better than unconditioned additives. Until the 8th trial, 100% reduction occurred much before 2 hrs of exposure. This probably happened due to the availability of more silver ion, which was attached on the surface of zeolites during functionalization following the conditioning process. The conditioned additives contain more silver than the raw one. Durability tests were carried out up to 15 trials with all four coated surfaces.

Table 4.9: Consecutive use of antimicrobial surfaces prepared with 5% additives (Raw LBN ion-exchanged with 0.05M $AgNO_3$ and 0.05M $Cu(NO_3)_2$)

No of microorganism present at particular time,10^9 cfu/ml

Time, hr	Trial 1	Trial 3	Trial 5	Trial 9	Trial 12	Trial 15	Control
0	0.27	0.23	0.28	0.22	0.3	0.24	0.23
2	0.03	0.02	0.01	0.02	0.06	0.03	2.0
4	0	0	0	0.0014	0.0027	0.0011	2.2
8	0	0	0	0	0	0	2.8
24	0	0	0	0	0	0	22.00

Table 4.10: Consecutive use of antimicrobial surfaces prepared with 5% additives (Conditioned LBN ion-exchanged with 0.05M $AgNO_3$ and 0.05M $Cu(NO_3)_2$)

No of Microorganism, present at particular time, 10^9cfu/ml

Time , hr	Trial 1	Trial 3	Trial 5	Trial 9	Trial 12	Trial 15	Control
0	0.22	0.26	0.27	0.21	0.29	0.31	0.25
2	0	0	0	0.006	0.003	0.001	2.0
4	0	0	0	0.0005	0.0003	0.0003	2.2
8	0	0	0	0	0	0	2.7
24	0	0	0	0	0	0	26.00

These samples were subjected to continuous exposures with the microorganism using the same procedures as discussed before. It should be mentioned here that the surfaces were cleaned with 70% ethyl alcohol solutions every time before spreading the microorganism.

A near constant reduction rate was observed until the last trial was checked. For conditioned chabazite containing surface, no viable microorganism was found at 2 hrs of exposure until 8 trials. So all microorganism died within 2 hrs of exposure. This is due to the presence of more silver in the additives in conditioned chabazites in compare to the unconditioned chabazites.

4.6.11 Bactericidal effect (Membrane Integrity/LDH Leakage)

LDH assay was used to measure the toxicity developed during exposure to the microorganism on the antimicrobial coated surface. Necrosis or apoptosis processes are the two way responsible for cells death. Apoptosis is a normal cell death that occurs for usual physiological changes but necrosis is unexpected and accidental cell damage, which occurs with the exposure to severe discrepancy from physiological conditions. Permeability of the plasma cell membrane increases due to these processes. LDH is a soluble enzyme found in all living cell and helps the conversion of NADH to NAD^+. This LDH releases into the medium due to the cell membrane integrity [48] and serves as an indicator to measure toxicity. With the increase of cell death and membrane damage, LDH leakage increases in the culture medium [49]. Fluorescence was used to measure the LDH amount at excitation and emission wavelengths of 560nm and 590nm respectively and measured data are reported as percentages of the control coated surface [50]. Toxicity analysis was done at different time of exposure to the microorganism on the antimicrobial coated surface. Toxicity analysis of silver and copper ions containing antimicrobial surfaces are shown in Figure 4.12. Percent of toxicity production with exposure of microorganism was increased with time. It should be noted that the same

coated antimicrobial surface used for 15 times produced similar toxicity after 24 hrs of exposure with the microorganism. Toxicity production proved the efficiency of the coated surface for prolonged period.

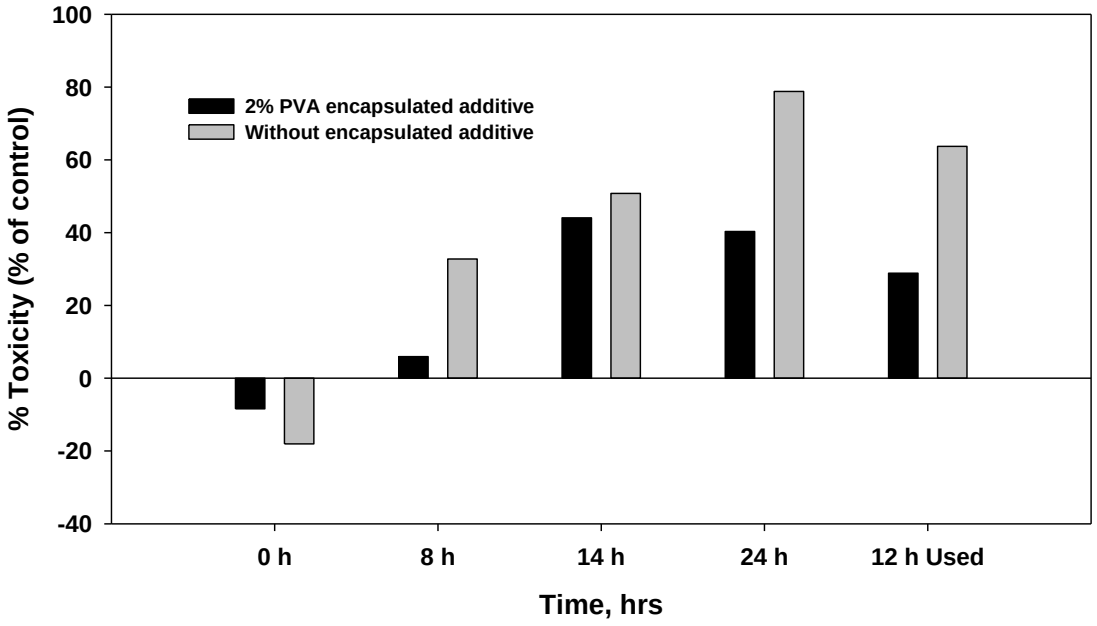

Fig 4.12: Toxicity analysis of conditioned and functionalized chabazite containing antimicrobial coated surface

4.7 Conclusions

Pre-treatment and conditioning of different natural zeolites helped remove loosely bonded cations from exchange sites and replaced those with more easily removable cations (mainly, sodium cation). Conversion of LBC and LBN chabazites to a near homo-ionic form was found in this study with improved CEC. Due to the lower hydrated cationic radius and lower electrostatic attractions with the structure of zeolites, these

sodium cations can be replaced more easily from zeolite channels than any other cations, such as calcium, magnesium, iron, etc. In addition, the removal of impurities and unwanted materials from zeolites during the pre-treatment process helped the uptake of sodium as well as silver and copper by reducing pore clogging. Therefore, it was possible to functionalize zeolites with silver and copper ions without difficulty by removing the existing sodium cations. Increasing the pH of the solution to pH 11 by adding NaOH in addition to mechanical treatment such as higher temperature, sonication and continuous stirring was found to have a strong influence on the higher values of CEC. Higher solid liquid ratios helped higher cationic movement through the channel of zeolites. Chabazites, which is known as LBC have a slightly higher Si/Al ratio than LBN. Again, the pre-treatment and conditioning process helped to increase the molar ratio of Na/Al for both zeolites, as well as their functionalization efficiency with silver and copper. It should be noted here that the addition of silver and copper salt at different time intervals has an effect on ion exchange as noted in the ICP-OES analysis. LBN is more efficient than LBC in terms of cationic configuration (silver, copper) after ion exchange and also required lesser time (24 hrs) than LBC (48 hrs) to achieve that efficiency. XRD of all additives showed similar peak with the raw zeolites including the standard one. As well no dissimilarities were found during the TGA analysis. As such, the conditioning and functionalization processes did not change the structure and behavior of chabazites, which could help them used as an antimicrobial additive for any industrial application. 5% of the additives as mentioned before were used in the final formulation in this study, which was found to be the most appropriate composition. But due to the flow characteristics and charging capabilities of additives and the resin powder during

spraying, it was evident that the percentage of additives in the coated surfaces remained as high as 85-87%. In the powder coating process we can reuse the overflow powder, which would make the process more efficient and economical than the liquid coating process. Color determination of the surface after curing is an important parameter to determine and fix the reduction rate of silver during curing, which was overcome by the addition of copper at different proportions.

To understand the leaching rate and the behavior of the coating, the surfaces were exposed to microorganism for different time periods to check its efficiency. It was found that the amount of silver that leached out from the coating was in ppm level with continuous contact of common cation available in the microorganism. No trace of silver was found during the leaching test with only DI water which also proved that silver did not leach out readily. Rather it needed some other cations for ion exchange and finally to leached out silver. Durability analysis of the prepared surfaces showed excellent performance against *E.coli* throughout 15 trials. The study also showed that the conditioned chabazites containing surfaces had better efficiency than the unconditioned ones. Conditioning helped the chabazites hold more active cations, which resulted in more durability and better performance.

The formulated surfaces were checked against *E.coli* only, which was a gram negative bacteria. Further efficiency of the surfaces can be checked against other gram negative and gram positive bacteria including some in-vitro and in-vivo analysis.

References:

1. BB Mamba, DW Nyembe, AF Mulaba-Bafubiandi, 2009, Removal of copper and cobalt from aqueous solutions using natural clinoptilolite, *Water SA*, vol.35 no.3, pages 237-243.

2. Vassilis J., Inglezakis, 2005, The concept of "capacity" in zeolite ion-exchange systems, *Journal of Colloid and Interface Science*, vol. 281, issue 1, pages 68–79.

3. Yousheng Tao , Hirofumi Kanoh , Lloyd Abrams and Katsumi Kaneko, 2006, Mesopore-Modified Zeolites: Preparation, Characterization, and Applications, *Chem. Rev.* vol.106, no.3, pages 896–910.

4. BB Mamba, DW Nyembe and AF Mulaba-Bafubiandi, 2010, The effect of conditioning with NaCl, KCl and HCl on the performance of natural clinoptilolite's removal efficiency of Cu2+ and Co2+ from Co/Cu synthetic solutions, *Water SA* vol. 36 no. 4 pages 437-444.

5. Nyembe dw, Mamba BB AND Mulaba AF, 2010, Adsorption mechanisms of Co^{2+} and Cu^{2+} from aqueous dolutions using natural clinoptilolite: equilibrium and kinetic studies. *J. Applied Sci.*, vol. 10, no.8, pages 599-610.

6. Panayotova M and Velikov B, 2003, Influence of zeolite transformation in a homoionic form on the removal of some heavy metal ions from wastewater. *J. Environ. Sci. Health A*, vol.38, pages 545-554.

7. Zamzow MJ and Murphy JE, 1992, Natural zeolites as cation exchangers for environmental protection. *Sep. Sci. Technol.* pages 1969-1984.

8. Coruh S, 2008, Treatment of copper industry waste and production of sintered glass-ceramic. *Waste Manage. Res.* vol. 24, pages 234-241.

9. Blanchard G, Maunaye M and Martin G, 1984, Removal of heavy metals from water by means of natural zeolites. *Water Res*. vol.18, pages 1501-1507.

10. Assenov A, Vassilev C and Kostova M, 1988, Simultaneous sorption of metal ions on natural zeolite clinoptilolite. In: Kallo D and Sherry HS (eds.) *Occurrence, properties and utilization of Natural zeolites.* pages 471-480.

11. Trgo M, Peric J and Vukojevic Medvidovic N, 2006, A comparative study of ion exchange kinetics in zinc/lead-modified zeolite-clinoptilolite systems. *J. Haz. Mater.* vol. 136, no.3 938-945.

12. Ghasemi Mobtaker H, Kazemian H., 2006, Investigation of the influence of the ionic interferences on the sorption of heavy metal cations with synthetic zeolite A and P,

synthesized from Iranian natural clinoptilolite. *Iranian Journal of chemistry and chemical Engineering* vol.25, page 87-95.

13. Kazemian H, Mallah MH., 2006, Elimination of Cd^{2+} and Mn^{2+} from wastewaters using natural clinoptilolite and synthetic zeolite-p. *Iranian Journal of chemistry and chemical Engineering*, vol.25, pages 91-94.

14. Kazemian H, Rajec P, Macasek F, Kufacakova JO., 2001, Iinvestigation of lead removal from wastewater by iranian natural zeolites using 212pb as a radiotracer. *In: Studies in surface science and catalysis*, vol. 135, page 369.

15. Faghihian H, Kazemian H. 2002. Ion exchange of Pb^{2+}, Ag^{+}, Ni^{2+} and Zn^{2+} in natural clinoptilolite, study of some parameters. *Iranian Journal of Science and Technology, Transaction A- Science*, vol 26, pages 357-361.

16, Mamba BB, Dlamini NP, Nyembe DW, Mulaba-Bafubiandi AF., 2009, Metal adsorption capabilities of clinoptilolite and selected strains of bacteria from mine water. *Physics and Chemistry of the Earth*, Parts A/B/C, vol 34, pages 830-840.

17. Faghihian H, Ghannadi Marageh M., Kazemian H., 1999, The use of clinoptilolite and its sodium form for removal of radioactive cesium, and strontium from nuclear wastewater and Pb^{2+} , Ni^{2+}, Cd^{2+}, Ba^{2+} from municipal wastewater, *Applied Radiation and Isotopes*,vol 50, no 4, pages 655–660.

18. Faghihian H, Kazemian H., 1999, Effect of different parameters on the uptake of Pb^{2+}, Ag^{+}, Ni^{2+}, Cd^{2+} and Zn^{2+} in natural clinoptilolite. *Asian Chemistry Letters*, vol 3, pages 279-283.

19. Kazemian H, H. Mallah M., 2008, Removal of chromate ion from contaminated synthetic water using mcm-41/ZSM-5 composite. *Iranian Journal of Environmental Health Science & Engineering*, vol 5, pages 73-77.

20. R. Menhaje-Bena, H. Kazemian, S. Shahtaheri, M. Ghazi-Khansari, M. Hosseini, 2004, Evaluation of iron modified zeolites for removal of arsenic from drinking water, *Studies in Surface Science and Catalysis* vol. 154, pages 1892-1899.

21. Ghadiri SK, Nabizadeh R, Mahvi AH, Nasseri S, Kazemian H, Mesdaghinia AR, 2010, Methyl tert butyl ether adsorption on surfactant modified natural zeolites. *Iranian Journal of Environmental Health Science and Engineering*, vol 7, pages 241-252.

22. Torkaman R, Kazemian H, Soltanieh M., 2010, Removal of btx compounds from wastewaters using template free mfi zeolitic membrane, *Iranian Journal of Chemistry and Chemical Engineering*, vol 29, pages 91-98.

23. Seifi L, Torabian A, Kazemian H, Bidhendi G, Azimi A, Charkhi A., 2011. Adsorption of petroleum monoaromatics from aqueous solutions using granulated surface modified natural nanozeolites: Systematic study of equilibrium isotherms. *Water, Air, & Soil Pollution*, pages 611-625.

24. Seifi L, Torabian A, Kazemian H, Bidhendi G, Azimi A, Farhadi F, et al., 2011. Kinetic study of btex removal using granulated surfactant-modified natural zeolites nanoparticles. *Water, Air, & Soil Pollution*, pages 443-457.

25. Langwaldt J, 2008, Ammonium removal from water by eight natural zeolites: a comparative study. *Sep. Sci. Technol.* vol 43, no.8, pages 2166-2182.

26. Rahmani AR, Samadi MT and Ehsani HR, 2009, Investigation of clinoptilolite natural zeolite regeneration by air stri`pping followed by ion exchange for removal of ammonium from aqueous solutions. *Iran. J. Environ. Health. Sci. Eng.* vol.6, no.3, pages 167-172.

27. Panayotova M and Velikov B, 2003, Influence of zeolite transformation in a homoionic form on the removal of some heavy metal ions from wastewater. *J. Environ. Sci. Health A*, vol. 38 no. 3. pages 545-554.

28. N.S. Flores-López, J. Castro-Rosas, R. Ramírez-Bon , A. Mendoza-Córdova, E. Larios-Rodríguez, M. Flores-Acosta, 28 November 2012, Synthesis and properties of crystalline silver nanoparticles supported in natural zeolite chabazite, *Journal of Molecular Structure,* vol. 1028, pages 110–115.

29. Masahiro Nitta, Shigemi Matsumoto, Kazuo Aomura, November 1974, Ion exchange scheme for silver exchange for sodium in the synthetic zeolite Linde 4A, *Journal of Catalysis*, vol. 35, issue 2, pages 317–319.

30. Li Z, Flytzani-Stephanopoulos M, 1997, Selective catalytic reduction of nitric oxide by methane over cerium and silver ion-exchanged ZSM-5 zeolites. *Applied Catalysis A: General*. vol.165, no.1-2,pages 15-34

31. Konstantinos P. Kitsopoulos, 1999, Cation exchange capapcity (CEC) of zeolite volcaniclastic materials: Applicability of the ammonium acetate saturation (AMAS) method, *Clays and Clay Minerals*, vol. 47, no. 6, pages 688-696.

32. *American Society for Testing and Materials*, 2006, "D 5630-06 Standard Test Method for Ash Content in Plastics".

33. Palesa. P. Diale, Edison Muzenda, and Josephat Zimba, 2011, A Study of South African Natural Zeolites Properties and Applications, *Proceedings of the World Congress on Engineering and Computer Science,* vol II, pages19-21.

34. M.C Barreto, P Ciambelli, G.del Re, A Peluso, 1987, A theoretical study of ion selectivity of zeolites—application to chabazite, Journal of Physics and Chemistry of Solids, vol.48, issue 1, pages 1–12.

35. I Nglezakis VJ and Grigoropoulou H, 2004, Effect of pore clogging on kinetics of lead uptake by clinoptilolite. *J. Haz. Mater.*vol. 112, pages 37- 43.

36. Vassilis J. Inglezakis, 2005, The concept of "capacity" in zeolite ion-exchange systems, *Journal of Colloid and Interface Science*, vol. 1, pages 68–79.

37. A.Z. Woinarskia,b, I. Snapeb, G.W. Stevensa, S.C. Starkb, 2003, The effects of cold temperature on copper ion exchange by natural zeolite for use in a permeable reactive barrier in Antarctica, *Cold Regions Science and Technology*. vol. 37, pages 159– 168.

38. Ayben Top, Semra U¨lku, October 2004, Silver, zinc, and copper exchange in a Na-clinoptilolite and resulting effect on antibacterial activity, *Applied Clay Science*, vol 27, issues 1–2 , pages 13–19

39. Jafar Talebi, Rouein Halladj, Sima Askari, 2010, Sonochemical synthesis of silver nanoparticles in Y-zeolite substrate, *Journal of Materials Science* ,vol 45, issue, pages 3318-3324.

40. S. Akbar, T.H. Shah, R. Shahnaz and G. Sarwar, 2007, Thermal studies of synthetic NaX Zeolite and its Zinc Exchanged Forms, *Journal of Chemical Society, Pakistan*, vol. 29, no.1, pages 5-11.

41. Cory O'Neill, Derek E. Beving, Wilfred Chen, and Yushan Yan, 2006, Durability of Hydrophilic and Antimicrobial Zeolite Coatings under Water Immersion, *Materials, interfaces, and electrochemical phenomena, AIChE Journal*, vol. 52, no. 3, page 1157-1161.

42. Fujing Wang, Robert Martinuzzi and Jesse (Jing-Xu) Zhu , 2004, Experimental study of particle trajectory in electrostatics powder coating process. *Journal of powder technology*, vol. 150, issue 1, pages 20-29.

43. Fernández A, Soriano E, Hernández-Munoz P, Gavara R., 2010, Migration of antimicrobial silver from composites of polylactide with silver zeolites. *J Food Sci*. vol. 75, no.3, pages 186–193.

44. Sabbani S, Gallego-Perez D, Nagy A, Waldman WJ, Hansford D, Dutta PK, 2010, Synthesis of silver-zeolite films on micropatterned porous alumina and its application as an antimicrobial substrate. *Micropor Mesopor Mat*. Vol.135, no.1–3, pages 131–136.

45. Kumar R, Howdle S, Münstedt H, 2005, Polyamide/silver antimicrobials: effect of filler types on the silver ion release. *J Biomed Mater Res B Appl Biomater, vol.*75, no.2, pages311-319**.**

46. Marjorie M. Cowan. Kelly Z. Abshire . Stephanie L. Houk. Suzanne M. Evans, 2003, Antimicrobial efficacy of a silver-zeolite matrix coating on stainless steel, *J Ind Microbiol Biotechnol*, vol. 30, pages102-106.

47. Abd El-Mohdy, H.L., 2013, Radiation synthesis of nanosilver/poly vinyl alcohol/cellulose acetate/gelatin hydrogels for wound dressing, J. Polym. Res., vol.20, pages 177-189.

48. Lun Li, Jie Sun, Xiaoran Li, Yan Zhang, Zhaoxu Wang, Chunren Wang, Jianwu Dai Qiangbin Wang, 2012, Controllable synthesis of monodispersed silver nanoparticles as standardsfor quantitative assessment of their cytotoxicity, *Biomaterials,* vol.33, pages 1714- 1721.

49. Thomas H. Sanderson, Sarita Raghunayakula, Rita Kumar, 2015, Release of mitochondrial Opa1 following oxidative stress in HT22 cells, *J Molecular and Cellular Neuroscience*, vol 64 pages 116–122.

50. C. Carlson, S. M. Hussain, A. M. Schrand, L. K. Braydich-Stolle, K. L. Hess, R. L. Jones, and J. J. Schlager, 2008, Unique Cellular Interaction of Silver Nanoparticles: Size-Dependent Generation of Reactive Oxygen Species, *J. Phys. Chem.* vol. 112,pages 13608–13619.

CHAPTER 5

Effectivity of Silver Ion on Enhanced Durability for Antimicrobial Powder Coated Surface

5.1 Abstract

The efficiency of antimicrobial products depends on the release of the active component (silver ions) embedded in the surfaces. An ion exchange process was used to incorporate the silver and copper ions into the synthetic zeolite A. Salts of these active agents in different combinations were used to optimize antimicrobial additives by achieving the highest amount of active components (Ag^{+},1.534meq/g, Cu^{2+}, 3.90 meq/g). Silver ions reduced to Ag^{o} during the curing step, so the surface became inactive against microorganism after few trials. The reduction of Ag^{+} can be controlled by the addition of Cu^{2+} ions and it made the surface very efficient since it showed 100% in reduction of microorganism within 2 hrs of exposure. The color of the coated surface containing Ag^{+} and Cu^{2+} was found comparable with the control surface. XPS data (binding energy and Auger Parameter) confirmed that copper prevented silver from reduction during the curing period of powder coating process. Transfer efficiency of the additives in the resin system during the spraying was improved by increasing the particle size of the final powder from 20μm to 30μm and 55 μm using different mechanical processes of pressing, grinding and sieving. Antimicrobial efficiency with enhanced additives was checked up to the 8th trial and found to be active against microorganism.

Curing promoters were used in the powder to lower the curing temperature. The effects of low curing additives on surface properties were analyzed and found comparable with

the surface cured at standard temperature (15 minutes at 200^{o}C). But the antimicrobial efficiency analysis did not show any appreciable results. The release rate of the active components from the surface to the contaminated environment can be further controlled by using a PVA coating on the additive and was found as an effective antimicrobial surface for prolonged period. Color of the coated surface is another indication for silver to remain active, which was determined at every stages of experiment. Effect of autoclave on the coated surface was also analyzed by considering the change of surface color and antimicrobial efficiency.

Key words: Silver ion, copper ion, antimicrobial activity, silver ion release, encapsulation, cation exchange capacity,

5.2 Introduction

Synthetic zeolites are micro porous crystal-structured aluminosilicate linked by shared oxygen atoms and weakly bonded exchangeable cations with water molecules. There is a negative charge imbalance due to the isomorphic exchange of Si (IV) by Al (III) in the tetrahedral, which is neutralized by the exchangeable alkali and alkaline earth cations. These cations do not reside in fixed position, that's why the negative charge of the zeolites is not confined, but are uniformly distributed throughout the frame. Frame-work charge is the main considering factor, which influences the ion exchange rate. Electrostatic attraction for the external cations is another factor responsible for a partial or complete ion exchange [1]. Transition metal cations have higher affinity for zeolite but lower affinity for non-polar organics and anions [2]. The amount of cations depends on the alumina content and the cation exchange capacity (CEC) depends on the amount

of exchangeable cations. The greater the alumina content, the smaller is the Si/Al ratio and the higher is the CEC. CEC is usually related to the replacement behavior of ammonium in synthetic zeolite, which in turn depends on the pore size, pore configuration and the CEC capacities of that zeolite. For Linde type A zeolite (LTA) with sodium, the ion exchange rate of silver ion decreases with reaction time due to its pore size, but for the Na-FAU, since the size of the pore is bigger than the LTA, later is not time depended [3].

These zeolites are generally produced by alkali treatment of silica and alumina, which is an expensive method, but produces high quality materials. These engineered zeolites possess very precise and desired chemical and physical properties suitable for highly specified applications in nanotechnology, electrochemistry, pharmacy, photochemistry, and in research. Based on the applications, zeolite can be prepared with the combination of different Si/Al ratio with single or multiple exchangeable cations. Synthetic zeolite NaA is one of the widely used zeolites known as LTA, with the chemical formulation of $Na_{12}\,Al_{12}Si_{12}O_{48}.27H_2O$, channel dimension 4Å and the CEC is 5.48 [2]. CEC is the main parameter that describes any zeolite from an applied perspective. The ion exchange capacity is considered to control the equilibrium behavior depending on its surrounding solution's concentration, the inherent characteristics of the ion exchange system and temperature [4]. It also depends on zeolites physical and chemical properties, e.g., composition, particle size, crystal structure, porosity and exchange site distribution, pH, and presence of surrounding cations etc. Cation selectivity depends on the cation charge, electronic structure, size and some-times temperature.

Through suitable modification of the physicochemical properties of zeolite A, it can be used in different and diverge applications. These modifications are possible with the incorporation of specific cation, which causes changes in their various properties following pore size and geometry. The changes improve their activity and enable them to act as a special additive with the replacement of native cations to some exotic metal ions. Exotic metal, silver for example, can provide broad spectrum antibacterial activity at very low concentrations, satisfactory safety in usages and inherent stability through the controlled release. Silver can be incorporated within zeolite A through ion exchange process followed by the incorporation of this zeolite into the resin system for the application of antimicrobial powder coating surfaces. Powder coated surface are normally required to be cured at $200^{o}C$ for 10 minutes. During this curing process ionic silver (Ag^{+}) is reduced to metallic silver (Ag^{o}), which makes the surface inactive against microorganisms. To overcome this problem some researchers incorporated copper into the additive with silver by ion exchange process and found to be effective [5]. The redox potential of these cations plays the main role to keep the silver ions in their original state.

Whenever common environmental cations such as sodium, calcium or potassium are available, control release of silver ions from silver zeolite takes place. Silver release cannot takes place unless another ion occupies its place in the zeolite. Silver comes out from the zeolite in the presence of moisture, until an equilibrium value of the silver concentration is reached. Silver does not release in dry condition and similarly microorganism also cannot survive without moisture. When moisture and such cationic species are not present, ions will not release from zeolite. So the active material is not consumed when it is not required, thus the duration of antimicrobial efficacy is enhanced

[6].Therefore, the antimicrobial activity of silver zeolite is controlled by gradual release of Ag^{+} from zeolite matrix. Zeolite has the enhanced water uptake properties which results in an increase in silver ion release in presence of other cations. Release of silver ion from zeolite occurs basically in three steps:

i) The diffusion of water into the zeolite

ii) The ion exchange due to the interaction between cations and water molecules and

iii) The release of silver ions to the aqueous environment [7].

To increase the durability of these additives, the controlled release rate of silver ions from the surface needs to be ensured. Encapsulation of zeolites would be the best solution for controlled release of active materials. Controlled release systems can provide the benefits of proper use of active materials and will prevent unnecessary leaching of silver and therefore increase the durability of the functionality of the surface.

The objective of this work is to incorporate highest amount of silver and proper amount of copper within zeolite A through ion exchange by applying proper conditions of such ion exchange and to make the zeolite a suitable additive for durable antimicrobial powder coatings.

5.3 Materials and Methods

5.3.1 Materials: Materials used for this study are listed below:

Synthetic zeolite: Synthetic zeolite was obtained from PQ Corporation, Malvern, PA, USA. This synthetic zeolite was designated as type A and contained only sodium cations for exchange. Average particle size of this zeolite was in the range of 2 to 3 micron.

Reagents: All chemicals used in this study were analytical grade reagents. DI water was used in all stages of the experiments. Test microorganism used for this experiment has been mentioned in Chapter 4.

Methods: A two-step method was employed fabricate the additives used in powder coating.

5.3.2 Functionalization of synthetic zeolite A:

Silver nitrate and copper nitrate were used to functionalize the zeolite samples. 25 gm zeolite in each batch was functionalized with 500ml of 0.05M $AgNO_3$ and 0.1M $Cu(NO_3)_2$ by adjusting the pH at 4-4.5 with concentrated HNO_3. All the zeolite samples were prepared by mixing with the aforementioned salt solutions at 60^oC by stirring them continuously at 500 rpm for 24 to 48 hours. Different addition protocols were used during functionalization to maximize the cations in the zeolite after ion-exchange. Silver loading of the zeolite was executed in the dark environment to stay away from the photo-oxidation of silver [18]. Two different phases were separated by centrifuging at 3500 rpm for 25 min. The solid phase was washed several times with deionized water to remove excessive ions. Later a 0.1N NaCl solution was used to identify any ionic silver species in

the supernatant fluid after centrifuging and washing. All functionalized samples were then dried at 80^{o}C for 5-6 hrs while maintaining the dark condition. After sufficient drying, the particles, were broken down into their initial respective particle sizes by a small grinder and kept in the dark container to avoid oxidation. Here after all the samples are referred to additive.

5.3.3 Encapsulation of additives: 2% and 6% PVA solutions were made by dissolving Poly (vinyl alcohol), [-CH_2CHOH-]$_n$, Mw 89,000-98,000, 99% hydrolyzed, Sigma 341584 in DI water at 80^{o}C for 45 minutes. The prepared additive was then added to the solution and mixed until became a thick slurry to avoid phase separation. Later the same was dried at room temperature followed by grinding. Powder spraying and curing process are mentioned in the earlier chapter.

5.3.4 XPS (X-ray photoelectron spectroscopy): To assess the change of Ag^{+} with and without the presence of copper during curing of the sprayed powder, X-ray photoelectron spectroscopy (XPS) analysis was carried out using a Kratos AXIS Ultra Spectrometer equipped with Mg Kα X-ray source and the XPS spectra were recorded at -5 to 1000eV with 2eV step size. The existence of silver is commonly determined by using the binding energy but it is difficult to assess the oxidation state of silver from XPS peaks due to very small chemical shift. So, MNN Auger electron analysis was used to determine the different states of silver.

5.3.5 Transfer efficiency of additives: Additives, which were added into the resin powder may have changed in concentration during the electrostatic spraying due to the different chargeability of two materials. Additive concentration was determined using ASTM D5630-06 Standard Test Method [8]. Powder was collected from the surface after spraying, which is called the transferred powder. This powder was heated at 550°C in a ceramic crucible for 90 minutes to remove all combustible material from the powder, leaving behind the non-combustible material in the form of ash. The amount of ash was then used to calculate the actual additive concentration of the transferred powder.

5.3.6 Impact resistance analysis (ASTM D2794): Impact resistance of any powder coated surface is one of the most important parameters which gives a indication of the mechanical performance of the same. It is done by an impact tester (Elcometer 157014) which imposes an instant stress by an object of a weight from a certain height. When the impact is given on the coated side of the testing surface, it is called direct impact. On the contrary, if the impact is given on the uncoated side of the surface, then it is called indirect impact. The objective of this test is to find out the threshold of the bearing load of the coated surface. The procedure which was followed for the evaluation of the impact resistance is given in the instructions of the "ASTM D2794 Standard Test Method". The apparatus consists of a vertical guide tube, 0.6m to 1.2m long through which a free falling cylindrical weight, which has a round impact head, can slide freely. The vertical guide has a length scale in millimetre attached next to its path of travel, which facilitates to keep record of the height of the weight from which it was dropped each time. The kinetic energy of the falling object was actually imparted on both side of the coated panel,

having a coating of 40-45 micron and the results of the load bearing test gave the impact resistance of the said surface.

5.3.7 Pencil scratch hardness test (ASTM D3363): The scratching resistance to any hard element was measured by this analysis following the "D3363 Standard Test Method for Film Hardness by Pencil Test" pencil with different hardness were used as the testing tool. The pencil that will not cut into or gouge the coated surface determines the hardness of the coated surface. A set of calibrated wood pencils with the following scale of hardness from the softest (6B) to the hardest (6H) were used (6B – 5B – 4B – 3B – 2B – B – HB – F – H – 2H – 3H – 4H – 5H – 6H). The coated surface was kept on a firm flat surface. The pencil was firmly held against the coated surface at an angle of 45°. Uniform pressure was applied forward and downwards and the stroke was around 6.5 mm long. In order to have consistent result, at least two strokes per lead were done on the coating.

5.3.8 MEK Test (Methyl Ethyl Ketone) ASTM D4752: This is a solvent rubbing testing for assessing the solvent resistance of the coating. To remove loose dirt, 6 inches long coated surface was cleaned with water and dried with cloth. A MEK saturated cotton bud was hold on the test surface at 45^{o} angle and rubbed with moderate pressure, away from the operator and then back towards the operator. Each double rubbing, one forward and back motion, was completed in approximately 1 sec and was continued up to 50 times. The rubbing effect was recorded after the test was completed.

5.3.9 FTIR (Fourier transform infrared spectroscopy): Additives prepared with silver and copper ions individually and together were characterized by ATR-FTIR spectroscope (Nicolet 6700 FTIR) with a single reflection diamond ATR accessory. The spectra were scanned between 4000 and 500 cm^{-1}.

5.3.10 Autoclave analysis: The antimicrobial coated surface including the control surface were autoclaved at 121°C for 15 minutes immediately after every exposure with microorganism. The pressure inside the autoclave was maintained at 15 psi and the same were repeated for four times. The color changes and antimicrobial efficiency of the coated surface were observed and recorded after every autoclave treatment.

All other analysis methods (XRF, ICP-OES, TGA, XRD, Antimicrobial analysis, Color analysis, Toxicity analysis) used in this study have reported earlier in Chapter 4.

The same coated surface was used repeatedly called as 'trial' to check the efficiency against microorganisms. It is to be noted that the aforesaid coated surface was cleaned with soap and water and dried before every use.

5.4 Results and Discussions

5.4.1 Elemental analysis of synthetic zeolite A by x-ray fluorescence (XRF):

The capacity of zeolites for ion exchange is one of its most important properties, which depends on its silica-alumina ratio and cations of alkali or alkaline earth metals, also known as counter cations. The interaction between the counter cations and the anionic frame-work (alumina content) exposed in the local environment expresses the ion

exchange behavior of that zeolite. The XRF analysis of synthetic zeolite A is shown in Table 5.1, which indicates that sodium was the main cation present for exchange and the silica alumina ratio was 1.17, which represents the ion exchange capability. The active negative charge of the zeolite structure comes from the alumina content which is the indicator for the entire charge of the exchangeable cations. It was determined that the ion exchange capacity of this zeolite by ammonia replacement method was 5.21meq/g. The intention was to use this zeolite as a carrier for an active antimicrobial additive and to make them suitable for use in the ultrafine powder coating surfaces.

Table 5.1: The main composition of zeolite A according to the XRF analysis, shown as % w/w content of mineral oxides and the corresponding bulk SiO_2/Al_2O_3 ratios

Samples	SiO_2	TiO_2	Al_2O_3	Fe_2O_3	MgO	CaO	K_2O	Na_2O	SiO_2/Al_2O_3 ratio
Synthetic Zeolite A	32.9	<0.04	28.1	<0.04	<0.11	<0.03	0.11	17.9	1.17

5.4.2 Functionalization of zeolite with silver and copper ions:

Functionalization of zeolite was done with silver and copper ions by replacing the native sodium cations. Different combinations of silver and copper salt solutions were added during functionalization. pH of the solution containing silver and zeolite was adjusted at 4-4.5 to make the cations more accessible for zeolites and to avoid precipitations. An acidic condition during ion exchange can slow down the process due to the presence of more H^+. Movement of the cations were accelerated inside the zeolite and also in the

surrounding medium through diffusion process by applying elevated temperature. This helps to disperse the zeolite within the solution properly and improves the mobility of the cations respectively. This diffusion process is the result of the concentration gradient of cations present between phases. The existing concentration differences are balanced through ion exchange and gradually equilibrium is established [9]. Functionalization of the zeolite with different combinations of salt was done to find the highest cationic concentration. The second combination reported in Table 5.2, was found to be the best of the combinations (Ag^{+} 1.534meq and Cu^{2+} 3.89meq) for this system, where silver was added first into the aqueous zeolite solution maintained at pH 4 with constant stirring and mixed for 24hrs at 60^{o}C followed by the addition of copper to the existing solution and mixing for another 24hrs.

In our hypothesis, the larger number of cation exchange occurs with copper (Cu^{2+}) compared to silver (Ag^{+}). This is mainly because of two following reasons:

a) Higher affinity of divalent cation to electronegative zeolite;
b) Higher chance of diffusion of smaller copper ions (ionic radius = 0.73Å) compared to that of silver ions (ionic radius =1.13 Å) into zeolite pores (4 Å);

Copper was added to the functionalization process to prevent the silver from reduction. By incorporating a higher amount of silver, it was anticipated that a higher activity with enhanced durability against microorganism can be achieved. The above mentioned combination was used to make the antimicrobial additives for ultrafine powder coating surfaces.

Table 5.2: Elemental analysis (milli eq) of functionalized zeolite by ICP-OES

Sample Labels	Ag	Cu	Na	Total cations
Raw Synthetic	0.00	0.00	6.98	6.98
Synthetic, Ag 24 hrs	1.66	0.00	5.26	6.92
Synthetic, Ag, then Cu 48hrs	1.53	3.89	1.46	6.88
Synthetic , Cu then Ag 48 hrs	1.30	3.32	2.35	6.97
Synthetic, Ag and Cu together 24 hrs	1.41	3.38	2.20	6.99
Synthetic, Ag and Cu together 48hrs	1.45	3.43	2.14	7.02

5.4.3 Thermo gravimetric analysis (TGA):

The thermal stability of polymer can be investigated by TGA analysis. Thermally stable polymers can withstand at least 300^{o}C in air and 500^{o}C in inert gases without any structural change and strength loss. Functionalization of zeolite A was done by adding silver and copper cations to replace the sodium cation present within the zeolite. So functionalized zeolite contains more charged cations (Cu^{2+}) and higher ionic radius containing cations (Ag^{+}) resulting in a lower void space in this zeolite than the raw zeolite. It was noted that the zeolite with high charge density in its frame work (Si/Al= 1.17) has a greater affinity for higher charged cations due to their electrostatic attractions. Small divalent cations (Cu^{2+}) are highly hydrated to replace the Na^{+} ion in the small cages of zeolite. Also there is a strong influence of cationic radius on the exchange process [11].

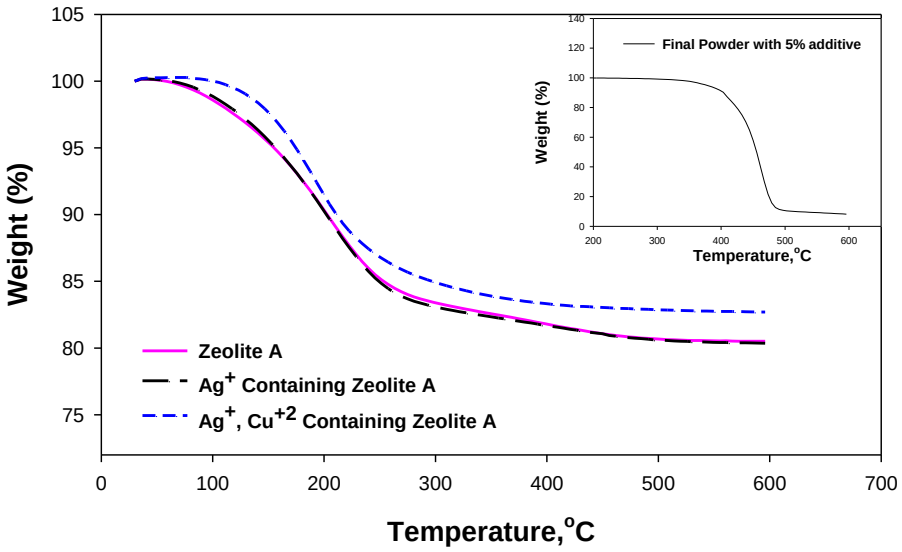

Figure 5.1: TGA of synthetic zeolite A and functionalized zeolites

The moisture content in zeolites NaA, AgNaA and AgCuNaA were investigated with the percent weight loss by TGA from 0^{o}C up to 600^{o}C. The characteristic thermo-grams of all zeolite samples and their DTGA profiles were shown in Figure 5.1 and 5.2, where the comparisons between the rates of weight loss with change in temperature were plotted. In general, TGA curves (in Figure 5.1) showed similar trends, but some small change in weight at high temperature after dehydration was observed. The thermograms were continuous and smooth, and the dehydration started at approximately 55^{o}C with the maximum weight loss (17.30-19.64%) was observed between 193-205^{o}C.

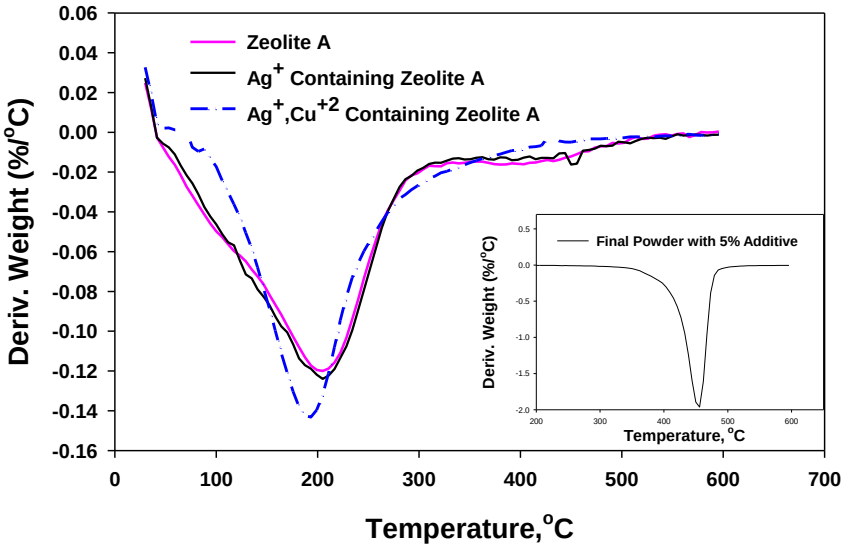

Figure 5.2: DTGA of synthetic zeolite A and functionalized zeolites

Data from all thermal analyses are summarized in Table 5.3. Zeolites have a non-stoichiometric hydrate structure because of the guest water molecules in the host structure. Water molecules interact in the framework with extra cations present and form hydrogen bonds with oxygen ions within the zeolite lattice [10]. The TGA and DTGA curves were correlated with each other and found with two types of water, mobile and immobile being present. Mobile water was in the wide pore sites and the immobile water was in the narrow pores. The TGA curves showed that maximum weight loss occurred between 280-300^{o}C, depending on the combination of cations being present or percentage of ion exchange of Na^{+} ions by Ag^{+} and Cu^{2+} ions. The higher rate of weight loss at this temperature range is assumed to be due to the loss of free mobile water and the weight loss above this range was assumed to be the immobile water. The immobile water formed hydration complexes with the cations being present and is tightly bonded with the

framework oxygen in the small cages [10]. The DTGA curves showed that the maximum dehydration temperature is 199^{o}C for NaA and 205^{o}C for AgNaA. But the zeolite containing silver and copper ions showed maximum dehydration at 193^{o}C and its corresponding weight loss was 17.30%, which was lower than the other two samples. The void space in the zeolite contained water molecules, which can be removed reversibly or replaced by other cations [12]. Due to the presence of higher copper ions than the silver ions in the third sample, the void space was small, so the water content was lower compared to the other two samples.

Table 5.3: Summary of the thermal property of the functionalized zeolite samples

Sample	Peak Area	Dehydration Temp. range, ^{o}C	Optimum Dehydration Temp, ^{o}C	Maximum Weight loss (%)
Zeolite A	16.57	53-333	199	19.48
Functionalized with silver	17.77	59-350	205	19.64
Functionalized with silver and copper	19.46	53-339	193	17.30
5% additive, Ag^{+}, Cu^{2+} in resin system	80.70	345-470	461	91.77

TGA analysis showed that even after 350^{o}C, some hydration water still remained in the sample [13] Small weight losses (~ 1-1.5%) were observed for all samples close to the end of the temperature range of the analysis. This water loss was probably due to the

immobile water, which required higher temperature to disrobe. On the contrary, the sample containing polyester resin with 5% additive (zeolite containing Ag^{+} and Cu^{2+}) showed weight loss at much higher temperature. This could be attributed ascribed to polymer degradation. DTGA curve for this sample showed a sharp endothermic peak at about $460^{o}C$, which was certainly due to the fusion of the crystalline phase of polymer. The area corresponds to DTGA peak was the enthalpy change and was not dependent on the heat capacity of the sample [14].

5.4.4 Fourier transform infrared spectroscopy (FTIR):

This functionalized zeolite A was further analyzed via the FTIR spectrum. Figure 5.3 showed combined FTIR spectra for synthetic zeolite A, synthetic zeolite A with Ag^{+} ions, synthetic zeolite A with Cu^{2+} ions and synthetic zeolite A with Ag^{+} and Cu^{2+}ions. From the FTIR spectra, the firmness of silicate structure and the non-band chemical interaction between zeolite structures and silver with copper ions in the matrix can be confirmed.

A broad band of weak intensity was observed at around $553cm^{-1}$, which indicates the presence of zeolite A. The band at this point represented the starting of crystallization of zeolite with double rings [15]. The band at $667cm^{-1}$ correspond to the internal linkage of the TO_4 (T represents Si or Al) tetrahedra which showed the asymmetric stretching of zeolite A. A similar band in the range of 540 to 680 cm^{-1} was defined as the characteristic spectra of synthetic zeolite A, which was again related to the SiO_2/Al_2O_3 ratio and the type of frame work [16]. Asymmetric stretching vibration were observed for all

characteristic bands in the range of 1250-950 cm^{-1}. This matched with the zeolitic materials [15].

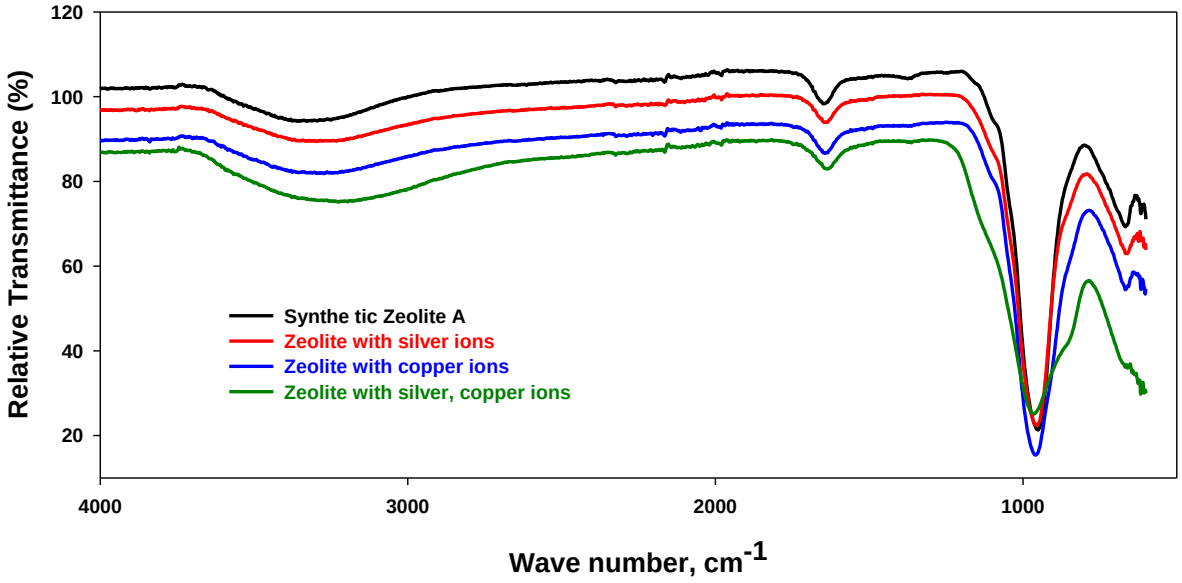

Figure 5.3: Fourier transform infrared spectroscopy (FTIR) analysis of synthetic zeolite A, synthetic zeolite A with Ag^{+}, synthetic zeolite A with Cu^{2+}, synthetic zeolite A with $Ag^{+}$and Cu^{2+}

The broad band at 3450 cm^{-1} and the other band at 1650 cm^{-1} were recognized as zeolitic water. The spectrum for zeolite A showed vibration bands for O-H stretching (H bonding) at 3295 cm^{-1} due to the presence of zeolitic water and at 1650 cm^{-1} for H-O-H bending. The strong vibrational band at 960 cm^{-1} corresponds to Si-O stretching, which suggested a three-dimensional silica phase. The band near 667 cm^{-1} was for Al-O stretching. The non-band chemical interaction between zeolite structure with silver and copper were associates with the peak at around 3200 cm^{-1} to 3275 cm^{-1}. The peak position at 3310 cm^{-1}, 3274 cm^{-1}, 3273 cm^{-1} and 3224 cm^{-1} were for zeolite A, zeolite A

with silver ions, zeolite with copper ions and, zeolite with silver and copper together respectively. With the addition of cations these peaks were shifted towards lower wave numbers. These broad bands were due to the van der Waals interactions between the hydroxyl groups present in the zeolite in the form of H_2O and the partial positive charge of dominating cations [17,38]. No bond displacement was observed in any of the spectrum indicated that there was no or few chemical interaction occurred in the matrix.

5.4.5 X-ray photoelectron spectroscopy (XPS):

XPS is an analytical method to characterize the surface which allows the elemental qualitative and quantitative analysis up to a thickness of less than 10 nm. This method also represents the chemical states of atoms based on shifts in binding energy [18]. Metallic ion with lower oxidation state shows higher experimental binding energy [19]. Most studies of silver systems showed negative shift in binding energy of the Ag 3d peaks with the increase of the oxidation state [20]. Binding energy at Ag $3d_{5/2}$ is reported from 367.9 to 368.4eV for Ag^o and 367.6 to 368.5 eV for Ag^+. These values are too close to differentiate [21].

To identify the silver oxidation state, the use of Auger Parameter is the more reliable method than the binding energy of Ag $3d_{5/2}$. Sample charge shift does not have any effect on the Auger Parameter and for this element, auger peaks usually show higher chemical shifts than photoelectron peaks.

One additive in this study contained Ag^+ and the other contained Ag^+ with Cu^{2+}. Binding energy for the sample containing Ag^+ was 368.44eV and for the other sample was

368.78eV shown in Figure 5.4. The Ag 3d photoelectron XPS region and AgMNN Auger structure of silver in different forms are shown in Figure 5.5. The positions of the Ag $3d_{5/2}$ for two samples with their respective comments are shown in Table 4. There was a negative shift of binding energy for the additive with Ag^{+} from the other additives after the heat treatment which confirmed the presence of Ag^{o} and complied with the literature results [22].

There was a very small difference of binding energy between these two additives, as such the present state of silver after the heat treatment within these additives was not very clear. Thus the Auger parameter for these additives was determined to verify the silver states. Auger parameter computed from the most intense peak existing in the Auger electron structure and from the binding energy of Ag $3d_{5/2}$. Auger parameters at $Ag3d_{5/2}$, $M_4N_{45}N_{45}$ and $M_5N_{45}N_{45}$ are shown in Table 5.4 for these two additives, which allowed to differentiate the reduced forms Ag^{o} from the oxidized forms. For the sample containing Ag^{+} and Cu^{2+} no peak was found at $Ag3d_{5/2}$, $M_4N_{45}N_{45}$, which only confirmed the presence of Ag^{+}. But the other additive contained a mixture of Ag^{o} with Ag^{+}. These Auger parameters showed a very clear difference between silver in its reduced form and silver in its oxidation state (725.4 for Ag^{o} and 719.6 and 718.9 for Ag^{+} form). However, it did not give any information about the number of oxidation state. The Auger parameter for the Ag^{+} containing additive was calculated to be 725.4, which was in the reported value range for metallic silver (726.1eV -724.8eV). For pure metallic silver the peak had

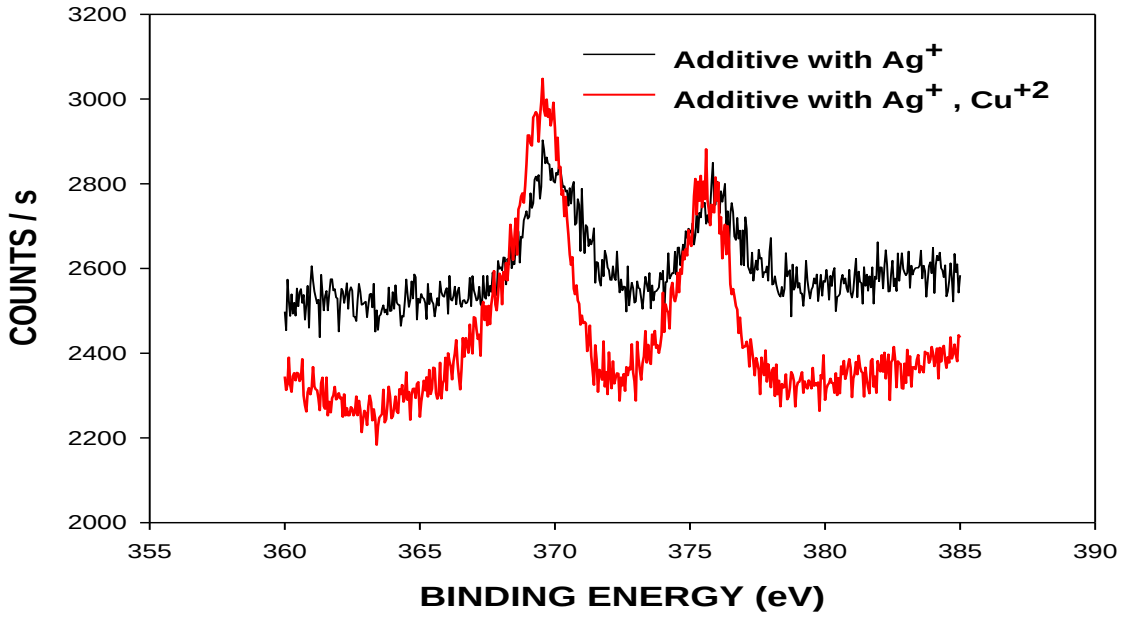

Figure 5.4: Binding Energy of two silver containing samples

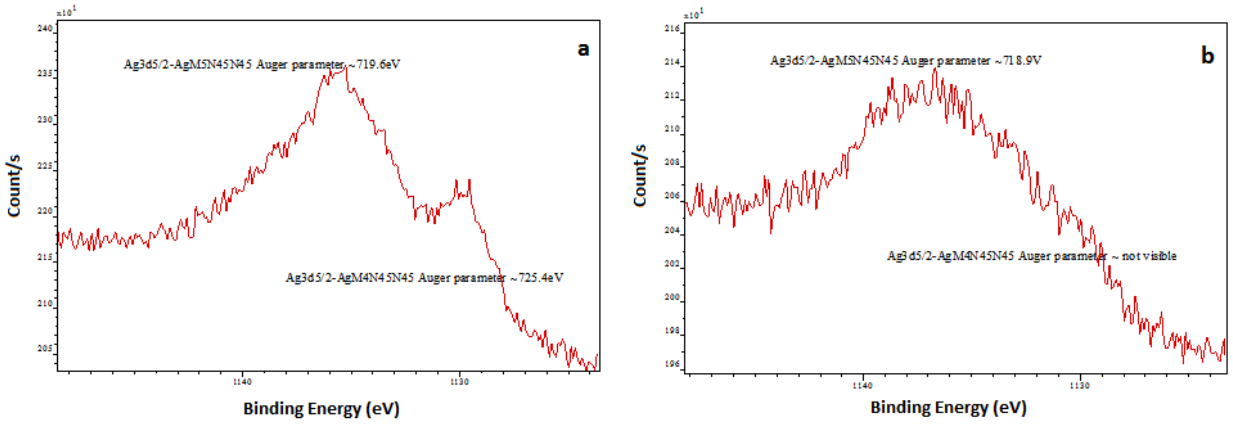

Figure 5.5: a. Auger parameter of additive containing with Silver ion (Ag^{+}) b. Silver ions (Ag^{+}) and Copper ions (Cu^{2+})

a sharper shape (lower FWHM values, 1.37) for metallic state and a wider peak (higher FWHM values, 1.54) for the non-metallic state [22].

The other additive, which contains Ag^{+} and Cu^{2+}, after the heat treatment was found to have most of Ag^{+} ions remaining in their original state. This was due to the presence of Cu^{2+}. Copper ions helped the silver ions to remain as Ag^{+} by reducing themselves. Silver has much lower affinity to oxygen than copper did, so copper reduced earlier than silver for the mixed additive [23]. The redox potential of silver ($Ag^{+}+e^{-} \rightarrow Ag^{o}$, +0.8) is reported to have higher values than copper ($Cu^{2+}+e^{-} \rightarrow Cu^{+}$, 0.16). Some researchers have pointed out that in the zeolite frame-work, copper ions (Cu^{2+}) can easily be reduced to Cu^{+} ions which are quite stable [24].

Because of the higher charges in the copper ions than silver ions, more electrostatic attraction was present in the zeolite for copper ions, which resulted restricted movement of silver ions. Water molecules can enter through the large and small cavities but oxygen can only enter through the larger cavities [25].

Different research work has been done based on the reduction of copper oxides. It was reported in some studies that the reduction of copper (II) oxide occurred by a direct transformation technique in place of sequential transformations [25]. The XPS/Auger analysis in this study strongly suggested that copper ions assisted silver to retain its original form during the heat treatment.

Table 5.4: Relative data for XPS analysis

SAMPLE	Ag 3d 5/2 Peaks			Position, Auger parameter, eV		Comments
	Binding Energy, eV	Counts/s	Area	$AgM_5N_{45}N_{45}$	$AgM_4N_{45}N_{45}$	
Additive with Ag^+	368.44	2615.4	2070.1	719.6	725.4	Mixture of Ag^o with small Ag^+
Additive with Ag^+, Cu^{2+}	368.78	2718.2	1256.4	718.9	Not Found	Only Ag^+ present

5.4.6 Powder X-ray diffraction (XRD):

XRD is a fast analytical technique mainly used for a crystalline phase identification of material which can make available information either as peak height intensity or as integrated intensity - the area under the peak [26]. The crystalline structure of the synthetic zeolite A matched with the standard XRD of typical diffraction peaks ranged from 10 to 350 at 2θ, which indicated the presence of zeolite. Ion exchange of this zeolite with 0.05M silver nitrate and 0.1M copper nitrate individually for 24 hrs showed the same trend as raw zeolite, since no change of peak position had taken place (Figure 5.6). XRD results are material dependent and are more related to the structural quality of the sample [27]. XRD technique has been utilized to detect changes in crystallinity along with the degree of crystallinity. There is a relationship between intensity and crystallinity; intensity changes with the internal order or disorder in the matrix [28].

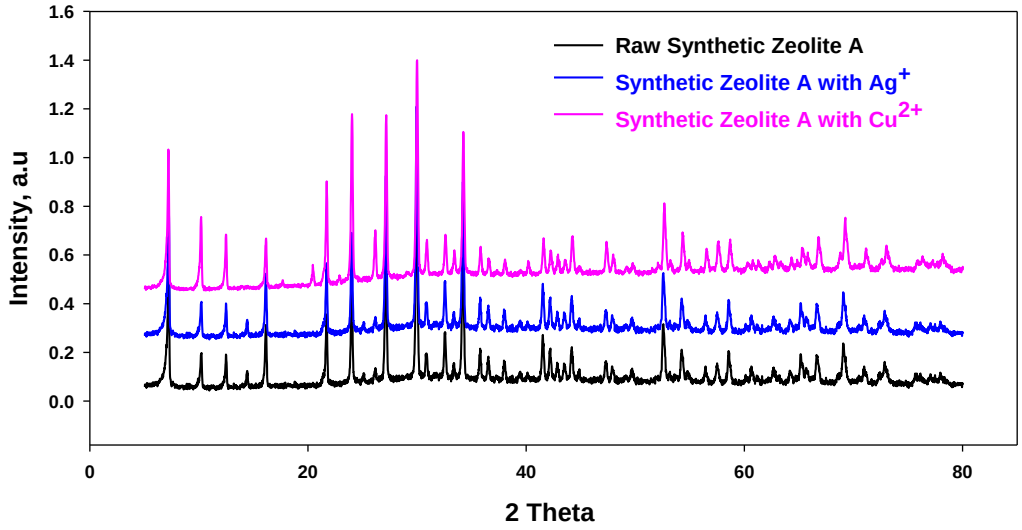

Figure 5.6: Powder X-ray diffraction patterns of synthetic zeolite A, silver with zeolite A and copper with zeolite A

But any remarkable change was not found after the ion exchange in this zeolite. Similar diffraction pattern was also observed without any significant lattice destruction and that complied with other research as well [20]. The functionalization process did not alter any substantial change in the topography of frame-work structure of zeolite as confirmed from the XRD results.

5.4.7 Transfer Efficiency of Additives:

Transfer efficiency of additive to the substrate surface during powder coating spraying is an important parameter for evaluating the efficiency of the powder coating. Transfer efficiency is defined as the mass ratio of the total deposited particles to that of the applied particles. Based upon the reported analysis, it was observed that under normal operating

condition, more powder deposition on to the surface during spraying can be achieved using the coarse powder (mean particle size above 30μm) [29]. But this can result in a thicker film with rough surface after curing [30]. Compared to the coarse powder, ultrafine powders (<25μm) can provide better smooth surface after curing. Although the fine powder can produce a better surface, but the transfer efficiency of the additive with fine powder to the substrate was found to be smaller under normal condition during electrostatic spraying due to the lower charge of the fine powder.

Table 5.5: Additive concentration before and after pressing at different combination of additive and polyester resin (clear coat)

Size of additive, μ	Size of polyester resin, μ	Before pressing		After Pressing and Spraying	
		Additive in powder before spraying, %	Additive on substrate after spraying, %	Additive on substrate (%), particle size, 30μ	Additive on substrate (%), particle size, 55μ
20	35	3.75	1.10	1.53	1.67
20	20	3.75	0.94	1.77	1.98
20	35	5.00	1.25	1.68	1.81
20	20	5.00	1.10	2.00	2.24

Additives (20μm) were mixed with the resin powder (clear coating powder) in a sequential order shown in Table 5.5. Here different combinations of additives (20μm) and resin powder (20 and 35μm) were made by varying the particle size and the ratios of additives (3.75 and 5%). By utilizing a pressing method, the ultimate particle sizes of the

mixture were increased to 30μm and 55μm. Transfer efficiency of additive were measured for all combinations. The best transfer efficiency values (underlined in Table5.5) were found for resin powder (20μm) for final size (30μm, 55μm) for both the additives ratio (3.75 % and 5%).

With additive ratios of 5%, the additive concentration was found much higher at the coated surface compared to the additive ratios of 3.75% based on coated surfaces appearance and color. It was also verified from the color analysis reported in Table 5.6, serial 3, the color (yellowness) increased with amount of additives. Taking into account the best of the reported results, 3.75% additive concentration was selected as the final powder compositions for further analysis. Detailed analysis report shown in Table 5.6 also include the antimicrobial efficiency against microorganisms.

Without any processing (pressing, grinding and sieving) of the final powder the transfer efficiency of the additive was 0.94%, when the particle sizes of both the additive and the resin were 20μm. But after processing when the final particle size changed from 20μm to 30μm, the transfer efficiency increased from 0.94 to 1.77% (increased 88.3%), due to the associated charge increased with the increase of particle size of the powder. The color of the coated surface was expressed in terms of brightness DL, yellowness Db and the overall difference DE from the control coated surface. The control surface was made with raw synthetic zeolite and polyester clear coating. The values shown in Table 5.6 for color analysis were the differences between control surface and the formulated surfaces. From the comparison study between processed (pressing, grinding and sieving) and unprocessed formulations shown in Table 5.6, it was found that the thickness of the coating increased with the increase of the particle size. Considering the merit of all

Table 5.6: Effect of treatments to improve of transfer efficiency on surface properties and antimicrobial efficiency

Treatment , Surface Appearance	Properties of Coating	Antimicrobial efficiency (microorganism present)
1. No treatment Coating surface is very smooth	Particle size 20µ Thickness of coating, 40-45µ Overall color difference from the control surface DL, -0.67, Db- 2.51, DE 2.97	Trial 1: 0 at 3hrs Trial 2: 0 at 4hrs Trial 3: 0 at 4hrs Trial 4: 0 at 4hrs Trial 5: 0 at 4hrs Trial 6: 0 at 4hrs Trial 7: 0 at 5hrs Trial 8: 0 at 5hrs
2. Pressing, grinding and Sieving with 100 mesh screen, coating surface was very smooth	Particle size 30 µ Thickness of coating,45-50µ Overall color difference from the control surface DL, -0.79, Db, -3.19, DE 3.29	Trial 1: 0 at 4hrs Trial 2: 0 at 5hrs Trial 3: 0 at 5hrs Trial 4: 0 at 5hrs Trial 5: 0 at 5hrs Trial 6: 0 at 5hrs Trial 7: 0 at 5hrs Trial 8: 0 at 5hrs
3. Pressing , grinding and Sieving with 150 mesh screen, coating surface has some orange peel	Particle size 55 µ Thickness of coating, 50-55µ Overall color difference from the control surface DL, -0.85, Db-3.43, DE 3.51	Trial 1: 0 at 4hrs Trial 2: 0 at 5hrs Trial 3: 0 at 5hrs Trial 4: 0 at 5hrs Trial 5: 0 at 6hrs Trial 6: 0 at 6hrs Trial 7: 0 at 6hrs Trial 8: 0 at 6hrs

*Db= Yellowness, DE=Overall difference

the factors that influenced the acceptability of the coated surfaces, the particular surface prepared from the powder with the particle size of 55µm found least acceptable in terms of smoothness and color.

All three parameters (DL, Db and DE) for color analysis were also increased with the increase of particle size. No considerable change was found in the antimicrobial efficiency between these three different formulations shown in Table 5.6. The yellowness of the surface is an indicator of the amount of silver reduction as well as the antimicrobial effectiveness against microorganism. Increased yellowness means that a part of the silver ions were reduced (Ag^{+} to Ag^{o}) during curing of the surfaces. As a result of this phenomenon, the antimicrobial efficiency is anticipated to reduce with time or number of exposures. Based upon all results reported in Table 5.6, number 2 Formulation was selected as the best combinations with improved transfer efficiency which is vital for durability as well as the antimicrobial effectivity.

The relative effects (shown in table 5.5) of major influencing factors (i.e. particle size (X_1), additive ratio (X_2) and final particle size (X_3) after treatment) on the response of additive (Y) is achieved by t-test, from the two levels three factors full factorial designs (2^3) matrix by statistical software MINITAB 15. From the experimental data (experimental conditions are shown in Table 5.7), the following regression model is established,

$$Y= 0.579667+ 0.0118667\ X_1 + 0.289607\ X_2+ 0.0124\ X_3 - 0.00533\ X_1X_2-2.4*10^{-4}X_1X_3+ 0.0032\ X_2X_3$$

Table 5.7: Development of regression model and relative effects of the variables

TERM	Coef	SE Coef	T-test	Probability
Constant	1.83500	0.005000	367.000	0.002
Resin Particle size, μ	-0.16250	0.005000	-32.500	0.020
Additive ratio, %	0.09750	0.005000	19.500	0.033
Final particle size, μ	0.09000	0.005000	18.000	0.035
Resin particle size * Ratio	-0.02500	0.005000	-5.000	0.126
Resin particle size * Final particle size	-0.02250	0.005000	-4.500	0.139
Ratio * Final particle size	0.00250	0.005000	0.500	0.705

The R-Sq (adj) value is 99.61% which represents that the data fit well in the regression model. It is found that the particle size, additive ratio and final particle size have a strong effect on the amount of additive (Y). A confidence level of 95% is used to examine the significance of the studied variables, and therefore the P-value less than 0.05 indicates that the effect of corresponding variable is significant. From the t-test results it is observed that the coefficient for the resin particle size, μ (P-value = 0.020) is more significant compared to the coefficients for either additive ratio, % (P-value = 0.020 < 0.033) or final particle size (P-value = 0.020 < 0.035). On the other hand, interaction effect of those factors are not found to be significant as the P-values are greater than 0.05. The P-values in table shows the order of significant factors as resin particle size > additive ratio > final particle size.

5.4.8 Effect of low curing additive:

Functionalization of synthetic zeolite A was done with silver nitrate and was used as an additive in the antimicrobial powder coatings. Normal powder coatings were cured at 180-200˚C for 10-15min. But the reduction of silver ions took place during the curing at that temperature range, as such the additives became inactive quickly resulting in remarkable drop in the antimicrobial efficiency. To impede this reduction process some low curing additives were added within the formulation, so that the curing process can be done at a lower temperature. Two different types of low curing additives were used where, one was known as promoter 1 (2 methylimidazole) and the other as promoter 2, TP 316 (Onium salt). Different proportions (0.5, 0.75 and 1%) of the promoter 1 were added to the antimicrobial formulations, of which one contained silver ions only and the

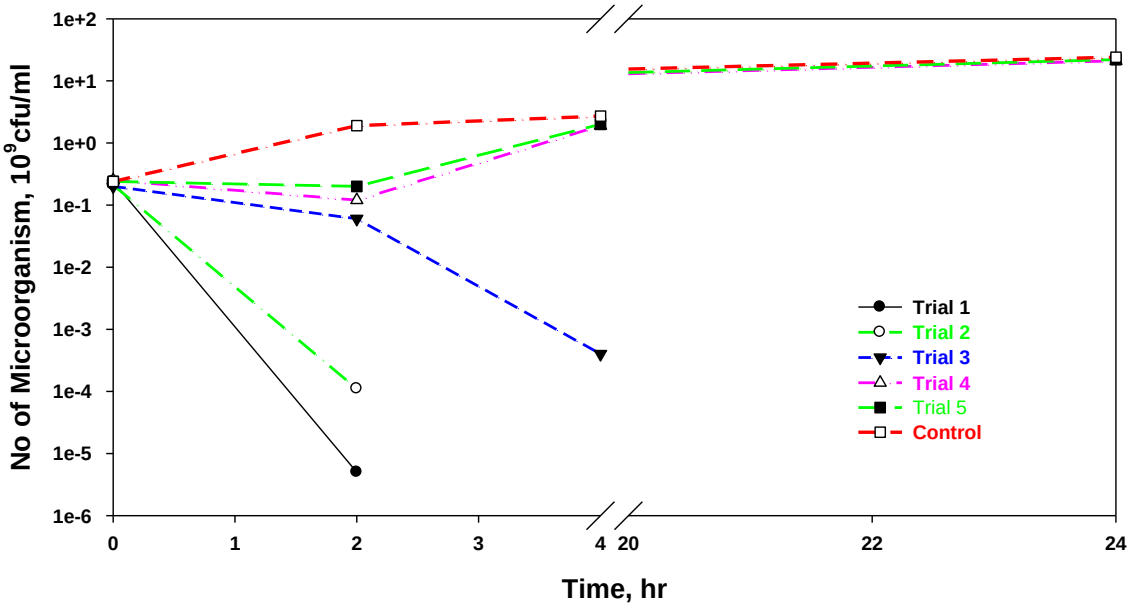

Figure 5.7: Synthetic Zeolite (Ion exchanged with 0.05M $AgNO_3$) cured at 200^{o}C for 15 min

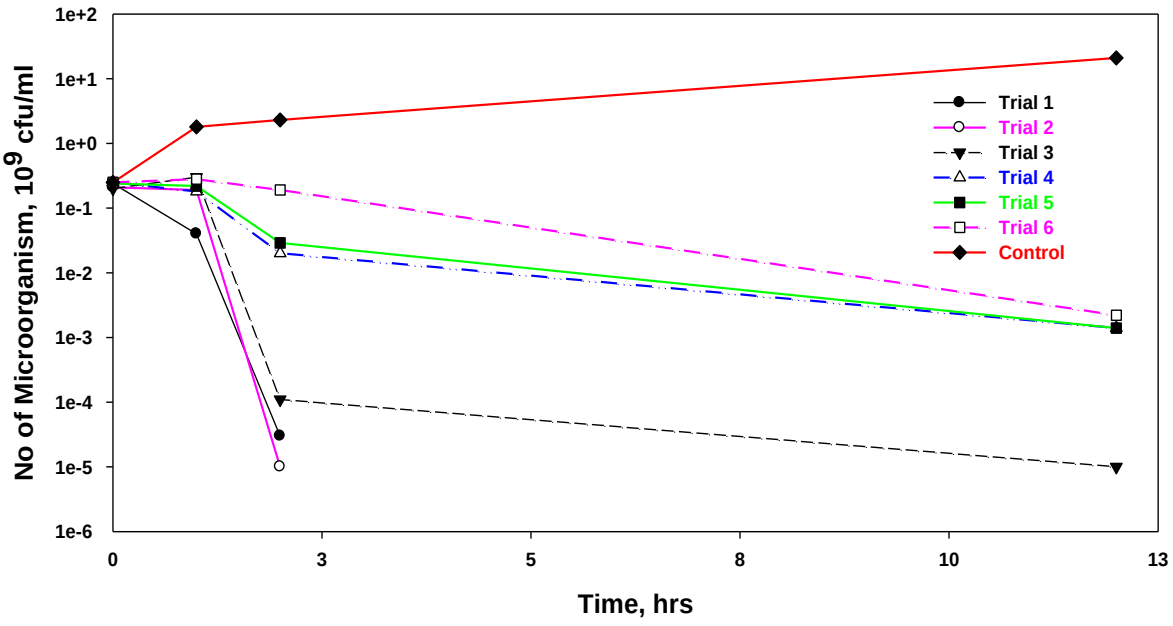

Figure 5.8: Synthetic Zeolite (Ion exchanged with 0.05 M $AgNO_3$) + 0.5% Promoter 1 cured at 150^oC for 1 hr

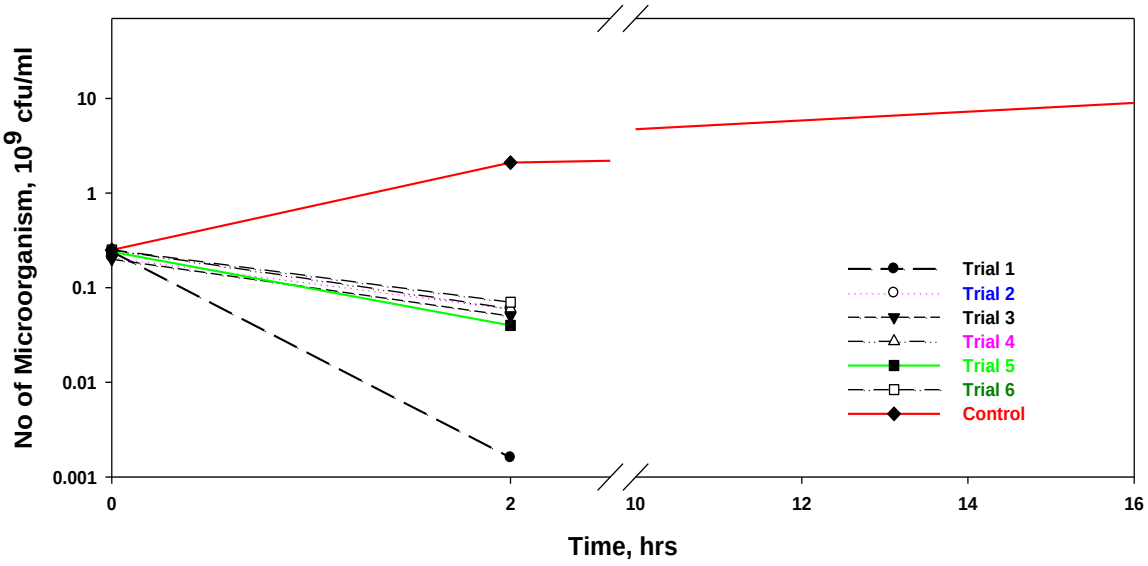

Figure 5.9: Synthetic Zeolite (Ion exchanged with 0.05 M $AgNO_3$, 0.1M$Cu(NO_3)_2$) cured at 200^oC for 15 min

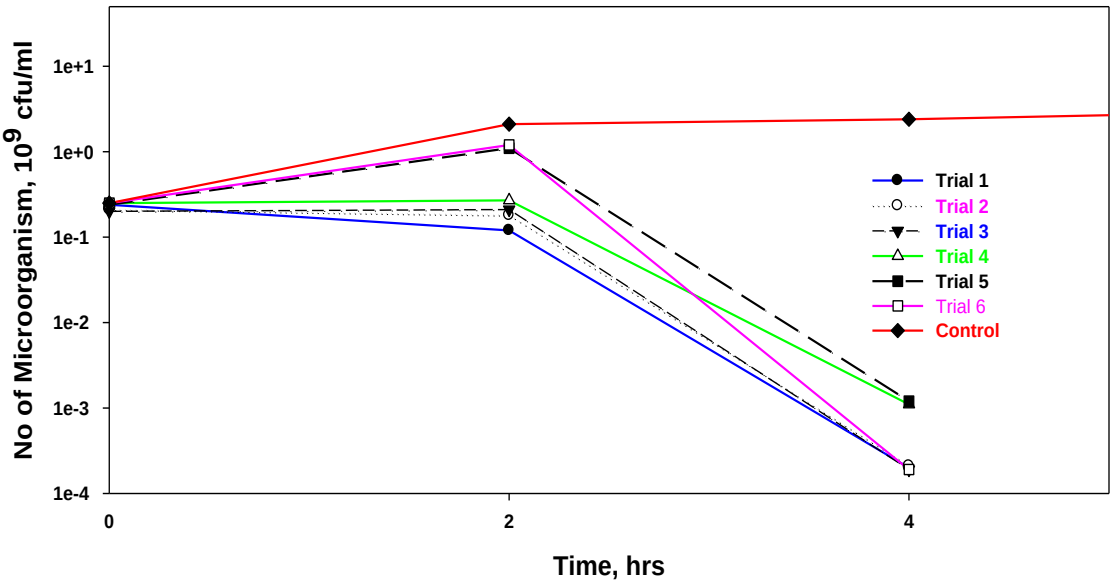

Figure 5.10: Synthetic Zeolite (Ion exchanged with 0.05 M $AgNO_3$, 0.1M$Cu(NO_3)_2$) + 0.5% Promoter 1 cured at 150^oC for 1 hr

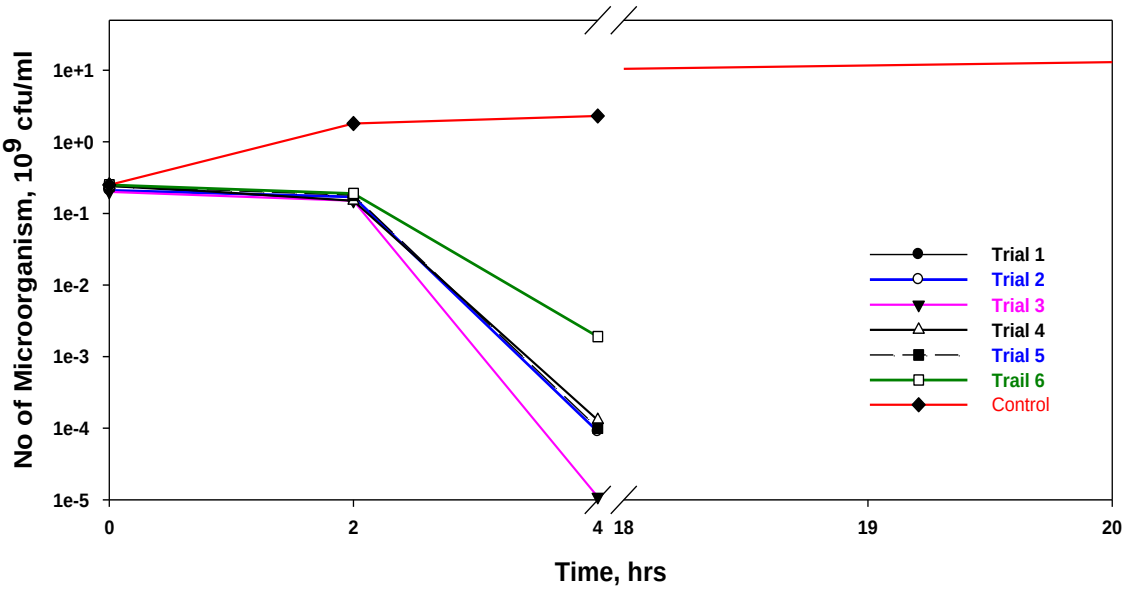

Figure 5.11: Synthetic Zeolite (Ion exchanged with 0.05 M $AgNO_3$, 0.1M$Cu(NO_3)_2$) + 0.5% Promoter 1 + 0.3% Promoter 2 cured at 150^oC for 1 hr

other contained silver with copper ions (6 in total). They were all cured at 150^{o}C for 40 and 60 minutes respectively. But the amount of promoter did not significantly affect the curing. Physical and chemical properties of those surfaces were tested by impact resistance, pencil hardness and rubbing test with MEK as well as the color of the coated surface. Surfaces cured for 40 minutes passed only the rubbing test. But the surfaces cured for 60 minutes at 150˚C have passed all the tests shown in appendix. To find the brightness and the yellowness of the coating and to compare with the control surface, the color of the surfaces were analyzed by Data color tools. Yellowness appeared due to the reduction of silver. One of the target of this study was to lessen the reduction of silver by lowering the curing temperature. The sample containing silver and copper with 5% promoter 1 and 0.3% promoter 2 showed the lowest yellow value (3.77) compared to other samples but lagged in providing improved efficiency than the surface containing only 5% promoter (yellowness 5.56).

Antimicrobial efficiency for all formulations were tested by exposing the same surface to microorganisms for several cycles to find its durability. Efficiency against microorganism for the surface made from additives containing silver ions only is shown in Figure 5.7 and Figure 5.8. These two surfaces contained higher concentration of silver ions, which has been reduced to Ag^{o} during the curing. The rate of reduction of microorganism on those surfaces reduced drastically with the exposure duration. The reason was simply due to the unavailability of the silver ions on those surfaces. On the contrary, surfaces containing low curing additives (Figure 5.8) showed better performance than the other surfaces (Figure 5.7) in terms of antimicrobial activity.

Antimicrobial efficiency of the surfaces prepared from additives containing silver and copper ions were also checked. It was mentioned earlier that the reduction of silver ions was retarded by the addition of copper ions in additives during the curing and this observation supported the justification for the enhanced antimicrobial efficiency as shown in Figures 5.9 and 5.10. But the addition of low curing additives (Figure 5.10) was not helpful to enhance the reduction rate of the microorganism from surfaces as shown in Figure 5.9. The reduced efficiency was observed during the durability analysis for the low curing additive containing surfaces. The reason behind this was due to the increase in disordered Cu^{2+} which may have blocked the pore of the zeolites that restricted the movement of the Ag^{+} ions [31].

On the other hand, the surfaces containing Promoter 2 (TP, (Figure 5.11) was more effective in terms of antimicrobial efficiency than the surfaces made for the test as shown in Figure 5.10. It can be concluded that the low curing additives which were used in the formulations of this study were not sufficiently effective for the enhancement of the antimicrobial efficiency as well as the durability of the surfaces.

5.4.9 Encapsulation of Ag^{+} and Cu^{2+} containing zeolite with PVA:

The main purpose of the encapsulation was to provide a barrier to decrease the release rate of active components from the coated surface as well as to increase the durability of the coated surface. A polymer barrier was applied to stabilize the morphology of the polymer ion composite, which is useful to control the silver ion release rate [7]. The release profile of silver ion can be tailored by polymer encapsulation with binding sites

[32]. The surface made from the additives containing Ag^{+} and Cu^{2+} ions was very active against microorganisms as shown in Figure 5.8. It showed a 100% reduction of microorganisms within 2 hrs. The reason was that, the ions were readily available for inactivation of the microorganisms and thereby resulting in very high release rate of the additives.

When this additive was mixed with 2% and 6% PVA solution for the encapsulation purpose, intra particle diffusion took place through PVA. Cu^{2+} and Ag^{+} ions were adsorbed within the PVA solution by the formation of ionic bonds with the hydroxyl groups in the PVA [33]. Table 5.8 showed the antimicrobial efficiency of an additive containing only with Ag^{+} and the other with Ag^{+} and Cu^{2+} ions.

Both of those surfaces were made on to the bare aluminium surface and also on to underneath coating (clear coat) with clear polyester coating. Surface coated on to the bare aluminium surface showed small cracks (<500µm interval) after some trials (no of cycle used), due to the presence of hydrophilic PVA encapsulation on the active zeolite component, though antimicrobial activity was prevailing on the surface. The hydrophilic polymer at that concentration absorb excessive amount of moisture in to the coated surface which causes corrosion on the aluminum substrate and gradually localized chemical instability and mechanical stress in the coated surface. This hydrodynamic pressure within the coating for the presence of hydrophilic polymer is responsible for the cracking on the surface. But when an additional clear coating was added underneath the active coating, these cracks disappeared. This additional coating prevents moisture absorption down to the metal surface.

The surfaces made from 6% and 2% PVA encapsulated additives were checked for antimicrobial efficiency against the microorganism until 10th trial shown in Table 5.9 and 15th trial shown in Table 5.10 respectively. There was a decrease of reduction rate observed upon trials with 6% PVA encapsulated additive containing coated surface. But 2% PVA encapsulated additive containing coated surface was found to the more active against microorganism in terms of release rate of additive. The combination of cations and the hydroxyl groups of PVA was needed to optimize for better cross-linking.

Table 5.8: Color analysis of coated surface containing PVA encapsulate and unencapsulate additives (Ag^{+} and Cu^{2+})

Sl.No	SURFACE (1:19)	DL	Da	Db	CIE DE
1	Syn + 0.05MAg^{+}	- 3.54	-1.34	17.05	19.34
2	Syn + 0.05MAg^{+}+ 6% PVA	-2.04	-1.37	12.41	12.63
3	Syn + 0.05MAg^{+}+ 2% PVA	-3.21	-1.87	13.66	14.81
4	Syn + 0.05MAg^{+}+ 0.1MCu^{2+}	-0.49	-1.45	4.41	4.66
5	Syn + 0.05MAg^{+}+ 0.1MCu^{2+}+ 6% PVA	-1.80	-1.56	4.08	4.57
6	Syn + 0.05MAg^{+}+0.1MCu^{2+} + 2% PVA	-2.09	-1.41	4.48	4.73

*Db= Yellowness, DE=Overall difference

It proved that the cross-linking here helped to hold the polymer which was working as the extra barrier for the cations, and also reduced the release rate of active agent. In this study, it was found that 2% PVA encapsulation was better fitted for this particular

additive than the 6% PVA encapsulation based on the antimicrobial efficiency following the release rate of the active agent.

Table 5.9: Antimicrobial Efficiency of 6 % PVA encapsulated additive containing surface

Sl. No	Surfaces	TRIAL 1	TRIAL3	TRIAL5	TRIAL 7	TRIAL 10
1.	Zeolite with Ag^{+}ions	0 at 6 hrs	0 at 6 hrs	0 at 7 hrs	Not active	Not active
2.	Zeolite with Ag^{+} ions on additional coating	0 at 6 hrs	0 at 6 hrs	0 at 7 hrs	0 at 7 hrs	Not active
3.	Zeolite with Ag^{+} and Cu^{2+} ions	0 at 5 hrs	0 at 5 hrs	0 at 6 hrs	0 at10 hrs	0 at 12 hrs
4.	Zeolite with Ag^{+} and Cu^{2+} ions on additional coating	0 at 5 hrs	0 at 5 hrs	0 at 6 hrs	0 at10 hrs	0 at 12 hrs

*Db= Yellowness, DE=Overall difference

Previously it was indicated that silver ions containing zeolite undergo reduction during curing process. Due to the conversion of Ag^{+} to Ag^{o}, silver has lost the instant antimicrobial property. For making the Ag^{o} active they needed a hydrophilic environment to release Ag^{+} from Ag^{o}. PVA encapsulation creates a favourable condition for this Ag^{o} to be active against microorganism, and helps to reduce the release rate of Ag^{+} from Ag^{o}. Color analysis of all coated surfaces are shown in Table 5.8 provided a clear picture about the yellowness (Db) of the coated surface, which came from the color of the metallic silver. PVA coated surfaces (2, 3) with only Ag+, showed less yellowness (Db) than coated surface 1, which was not encapsulated with PVA. This was an indication of lower reduction of silver happened during the curing process and thus it was found to

have a similar trend of microorganisms reduction efficiency. Effectiveness against microorganism in Sample 2 and 3 are presented in Table 5.9 and 5.10 respectively. When considered the samples containing both of the ions, the color of the surface after curing

Table 5.10: Antimicrobial Efficiency of 2 % PVA encapsulated additive containing surface

Sl. No	Surfaces	TRIAL 1	TRIAL 4	TRIAL 7	TRIAL 10	TRIAL 15
1.	Zeolite with Ag^{+} ions	0 at 8 hrs	0 at 8 hrs	Not active	Not active	Not active
2.	Zeolite with Ag^{+} ions on additional coating	0 at 8 hrs	0 at 8 hrs	0 at10 hrs	Not active	Not active
3.	Zeolite with Ag^{+} and Cu^{2+} ions	0 at 6 hrs	0 at 7 hrs	0 at 8hrs	0 at 8 hrs	0 at 9 hrs
4.	Zeolite with Ag^{+} andCu^{2+} ions on additional coating	0 at 6 hrs	0 at 7 hrs	0 at 8 hrs	0 at 8 hrs	0 at 9 hrs

showed comparable values with the control surface. All the values shown in Table 5.8 were obtained from the difference between the antimicrobial coated surface and the control surface. Due to the presence of copper ions in those surfaces, silver seems to remain as Ag^{+}, which can also be correlated with the yellowness of the surface from b values. All these samples had very effective efficiency against microorganism as shown in Tables 5.9 and 5.10. Moreover the decrease of Ag^{+} ion release rate was due to the decrease of electrolyte movement, as the barrier thickness had increased. This extra polymer coating also delayed the movement of silver ion from additive to the coating surface with the microorganism, which lead to a lower release rate of silver ions [34].

5.4.10. Leaching analysis by ICP-OES:

The release rate of Ag^+ from the coated surface in presence of microorganism was analysed by ICP-OES after extracting the microorganism from the exposed coated surface at certain time shown in Table 5.11. It was found that the additive encapsulated with 2% PVA gave extra shield for the active agent incorporated into the coated surface. The amount of leached Ag^+ from the surface was 0.16ppm after 8 hrs of exposure, but the amount of Ag^+ from the surface containing additive which is not encapsulated with PVA was 0.19ppm at same time. During the durability analysis it was observed from previous experiment that all microorganisms died within first 2 hrs after the exposure on the coated surface containing additives with silver and copper in ionic form.

Table 5.11: Leaching test of silver ion during exposure of microorganism

Additive with	Amount of silver (ppm) at the exposed time				No of microorganism remain, 10^9cfu /ml
	2 hrs	4 hrs	8 hrs	24 hrs	
Control	0	0	0	0	21 after 24 hrs
Ag^+, Cu^{2+}	0.14	0.16	0.19	0.22	0 after 2 hrs
Ag^+, Cu^{2+} encapsulated with 2% PVA	0.031	0.10	0.16	0.19	0 after 6 hrs

The amount of silver leached out from the same coated surface was found 0.14 ppm after 2hrs and 0.16 ppm after 4 hrs. There was no significant leaching observed on the control surface even after 24 hrs of exposure. But when the additive was encapsulated with 2% PVA, the leaching rate of silver ion was reduced and took 6 hrs for complete reduction of

microorganism from 10^6cfu/ml. Excessive silver leached out from the additive without PVA encapsulation after 2hrs does not needed for killing the microorganisms, so PVA encapsulation helps to reduce the extra leaching of Ag^+ as well as increasing the durability of that coated surface.

5.4.11. Effect of autoclave on coated surface:

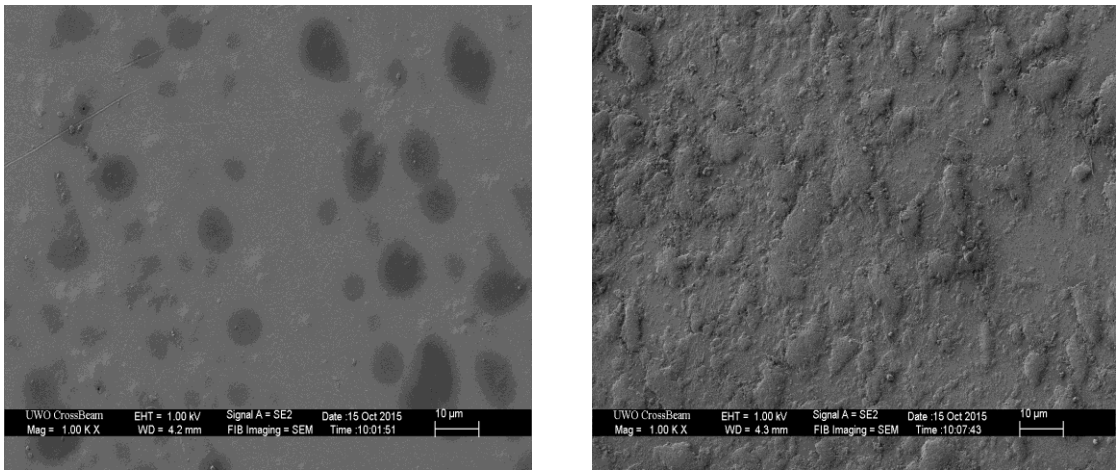

Antimicrobial surface before Autoclaving

Antimicrobial surface after Autoclaving

Figure 5.12: Surface morphology of coated surface after autoclave test

Autoclave testing of protective coatings was done to compare competing coating products as well as, to evaluate new coatings and to determine the effect of corrosion and chemical inhibitors on the coating integrity. Steam sterilization is normally used due to its short operation time, non-toxicity and safety [35]. During the autoclaving analysis of this study, the coated surfaces were exposed to relatively high temperature and water vapor in

a very highly concentrated form. These tests were also carried out to monitor the changes in surface morphology and the phase composition of coatings which possessed resistance to the worst corrosion. These were characterized by antimicrobial efficiency

Table 5.12: Effect of Autoclave on surface color and antimicrobial effectivity

Zeolite containing Ag^{+}, Cu^{2+} ions coated with 6% PVA sprayed on Initial clear coating	DL	Da	Db	CIE DE	Microorganism present
1st	-4.85	-1.91	7.92	8.36	0 at 24 hrs
2nd	-5.72	0.64	16.92	17.87	0 at 24 hrs
3rd	-13.92	3.30	23.84	27.80	0 at 24 hrs
4th	-15.9	4.29	27.05	31.67	0 at 24 hrs

*Db= Yellowness, DE=Overall difference

and the change in color of the coating. A flocculent structure (Figure 5.12) with non-uniform surface might have changed the orientation of additive containing silver and copper ions within the coating, which prevented the silver to move out easily in contact with the microorganism and have formed the oxides due to this adverse effect [36]. Antibacterial efficacy tests also revealed the same conclusions as it gradually reduced its activity from 1st autoclaving run to the 4th run but showed full reduction of microorganisms until 4th autoclaving. Color change of the coated surfaces was also observed using the color meter after every autoclaving run shown in Tables 5.12 and 5.13. Coated surface lost their initial color and became light brown, probably due to

silver present in the coating during autoclaving. It should be mentioned that control coated surfaces which had no silver, did not show any color change. The result of this study had similarity to that of the microbial testing tape which contains silver thiosulphate decomposed to black silver sulfide using the steam sterilization

Table 5.13: Effect of Autoclave on surface color and antimicrobial effectivity

Zeolite containing Ag^{+}, Cu^{2+} ions coated with 2% PVA sprayed on Initial clear coating	DL	Da	Db	CIE DE	Microorganism present
1st	-5.38	-1.42	7.62	8.85	0 at 24 hrs
2nd	-6.28	0.13	18.51	19.54	0 at 24 hrs
3rd	-7.68	0.58	18.48	20.02	0 at 24 hrs
4th	-10.75	0.8	18.41	21.33	0 at 24 hrs

*Db= Yellowness, DE=Overall difference

conditions (US patent, 4857450). Autoclaving could alter the ionic silver to insoluble hydroxides and oxides. Other sterilization method, such as ultraviolet treatment is also challenging, due to the photo sensitivity of silver [37].

5.4.12. Bactericidal effect (Membrane Integrity/LDH Leakage):

Toxicity analysis was done to find the loss of cell membrane integrity and was measured based on the production of lactate dehydrogenase (LDH), is a soluble cytosolic enzyme, which exposes due to the damage of loss of cell membrane. The amount of fluorescence

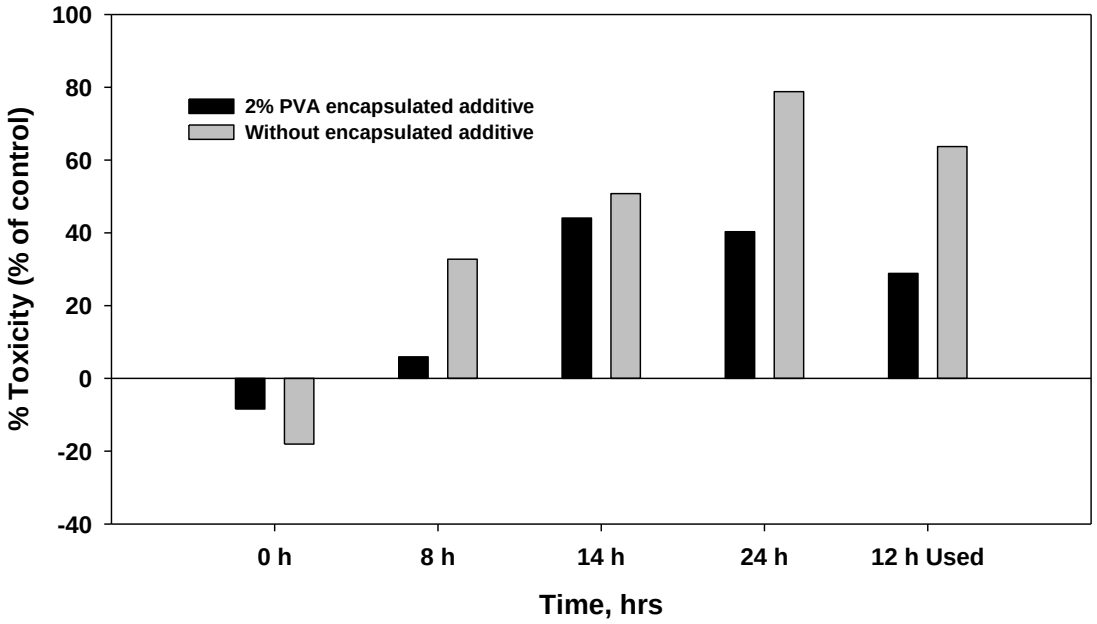

Figure5.13: Toxicity analysis of antimicrobial surfaces with Ag^{+} and Cu^{2+} for extended time and period

produced is used to assess the toxicity resulting from the toxic effects of silver to the microorganisms [38]. Fluorescence was used to measure the LDH amount at excitation and emission wavelengths of 560nm and 590nm respectively and measured data are reported as percentages of the control coated surface [39]. No of lysed cells are comparative to the fluorescence. Production of LDH was calculated after exposure to the microorganism on the new coated surface at different times. An increase in LDH leakage in the culture medium was observed with the increase of contact time with the microorganism due to the plasma membrane damage of cells. LDH production was also confirmed from the observation for the analysis with the 15 times used coated surface and proved the effectivity of the formulation. The fluorescence produced for the analysis where the coated surface contains the encapsulated additives with 2% PVA was lower than the PVA un-encapsulated additives. This also again proved that leaching of silver

from the surface was low for the PVA encapsulated additives, which will help to increase the durability of the surface.

5.5 Conclusions

Silver has been used as an antimicrobial agent from ancient time, but with the rapid improvement of modern technology and consumer demand, improved products with much higher efficiency and durability are more demanding in every sector of our daily life. For the application of ultra-fine powder coating as an antimicrobial surface, additives were prepared by the incorporation of silver and copper ions into zeolite by ion-exchange and effectiveness with durability of the surfaces were checked against microorganisms.

It was found that incorporation of copper was needed to reduce the reduction rate of silver during the curing period of the powder coating process. Copper ions prevented the reduction of silver ions and helped silver ions to remain in its original state inside the additive by getting reduced itself. The amount of copper ions at particular concentration of silver ions was an important factor for a transparent coated surface, which was optimized by ion exchange process with different combinations of silver and copper. XPS analysis in this study proved that copper ions in the additive had reduced before silver ions and thereby was protecting the silver ions from reduction.

Different characterization techniques (ICP, XRD and TGA) were used for identifying the physical changes after functionalization of synthetic zeolite A with silver and copper. It is known that silver ion is more active than any other form of silver but its efficiency against microorganism is directly related to the concentration of silver ion and

availability. Leaching of silver ions from the coated surface into the microorganism was analyzed by ICP. The release rate of the active agents is reported to have slowed down by encapsulation of the additives with 2% PVA. This polymeric encapsulation helped to reduce the release rate of active agent as well as increased the durability of the formulated antimicrobial coated surface. Additional coating was applied underneath the active coating to avoid cracking in the coating as cracking appeared due to the encapsulation of 6% PVA on the additives from the development of hydrodynamic pressure inside the coating.

However, the transfer efficiency of the additives during spraying was improved by increasing the particle size of the final powder, which also helped to reduce the production cost as well as the system loss. The curing process of the powder coated surface was done at 200^{o}C for 15 minutes. Silver ions were reduced to metallic silver during this curing process. Low curing additives were incorporated into the resin system, which helped to cure the surface at lower temperature than 200^{o}C. The effect of low curing additives on the reduction rate of silver ions was analyzed by checking the antimicrobial efficiency analysis, which was found not very satisfactory. Mechanical and chemical properties of low curing additives containing surface in this study were also checked by following ASTM standards.

The effect of autoclave on the surface color and antimicrobial efficiency was checked to find the applications of these coatings on the products that require sterilization process. Hydrophilic polymer encapsulation of the additive containing silver and copper ions can be used for better surface and coating property, which has huge potential in biomedical applications.

References:

1. Inglezakis Vassilis J. The concept of capacity in zeolite ion-exchange systems (2005) *Journal of Colloid and Interface Science*. vol 281, no. 1, Pages 68-79.

2. Haggerty GM, Bowman RS.,1994, Sorption of chromate and other inorganic anions by organo-zeolite, *Environ. Sci. Technol.* vol. 28, no.3,pages 452– 458.

3. Watanabe Y, Yamada H, Tanaka J, Komatsu Y, Moriyoshi Y, 2005, Ammonium Ion Exchange of Synthetic Zeolites: The Effect of Their Open- Window Sizes, Pore Structures, and Cation Exchange *Capacities, Separation Science and Technology*, vol. 39, no. 9, pages 2091-2104.

4. Shoumkova A.,2013, Zeolites for water and wastewater treatment: An overview. *Australian Institute of High Energetic Materials*.

5. Inglezakis VJ, Loizidou MD, Grigoropoulou HP (2002) Equilibrium and kinetic ion exchange studies of Pb^{2+}, Cr^{3+}, Fe^{3+} and Cu^{2+} on natural clinoptilolite. *Water Res*. vol.36, pages 2784– 2792.

6. Feied, Craig. (2004). Novel Antimicrobial Surface Coatings and the Potential for Reduced Fomite Transmission of SARS and Other Pathogens. *MD*. vol.1, 1-22.

7. Alissawi N, Zaporojtchenko V, Strunskus T, Hrkac T, Kocabas I, Erkartal B, Chakravadhanula VSK, Kienle L, Grundmeier G, Garbe-Schönberg D, Faupel F, 2012, Tuning of the ion release properties of silver nanoparticles buried under a hydrophobic polymer barrier. *J Nanopart Res.* vol 14, pages 928.

8. Rana DS, Chaturvedi DK, Quamara JK, 2011, XRD and SEM Investigation of Swift Heavy Ion-Irradiated Polyvinylidene Fluoride Thin Films. Journal of Materials Engineering and Performance, vol. 20, pages276–282.

9. Coruh S (2008) Treatment of copper industry waste and production of sintered glass-ceramic. *Waste Manage. Res.* vol. 24. pages 234-241.

10. Akbar S, Shah TH, Shahnaz R, Sarwar G. , 2007, Thermal studies of synthetic NaX Zeolite and its Zinc Exchanged Forms. *Journal of Chemical Society*, Pakistan, vol. 29.no.1, pages 5-11.

11. Fiddy S, Petranovskii ,V Ogden, Steve, Iznaga, Inocente Rodriguez, 2007, Characterization of Binary Ag-Cu Ion Mixtures in Zeolites: Their Reduction Products and Stability to Air Oxidation, *Vaccum*, vol.882, no. 1, page 631

12. Breckw DW, Eversoler G, Miltont M, Reeda B, 1956, Thomas TL. *Journal of the American Chemical Society*. vol.78, no.23,

13. De Cremer G, Gonzalez EC, Maarten B, Roeffaers J, Moens B, Ollevier J, Van der Auweraer M, Schoonheydt R, Jacobs PA, De Schryver FC, Hofkens J, De Vos DE, Sels BF, Vosch T., 2009, Characterization of Fluorescence in Heat-Treated Silver-Exchanged Zeolites. A*m. Chem. Soc*., vol. 131, pages 3049–3056.

14. Chiai H, Fukushima S, Fujikawa M, Yamamura H., 1976, Mechanical and thermal properties of Poly (vinyl alcohol) crosslinked by borax. *Polymer Journal,* vol 8, no 1, pages 131-133.

15. Gougazeh M, Buhl J., April 2014, Synthesis and characterization of zeolite A by hydrothermal transformation of natural Jordanian kaolin. *Journal of the Association of Arab Universities for Basic and Applied Sciences,* vol. 15, pages 35–42.

16. Shikunov I, Lafer LI, Yakerson VI, Mishin IV, Rubinshtein AM, January 1972, Infrared spectra of synthetic zeolites. *Bulletin of the Academy of Sciences of the USSR, Division of chemical science*, vol 21, no.1, pages 201-203.

17. Shameli K, Ahmad MB, Zargar M, Yunus W, Ibrahim NA., 2011, Fabrication of silver nanoparticles doped in the zeolite framework and antibacterial activity *International Journal of Nanomedicine Dovepress*, vol.6, pages 331-341.

18. Standard guide to charge control and charge referencing techniques in X-ray photoelectron spectroscopy, *ASTM standard*. E 1523 e 03; 2003.

19. Ferraria AM, Carapeto AP, Botelho do Rego AM. July 2012, X-ray photoelectron spectroscopy: Silver salts revisited, *Vacuum*, vol.86, no. 12, pages 1988-1991.

20. Nima ZA, Mahmood M, Xu Y, Mustafa T, Watanabe F, Nedosekin DA, Juratli MA, Fahmi T, Galanzha EI, Nolan JP, Basnakian AG, Zharov VP, Biris AS., May 2014, Circulating tumor cell identification by functionalized silver-gold nanorods with multicolor, super-enhanced SERS and photothermal resonances, Scientific Report 4, article no 4752, Volume 4,

21. Yasuda Y, Ide E, Morita T. 2011, Evaluation of Copper Oxide-Based Interconnecting Materials. *The Open Surface Science Journal*, vol.3, pages 123-130.

22. Petranovskii V, Gurin V, Bogdanchikova N, Licea-Claverie A, Sugi Y, Stoyanov E. 2002, The effect of SiO_2/Al_2O_3 molar ratio in mordenite upon the optical appearance of reduced copper *Materials Science and Engineering* A, vol. 332, pages 174–183.

23. Reed TB, Brec DW.,1956, Crystalline Zeolites. II. Crystal Structure *of* Synthetic Zeolite, Type A, Journal of americal Chemical Society, vol 78, pages 5972-5977.

24. Hutson ND, Reisner BA , Yang RT , Toby BH. 2000, Silver Ion-Exchanged Zeolites Y, X, and Low-Silica X: Observations of Thermally Induced Cation/Cluster Migration and the Resulting Effects on the Equilibrium Adsorption of Nitrogen. *Chem. Mater.*, vol. 12, no.10, pages 3020–3031.

25. Ashrafi F, Babanejad SA, Rajabnia Baboli A, 2010, A study on optical characteristics of amorphous structure (Vitreous) including oxides of main and transitional elements in binary system B2O3 – CaO, *Der Chemica Sinica*, vol.1,no. 3,pages 1-6.

26. Mohd Bakhori S. K, Abd. Raof N.H, Ng S.S. H. Abu Hassan, Hassan Z, 2011, Photoluminescence and XRD Crystalline Studies of InxAlyGa1-X-Yn Quaternary Alloys. *IOP Conf. Series: Materials Science and Engineering*. 17

27. Naoto Yagi, 2003, An X-Ray Diffraction Study on Early Structural Changes in Skeletal Muscle Contraction, *Biophys J*, vol.84, no. 2, pages 1093–1102.

28. Meng X., Zhang H., Zhu J., 2009, Characterization of particle size evolution of the deposited layer during electrostatic powder coating processes, *Powder Technology*, vol.195, no.3, pages 264-70.

29. Zhu J., Zhang H., 2004, Fluidization additives to fine powders, *US Patent* 6833185.

30. Top A, Ülku S., 2004, Silver, zinc, and copper exchange in a Na-clinoptilolite and resulting effect on antibacterial activity. *Applied Clay Science*, vol 27, pages 13–19.

31. Reidy B, Haase A, Luch A, Dawson KA, Lynch I, 2013, Mechanisms of Silver Nanoparticle Release, Transformation and Toxicity: A Critical Review of Current Knowledge and Recommendations for Future Studies and Applications. *Materials*, vol. 6, pages 2295-2350.

32. Jamnongkan T, Wattanakornsiri A, Wachirawongsakorn P, Supranee Kaewpirom S., 2014, Effects of crosslinking degree of poly(vinyl alcohol) hydrogel in aqueous solution: kinetics and mechanism of copper(II) adsorption. *Polym. Bull.* vol. 71, pages1081–1100.

33. Yliniemi K, Özkaya B, Alissawi N, Zaporojtchenko V, Strunskus T, Wilson BP, Faupel F, Grundmeier G,2012, Combined in situ electrochemical impedance

spectroscopy- UV/Vis and AFM studies of Ag nanoparticle stability in perfluorinated films. *Mater Chem Phys* ,vol. 134, pages 302–308.

34. Senthilkumar V, Vickraman P.,(2010 Structural, optical and electrical studies on nanocrystalline tin oxide (SnO_2) thin films by electron beam evaporation technique, *Journal of Materials Science, Materials in Electronics*, vol.21, no. 6, pages 578-583.

35. Chen Y, Nie X, Northwood DO, 2010, Investigation of Plasma Electrolytic Oxidation (PEO) coatings on a Zr–2.5Nb alloy using high temperature/pressure autoclave and tribological tests. *Surface & Coatings Technology*, vol. 205, pages 1774–1782.

36. Nagy A, Harrison A, Sabbani S, Munson RS Jr, Dutta PK, Waldman W J., 2011, Silver nanoparticles embedded in zeolite membranes: release of silver ions and mechanism of antibacterial action. *Int J Nanomedicine*. vol. 6, pages 1833–1852.

37. Soh Fonglim, Yu Mingzheng, Shuai Wenzou, Andj Paulchen, 2008,Characterization of Copper adsorption onto an Alginate Encapsulated Magnetic Sorbent by a Combined FT-IR, XPS,andMathematical Modeling Study,*Environ. Sci. Technol.*, vol. 42, 2551–2556.

38. Lun Li, Jie Sun, Xiaoran Li, Yan Zhang, Zhaoxu Wang, Chunren Wang, Jianwu Dai Qiangbin Wang, 2012, Controllable synthesis of monodispersed silver nanoparticles as standards for quantitative assessment of their cytotoxicity, *Biomaterials,* vol.33, pages 1714-1721.

39. C. Carlson, S. M. Hussain, A. M. Schrand, L. K. Braydich-Stolle, K. L. Hess, R. L. Jones,and J. J. Schlager, 2008, Unique Cellular Interaction of Silver Nanoparticles: Size-Dependent Generation of Reactive Oxygen Species, *J. Phys. Chem.* vol. 112,pages 13608–13619.

CHAPTER 6

Efficiency of Silver Nanoparticles on Zeolite Surface as an Antimicrobial Additive Embedded in Ultra-fine Powder Coated Surfaces

6.1 Abstract

Silver nano particles were synthesized on the surface of synthetic zeolite A by a chemical reduction method followed by addition of copper ions through ion exchange. These zeolites containing nanoparticles and copper ions, referred to as additives, were incorporated into the resin system for making the ultrafine-antimicrobial- powder coated surface. Uniform distribution of silver nanoparticles on the zeolite surface plays an important role for the generation of silver ions. Hydrophilic encapsulation of these additives is essential for the generation of silver ions from nanoparticles, which were embedded in the powder coated surface to make it effective against microorganism. Different water soluble hydrophilic polymer encapsulations were used to find the best combination for this purpose. External cross-linkers were used to stabilize the polymer during encapsulation. Due to the high hydrophilicity of the encapsulation, fine cracks were found in the coated film after several exposures to the microorganism. This problem was solved by applying additional clear coating underneath the active coating. Polymers which contain more hydroxyl groups are difficult to optimize for uniform release of silver ion from the nanoparticles for prolonged use. Encapsulation with anionic polymers is the most effective solutions for releasing the silver ions from the ultrafine powder coated surface. The strength of the encapsulation within the matrix was found to depend on the cations present in the additives, which increases with the concentration of cations. Non-

ionic and anionic polymer encapsulations were found more effective than the high hydroxyl-containing polymers. Non-polymeric hydrophilic encapsulation was also used, made from the precipitation of calcium nitrate and sodium phosphate. This encapsulated additive showed efficiency against microorganism but was not as good as the polymer encapsulated additives.

Key words: Silver nano particles, hydrophilic polymer, antimicrobial efficiency, powder coating, encapsulation

6.2 Introduction

Microbial growth in medical and food industries is a big concern now a days, so there is an urgent need for developing effective coating strategies to fight against microbial infections. Due to the rise of resistant strains, bacterial resistance towards various disinfectants and antibiotics have increased. There is a high demand for safe and cost effective biocidal formulations instead of toxic and harmful antimicrobial agents. Silver in different forms such as silver ions and silver-based compounds, as well as silver nanoparticles (AgNP) have been proved to be the best and most used active agent against microorganisms [1]. The antimicrobial efficiency and durability depend on the adequate availability of silver ions with controlled release in the affected area of interest. Thus the higher the microbial load, the higher the efficiency and the longer the function lasts. To have high silver ion concentrations, modern techniques such as nanotechnology can be applied e.g., the use of nano silver [2]. Nano-sized inorganic particles are being demonstrated as an important material for making the novel nano-devices used in physical, biological, biomedical and pharmaceutical areas. Presently, nanosilver is

incorporated into different consumer products, such as food storage containers, textiles, antiseptic sprays, bandages, catheters etc. [3]. The biocidal effect of silver nanoparticles is creating demands for their use in consumer and medical products. Metallic nanoparticles, like silver have already been established as an atomic scale tailoring material to fight and prevent growth of microorganism. Nanometer size metal particles exhibit remarkable properties which are different from the bulk due to their highly active morphological surfaces. There is a hypothesis on activation of silver nanoparticle, which explains that antimicrobial activity is only due to the release of silver ion from nano particles but the nanoparticles themselves do not work for the inactivation process and serve as a vehicle to release silver ion more efficiently [4]. Release of silver ions from nano particles embedded in substrates is the focal point to achieve the effective result against biological activity. Recent studies have shown that the majority of silver ions come from zero valent metallic silver, from the reaction with dissolved oxygen, which is mediated by protons and surrounding fluid. Ion release from nanoparticles is also dependent on the exposed surface area and the particle size, which increases with the decrease of the nano-particle's size [5]. Due to the highly reactive large surface areas, nano-particles have potential for rapid dissolution and oxidative production.

The long term release of silver ions from the nano-particles results in the oxidation of metallic silver (Ag^0) in the presence of water [6].

$$2Ag(s) + ½\ O_2\ (aq) + 2H^+ \rightarrow 2Ag^+\ (aq) + H_2O\ (aq)$$

Incorporation of these nano particles into the hydrophilic polymer environment enables the nano particles to become active for the synthesis of silver ions. There are some water

soluble synthetic and natural polymers with very high hydrophilic properties, those are now used in drug delivery and different biomedical applications including nanotechnological research. Some hybrid polymers are also used in different sophisticated research. Hybrid polymers are formed by covalently cross-linked synthetic and natural polymers, to achieve high mechanical strength and elasticity even in swelling states. Natural polymers are biocompatible and biodegradable but the synthetic polymers besides being biocompatible have better physical and mechanical properties [7]. So by cross-linking these two types of polymers it is possible to generate an interpenetrating polymeric network, which is known as hybrid super porous hydrogel with very good water absorption capacity [8].

A different studies showed that polymer barrier can stabilize the morphology of silver nano particle polymer composites and represents a simple as well as an effective way to stabilize the controlled dispersion of silver ions [9]. Solubility and mobility of water molecules indicate the rate of water uptake into the polymer and have an effect on ion release. The release of ion takes place when the water molecules reach the particle surface [9]. The release of silver ion from nanoparticles is also governed by the diffusion coefficient of water in the hydrophilic polymer because most of the silver ions need to move from the interior to the surface. The silver ion is generated by the oxidation of elemental silver on the surface of the silver particles and then transported to the surface of the specimens [10]. Some researchers have reported that the positive charge of the silver ion, and in cases, possibly the silver nano-particle itself, results electrostatic attraction with the negatively charged bacterial cell membrane. Also it has been reported

that the nano particles coated with a negatively charged carboxyl group containing polymers still results in significant attraction [11].

To utilize the effectiveness of nanoparticles against microorganism and to overcome the present concerns regarding the leaching of nano particles into the environment, a novel antimicrobial surface coating containing silver nanoparticles against microorganisms was investigated.

6.3 Materials and Methods

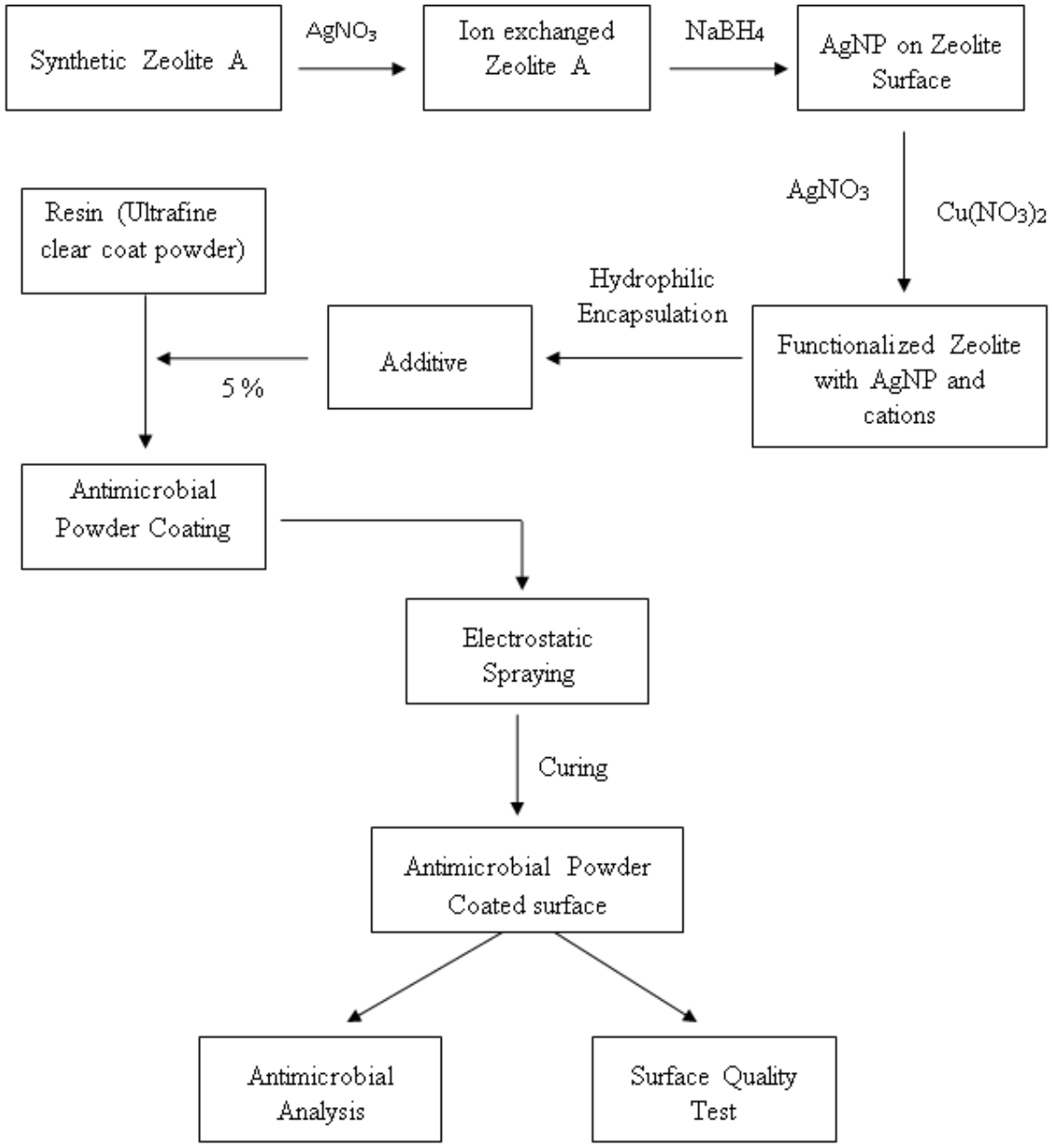

Flow sheet 6.1: Fabrication of antimicrobial powder coated surface

6.3.1 Materials

List of chemicals used for the encapsulation of additives are shown below;

1. Poly(vinyl alcohol), $[-CH_2CHOH-]_n$, Mw 89,000-98,000, 99% hydrolyzed, Sigma 341584

2. Poly(ethylene oxide), $[-CH_2CH_2O-]_n$, Mw 100,000, Sigma 181986

3. Polyacrylamide, $[-C_3H_5NO-]_n$, Nonionic, Mw 5,000,000-6,000,000, Sigma 92560

4. Alginic acid sodium salt, $[-NaC_6H_7O_6-]_n$, Mw-Not specified, Sigma 180947

5. Sodium carboxymethyl cellulose $[-C_8H_{15}NaO_8-]_n$ Mw-90,000, Sigma 419273

6. Polyester- Crylcoat 4646-3 polyester resin

7. Calcium phosphate (Calcium nitrate tetrahydrate, Sigma 1396 + Sodium phosphate, Sigma 342483)

8. Silver nano powder: Sigma 484059, particle size < 150nm

All other materials used in this work have been described in the earlier chapters.

6.3.2 Formation of silver nano particles

Ion-exchange of synthetic zeolite A with silver nitrate of different concentrations (0.001M, 0.01M, 0.03M, 0.05M) was done for 24hrs with constant stirring at 300rpm. The temperature was maintained at 60^oC and the pH was adjusted below 5 with concentrated HNO_3. The samples were centrifuged after 24 hrs at 3500 rpm for 30 min to separate from the liquid and the liquid was preserved for further use. The slurry was washed with fresh DI water twice to remove the overloaded silver ions from the zeolite

surface. These silver ions in zeolite were then reduced to silver nano particles with sodium borohydride at different concentrations. Based upon the elemental analysis of ion-exchanged zeolites, this reducing agent was added at different proportions ranging from 0.5, 1.0, 1.5 to 2 times the molar no of silver. Different amounts of borohydride were dissolved in 300ml of DI water and then added slowly to the ion exchanged zeolite slurry with constant stirring and mixing for 1 hr. After centrifugation for 30 min at 40^{o}C, the sample was washed with DI water two times. In some formulations previously separated ion exchanged solution was added with different amount of $Cu(NO_3)_2$ and the sample was stirred for another 24 hrs. Entire mixing processes were done by covering the mixing container to protect the content from light. Finally, the sample was centrifuged and washed with DI water two times and dried at 80^{o}C for 6-8 hours. After grinding, the ground powder was kept in an airtight dark container for further use, which referred as additive. In some other formulation fresh silver nitrate was added with copper nitrate during the functionalization of the additives.

6.3.3 Encapsulation of zeolites containing nano particles with hydrophilic coating

Five different hydrophilic water soluble polymers were used for the encapsulation process at different concentrations. Mixed polymers were also used for encapsulation with or without the presence of external cross linkers. Commercially available silver nanoparticles were used in some additive formulation and rest additives were prepared with synthesized nanoparticles on zeolite surface. One set of additives was prepared by the encapsulation of calcium phosphate at different concentrations. Calcium phosphate

encapsulation was prepared by the chemical reaction of calcium nitrate and sodium phosphate. Encapsulation was also done with polyester.

6.3.4 List of functionalized additives prepared on zeolite:

Through the above mentioned procedures, following functionalized additives were prepared;

1. Nano particles prepared with 0.03M silver nitrate ($AgNO_3$), reduced by 1.5 times borohydride

2. Nano particles prepared with 0.03M silver nitrate and functionalized with 0.06M copper nitrate, $Cu(NO_3)_2$

3. Nano particles prepared with 0.03M silver nitrate and functionalized with 0.03M silver nitrate and 0.06M $Cu(NO_3)_2$

4. Nano particles prepared with 0.03M silver nitrate and functionalized with 0.1M $Cu(NO_3)_2$

5. Synthetic zeolite functionalized with 0.03M silver nitrate and 0.06M $Cu(NO_3)_2$

6. Synthetic zeolite functionalized with 0.06M $Cu(NO_3)_2$

7. Nano particles prepared with 0.05M silver nitrate and functionalized with 0.1M $Cu(NO_3)_2$

8. Nano particles prepared with 0.01M silver nitrate and functionalized with 0.02M $Cu(NO_3)_2$

9. Nano particles prepared with 0.001M silver nitrate and functionalized with 0.002M $Cu(NO_3)_2$

6.3.5 Analysis

Scanning Electron Microscopy (SEM): Hitachi S-4500 field emission SEM with a Quartz PCI XOne SSD X-ray analyzer was used to get high resolution images of the surface topography of zeolite particles with silver nano particles.

All other analyses (XRD, ICP-OES, Antimicrobial analysis, Color analysis and Autoclave) done for this study have been mentioned earlier. Mean values of all analysis are used here.

The same coated surface was used repeatedly called as 'trial' to check the efficiency against microorganisms. It is to be noted that the aforesaid coated surface was cleaned with soap and water and dried before every use.

6.4 Results and Discussions

6.4.1 Formation of nanoparticles:

Silver nanoparticles (AgNPs) are subjected to new engineering technologies with extraordinarily resultant novel morphologies and characteristics. Smaller nanoparticles were formed by using strong reducing agent whereas the larger silver nanoparticles were formed as the result of weaker reducing agent [12]. Nano particles were formed on the surface of the synthetic zeolite A by the reduction of silver ions with different proportions of strong reducing agents (sodium borohydride, $NaBH_4$). The concentrations of silver nitrate used for ion-exchange were 0.001M, 0.01M, 0.03M, 0.05M and the amounts of $NaBH_4$ were 0.5, 1, 1.5 and 2 times of silver ions which remain after ion exchange. Copper was incorporated into all additives to partially balance the zeolite charge. The color of the nanoparticles containing zeolites changed from light to dark brown with the

change of silver concentration (0.03M-0.05M). But the color of the additives prepared with 0.001M silver nitrate was light gray and with the ones 0.01M silver nitrate was slight dark gray. The gray color of additives denotes the reduction of silver ions to metallic silver crystals. All nano particles formation processes were done at 60^{o}C to accelerate the movement of components within the solution. Another set of additives was prepared for every combination of silver and reducing agent with extra silver ions. Extra silver ions were added for the instant use of active agent. Some additives were also prepared by mixing with commercially available silver nano particles.

6.4.2 X-ray Powder diffraction (XRD):

The powder X-ray diffraction spectra of the zeolite supporting silver nano particles are shown in Figure 6.1. Additives prepared from different concentrations of silver nitrate on the zeolite surface showed characteristic peaks for silver at the same angles but with different intensities. The existence of crystalline phase of silver nanoparticles was found and became pronounced with the increase of concentration of silver nitrate used. The characteristic peaks matched with the standard silver XRD patterns (based on the silver standard diffraction pattern of REF. 01-087-0720). The intensity of the silver peaks was prominent for nano particles prepared from 0.03M and 0.05M silver nitrate and matched with the standard diffraction pattern. The peak intensity of synthetic zeolite A can easily be tracked including the peak intensity for silver in the XRD diffraction spectra for the additive prepared by 0.03M silver nitrate. But no peak for zeolite A was found when

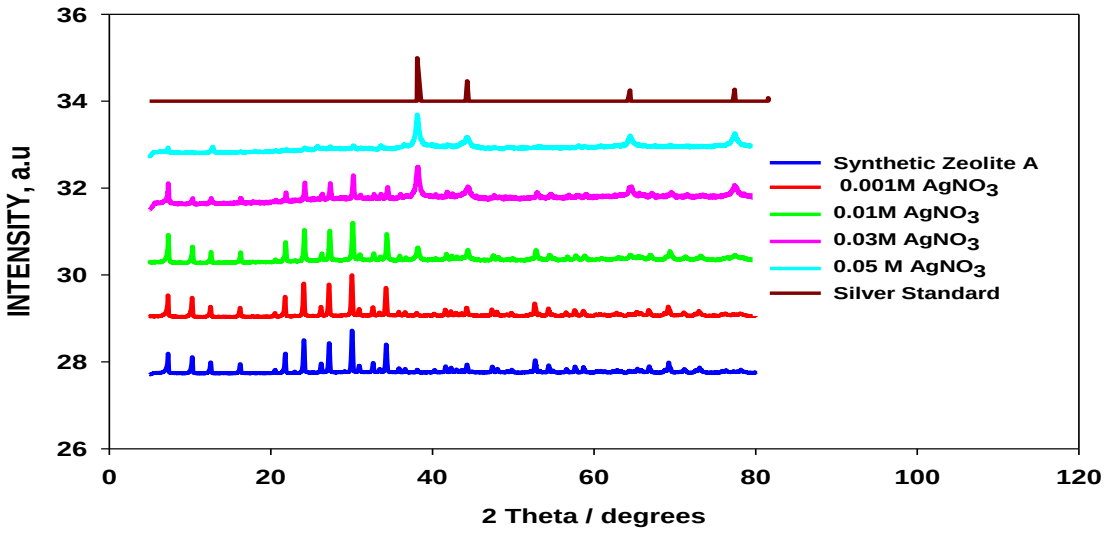

Figure 6.1: Powder X-ray diffraction patterns of standard zeolite A and silver with silver zeolite nano composites synthesized by using different silver nitrate concentrations (0.001, 0.01, 0.03, 0.05M)

higher concentration (0.05M) of silver nitrate was used for the preparation of nanoparticles. It confirmed the presence of thicker layer of nano-particles on the zeolite surface, prepared from 0.05M silver nitrate. The characteristic peaks for only silver were observed at that XRD spectra. Since efficiency of nanoparticles is size and dispersity dependent, it is required to have a good control over their size and distribution. The prominent peaks at 2θ having values of about 38.59^{o}, 44.49^{o}, 64.56^{o}, and 77.51^{o} could be characterized to the 111, 200, 220 and 311 Bragg's reflections of crystallographic planes of the face-centered cubic (FCC) crystal of silver. Similar results were shown in previous research [13].

With the increase of silver nitrate concentration used during nano particles synthesis, the intensities of 111, 200, 220 and 311 reflections were also increased due to the formation of silver nano particles on the zeolite surface. It should be noted that no other additional

peak was observed other than zeolite and silver, which confirmed the purity of synthesized silver nanoparticles on the zeolite surface. Moreover, the increase of silver concentration in the ion exchange medium had led to the development of the characteristic peaks of silver, indicating the development of crystalline silver nano particles. The typical diffraction peaks of synthetic zeolite A ranged from 10^{o} to 35^{o} at 2θ indicate the presence of zeolite (zeolite A standard diffraction pattern of REF. 00-056-0610). At lower concentrations of silver nitrate (0.001M and 0.01M) diffraction peaks for zeolite A were found along with small diffraction peaks for silver. No characteristic peak for copper crystal was found in any of these additives, which confirmed the presence of copper as an ionic form.

6.4.3 Inductively coupled plasma optical emission spectrometry (ICP-OES):

ICP-OES analysis was used to determine the elemental composition of the additives after functionalization of synthetic zeolite A. The nano particles were synthesized using the chemical reduction process after ion-exchange of zeolite with different concentrations of silver nitrate followed by the incorporation of copper ions into the zeolite matrix. After synthesizing the nano patarticles, extra silver ions were added to the zeolite matrix for the preparation of some of the additives. These silver ions were added afterwards by further ion exchange with the the remaining solution (preserved after first ion-exchange) or by using fresh silver nitrate solution. The second ion-exchange was done with silver nitrate to increase the silver content. This extra silver will remain in an ionic form. After chemical reduction of silver ions with $NaBH_4$, the Ag^{+} was transformed to Ag^{o}, as such, there were some extra charges available in the zeolite to compensate the chrages. Based

on the ICP analysis the increase of silver concentration was found in these fromulations. By this analysis one can only find the total concentration of silver; and neither the concentration of the silver ion nor the concentration of the nanoparticles, can be found. Different amounts of borohydride were used based on the amount of silver ions present following the ion-exchange process. One mole of borohydride was needed for the reduction of one mole of silver.

$$AgNO_3 + NaBH_4 \rightarrow \quad Ag + NaNO_3 + 1/2\ H_2 + 1/2\ B_2H_6$$

However different combinations of borohydride were used to optimize the reduction process shown in Table 6.1. Excess reducing agents were used to make sure for complete reduction of silver ions. The intention was to incorporate as much silver as possible into the additives. The ICP-analysis did not show any big difference in terms of silver content

Table 6.1: Elemental analysis (milli eq) of additives containing silver nanoparticle (0.05M $AgNO_3$) synthesized with different amount of borohydride with additional silver and copper ions

Additive formulation	Ag	Cu	Na	Total
[1]Zeolite + Ag^+	1.66	0.00	5.26	6.92
[2]Zeolite + Ag^+ + Cu^{2+}	1.53	3.89	1.46	6.88
[3]Zeolite + AgNP (2 $NaBH_4$)+ Ag^+(pre)+ Cu^{2+}	1.65	3.47	1.07	6.19
[4]Zeolite + AgNP (1.5 $NaBH_4$)+ Ag^+(pre)+ Cu^{2+}	1.69	3.51	1.07	6.27
[5]Zeolite + AgNP (1 $NaBH_4$)+ Ag^+(pre)+ Cu^{2+}	1.59	3.78	1.08	6.45
[6]Zeolite + AgNP (0.5 $NaBH_4$)+ Ag^+(pre)+ Cu^{2+}	1.61	3.86	1.09	6.56

1. Zeolite + 0.05M $AgNO_3$ **2**. Zeolite + 0.05M $AgNO_3$ + 0.1M $Cu(NO_3)_2$, **3.** Zeolite + 0.05M $AgNO_3$+ 2 times $NaBH_4$ + previous silver soln + 0.1M $Cu(NO_3)_2$ **4.** Zeolite + 0.05M $AgNO_3$+ 1.5 times $NaBH_4$ + previous silver soln + 0.1M $Cu(NO_3)_2$ **5**. Zeolite + 0.05M $AgNO_3$+ 1 times $NaBH_4$ + previous silver soln + 0.1M $Cu(NO_3)_2$ **6**. Zeolite + 0.05M $AgNO_3$+ 0.5 times $NaBH_4$ + previous silver soln + 0.1M $Cu(NO_3)_2$

Table 6.2: Elemental analysis (milli eq) of additives containing silver nanoparticle (0.05M $AgNO_3$) synthesized with 1.5 times borohydride with additional silver and copper ions

Additive formulation	Ag	Cu	Na	Total
[1]Zeolite +Ag^+	1.66	0.00	5.26	6.92
[2]Zeolite +Ag^+ + Cu^{2+}	1.53	3.89	1.46	6.88
[3]Zeolite +AgNP (1.5$NaBH_4$)	1.64	0.00	4.89	6.53
[4]Zeolite + AgNP (1.5$NaBH_4$) + Cu^{2+}	1.62	3.29	1.11	6.02
[5]Zeolite + AgNP (1.5$NaBH_4$)+ Ag^+(fresh)+ Cu^{2+}	1.87	3.31	1.09	6.27
[6]Zeolite + AgNP (1$NaBH_4$)+ Ag^+(fresh)+ Cu^{2+}	1.73	3.51	1.09	6.33

1. Zeolite + 0.05M $AgNO_3$ **2**. Zeolite + 0.05M $AgNO_3$ + 0.1M $Cu(NO_3)_2$, **3**. Zeolite + 0.05M $AgNO_3$+ 1.5 time $NaBH_4$ **4**. Zeolite + 0.05M $AgNO_3$+ 1.5 time $NaBH_4$ + 0.1M $Cu(NO_3)_2$, **5**. Zeolite + 0.05M $AgNO_3$+ 1.5 time $NaBH_4$ + 0.05M $AgNO_3$ (fresh) + 0.1M $Cu(NO_3)_2$**6**. Zeolite + 0.05M $AgNO_3$+ 1 time $NaBH_4$ + 0.05M $AgNO_3$ (fresh) + 0.1M $Cu(NO_3)_2$

Table 6.3: Elemental analysis (milli eq) of additives containing silver nanoparticle (0.03M $AgNO_3$) synthesized with 1.5 times borohydride with additional silver and copper ions

Additive formulation	Ag	Cu	Na	Total
[1]Zeolite +Ag^+	1.19	0.00	5.06	6.25
[2]Zeolite +Ag^++Cu^{2+}	0.92	3.37	2.20	6.49
[3]Zeolite +AgNP (1.5$NaBH_4$)	1.21	0.00	5.00	6.21
[4]Zeolite + AgNP (1.5$NaBH_4$)+ Cu^{2+}	1.09	3.43	2.19	6.71
[5]Zeolite +AgNP (1.5$NaBH_4$)+Ag^+(fresh)+Cu^{2+}	1.46	2.82	2.21	6.49
[6]Zeolite +AgNP (1$NaBH_4$)+Ag^+(pre)+Cu^{2+}	1.19	3.33	2.19	6.68

1. Zeolite + 0.03M $AgNO_3$, **2**. Zeolite + 0.03M $AgNO_3$+ 0.06M $Cu(NO_3)_2$, **3.** Zeolite + 0.03M $AgNO_3$+ 1.5 time $NaBH_4$, **4**. Zeolite + 0.03M $AgNO_3$+ 1.5 time $NaBH_4$+ 0.06M $Cu(NO_3)_2$, **5.** Zeolite + 0.03M $AgNO_3$+ 1.5 time $NaBH_4$ + 0.05M $AgNO_3$ (fresh) + 0.1M $Cu(NO_3)_2$, **6**. Zeolite + 0. 03M $AgNO_3$+ 1.5 time $NaBH_4$ + previous silver soln + 0.1M $Cu(NO_3)_2$

between formultions with 1.5 and 2 times borohydride used for reduction as shown in Table 6.1. Some additives were prepared with further addition of previously seperated solution to increase the amount of silver ions in the addtives. In all formulations nanoparticle worked as a reservoir for silver ions. The reason for adding extra silver ions into the additives was to make the additive more active, so that it can act instantly and the nanoparticle will work as a reservor and copper ions were added to neutralize the charge of the zeolite. After fixing the amount of reducing agents, finally the additives were prepared in four different and distinct combinations; a) with only silver ions, b) only silver nanoparticles, c) nanoparticles with copper ions and d) nanoparticles with siver and

Table 6.4: Elemental analysis (milli eq) of additives containing silver nanoparticle (0.01M $AgNO_3$) synthesized with 1.5 times borohydride with additional silver and copper ions

Additive formulation	Ag	Cu	Na	Total
[1]Zeolite +Ag^+	0.51	0.00	6.14	6.65
[2]Zeolite +Ag^+ + Cu^{2+}	0.48	1.43	4.72	6.63
[3]Zeolite +AgNP (1.5$NaBH_4$)	0.52	0.00	5.91	6.43
[4]Zeolite + AgNP (1.5$NaBH_4$) + Cu^{2+}	0.49	1.44	4.59	6.52
[5]Zeolite +AgNP(1.5$NaBH_4$)+Ag^+(fresh)+Cu^{2+}	0.73	1.38	4.08	6.19
[6]Zeolite +AgNP(1.5$NaBH_4$)+Ag^+(0.03M fresh)+Cu^{2+}(0.06M)	0.90	3.21	2.54	6.64
[7]Zeolite +AgNP(1.5$NaBH_4$)+Ag^+(pre)+Cu^{2+}	0.68	1.43	4.26	6.37

1. Zeolite + 0.01M $AgNO_3$, **2**. Zeolite + 0.01M $AgNO_3$+ 0.02M $Cu(NO_3)_2$, **3**. Zeolite + 0.01M $AgNO_3$+ 1.5 time $NaBH_4$, **4**. Zeolite + 0.01M $AgNO_3$+ 1.5 time $NaBH_4$ + 0.02M $Cu(NO_3)_2$, **5**. Zeolite + 0.01M $AgNO_3$+ 1.5 time $NaBH_4$ +0.01M $AgNO_3$ (fresh) +0.02M $Cu(NO_3)_2$, **6**. Zeolite + 0.01M $AgNO_3$+ 1.5 time $NaBH_4$ +0.03M $AgNO_3$ (fresh) +0.06M $Cu(NO_3)_2$, **7.** Zeolite + 0. 01M $AgNO_3$+ 1.5 time $NaBH_4$ +previous silver soln +0.02M $Cu(NO_3)_2$

copper ions. 0.05M silver nitrate was used for this set of four additives. Elemantal analysis of these additives is shown in Table 6.2. Another set of additives was also prepared with the same combinations but by changing the concentration of silver nitrate to different values such as, 0.03M and 0.01M as shown in Tables 6.3 and 6.4 respectively. The purpose of preparing all these additives were to find the best effective formulation for the preparation of active antimicrobial surface. Different antimicrobial surfaces were prepared with all these additives and the efficiencies against the microorganisms were checked. The sample containing only silver nanoparticles and copper ions did not show any activity against microorganisms but the additives containing silver nanoparticles including silver and copper ions showed excellent efficiency. This does not mean that the nanoparticles present in those additives were not good enough to kill the microorganisms, as they need the proper environment to become active. So the nanoparticles present within the coated surface are not readily active. The activity against microorganisms is exclusively due to silver ions release, which suggests that the silver nanoparticles themselves do not influence the biological activity of microorganisms instantly. In presence of proper surroundings it can release silver ions more effectively according to the requirement and also can works as a reservor for silver ions [4]. All prepared additives showed antimicrobial activity, when they were used directly into the microcrobial solutions. From those observations, it was proved that silver nanoparticles needs hydrophilic environment to release silver ions from the coated surface.

6.4.4 Scanning Electron Microscopic (SEM) analysis:

Morphological analyses of these additives were done with SEM. These images (Figures 5.2-5.5) demonstrated the formation of nano particles on the zeolite surface and their dispersity. When ion exchange was done with lower concentrations of silver nitrate (0.001M, 0.01M), maximum ions were able to enter into the zeolite pore. During the reduction process, silver ions within the pore were reduced to Ag^{o}, the ionic interactions between silver ion and the zeolite were changed to van der Waals interactions. Change of interactions with the zeolite led them to hold weakly in the zeolite cavities, so they were able to move out from the cavities and started to grow outside [14].

With the increase of concentration of silver nitrate from 0.001M to 0.01M, some small nano particles were found on the zeolite surface. Figures 6.2 and 6.3 showed the SEM images of zeolite with synthesized nanoparticles prepared by different concentrations of silver nitrate (0.001M, 0.01M) as mentioned before. Some of the nano particles which formed outside the zeolite surface aggregated together. It is known that the aggregated particles had lower exposed surface areas for available activity than the well dispersed ones. This was proven by the antimicrobial analysis from which it was found that surfaces made with those additives with well dispersed nanoparticles had good efficiency against microorganisms. The nanoparticles prepared on the surface of zeolite using 0.03M and 0.05M silver nitrate is shown in Figures 6.4 and 6.5 respectively. Nanoparticles prepared with 0.03M silver nitrate were well dispersed on the zeolite surface and their particle size was around 10-20nm. The figure 6.4 exhibited below show a homogeneous morphology, so the zeolite surfaces were covered with uniformly grafted

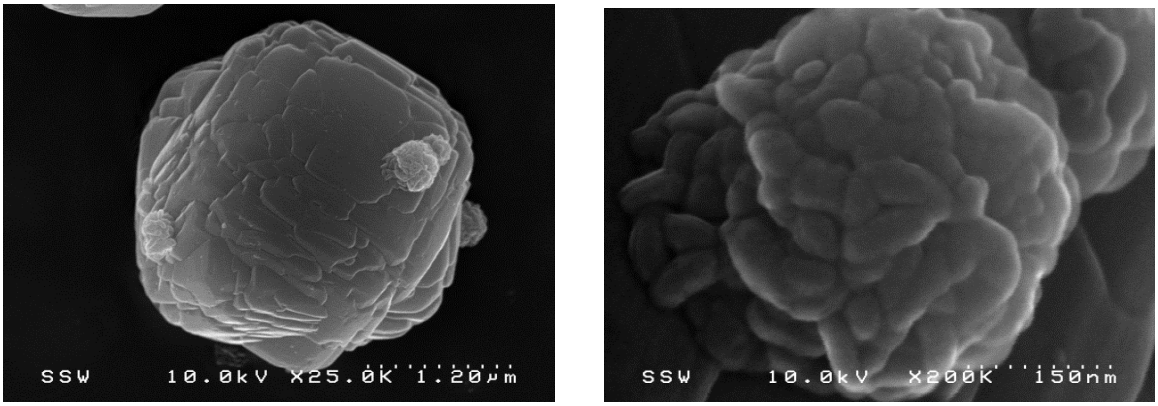

Figure 6.2: Silver Nano particles (0.001M Ag reduced with 1.5 time $NaBH_4$) on Synthetic Zeolite

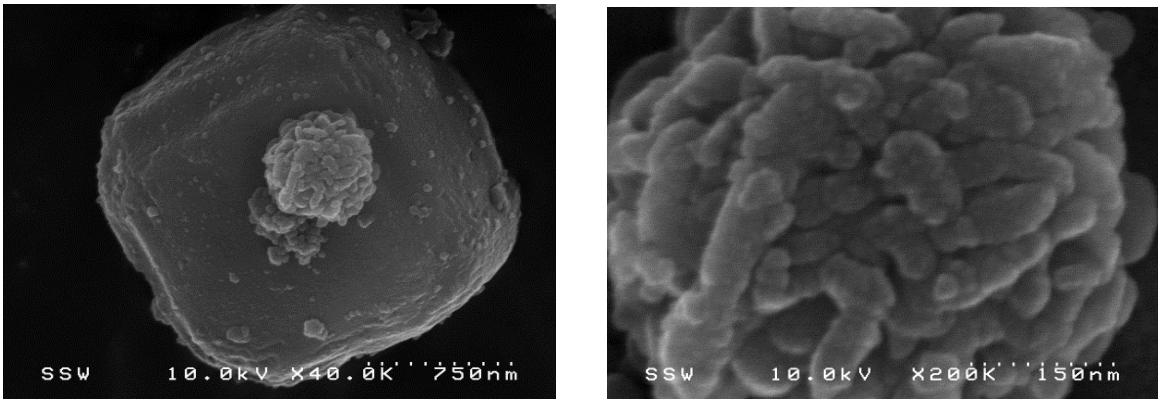

Figure 6.3: Silver Nano particles (0.01M Ag reduced with 1.5 time $NaBH_4$) on Synthetic Zeolite

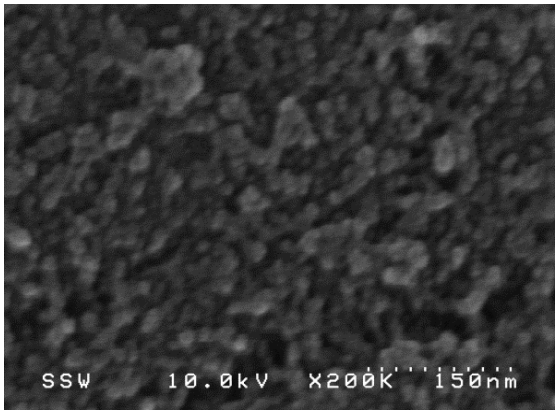

Figure 6.4: Silver NP (0.03M Ag reduced with 1.5 time $NaBH_4$) on Synthetic Zeolite

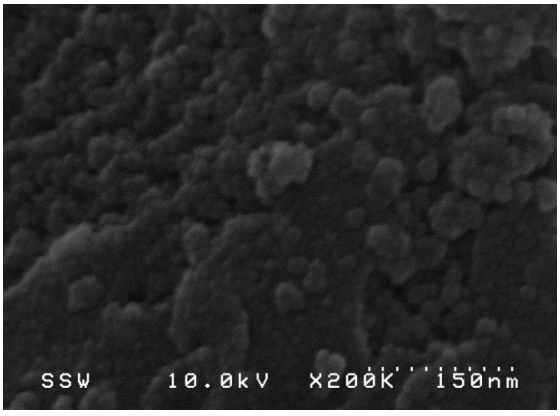

Figure 6.5: Silver NP (0.05M Ag reduced with 1.5 time $NaBH_4$) on Synthetic Zeolite

silver nano particles. It was confirmed from the antimicrobial analysis, that the ultra small particle size had ultra large exposed surface areas, where a large number of atoms were able to come in direct contact and was readily available for action.

But the nanoparticles in the other additives prepared with 0.05M silver nitrate over lapped on top of each other and their particle size was also bigger (Figure 6.5). It was observed that the surface of zeolite consisted of nano agglomerates of silver particles. Based on the uniform distribution and the size of the nano particle shown in Figure 6.4, it was decided to work further with the additive prepared by 0.03M silver nitrate and reduced with 1.5 times $NaBH_4$. It should also be noted that the bare surface shown in Figure 6.2 did not contain any silver which was confirmed from the EDX analysis shown in appendix.

6.4.5 Encapsulation of additives with hydrophilic polymers:

Presently the main concern is the release of silver nanoparticles while using any product that contains silver nanoparticles. If the nanoparticles can be incorporated on a substrate in such a way that no leaching of nanoparticles would occur except only the active Ag^+, when required. So the proper process optimization is needed to achieve the required product performance and safety [4, 15, 16]. Different hydrophilic encapsulations were used to coat the surface of the additives containing silver and copper in different forms to initiate the nano particles for oxidation. The main source of ions was the oxidation of nanoparticles and it was hypothesized that ion release could initiate the management of the oxidation pathway through hydrophilic polymer encapsulation. The cations present on the zeolite surface were bound with the polymer used for encapsulation by ionic

interaction through physical cross-linking [17]. Following water soluble hydrophilic polymers were used for the encapsulation purpose.

Poly-vinyl-alcohol (PVA): PVA is a nontoxic and biocompatible polymer with excellent mechanical properties, thermal and pH stability. This polymer possess extreme hydrophilicity due to the presence of huge hydroxyl groups in the large molecular chain. Cross-linking by chemical reactions can create the three dimensional polymeric network and can alter their chemical stability and mechanical strength with hydrophilicity [18]. 6% PVA was used to encapsulate the additives made from different combinations of silver nanoparticles, copper ions, silver ions and commercially available nanoparticles as mentioned in the Flow sheet 6.2 (samples 1-6). 5% each of these encapsulated additives were incorporated into the resin system (clear coat) to prepare the antimicrobial surfaces. These same surfaces were used to check the efficiency against microorganism several times after washing with soap water and drying at the end of each exposure of microorganisms. Very small cracks (<500µm interval) on the coated surface made with the additive containing only silver nanoparticles were found (sample 1) immediately after 1st use and the surfaces also lost their antimicrobial efficiency. But cracks on the surface were not found until 5th trial, made with the additive, which contains nanoparticles and copper ions (sample 5).

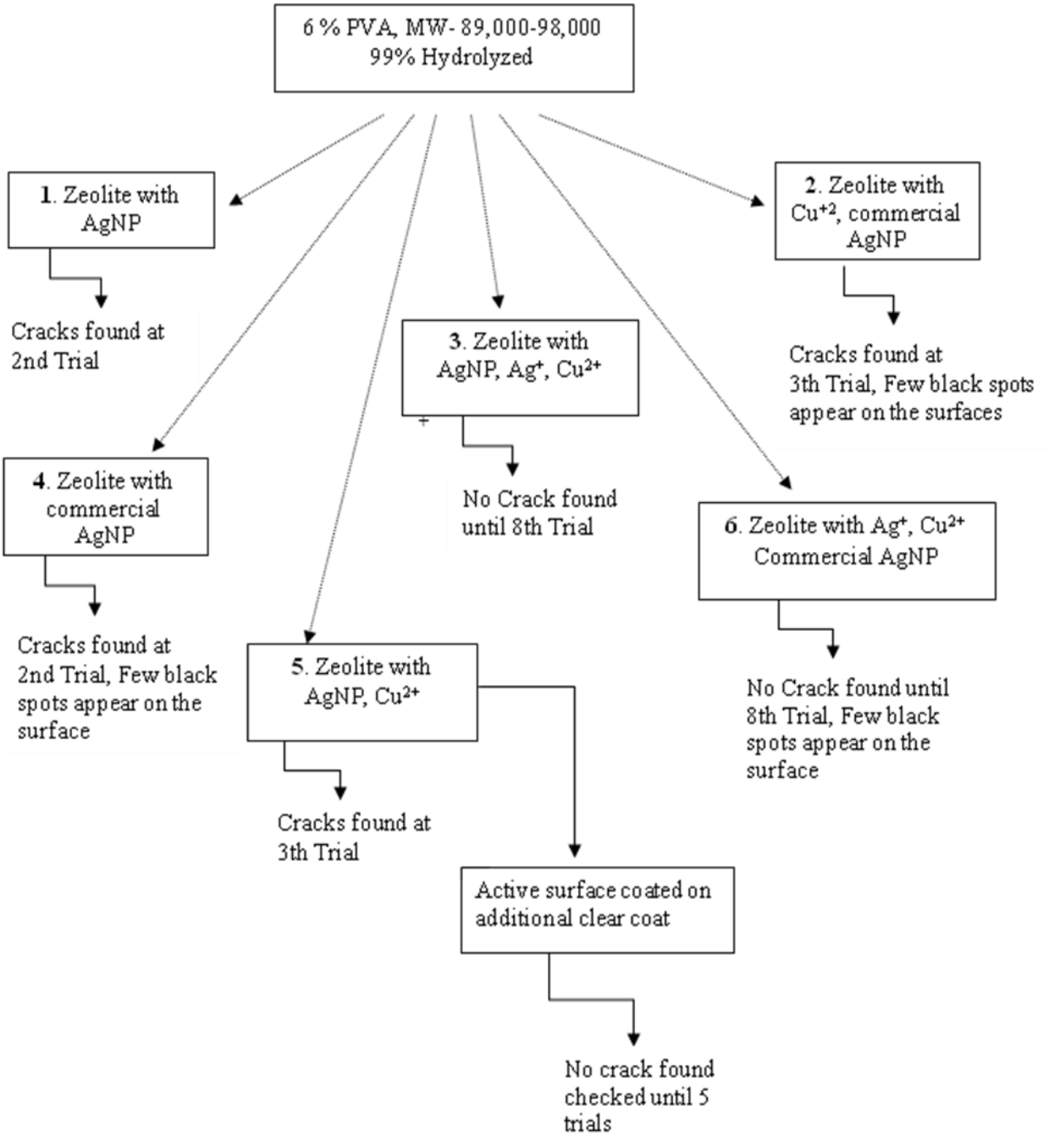

Flow Sheet 6.2: 6% PVA encapsulated additives containing silver nanoparticles, silver ions, copper ions and commercially available nanoparticles.

Physical bonds by ionic interaction between the hydroxyl groups in the polymer and the copper ions were formed. This bonding helped to increase the insolubility of the polymer to some extent simultaneously helped to reduce the leaching of additives while keeping the hydrophilicity of the matrix. As PVA has very high hydrophilic properties, its water absorption was also very high. The proportion of hydroxyl groups are far more than the proportion of cations, so the available hydroxyl groups are huge, though this bonding is not a stable or strong one. But there is a possibility of leaching of the additives from the surface with the diffused water due to high hydrophilicity.

But the surface containing nanoparticles, copper and silver ions (sample 3) did not show any crack until the 8th trial. This formulation also demonstrated high rates of microorganism reduction. The more cations present in the formulations, the better physical cross-linking took place with the polymer. Here silver ions will be readily available for inactivation of microorganisms. It was reported in literature that the hydrogel prepared by PVA/Ag nano particles showed considerable antimicrobial activity against *E.coli* [20]. This hydrogel also possess superior water permeability and transmission rate. Many researchers have found sufficient water absorbing capacity for this hydrogel with the addition of silver nano particles and other hydrophilic polymers [19]. But there is no report of any work been done on the assessment of durability for this type of hydrogel used in surface coating.

The surfaces prepared with additives (sample 4, 2, 6), which contained commercial nanoparticles with the combination of Ag^{+} and or Cu^{2+}, showed similar results as noted in samples (samples 1, 5, 3), but after few trials some black spots appeared on the surface. These black spots were the commercial nanoparticles that were added externally into the

formulation during encapsulation. Due to the size of nanoparticles (100nm) these are not strongly adsorbed on the zeolite surface or any other places in the matrix. But there is possibility of trapping these nanoparticle in to the polymer network, if a proper dense cross-linking can be formed between the polymer encapsulation. A new surface was prepared with the additive (sample 5), which contained AgNP and Cu^{2+}, where an additional clear coat was applied underneath the active coating. This surface showed good efficiency against microorganism and found better resistance from cracking until the 5th trial than the surface without additional coating. So the additional underneath coating helped to reduce the cracking though all these formulation which were encapsulated with 6% PVA did not show very promising results in term of antimicrobial activity and surface property.

It was found that moisture is essential for the generation of Ag^{+} from silver nanoparticles on zeolite surface. High hydrophilic encapsulation (6% PVA) allowed more water to penetrate through the surface and entrapped moisture in the bulk of the coating. This moisture causes its defects like cracking due to the corrosion on the aluminum substrate and eventually localized chemical instability and mechanical stress in the coated surface. Underneath coating is helping to reduce the corrosion problem finally keeping the surface from crack free.

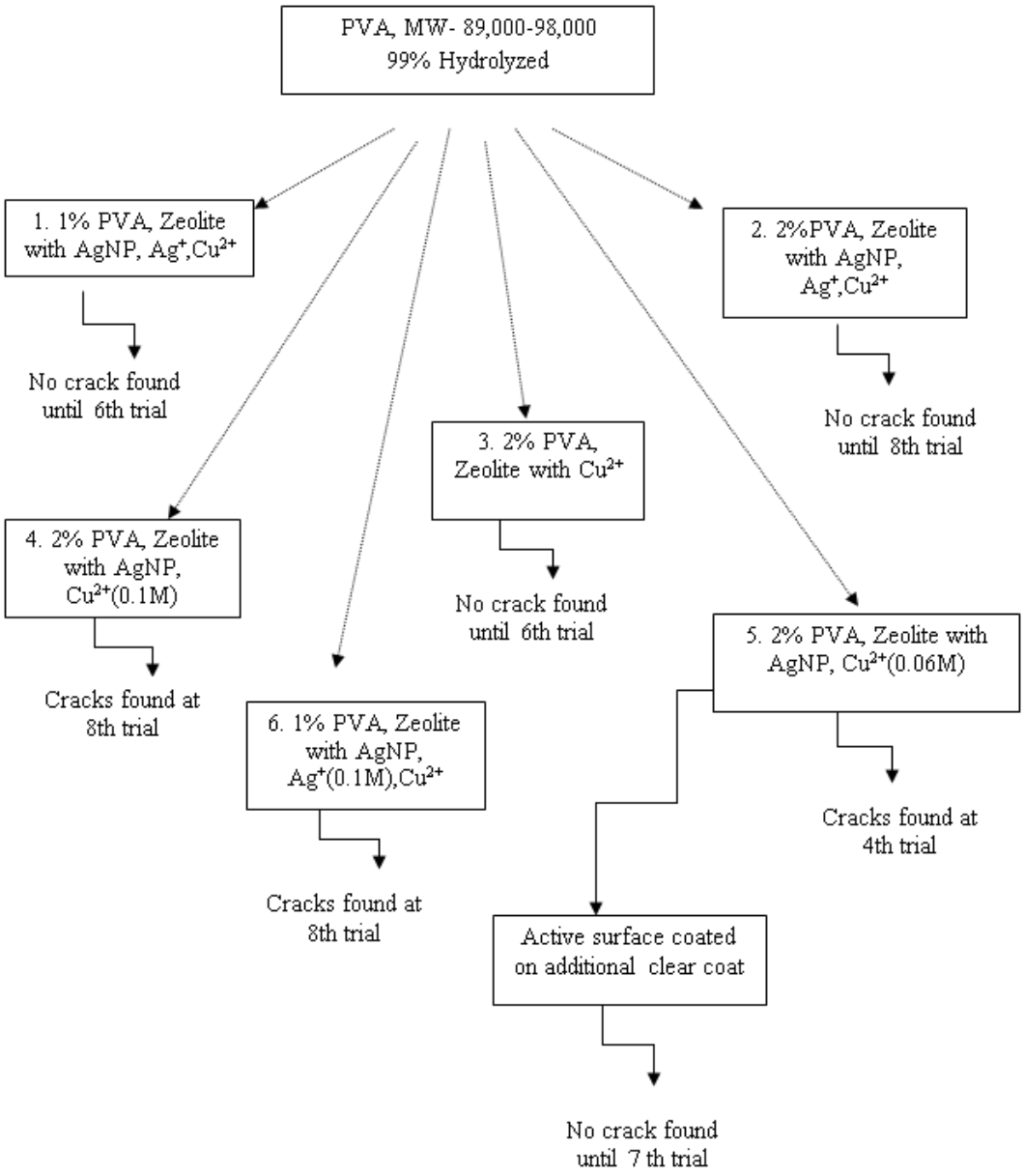

Flow Sheet 6.3: PVA encapsulated additives containing silver nanoparticles, silver ions, copper ions and commercially available nanoparticles.

Another set of surfaces were made with different reduced amounts of PVA encapsulation to optimize the combination of additives and the hydrophilic polymers (PVA). The polymer- holding capacity of different additives is mentioned in Flow sheet 6.3 on the

basis of cracks observed in the coated surface. A better correlation was found with the additives and the polymer for this set of surfaces than the set mentioned earlier in Flow sheet 6.2. The number of hydroxyl groups that are present in the polymer and the ions present in the additives bound more than those in the previous set during the encapsulation process. Although the amount of cracks were appeared after few trials, but it was not completely eliminated. Additive of sample 3, which contained only copper ions and encapsulation was done by 2% PVA, did not show any cracks even after several trials (6th), but this surface did not show any antimicrobial efficiency.

The copper ions were believed to have helped to hold the polymeric encapsulations. Cracks were found on all the surfaces made with the nanoparticles containing additives following their use for several trials. But again this problem was solved with the application of additional coating underneath the active coating, which reduced the interaction between the bare aluminium surface and the moisture in the coating. The increase in coating thickness can help to reduce this cracking problem [21].

Here silver nano particles does not have any attraction with any functional group, so with the diffused water, there is a possibility of leaching those nanoparticles. This leaching can be reduced by making the polymer encapsulation more cross-lined, so the nanoparticles can tightly bounded within the polymer network. Functionalized zeolite with only silver and copper ions was encapsulated with 2% and 6% PVA, which is reported in chapter 5. Cracks did not appear at the coated surfaces which contained 2% PVA encapsulated additive and the antimicrobial efficiency was excellent as they were checked until 15 trials. So during encapsulation cross-linking occurred between cations and the hydroxyl groups, which reduced the hydrophilicity.

The cross-linking of the hydrophilic polymer with external cross linker is a process of joining two or more molecules by covalent bonding that helped to decrease the hydrophilicity of that polymer and making them insoluble. This cross-linked polymer acted as a binder for divalent transition metals like Co, Ni, Cu and Zn, by decreasing the salvation shell [20]. PVA can be used potentially as an absorbent of different cations due to its biocompatibility. Copper (II) ions can be adsorbed into PVA in the presence of cross-linkers (glutaraldehyde) from a water solution [18]. This copper adsorption depended on the degree of cross-linking and it decreases with the increase in cross-linking. Reactive sites of PVA decreased with the increase in cross-linking, resulting in the decrease of interaction with as well as adsorption of copper (II) into the PVA matrix. The intra particle diffusion takes place by the adsorption mechanism [18].

From previous experiments it was found that copper in the ionic form helped to hold the polymer. Copper nitrate (0.06M) solution was used during functionalization after preparing the silver nano particles for additive preparation. An additive (sample 4) with 0.1M copper nitrate was also prepared to check the effect of excess copper ions for the binding of the polymer. Copper concentration is the only difference between sample 4 and sample 5. It was again proved that ionic concentration has significant effect on reducing cracks of the coated surface. Same correlation was also found between sample 1 and sample 6. The difference between these two samples was only the silver ion concentration, 0.05M for sample 1 and 0.1M for sample 6.

Different amounts of glutaraldehyde (5-10 µl) were used to cross-link the polymer (2% PVA) during the encapsulation of additives containing AgNP and copper ions. No cracks were found on the coated surface until several trials (4-6). But attempts to optimize the

combination between the cross-linker, and polymer, including nanoparticles and copper ions were failed. All formulations showed reduced reduction rates of microorganisms after several trials. More GA is providing more cross-linking and making the polymer less hydrophilic. Borax at different combinations with PVA was used as another cross-linker. Any satisfactory result was not observed in terms of antimicrobial activity from these coated surface. Due to the excess amount of hydroxyl groups present in the PVA, it was difficult to optimize the perfect combination for the encapsulation of nanoparticles containing additives, for the application in powder coating antimicrobial surface with enhanced durability. These results were not shown here.

Poly-ethylene oxide (PEO): The next used polymer in this study for encapsulation was the poly ethylene oxide (PEO), which has lower hydrophilicity than PVA. Use of polymer-metal composites is another approach that further broaden the purposes of biocide metals. The release of these metals can be controlled by water uptake-swelling, water diffusion within the matrix and by the interactions between polymers with the active agents. The release was also governed by the hydration number of PEO and the degree of cross-linking with the metallic cations [23]. 6% PEO was used to encapsulate both additives of which one contains Ag^{+}, Cu^{2+} with the nanoparticles (sample 2) and the other contains only Cu^{2+} with the nanoparticles (sample 1) as mentioned in flow sheet 6.4. The sample (no.2) which contains more cations found to be more resistant from cracking than the sample (no 1). No significant difference was observed between

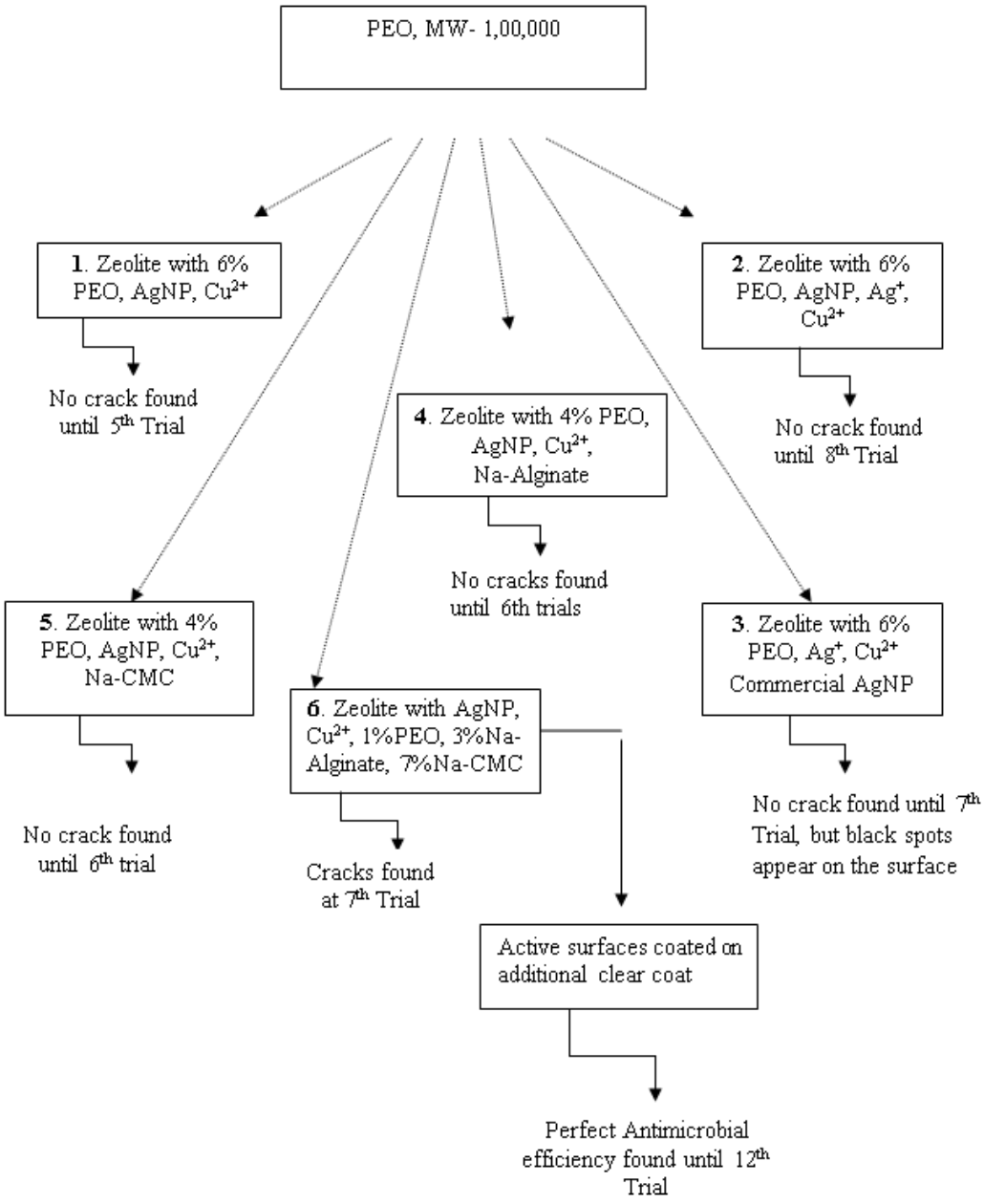

Flow Sheet 6.4: PEO encapsulated additives containing silver nanoparticles, silver ions, copper ions and commercially available nanoparticles

encapsulation with PVA (sample 3, flow sheet, 6.2) and PEO (sample 2, flow sheet 6.4) in terms of surface cracking (until 8th trials). But 6% PEO encapsulation was found as

the better combination for the additive containing AgNP and Cu^{2+} than the 6% PVA encapsulation. Cracks did not appear until 5th trials for 6% PEO encapsulation. Lower hydrophilicity of PEO made the formulation more promising for this particular combination of additive. The additive containing external nanoparticles also showed similar efficiency to PVA in terms of antimicrobial efficiency.

The blending process of natural and synthetic polymer results in bio-artificial polymeric materials, which posses unique structural and mechanical properties and is mainly used in biomedical applications. Dissolution of these two polymers in the same solvent can avoid denaturation of the active component present within the matrix. The interaction between blended polymers is mainly due to the hydrogen bonding [23]. Attempts were made to check the effectivity of blended polymers for encapsulation of the additives as shown in Flow sheet 6.4 (samples 4-6). Every surface showed antimicrobial activity until a certain trial, but the formulations for the encapsulation in sample 6 which contained 1% PEO, 7% Na-CMC, and 3% Na-Alginate was found to be the most useful for the additive to generate the silver ions. The underneath coating on the bare surface also helped to reduce the cracking of the coated surface during continuous exposure to microorganisms.

The same additive was used in the formulation mentioned in flow sheet 6.3 (sample 5) and in flow sheet 6.4 (sample 6), and the only difference was the polymer or combination of polymers used for encapsulations. The blended polymer encapsulation was found to provide better protection and showed enhanced antimicrobial activity in terms of number of exposures cycle to the microorganism. It was also mentioned in many previous works about the better performances of blended polymers in terms of physical and mechanical properties [23]. But no research has yet been conducted on the use of blended polymers

in the powder coating process for the production of antimicrobial surfaces. The reason behind that combination which used for encapsulation in sample 6 in flow sheet 6.4 found to be the cross-linking of the natural polymers with the cations present in the matrix. Copper cross- linked with the carboxylate groups of Na-CMC and Na-alginate by coordination-covalent bonds [24].

Polyacrylamide (PAM): The polymeric encapsulations were made with PAM alone and in combinations of other natural polymers. Polyacrylamides are known to be inert in nature and hydrophilic, which made them suitable for medical and pharmaceutical applications [10]. Graft copolymerization by synthetic and natural polymers is one of the ways to increase the polymeric properties [22]. Recently, physical cross-linking e.g., ionic interaction, has been found to be more effective in terms of toxicity and stability than the chemical cross-linking by toxic compounds. Physical cross-linking do not required any complicated processing and does not alter any properties of additives [25, 26]. Polysaccharides are biological polymers, which are being used in biomedical applications intensively nowadays. Alginate and carboxymethylcellulose is an anionic linear polysaccharide polymer that can be blended with PVA to achieve thermally stable, highly elastic and good water swelling properties [27]. Due to their flexible nature, synthetic polymers are more effective than the natural ones [22].

The additives used in this set of formulation are different combination of synthesized silver nanoparticles on zeolite surface, silver ions, copper ions, and commercial silver nanoparticles. Polyacrylamide contains the reactive amide (NH_2) groups and provides ionic character. Since the $-COO^-$ groups can be generated by the hydrolysis of $-CONH_2$ in PAM [28], thereby, the copper ions can be adsorbed with the $-COO^-$ groups by forming a

physical bond through the ionic interaction. But this hydrolysis at low pH is a very slow reaction [29]. So the cross-linking between copper and amide groups will be less, as well as the stability of the polymer in the matrix. Different combinations of polymers were

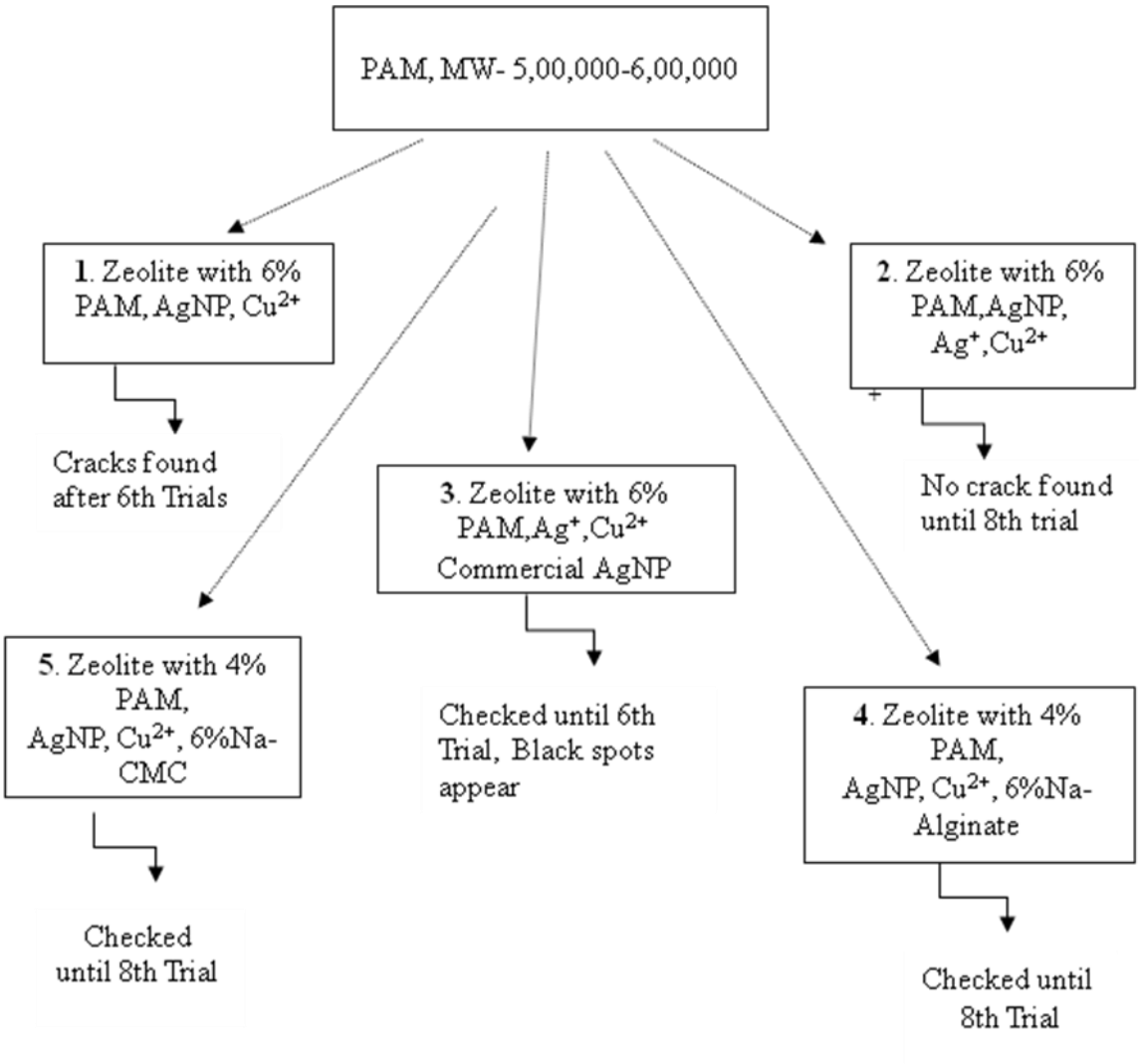

Flow Sheet 6.5: PAM encapsulated additives containing silver nanoparticles, silver ions, copper ions and commercially available nanoparticles

used to encapsulate the zeolites containing nanoparticles. Similar antimicrobial activity and coated surface property in terms of avoiding cracking were found from all coated

surfaces prepared by the additives which contain silver and copper ions in presence of silver nano particles. This was due to the physical bonding between polymer and the cations present in the additives.

Formulations of sample 1 in flow sheet 6.4 and the sample 1 in flow sheet 6.5 are same, but the polymer used for encapsulation were PEO and PAM respectively. Hydrophilicity provided by 1% PEO and 1% PAM is different due to their molecular weight and functional groups. The polymer-cation interaction for these two polymers is also different. Copper ions formed ionic bond with hydroxyl group of PEO and co-ordination covalent bond with generated $-COO^-$ in PAM. Though the bonding number will be low but the bonding strength will be more than the ionic bond formed with PEO.

Sample 5 and the sample 4 in flow sheet 6.5 are made by similar formulation, only the polymer used for encapsulation is different, but these are same kind of polymer. Similar surface cracking was also found from these two formulated samples. Better co-relation with the cations and the polymer was found here for those two samples in compare to other samples reported in this flow sheet (6.5). The reason behind that is same as above, the co-ordination covalent bonding between the cations and the polymer.

Non polymeric hydrophilic encapsulation: Insoluble calcium phosphate was used to encapsulate the additive. It was prepared to evaluate the water absorption capacity and dissolution of silver ions from the silver nanoparticles. Calcium nitrate and sodium phosphate solution were added into the suspension of zeolite containing silver nano particles. The insoluble encountered as particle form and precipitated on zeolite surfaces.

This precipitate was aimed to work as a hydrophilic coating on zeolite, which is anticipated to help in absorbing water and to accelerate the oxidation process of silver

Table 6.5: Comparative studies of encapsulation used on additives

Additive containing AgNP, Cu^{2+}	Effectivity against microorganism	Autoclave test		
		Initial color of the surface	Color after 4 autoclave cycles	No of microorganism after 4 autoclave cycles
6% PVA	Until 5th trial	Db = 5.34, DE=7.43	Db = 7.81, DE=10.09	0 at 24 hrs
6% PEO	Until 5th trial	Db = 5.55, DE=8.13	Db = 9.81, DE=12.88	0 at 24 hrs
6% PAM	Until 6th trial	Db = 4.09, DE=4.97	Db = 7.91, DE=9.29	0 at 18 hrs
6% Na-CMC	Until 12th trial	Db = 6.09, DE=8.59	Db = 12.07, DE=13.82	0 at 16 hrs
6% Na-Alginate	Until 12th trial	Db = 6.41, DE=8.91	Db = 13.18, DE=15.67	0 at 16 hrs
6% Polyester resin	Until 6th trial	Db = 3.63, DE=4.05	Db = 7.93, DE=10.11	0 at 20 hrs
$Ca(PO_4)_2$	Until 8th trial	Db = 3.49, DE=4.41	Db = 6.97, DE=10.79	0 at 20 hrs

*Db= Yellowness, DE=Overall difference

nanoparticles to silver ions. These encapsulated additives were used to make the antimicrobial coated surfaces and checked for the efficiency.

It was found that these surfaces had better antimicrobial efficiency than the surfaces containing 6% PAM (sample 1, flow sheet 6.5), and were active against microorganism until 8th trials. 6 % polyester resin was also used for encapsulation. From the comparative study as shown in Table 6.5, the two natural polymer encapsulated additives (Na-CMC, Na-Alginate) were more active against microorganism than any other encapsulated additive due to the formation of comparatively stronger bonds between copper ions and the polymers functional groups. Effects of autoclave on these surfaces were analyzed in terms of color change and antimicrobial efficiency. Synthetic polymer encapsulated additives had better protecting capabilities than the surfaces prepared with the natural polymers, because the change of yellowness was found to increase more for natural polymer encapsulated additives than the synthetic ones.

6.5 Conclusions

Silver in different forms are being used from ancient time as an antimicrobial agent. Nano silver possess highly reactive available large surface areas and have potential for rapid dissolution and oxidative production. The main source of silver ions is through oxidation and nano silver can remain as a reservoir.

Uniform distribution of silver nano particles on zeolite surface was achieved through ion-exchange of zeolite with 0.03M silver nitrate followed by reduction with sodium boro-hydride, a strong reducing agent. Nanoparticles containing zeolite was functionalized with copper nitrate to balance the charge of the zeolite. SEM picture confirmed that the

nanoparticles produced with 0.05M silver nitrate overlapped each other on zeolite surface.

Intensity recorded from XRD analysis has confirmed the formation of silver nano particles on zeolite surface. Change of intensities with the increase of concentration of silver nitrate were also observed. But no peak for zeolite A was found when higher concentration (0.05M) of silver nitrate was used for the preparation of nanoparticles. It confirmed the presence of thicker layer of nanoparticles on the zeolite surface, prepared from 0.05M silver nitrate. Since efficiency of nanoparticles is size and dispersity dependent, it is required to have a good control over their size and distribution.

Uniform distribution of nanoparticles on the zeolite surfaces enhances the efficiency of the oxidation of nanoparticles in the presence of moisture. Different hydrophilic encapsulations were used in this study to provide a better insight for this purpose. Cross-linking between the polymers and the cations present within the additives plays an important role in holding the polymers so does the hydrophilic environment. The additives that contain only the nanoparticles did not show such holding capacity. Copper ions present within the additive helped to hold the polymer as well as preventing the silver ion already available from reduction during the curing process. The more cations present in the formulations, the stronger is the holding capacity as well as the greater the durability against microorganisms. So the release of silver ions from the coated surface depends on the hydrophilic polymeric compositions, concentration of cations, the valences and the polymer holding capacity. Although the addition of external nanoparticles within the formulations was found to be effective but on the contrary, after

several trials some black nanoparticles were found to leach out from the encapsulation and appeared on the surface.

At the beginning of the antimicrobial efficiency analysis, silver ion released from the surface of the specimen was found to dominate the process which resulted in achieving the antimicrobial efficiency in short time. Silver ion movement from the bulk to the surface became more significant after a certain time. So sufficient amount of silver ions is required to be produced and stored for longer antimicrobial durability, with control release. Natural polymeric encapsulation found to be the best option for this powder coated surface which can bind the cations by comparatively stronger bonds than the synthetic polymer encapsulation and can release ions by initiating better management of the oxidation pathways.

Through proper incorporation of the zeolite containing nanoparticles into the coated surface and to create the proper environment for these nano particles to release ions, direct release of nanoparticles can easily be minimized. This coated surface was successfully and efficiently able to inhibit the growth of *Escherichia coli*. Thus this novel antimicrobial coating can be an effective alternative in inhibiting the microbial growth and thereby the toxic ecological effect from direct release of nanoparticles into the environment can be avoided.

References:

1. Morones JR, Elechiguerra JL, Camacho A, Holt K, Kouri JB, Ramırez JT, Yacaman MJ. 2005, The bactericidal effect of silver nanoparticles. *Nanotechnology*, vol.16, pages 2346–2353

2. Guridi A, Diederich AK, Aguila-Arcos S, Garcia-Morenoa M, Blasi R, Broszat M, Schmieder W, Clauss-Lendzian E, Sakinc-Gueler T, Andrade R, Alkorta I, Meyer C, Landau U, Grohmann E, 2015. New antimicrobial contact catalyst killing antibiotic resistant clinical and waterborne pathogens. *Materials Science and Engineering*, vol. 50, pages 1–11.

3. Liu J, Hurt RH, 2010, Ion Release Kinetics and Particle Persistence in Aqueous Nanosilver Colloids. *Environ. Sci. Technol.* vol. 44, pages 2169–2175.

4. Xiu ZM, Zhang QB, Puppala HL, Colvin VL, Alvarez PJ, 2012, Negligible particlespecific antibacterial activity of silver nanoparticles, *Nano Lett.* vol.12, no. 8, pages 4271–4275.

5. Lok C, Ho, C, Chen R, He Q, Yu W, Sun H, Tam PK, Chiu J, Che C. ,2007,Silver Nanoparticles: Partial Oxidation and Antibacterial Activities. *J. Biol. Inorg. Chem.* vol.12, pages 527–534.

6. Lee YJ, Kim J, Oh J, Bae S, Lee S, Hong IN, Kim SH., 2012, Ion-release kinetics and ecotoxicity effects of silver nanoparticles. *Environmental Toxicology and Chemistry*, vol. 31, no. 1, pages 155–159.

7. Rahul Tripathi and Brahmeshwar Mishra, 2012, Development and Evaluation of Sodium Alginate–Polyacrylamide Graft–Co-polymer-Based Stomach Targeted Hydrogels of Famotidine, *AAPS PharmSciTech*, vol. 13, no. 4, pages 1091-1102.

8. Calo E, Khutoryanskiy VV. 2015, Biomedical applications of hydrogels: A review of patents and commercial products. *European Polymer Journal*, vol. 65 pages 252–267.

9. Alissawi N, Zaporojtchenko V, Strunskus T, Hrkac T, Kocabas I, Erkartal B, Chakravadhanula VSK, Kienle L, Grundmeier G, Garbe-Scho¨nberg D, Faupel F. 2012, Tuning of the ion release properties of silver nanoparticles buried under a hydrophobic polymer barrier, *J Nanopart Res.* vol.14, page 928.

10. H Münstedt, 2008, Kinetic aspects of the silver ion release from antimicrobial polyamide/silver nanocomposites c. dam. *Appl. Phys.* vol. 91, pages 479–486.

11. Xu H, Qu F, Xu H, Lai W, YA Wang, Aguilar ZP, Wei H., 2012, Role of reactive oxygen species in the antibacterial mechanism of silver nanoparticles on Escherichia coli O157:H7. *Biometals,* vol. 25, pages 45–53.

12. Behra R, Sigg L, Clift MJD, Herzog F, Minghetti M, Johnston B, Petri-Fink A, Rothen-Rutishauser B. Oct. 6, 2013, Bioavailability of silver nanoparticles and ions: from a chemical and biochemical perspective. *Journal of Royal Society, Interface* vol 10, page 87.

13. Cheng HH, Hsieh CC, Tsai CH., 2012,Antibacterial and Regenerated Characteristics of Ag-zeolite for Removing Bioaerosols in Indoor Environment. *Aerosol and Air Quality Research,* vol. 12, pages 409–419.

14. Ayben Top, Semra U lku, October 2004,Silver, zinc, and copper exchange in a Na-clinoptilolite and resulting effect on antibacterial activity. *Applied Clay Science*, vol.27, no. 1-2, pages 13-19.

15. Carlson C, Hussain SM, Schrand AM, Braydich-Stolle LK, Hess KL, Jones RL, Schlafer JJ. 2008, Unique Cellular Interaction of Silver Nanoparticles: Size-Dependent Generation of Reactive Oxygen Species. *J. Phys. Chem. B.*, vol.112, pages 13608–13619.

16. Asharani PV, Mun GLK, Hande MP, Valiyaveettil S. 2009, Cytotoxicity and Genotoxicity of Silver Nanoparticles in Human Cells. *ACS Nano,* vol. *3*, pages 279–290.

17. Elbadawy A. K., Xin C. B., Mohamed S. Mohy E. A., El-Refaie S. K., 2015, Crosslinked poly(vinyl alcohol) hydrogels for wound dressing applications: A review of remarkably blended polymers, *Arabian Journal of Chemistry*, vol.8, pages 1–14.

18. Chen M, Yan L, He H, Chang Q, Yu Y, Qu J. 2007, Catalytic Sterilization of *Escherichia coli* K12 on Ag/Al2O3 Surface. *J. Inorg. Biochem.*, vol. 101, pages 817–823.

19. Jamnongkan T, Wattanakornsiri A, Wachirawongsakorn P, Kaewpirom S. 2014, Effects of cross-linking degree of poly(vinyl alcohol) hydrogel in aqueous solution: kinetics and mechanism of copper(II) adsorption. *Polym. Bull*. vol.71, pages 1081–1100.

20. Gonzalez JS, Maiolo AS, Ponce AG, Alvarez VA, 2011. Composites based on poly(vinyl alcohol) hydrogels for wound dressing. *XVIII The Argentine Congress of Bioengineering and Clinical Engineering Conference VII*, SABI, pages 1–4.

21. Composition for forming hydrophilic coating. US 4466832 A.

22. Saeed R, Masood S, ul Abdeen Z. February 2013, Ionic Interaction of Transition Metal Salts with Polyvinyl Alcohol-Borax- Ethyl Acetate Mixtures *International Journal of Science and Technology*. vol. 3, no.2, pages 132-142.

23. Shekunov BY, Chattopadhyay P, Tong HHY, Chow AHL, Grossmann JG. May 2007, Structure and drug release in a crosslinked poly(ethylene oxide) hydrogel *Journal of Pharmaceutical Sciences*. vol. 96, no. 5, pages 1320–1330

24. Pierre Agulhon, Velina Markova, Mike Robitzer, Françoise Quignard, and Tzonka Mineva, 2012, Structure of Alginate Gels: Interaction of Diuronate Units with Divalent Cations from Density Functional Calculations, *Biomacromolecules*, vol.13, no.6, pages 1899–1907.

25. Kamoun EA, Chen X, Eldin MSM, Kenawy ES. 2015, Crosslinked poly(vinyl alcohol) hydrogels for wound dressing applications: A review of remarkably blended polymers. *Arabian Journal of Chemistry* , vol. 8, pages 1–14.

26. Molina I, Li S, Martinez MB, Vert M., 2001, Protein release from physically crosslinked hydrogels of the PLA/PEO/PLA triblock copolymer-type. *Biomaterials* vol.*22*, pages 363-369.

27. Ramakrishna P, Madhusudana Rao K, Sekharnath KV, Kumarbabu P, Veeraprathap S, Chowdoji Rao K, M.C.S. Subha. March, 2013, Synthesis and characterization of Interpenetrating polymer network microspheres of acryl amide grafted Carboxymethylcellulose and Sodium alginate for controlled release of Triprolidine hydrochloride monohydrate. *Journal of Applied Pharmaceutical Science* vol. 3, no.3, pages 101-108.

28. Chang Q, Hao X, Duan L. 2008, Synthesis of crosslinked starch-graft-polyacrylamide-*co*-sodium xanthate and its performances in wastewater treatment. *Journal of Hazardous Materials* vol.159 pages 548–553.

29. Hand book of Polymeric Engineering Materials, 1997, Nicholas P. Cheremisinoff, ISBN :0-8247-9799-X

CHAPTER 7

Encapsulation of Zeolite Containing Nanoparticles with Blended Polymers and their Antimicrobial Efficiency in Powder Coated Surface

7.1 Abstract

The antimicrobial efficiency of the silver nanoparticles embedded in the ultra fine powder coated surface was resolved. The hydrophilic polymer encapsulation of the silver nanoparticles with copper ions dispersed on the zeolite surface helped to generate the silver ions. Synthetic and natural polymer blends were found to be the best combination for this particular formulation. The polymer blend was prepared with Na-alginate and Na-CMC at different proportion with polyacrylamide, which helped to form physical cross-linking with cations in the additive and carboxylate groups in the polymers. Cross-linking helps to prepare hydrophilic three dimensional polymeric structures. This hydrophilic encapsulation helps to provide moisture for the nanoparticles to oxidize, and as such, this oxidation process can help to produce the Ag^{+} ions. Glutaldehyde was added in one formulation to join the different molecular chains by covalent bonds to make the polymer more stable. For this particular combination of polymers, chemical cross linkers (GA) did not show any difference in respect to the reduction of number of microorganisms. But higher proportion of natural polymers, used for encapsulation of additives seems to be more stable and capable of holding more moisture within the polymer matrix through interpenetrating cross-linking as proven by its antimicrobial efficiency. Transfer efficiency of the additive to the coating substrate was 80% during

spraying. The finally formulated surface was found to be active against microorganisms after autoclave and UV treatment. Lactate dehydrogenase (LDH), released from damaged or destroyed cells in the surrounding media also proved the efficiency of the coated surface even after prolonged use.

Key words: Blended polymer, antimicrobial efficiency, encapsulation, hydrophilic

7.2 Introduction

Silver nano particles have already been established as highly effective antimicrobial agent against bacteria, viruses and fungi [1]. There is some concern about the direct release of these nano particles, which may cause potential risk to the environment. In order to minimize this risk, the incorporation of these nano particles was done within different polymeric matrixes in the form of multilayered films, nano-fibers, hydrogels, and micro-particles all of which had certified adequate stabilization with minimum release of silver nano particles from the matrix [2,3,4,5]

Natural polymers are biocompatible and biodegradable, but synthetic polymers, besides being biocompatible, have better physical and chemical properties. The mechanical, thermal and physico-chemical properties of the natural polymers can be improved by blending them with synthetic polymers or by chemical modifications such as grafting, interpenetrating polymer networks and chemical cross-linking [6].

Hydrogels are cross-linked hydrophilic water insoluble polymeric networks, which swell in water and can retain significant amounts of water. This water retaining capacity is due to the presence of different functional groups such as amides, hydroxyl and carboxyl

groups in the polymers [7]. When a polymer chain contains ionic units, it shows a distinct effect in the polymeric network. Inter and intra molecular ionic interactions take place due to the Coulombic attraction between oppositely charged sites, which is stronger than van der Waal forces but not as strong as covalent bonds. By changing the degree of cross-linking, ionic strength, solvent composition, and charge density, the swelling property of the polymeric network can be altered from highly swollen hydrogels to collapsed networks [7]. The structure of the hydrogels can be modified for adaptable functionality and for the enhanced release profile [8]. These hydrophilic hydrogels can stabilize the nanoparticles within the polymeric matrix [9].

Cross-linking can be formed by covalent or ionic bonds with the formation of three dimensional networks, which helps to join the polymer chains and thereby decrease the molecular freedom. These bonds are formed between the charged polymer chains and the ions of opposite charge. So, cross-linking is formed as an effect of charge association. Generally polymers are cross-linked to avoid dissolution, which contains ionic functional groups to encourage diffusion of water within the matrix. Three dimensional networks formed by cross-linking reduce swelling and make the matrix insoluble in water [10]. This is due to the reduction of elasticity in the network, disorder in the original form and the reduction of the entropy of the chain. They also become stiffer from their formerly coiled state [11]. This network permits the liquid to absorb in the empty spaces within the polymer chains and prevents dissolution of the polymer due to the withdrawal forces of the polymer matrix [10]. Presently, cross-linking by ionic interaction, which is known as physical cross-linking, establishes a more effective method based on toxicity and stability than the chemical cross-linking with toxic compounds [12].

Polymeric properties can also be modified by graft copolymerization with synthetic and natural polymers, which have imminent applications in the biomedical field [13]. Graft co-polymerization is also an effective way to modify the physico-chemical property of polysaccharides. Here, polymers are grafted on the backbone of polysaccharides. This process helps to reduce the hydrophilicity and introduce steric bulkiness, and as a result rapid dissolution and erosion of the matrix is prohibited. It also helps to control the release rate of incorporated active agents. Interpenetrating three dimensional networks is possible to develop using this process, and will help to impart additional firmness to the matrix [14].Interpenetrating polymeric networks are possible by the cross-linking of these two different types of polymers with high water absorption capacity [15].

Synthetic polymers, like PVA, PEO, and PAM, can be blended with natural polymers. Polysaccharides are known as biological polymers, which are being used extensibly now a days in biomedical application. Sodium alginate is a natural, anionic, linear polysaccharide. Easy water solubility, and extensive swelling are the two important limitations of sodium alginate, which make it a non-effective matrix material. Physical cross-linking through the iono-tropic gelation process with other cations or other polymers is one of the easiest options by which to overcome these problems. Chemical modification is another way to modify the properties of sodium alginate [16, 23]. A polymer blend with PVA and sodium alginate enhances thermal stability, and provide higher elasticity and enhanced water swelling properties [12]. This was utilized for encapsulation followed by ionic interaction with calcium. This blended polymer was used in food processing [17]. Sodium alginate can also be used as microspheres and membranes. This polymer can be cross linked chemically with glutaraldehyde and

physically with Ca^{2+} ions. The cross-linking of chitosan and sodium alginate has also been reported by others [18].

Carboxymethylcellulose (CMC) is another anionic polyelectrolyte natural cellulose derivative used in a wide range of applications in vast areas. Sodium carboxymethyl cellulose has very good stability under shear stress [13]. The carboxyl and hydroxyl groups of CMC can easily form complexes with divalent metals [19].

Polyacrylamide is a non-ionic polymer, which is inert in nature and is hydrophilic. This can be blended with natural polymers to obtain improved properties. Synthetic polymers are more effective due to their flexible tailor-ability compared to the natural polymers but these are not resistant to shear [13].

Antimicrobial agents like silver nano particles, have been found to be effective after incorporating into blended polymers, i, e., PVA and alginate [20]. It is also reported in the literature that composites of PVA, chitosan and silver nanoparticles showed strong inhibition against microorganisms [21]. Copper ions were used as cross linkers in PVA followed by the preparation of copper - PVA nano cables by a reduction process. But silver ions in PVA are more difficult to reduce during cross-linking reactions under hydrothermal conditions [22].

Different blended hydrophilic polymeric encapsulations have been used for drug delivery and in the biomedical field. Blended polymers are known for their control release capability. Based upon all information mentioned in different studies it was decided to formulate a hydrophilic polymeric encapsulation for the additives that would contain silver nano particles and copper ions on a zeolite surface. Hydrophilic encapsulation is

needed for the silver nanoparticles to generate silver ions by an oxidation process. The antimicrobial activity of the surface containing these encapsulated additives was checked against *E.coli*.

7.3 Materials and Methods

Different methods employed in this study, are shown below;

7.3.1 Encapsulation of additives: Zeolite containing silver nano particles was used as the additives. These nano particles were prepared by the reduction of silver ions after the ion-exchange with 0.03M silver nitrate and copper ions. These additives were encapsulated with water soluble and hydrophilic blended polymer at different compositions as shown in Flow Sheet 1. Polymers used for encapsulation were polyacrylamide (PAM), sodium alginate (Na-alginate) and sodium carboxy methyl cellulose (Na-CMC). Glutaraldehyde (GA) was used as a cross linker. Formulation 1 and 2 are similar in polymeric composition, but the GA used in Formulation 2 as a chemical cross linker employed sulphuric acid to accelerate the cross-linking reaction. Formulation 3 consists of more natural polymers without any chemical cross linker. All other materials used for this work are mentioned in previous Chapters.

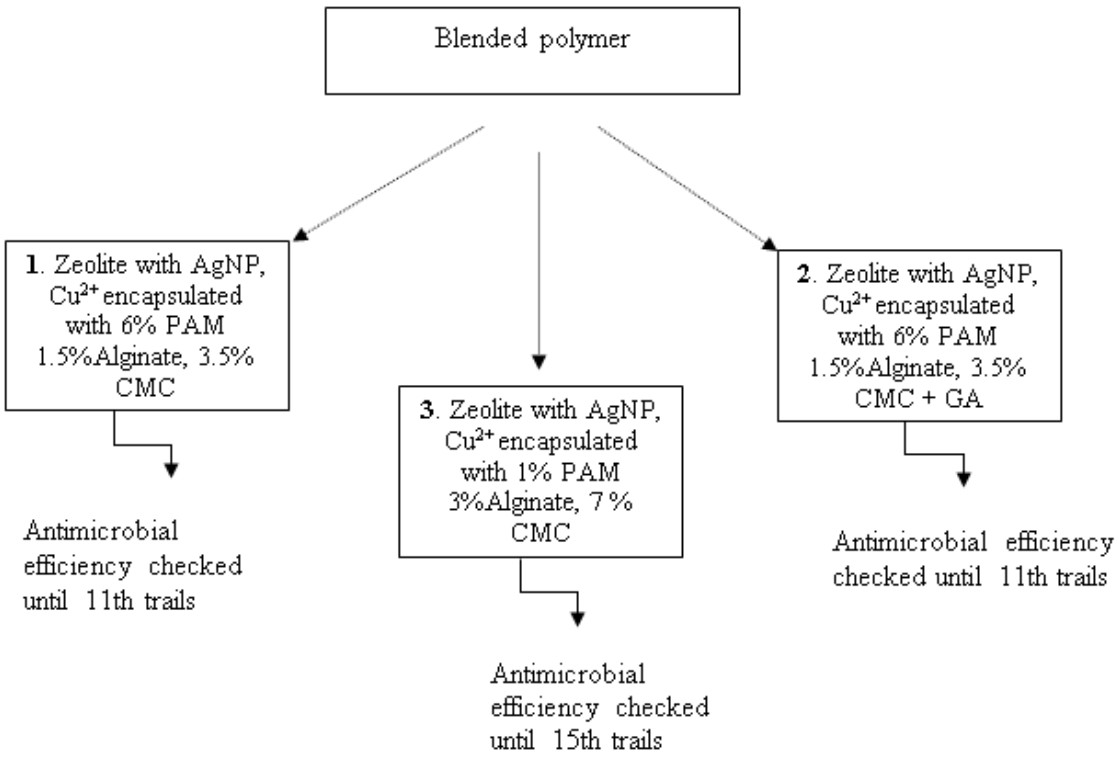

Flow sheet 7.1: Blended polymer encapsulated additives containing silver nanoparticles and copper ions

7.3.2 Leaching test of silver ion during exposure of microorganism: The coated surface was exposed to 10 ml of 10^6cfu/ml microorganism and incubated for different time durations at 37°C. The exposed microorganisms were collected for ICP analysis after digestion. One control surface without the additive was also used as a reference.

7.3.3 Weather test: Q-sun Xenon's Accelerated Light Stability and Weather Test Chamber (Q-Lab Corporation, Ohio, USA) was used to test the compatibility of the coated surface, including the control sample, at different weather conditions. Parameters used were UV 340nm, Irradiance: 0.55 W/m^2 (with 0.68 being the intensity of noon

summer sunlight at 340nm), day light temperature at 65°C for 8 hours and 4 hours condensation at 55°C. This pattern was used for total periods of 250, 500, 750 and 1000 hours. The total procedures were done following circle A in the standards ASTM D 4329.

All other methods of analysis (TGA, FTIR, Antimicrobial analysis, color analysis) used in this work are mentioned in the earlier chapters.

The same coated surface was used repeatedly called as 'trial' to check the efficiency against microorganisms. It is to be noted that the aforesaid coated surface was cleaned with soap and water and dried before every use.

7.4 Results and discussion

7.4.1 Polymeric encapsulation:

To make the silver nanoparticles active for the synthesis of silver ions, different blended polymeric encapsulated formulations were analyzed and their efficiency against microorganisms were checked after incorporation into the ultrafine powder coated surface. Sodium alginate and sodium CMC were used in combination as a natural source of polysaccharide. Gel strength of Na-alginate is low. Blending with Na-CMC helps to decrease the dissolution of this alginate in water due to the formation of hydrogen bond between these two polymers [23]. But maximum water absorbency can be achieved by Na-alginate/Na-CMC weight ratio of 0.54. Increase of alginate amount leads to the decrease of swelling capacity, due to the increase of viscosity of the mixture which hindered the movement of the reactant [24]. Graft co-polymerization was done with

polyacrylamide (PAM) as a source of synthetic polymer into the backbone of polysaccharides. PAM undergoes hydrolysis under basic condition and forms -COO^-, which is a binding site for cations [25]. In presence of water this polysaccharides can provide the basic environment. Combination of different polymers in 3 formulations are shown in Table 7.1 and the corresponding molar ratio of PAM and polysaccharide (mixture of Na-CMC and Na-Alginate).

-COONa present in CMC and alginate has a high solubility and can be present as carboxyl anions (-COO^-) and sodium cations (Na^+) in presence of water. The positively charged copper ions (Cu^{+2}) shows a stronger electrostatic interaction with the negatively charged carboxylic group (-COO^-) than the amide group (-$CONH_2$) present in polyacrylamide [26]. And it was also proven by thermo-gravimetric measurements that one divalent cations can bind by physical cross-linking through ionic bond with two -COO^- site of alginate or CMC [27]. Copper ions forms co-ordination covalent bond with -COO^- and the interaction energy has the highest value for Cu^{+2} then Co^{+2} , Zn^{+2} and Mn^{+2} [28]. Polyacrylamide contains amine groups, and they possess two hydrogen atoms, which can form hydrogen bond with other functional groups where lone pairs of electrons are available for bonding [29]. But hydrogen bonds are more flexible than ionic or coordination covalent bonds. The mechanism of interaction between the matrix during encapsulation can be hypothesized as follows; the experimental formulation mentioned in Table 7.1 contains 0.171moles of copper cations in the polymer matrix which can bind 0.3421 (0.171 x 2) moles of total carboxylate units. Total carboxylate units present in the first two formulations and the third formulation are 0.0203 and 0.0407moles respectively,

Table 7.1: Moles of cations and functional unit per 100 gm of additives

Sl. No	Formulation	Molar ratio PAM : Poly saccharide	Copper ions, moles	Na-CMC moles monomer unit	Na-Alginate moles monomer unit	Total $-COO^-$ moles	Molar ratio Cu^{+2} : $-COO^-$
1.	6% PAM, 3.5 % CMC, 1.5%Alginate	4:1	0.171	0.0133	0.007	0.0203	8.42
2.	6% PAM, 3.5 % CMC, 1.5%Alginate GA	4:1	0.171	0.0133	0.007	0.0203	8.42
3.	1% PAM, 7 % CMC, 3% Alginate	1:4	0.171	0.0267	0.014	0.0407	4.20

* Polysaccharide = Mixture of Na-CMC and Na-Alginate

so all carboxylate sites will be cross-linked physically by copper ions through co-ordination covalent bond. It is known that one copper ion can bind two carboxylate so the neutralization point is 0.5, but the molar ratio between Cu^{+2} and-COO^- is 8.42 and 4.20 for formulations 1 and 2 and formulation 3 respectively. So the adsorption capacity of copper present in the system is much higher than the present compositions. The interaction energy between the two ends of cross-linking is depended on ionic radius and the binding strength, which also depends on the nature of the cations and ionic character of the binding. Large cationic radius (Cu^{2+} 7.3) forms a tighter arrangement of cross-linked polymers, which is expected to fill a larger space between the blocks of polymers [30] Copper has the highest binding strength towards the $–COO^-$ and it is dependent on the nature of the metal cation, which follows the order: Cu^{+2}> Co^{+2} > Zn^{+2} > Mn^{+2} >>

Mg^{+2}> Ca^{+2}>Sr^{+2} [28]. In formulation 2 glutaraldehyde was added to the polymer matrix as a chemical cross-linker, two of the aldehyde groups will form covalent bonds with the –OH group present in the system [31, 32]. This external cross-linker helped to join the different molecular chains by covalent bond to make the polymer more stable.

OH^- groups of polymers will be responsible for the hydrophilicity of that encapsulation, which help to swell the polymer matrix for the synthesis of silver ions from the nanoparticles. When more copper ions will get chance to crosslink with carboxylate, more insoluble will be the polymeric composition and more stable will be the polymer matrix. In this case additives will not be vulnerable from the matrix. GA reduces the hydrophilicity of the polymeric matrix due to the formation of covalent bonds between aldehyde groups and the hydroxyl groups but copper makes the polymer insoluble while keeping the hydrophilicity intact.

7.4.2 Thermo gravimetric analysis:

TGA measures the mass change as a function of temperature in a controlled atmosphere. It is used to determine thermal and oxidative stability and is especially useful for polymeric materials studies. The derivative of the TGA curve gives the exact value for the decomposition process with enhanced resolution. The number of peaks at the derivative curve is confirmed by the number of distinct thermal changes taking place during such an analysis.

Free radical sites of the polymers were cross linked together with the cations present in the additives and formed three dimensional networks. Weight loss for additive containing

only nanoparticles, and copper ions and the encapsulated additives (Formulation 2 and Formulation 3) from the TGA analysis was found to be 19.5, 27.5 and 26% respectively. Weight loss occurred at the beginning of analysis around 85-120^{o}C and was due to the loss of moisture for all samples. But the fact that, samples containing polymer encapsulation losses more at that range were due to the presence of sugar units, galactose and mannose [16]. Their weight (moisture) loss occurred below 100^{o}C.

Formulation 3 contained more polysaccharides (Na-CMC and Na alginate) than Formulation 2, and so slightly higher moisture loss occurred at this thermogram than at lower temperatures. Maximum weight loss for the additive only occurred at 165^{o}C. But the encapsulated additives showed weight loss at two different stages of temperature in the DTGA curve in Figure 7.1. The weight loss for Formulation 2 occurred at 170^{o}C and at 392^{o}C. But Formulation 3 lost slightly less weight, and this occurred at 173^{o}C, almost at the same temperature as Formulation 2.

But the second reduction of weight loss in Formulation 3 was observed at higher temperatures between 470-520^{o}C. The weight loss at higher temperatures for the encapsulated additives were because of the loss of volatile compounds, fragmentation of chains and finally from the decomposition of polymers [16]. Total weight loss for Formulation 3 was found lower than Formulation 2 (27.5% water content) due to the reduced mobility of the internal water and volatile compounds through the polymeric encapsulation with higher polymeric matrix cross-linking, which also has high water

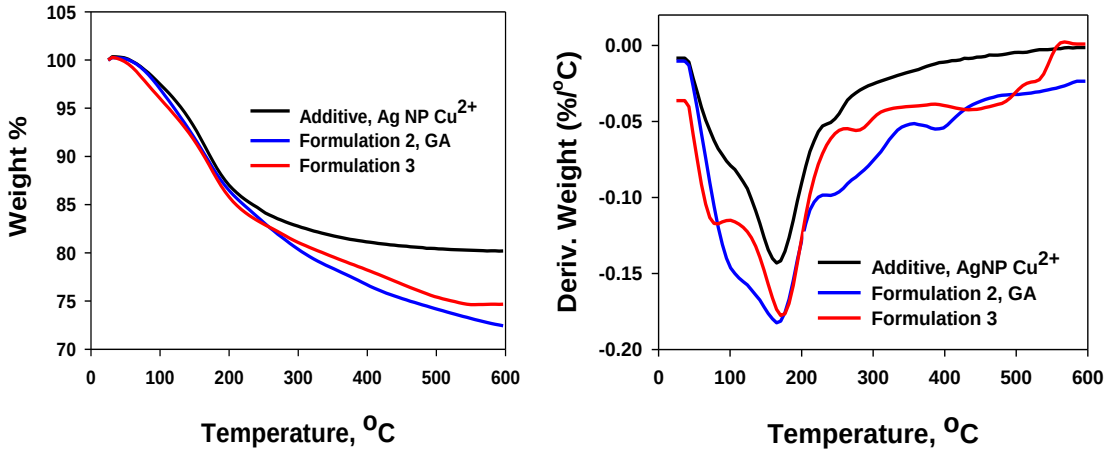

Figure 7.1: TGA and DTGA curves for additive used only (black), encapsulated additive with GA (formulation 2, blue), Encapsulated additive with more natural polymer (formulation 3, red)

retention capacity. So polymeric network is playing the key role for less weight loss for Formulation 3. It is working as heat barrier, so delaying the diffusion of volatile products. Similar effect was reported in previous studies for the polymer matrix [33].

7.4.3 FT-IR analysis:

The FTIR spectrum of the additives, containing synthetic zeolite with silver nanoparticles and copper ions encapsulated by three different blended polymeric compositions is shown in Figure 7.2 to demonstrate the changes in peaks or peak fluctuations, which could reveal the changes of bonding or interaction between functional groups. Stretches normally appear at around 3450 cm^{-1} and are due to the vibration of hydroxyl groups (-O-H stretching) present in the Na-alginate and Na-CMC. The interaction between the –H atom of Na Alginate/ Na-CMC and the lone pair of electrons at –O– of polyacrylamide results in the intermolecular hydrogen bonds [16]. It was also found in another study that

hydrogen bond formed between the hydrogen atoms in the amine groups of polyacryamide and the functional groups that possess a lone pair of electrons [29]. It was also noted that the intermolecular hydrogen bonding formed between polyacryamide and alginate or CMC [16].

Because of the formation of hydrogen bonds, the reduction in wave number of hydroxyl peaks occurred from 3440 to 3382 cm^{-1}[34]. The peaks for the vibration of hydroxyl groups found in the spectrums in Figure 7.2 were at around 3250cm^{-1}, which is lower than the normal stretching (3450 cm^{-1}) for hydroxyl groups. The characteristic band that occurred at 1691 cm^{-1} and 1692 cm^{-1} was due to the amide group (-$CONH_2$) of polyacrylamide (>C=O stretching) for the two formulations (1, 2) and contained more polyacrylamide (6%) than the Formulation 3 (1%). But this band shifted to a lower wavelength in the case of the Formulation 3 at 1626 cm^{-1}, due to the formation of -COO^- at the basic environment of the polymer blend, where Cu^{2+} can bound. The presence of symmetric –COO^- stretching vibrations [35] appeared at 1415 cm^{-1} for all formulations, but the intensity of those vibration for Formulation 3, which contained 10% of total CMC and alginate was more than the other two formulations with 5% total CMC and alginate. Some researchers pointed out that the interaction between negatively charged carboxylate

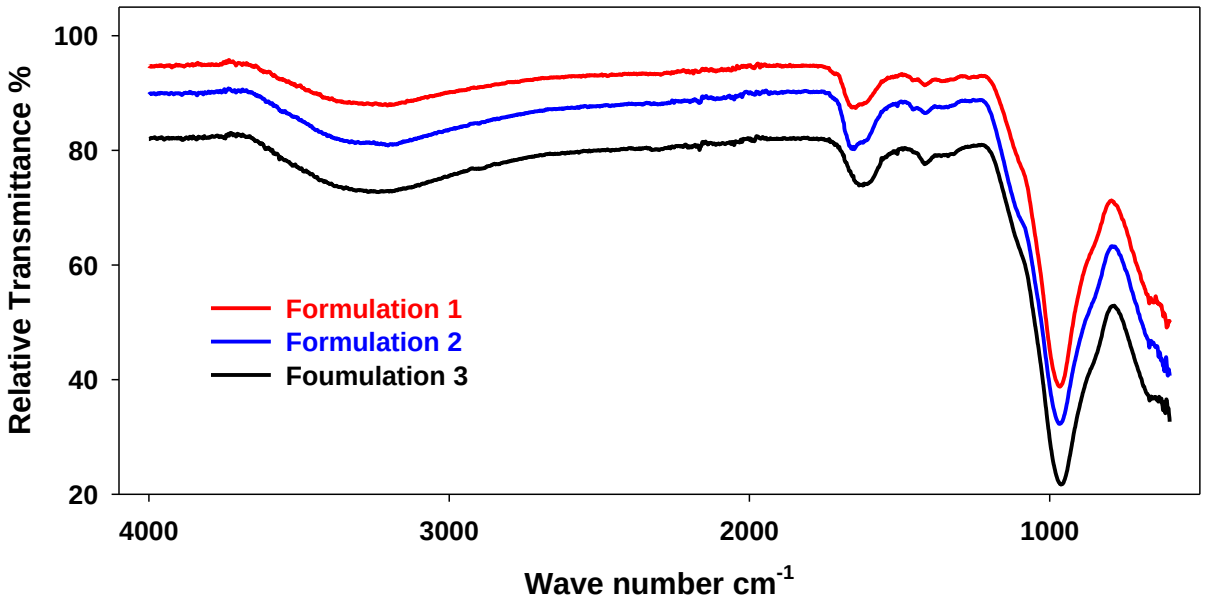

Figure 7.2: FTIR analysis of additives encapsulated by three different polymeric formulation

groups of carboxymethylcellose (CMC) and alginate and positively charged copper ions led to the formation of physical cross-linking due to the electrostatic interaction. And this interaction leads to the formation of coordination covalent bonds [28]. Other peaks found at around 970 cm^{-1} in all spectrums were the characteristic peak for zeolite, which is associated with the stretching vibration of Si-O, as suggested in the three dimensional silica phase [36].

7.4.4 Anti-microbial efficiency:

Antimicrobial efficiency test were performed against Gram-negative bacteria, *E.coli*. The efficiency depends on the silver ion release. The effects of antimicrobial activity for the

coated surface made with the additives from Formulation 1 and 2 are shown in Table 7.1 and 7.2 respectively. Similar trends were observed for the inactivation of the microorganisms. There was no significant effect observered from the antimicrobial analysis due to the formation of more stable cross-linking by GA for this particular composition of polymers. But the surface made from Formulation 3, which contained smaller amounts of synthetic polymers, showed very good efficiency in terms of inactivation of microorganisms (Fig. 7.3). This surface was found to be the most active antimicrobial surface made by the ultrafine powder coating method with the additive, which contains silver nanoparticles. The reason for this, is that the formulation contains higher amount of anionic polymer (Na-CMC, Na-Alginate). Anionic polymer contains chain $–CH_2COONa$, which can dissociate into $–COO^-$ when dissolved in water. The copper ions present in the additives can easily be cross-linked between two polymeric chains.

Table 7.2: No of microorganisms present (10^9 cfu/ml) after exposure on the coated surface made with Formulation 1

Time, hr	Trial 1	Trial 2	Trial 4	Trial 6	Trial 8	Trial 10	Trail 11
0	0.23	0.28	0.24	0.30	0.21	0.23	0.26
4	0.11	0.24	0.27	0.23	0.3	0.29	0.27
8	0	0	0.0021	0.0027	0.003	0.023	0.025
12	0	0	0	0	0	0.01	0.03
18	0	0	0	0	0	0.0017	0.0005
24	0	0	0	0	0	0	0

Table7.3: No of microorganisms present (10^9 cfu/ml) after exposure on the coated surface made with Formulation 2

Time, hr	Trial 1	Trial 2	Trial 4	Trial 6	Trial 8	Trial 10	Trail 11
0	0.23	0.28	0.24	0.30	0.21	0.23	0.26
4	0.22	0.28	0.19	0.31	0.28	0.25	0.2
8	0	0	0.0027	0.0021	0.0028	0.024	0.027
12	0	0	0	0	0	0.009	0.0032
18	0	0	0	0	0	0.005	0.0010
24	0	0	0	0	0	0	0

Excess copper ions can easily be cross-linked with excess $–COO^–$ and make the polymer matrix more insoluble and stable while keeping the hydrophilicity of the encapsulation. The co-grafting of PAM into that network makes its backbone more rigid and flexible with enhanced mechanical properties [37]. Penetration of water dominates the transport process and the rate of relaxation of the polymer chain. In the beginning, silver ion release is governed by the dissolution of silver particles at the surface, where the diffusion process is not needed. But after consumption of the surface particles, the transport of silver ions to the surface from the bulk is necessary. For that, diffusion of water is important and the free volume of the polymer is needed for this diffusion process, which can be obtained by cross-linking [38].

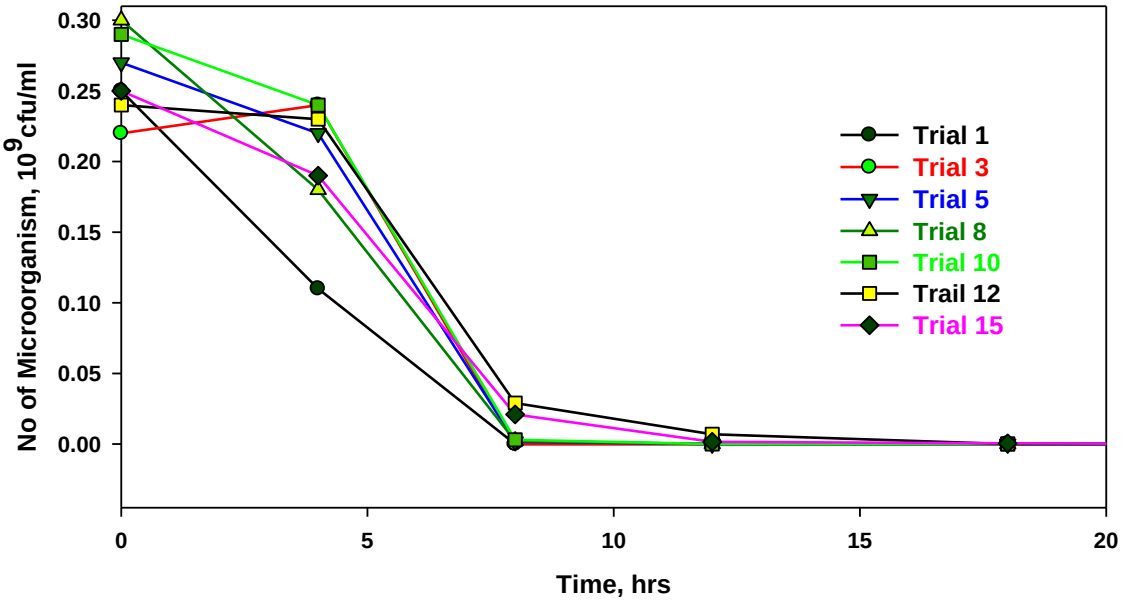

Figure 7.3: No of microorganisms present (10^9 cfu/ml) after exposure on the coated surface made with Formulation 3

7.4.5 Leaching analysis:

It was observed from previous experiments (reported in Chapter 5) that all microorganisms died within the first 2 hrs after exposure to the coated surface containing additives with silver and copper in ionic form. Whereas the amount of silver leached out from the same coated surface was found to be 0.14 ppm after 2 hrs and 0.16 ppm after 4 hrs. there was no significant leaching observed on the control surface even after 24 hrs of exposure. But when the additive was encapsulated with 2% PVA, the leaching rate of silver ion was reduced and it took 6 hrs for complete reduction from 10^6cfu/ml.

Table 7.4: Leaching test of silver ion during exposure of microorganism

Additive with	Amount of silver (ppm) at the exposed time				No of microorganism remain, 10^9cfu /ml
	2 hrs	4 hrs	8 hrs	24 hrs	
Control	0	0	0	0	21 after 24 hrs
AgNP, Cu^{2+}, encapsulated with 6% PAM, 1.5% Na-Alginate, 3.5% Na-CMC	0	0.04	0.14	0.24	0 after 8 hrs
AgNP, Cu^{2+}, encapsulated with 1% PAM, 3% Na-Alginate, 7% Na-CMC	0	0.03	0.13	0.17	0 after 8 hrs

The release of silver ion from the elemental silver is due to the oxidation of the elemental silver in the presence of moisture [39]. So the release was assumed to increase with the increase in moisture content of the encapsulated polymer. Since the diffusion coefficient of water is polymer dependent, the polymer composition plays an important role in the release of silver ions. For the hydrophilic polymer encapsulated additives, it was found that the complete reduction of microorganisms commenced after 8 hrs.

The amount of silver in the extracted microorganisms was found to be 0.14ppm and 0.13ppm for 6% PAM (Formulation 2) and 1%PAM (Formulation 3) respectively. Cross-linking between cations and polymers and the inter cross-linking between polymers in additives containing 1%PAM made the formulation more insoluble, so the release rate of silver ion was slowed down. Also the transport rate of water, which includes water diffusion and silver ion movement was usually found to be slower than the polymer relaxation processes. So the durability of this coated surface would be higher

than the surfaces coated with other additives. The release of active component always depends on the population of microorganisms, humidity and temperature. The transfer efficiency of the additives during powder spraying to the surface or object was 80% .

7.4.6 Autoclave analysis:

Autoclave testing of protective coatings was done to compare competing coating products to assess new coatings and to determine the effect of corrosion on the coating integrity. Continuous autoclaving with microorganism exposure is an accelerated corrosion testing method and was carried out to simulate the service conditions for sterilization purposes. Steam sterilization is normally used owing to its short processing time, non-toxicity and safety. During the autoclaving, the coated surfaces were exposed to relatively high temperatures and concentrated water vapors. These tests were also carried out to observe the changes in antimicrobial efficiency and color of the surface due to the change of surface morphology of the coating. The coating possesses the best and the worst deterioration resistance. The silver particles were active to produce the ions, which were found from the antimicrobial efficiency test, even after four cycle autoclaving. The test surfaces were prepared with the additives prepared following the composition of Formulation 3.

Color analysis revealed the increase in yellowness of the surface as well as the overall color difference after the 1st autoclaving. But there was no significant color change observed after the remaining autoclave treatments. Silver in the additive was incorporated as nano particles, so there was no scope for any reduction of silver, where this reduction

is responsible for change the color after every autoclave treatment. It should be mentioned here that the control surface without silver did not show any color change. As per US patent 4857450, it is reported that the Silver thiosulphate used in the microbial testing tape decomposed to black silver sulfide under the steam sterilization conditions. Other sterilization methods, such as ultraviolet treatment are also challenging, because of the photo sensitivity of silver [40]. But this formulation can easily be applied to the dark colored surface, where changes in color during autoclaving would not show any significant effect.

Table 7.5: Effect of Autoclave on surface color and antimicrobial effectivity against microorganism

Surface made with formulation 3 additive	DL	Da	Db	CIE DE	No of microorganism remain
0	-1.34	-0.45	4.01	4.29	0 at 08 hrs
1st	-3.74	-1.89	10.14	11.84	0 at 18 hrs
2nd	-4.15	-2.56	11.48	12.78	0 at 24 hrs
3rd	-4.99	-2.76	11.67	14.04	0 at 24 hrs
4th	-5.01	-2.80	11.71	14.05	0 at 24 hrs

*Db= Yellowness, DE=Overall difference

7.4.7. Compatibility analysis of the coated surface at different weather conditions:

To predict the durability of coatings exposed to outdoor environments, accelerated weather testing experiments were done. This was a laboratory simulation of the damaging forces of weather. Depending upon the purpose and use of the coating, either physical

and or chemical properties could be used to check the effects of weather. According to ISO 4582, general appearance, color change and antibacterial activity of the coating were selected to address the effect of weather in the accelerated conditions. Essentially, if the light source was comparable to sunlight, the best simulation with natural exposure could be achieved. The spectral power circulation of sunlight at the UV and visible regions can be reproduced by the filtered xenon arc. The stresses of swelling and drying are dependent on moisture [40].

Table 7.6: Effect of UV radiation on surface color and antimicrobial effectivity against microorganism

Surface made with formulation 3 additive	DL	Da	Db	CIE DE	No of microorganism remain
0	-1.34	-0.45	4.01	4.29	0 at 08 hrs
250 hrs	-1.35	-0.43	3.98	4.27	0 at 18 hrs
500 hrs	-1.49	-0.54	4.11	4.53	0 at 24 hrs
750 hrs	-1.74	-0.68	4.35	4.72	0 at 24 hrs
1000 hrs	-2.32	-0.84	4.51	4.91	0 at 24 hrs

*Db= Yellowness, DE=Overall difference

Table 7.6 shows the results of antibacterial activity of a coated surface (Formulation 3) exposed to accelerated weather conditions at different time periods. With an increase of time of exposure, antibacterial activity reduced gradually but it was quite active against microorganisms. There was no significant color effects like autoclaving analysis after 1000hrs of UV exposure and the antimicrobial efficiency was intact. So this formulation has a potential future for the surface which needs to use at the detrimental weather.

7.4.8 Bactericidal effect (Membrane Integrity/LDH Leakage):

Lactate dehydrogenase (LDH), is a soluble cytosolic enzyme, which exposes due to the loss of cell membrane integrity. To assess the cytotoxicity resulting from the toxic effects of silver to the microorganisms, lactate dehydrogenase (LDH) production is used [41] by the amount of fluorescence produced. Fluorescence was used to measure the LDH amount at excitation and emission wavelengths of 560nm and 590nm respectively and measured data are reported as percentages of the control coated surface [42]. This fluorescence is related to the number of lysed cells. Toxicity analysis was done at different time of exposure to the microorganism on the antimicrobial coated surface. An increase in LDH seepage in the culture medium was observed with the increase of contact

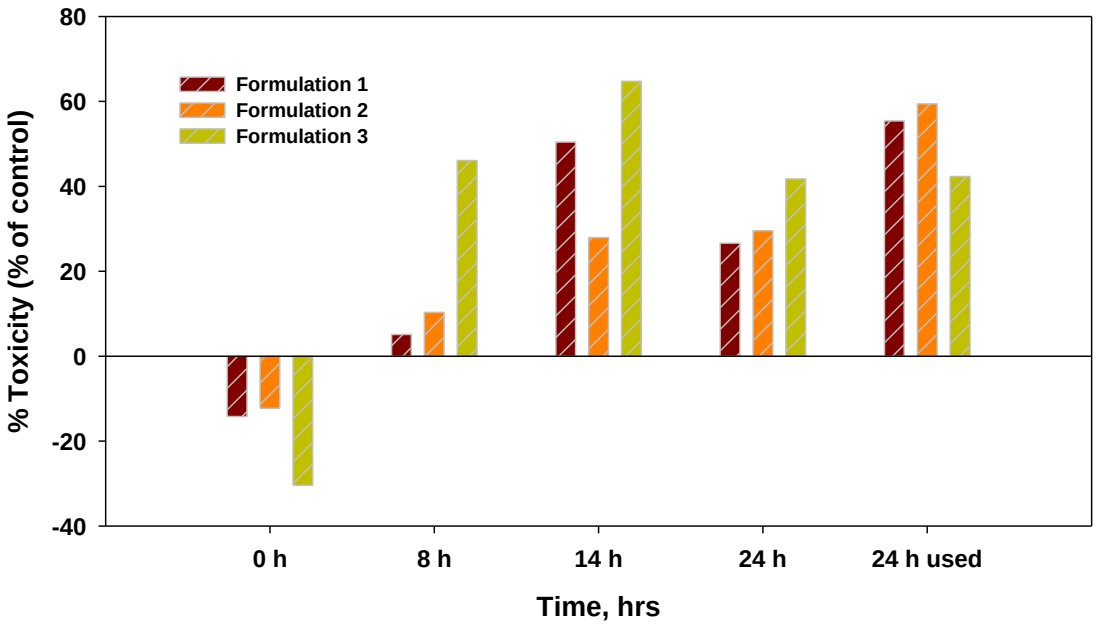

Figure 7.4: Toxicity analysis of antimicrobial surfaces with AgNP for extended time and period

time with the microorganism due to the plasma membrane damage of cells. LDH production from the observation of toxicity analysis even after 15 times (cycle of exposure) used coated surface also proved the efficiency of the formulation.

7.5 Conclusions

Use of nano particles for novel applications is opening the door for some critical toxicological and environmental issues to be resolved. Hydrophilic polymer blends are the promising encapsulation formulation for nanoparticles to produce their respective ions. Graft polymerization with synthetic and natural polymer combinations, followed by physical cross-linking with cations between these polymers and additives, are the best encapsulation combinations for the antimicrobial surface preparation. This hydrophilic encapsulation helps to provide moisture for the nanoparticles in which to oxidize, and as such, this oxidation process can help to produce the Ag^{+} ions.

Cross-linking helps to prepare hydrophilic three dimensional polymeric structures. The external cross-linker, like glutaldehyde, can join the different molecular chains by covalent bond to make the polymer more stable. For this particular combination of polymers, a chemical cross-linker (GA) did not show any difference in respect to the reduction of microorganisms. But with increased proportions of natural polymers, encapsulation of additives seems to be more stable and capable of holding more moisture within the polymer matrix by interpenetrating cross-linking. Physical cross-linking with natural and synthetic polymers make the polymer relaxation slower so that the release of silver ions also follows the same trend.

It was found from the calculation of moles of cations and carboxylate groups present in the system, that more carboxylate can be added to the system to bond the excess copper ions available in the matrix. More carboxylate source will afford more insolubility of the polymer due to the bonding between copper and the carboxylate and it will provide excess hydrophilicity. Extra polymer encapsulation also helped to protect the color of the surface to some extent during autoclave treatment. Toxicity analysis is another way to understand the efficiency of the coated surface by the formation of silver ions, which is responsible for the production of lactate dehydrogenase (LDH), released from damaged or destroyed cells in the surrounding medium.

References:

1. Li WR, Xie XB, Shi QS, Zeng HY, Ou-Yang YS, Chen YB, 2010, Antibacterial activity and mechanism of silver nanoparticles on *Escherichia coli*. *Appl Microbiol Biotechnol* vol. 85, no. 4, pages 1115–1122.

2. Zhang J, Xu S, Kumacheva E (2004) Polymer microgels: reactors for semiconductor, metal, and magnetic nanoparticles. *J Am Chem Soc*, vol.126, pages 7908–7914.

3. Wu Y, Jia W, An Q, Liu Y, Chen J, Li G, 2009, Multiaction antibacterial nanofibrous membranes fabricated by electrospinning: an excellent system for antibacterial applications, *Nanotechnology,* vol. 20, no 24, pages 245.

4. Yuana W, Fua J, Sua K, Ji J, 2010, Self-assembled chitosan/heparin multilayer film as a novel template for in situ synthesis of silver nanoparticles. *Coll Surf B Biointerface,* vol. 76, pages 549–555.

5. Ma YQ, Yi JZ, Zhang LM, 2009, A facile approach to incorporate silver nanoparticles into dextran-based hydrogels for antibacterial and catalytical application, *J Macromol Sci* vol. 46, no. 6, pages 643–648.

6. Chandy T, Sharma CP, 1992, Prostaglandin E1-immobilized poly (vinyl alcohol)-blended chitosan membranes: Blood compatibility and permeability properties, *J Appl Polym Sci* vol. 44, no12, pages 2145–2156

7. Peppas NA, Khare AR, 1993, Preparation, structure and diffusionalbehavior of hydrogels in controlled release. *Adv Drug Del Rev* , vol.11, no 1–2, pages1–35.

8. Mukherji S, Ruparelia J, Agnihotri S, 2012, Antimicrobial activity of silver and copper nanoparticles: variation in sensitivity across various strains of bacteria and fungi. *Nano-antimicrobials–progress and prospects*, pages 225–251.

9. Juby K. A., Dwivedi C., Kumar M., Kota S., Misra H. S., Bajaj P. N., 2012, Silver nanoparticle-loaded PVA/gum acacia hydrogel: synthesis, characterization and antibacterial study, *Carbohydrate polymers* vol.89, pages 906-913.

10. Auda J. B., Sihama I. S., Fadhel A. H., Jaleel K. A., 2014, Proposed cross-linking model for carboxymethyl cellulose/starch superabsorbent polymer blend, *International Journal of Materials Science and Applications*, vol.3, no. 6, pages 363-369.

11. M. Elliot 2010,"Superabsorbent Polymers" BASF,

12. Elbadawy A. K., Xin C. B., Mohamed S. Mohy E. A., El-Refaie S. K., 2015, Crosslinked poly(vinyl alcohol) hydrogels for wound dressing applications: A review of remarkably blended polymers, *Arabian Journal of Chemistry*, vol.8, pages 1–14.

13. P. Ramakrishna, K. Madhusudana Rao, K.V. Sekharnath, P. Kumarbabu, S. Veeraprathap, K. Chowdoji Rao, M.C.S. Subha, March, 2013, Synthesis and characterization of Interpenetrating polymer network microspheres of acryl amide grafted Carboxymethylcellulose and Sodium alginate for controlled release of Triprolidine hydrochloride monohydrate, *Journal of Applied Pharmaceutical Science*, vol. 3,no.03, pages 101-108.

14. Sanchita Mandal, Sanat Kumar Basu, Biswanath Sa, 2010, Ca^{2+} ion cross-linked interpenetrating network matrix tablets of polyacrylamide-grafted-sodium alginate and sodium alginate for sustained release of diltiazem hydrochloride, *Carbohydrate Polymers*, vol 82, no.3, pages 867–873.

15. Enrica C., Vitaliy V. K., 2015, Biomedical applications of hydrogels: A review of patents and commercial products, *European Polymer Journal*, vol.65, pages 252–267.

16. Rahul Tripathi and Brahmeshwar Mishra, 2012, Development and Evaluation of Sodium Alginate–Polyacrylamide Graft–Co-polymer-Based Stomach Targeted Hydrogels of Famotidine, *AAPS PharmSciTech*, vol. 13, no. 4, pages 1091-1102.

17. Levic S., Rac V., Manojlovic V., Rakic V., Bugarski B., Flock T., Krzyczmonik K.E., Nedovi N., 2011, Limonene encapsulation in alginate-poly (vinyl alcohol), *Procedia Food Sci.*, vol.1, pages 1816–1820.

18. Djamel Tahtat , Mohamed Mahlous, Samah Benamer, Assia Nacer Khodja, Habiba Oussedik-Oumehdi, Fatima Laraba-Djebari, 2013, Oral delivery of insulin from alginate/chitosan crosslinked by glutaraldehyde, *International Journal of Biological Macromolecules,* vol.58, pages 160–168.

19. B.Mahalakshmi Devi, Srinivasan Latha, D. Umamaheshwari, K. Vijayalakshmi,Thandapani Gomathi and P. N. Sudha, 2014, Synthesis and characterisation of chitosan/sodium alginate/carboxymethyl cellulose beads, *Der Pharmacia Lettre*, vol. 6, no 6, pages 389-395.

20. Abd El-Mohdy, H.L., 2013. Radiation synthesis of nanosilver/polyvinyl alcohol/cellulose acetate/gelatin hydrogels for wound dressing. *J. Polym*. Res. Vol.20, pages 177–188.

21. Li C., Fu R., Yu C., Li Z., Guan H., Hu D., Zhao D., Lu L., 2013, Silver nanoparticle/chitosan oligosaccharide/poly(vinyl alcohol) nanofibers as wound dressing: a preclinical study, *Int. J. Nanomed*, vol.8, pages 4131–4145.

22. Junyan G., Linbao L., Shu-Hong Y., Haisheng Q., Linfeng F., 2006, Synthesis of copper/cross-linked poly(vinyl alcohol) (PVA) nanocables via a simple hydrothermal route, *J. Mater Chem.*, vol16, pages 101-105.

23. Sa-Ad Riyajan and Janthanipa Nuim, 2013, Interaction of Green Polymer Blend of Modified Sodium Alginate and Carboxylmethyl Cellulose Encapsulation of Turmeric Extract, *International Journal of Polymer Science*, pages 1-10.

24. A. Pourjavadi, Sh. Barzegar, G.R. Mahdavinia, 2006, MBA-crosslinked Na-Alg/CMC as a smart full-polysaccharide superabsorbent hydrogels, Carbohydrate Polymers, vol.66, no. 3, pages 386-395.

25. Cavus, S., G. Gurdag, K. Sozgen and M.A. Gurkaynak, 2009,The preparation and characterization of poly(acrylic acid-co-methacrylamide) gel and its use in the noncompetitive heavy metal removal, *Polymers for Advanced Technologies*, Vol.20, no.3, pages 165-172.

26. Hand book of Polymeric Engineering Materials, 1997, Nicholas P. Cheremisinoff, ISBN :0-8247-9799-X

27. Pierre Agulhon, Mike Robitzer, Laurent David, and Françoise Quignard, 2012**,** Structural Regime Identification in Ionotropic Alginate Gels: Influence of the Cation Nature and Alginate Structure, *Biomacromolecules*, vol.*13, no.*1, pages 215–220.

28. Pierre Agulhon, Velina Markova, Mike Robitzer, Françoise Quignard, and Tzonka Mineva, 2012, Structure of Alginate Gels: Interaction of Diuronate Units with Divalent Cations from Density Functional Calculations, *Biomacromolecules*, vol.13, no.6, pages 1899–1907.

29. Zhi Wei Low, Pei Lin Chee, Dan Kai and Xian Jun Loh, 2015, The role of hydrogen bonding in alginate/poly(acrylamide-co-dimethylacrylamide) and alginate /poly (ethylene glycol) methyl ether methacrylate-based tough hybrid hydrogels, *Royal Society of Chemistry*, vol.5, pages 57678-57685.

30. Can Hui Yang, Mei Xiang Wang, Hussain Haider, Jian Hai Yang, Jeong-Yun Sun, Yong Mei Chen, Jinxiong Zhou, and Zhigang Suo, 2013, Strengthening Alginate/Polyacrylamide Hydrogels Using Various Multivalent Cations, *Appl. Mater. Interfaces*, vol.*5* no.21, pages 10418–10422.

31. A review of: "Affinity Chromatography J. Turková Elsevier Amsterdam, New York, 1978; hardbound, 405 pages

32. Oya Şanlı, Nuran Ay, Nuran Işıklan, 2007, Release characteristics of diclofenac sodium from poly(vinyl alcohol)/sodium alginate and poly(vinyl alcohol)-grafted-poly(acrylamide) /sodium alginate blend beads, *European Journal of Pharmaceutics and Biopharmaceutics*, vol. 65, no. 2, pages 204–214.

33. Junping Zhang, Qin Wang, Aiqin Wang, 2007, Synthesis and characterization of chitosan-g-poly(acrylic acid)/attapulgite superabsorbent composites, *Carbohydrate Polymers*, vol.68, pages 367–374.

34. Wimonwan Klinkajon and Pitt Supaphol, 2014, Novel copper (II) alginate hydrogels and their potential for use as anti-bacterial wound dressings, *Biomedical materials*, vol.9, page 1-11.

35. Sergios K. Papageorgiou, Evangelos P. Kouvelos, Evangelos P. Favvas, Andreas A. Sapalidis, George E. Romanos, Fotios K. Katsaros, 2010, Metal–carboxylate interactions in metal–alginate complexes studied with FTIR spectroscopy, *Carbohydrate Research* vol 3, no.45 pages 469–473.

36. Kamyar Shameli, Mansor Bin Ahmad, Mohsen Zargar, Wan Md Zin Wan Yunus, and Nor Azowa Ibrahim, 2011.Fabrication of silver nanoparticles doped in the zeolite framework and antibacterial activity *Int J Nanomedicine*. Vol. 6, pages 331–341.

37. A. Li, R.F. Liu, A.Q. Wang, 2005, Preparation of starch-graft-poly(acrylamide)/ attapulgite superabsorbent composite, *J Appl. Polym. Sci*., vol.98, pages 1351–1357.

38. N. Alissawi, V. Zaporojtchenko, T. Strunskus, T. Hrkac, I. Kocabas, B. Erkartal, V. S. K. Chakravadhanula, L. Kienle, G. Grundmeier, D. Garbe-Scho¨nberg, F. Faupel, 2012, Tuning of the ion release properties of silver nanoparticles buried under a hydrophobic polymer barrier, *J Nanopart Res*, vol.14, page 928.

39. Amber N., Alistair H., Supriya S., Robert S. M. Jr., Prabir K. D., James W., 2011, Silver nanoparticles embedded in zeolite membranes: release of silver ions and mechanism of antibacterial action, *Int J Nanomedicine*, vol.6, pages 1833–1852.

40. Brown R. P., 1993, Test procedures for Artificial Weathering, *Polymer Testing* vol. 12, pages 459-466.

41. Lun Li, Jie Sun, Xiaoran Li, Yan Zhang, Zhaoxu Wang, Chunren Wang, Jianwu Dai Qiangbin Wang, 2012, Controllable synthesis of monodispersed silver nanoparticles as standards for quantitative assessment of their cytotoxicity, *Biomaterials,* vol.33, pages 1714- 1721.

42. C. Carlson, S. M. Hussain, A. M. Schrand, L. K. Braydich-Stolle, K. L. Hess, R. L. Jones, and J. J. Schlager, 2008, Unique Cellular Interaction of Silver Nanoparticles: Size-Dependent Generation of Reactive Oxygen Species, *J. Phys. Chem.* vol. 112,pages 13608–13619.

CHAPTER 8

CONCLUSIONS AND GENERAL DISCUSSIONS:

Surface bio-contamination is a severe problem which contributes to outbreak of nosocomial infections. An effective antimicrobial surface coating can significantly reduce the average surface population of pathogens available for transmission to a susceptible host. To respond to these problems, functional antibacterial surface was developed using ultrafine powder coating technology. Compared to traditional liquid coating, powder coating is highly efficient and enables nearly 100% recycle ability. Powder coating is also environmentally friendly. Particle size in all developed powder below 25μm is defined as ultrafine powder and it can produce a very smooth coating surface similar to those made from using liquid coatings.

Zeolites are a porous crystal structured-material, in which metal ions within their pores and metal nano particles on their surface can be incorporated by ion-exchange and reduction method respectively, therefore they are capable of releasing ions at a regulated rate for prolonged duration while maintaining their antimicrobial properties.

This study investigated the antimicrobial efficiency of ultrafine powder coated surfaces prepared with silver in different forms as an active agent. For the application of ultra-fine powder coating as an antimicrobial surface, additives were prepared by incorporation of silver and copper ions into the zeolite by ion-exchange method. Chabazites and synthetic zeolite A were used as carriers for these active agents during the course of fabrication by the ion-exchange method and the effectiveness with durability of the surfaces were checked against *E.coli.* Overall conclusions of this research are stated as follows:

Two different forms of chabazite, LBC and LBN, were used as carrier for the active agents. Pre-treatment and conditioning of chabazites were done to remove loosely bonded cations from the exchange sites and replaced with more easily removable cations (mainly sodium cations). The removal of impurities and unwanted materials from the zeolites during the pre-treatment process helped the uptake of sodium as well as silver and copper ions by reducing pore clogging during the functionalization process.

Conditioning helped to convert those chabazites to a near homo-ionic form as found in this study, with improved cation exchange capacity (CEC). Increasing the pH of the solution to pH 11 by adding NaOH in addition to mechanical treatments such as elevated temperature, sonication and continuous stirring were found to have strong influence for the higher values of CEC. Higher cationic movement through the channels of zeolite can be achieved through higher solid-liquid ratios. XRF analysis showed that the chabazites known as LBC had a slightly higher Si/Al ratio than LBN. The molar ratio of Na/Al of both zeolites were increased by pre-treatment and conditioning process as were their functionalization efficiency with silver and copper ions.

The addition of silver and copper salts, while varying the time interval, had substantial effect on ion exchange as noted in the ICP-OES analysis. In terms of cationic configuration (silver, copper) after ion exchange, LBN was found to be more efficient than LBC and also required less time to achieve that efficiency. The conditioned LBN can readily be functionalized within 24hrs of the ion-exchange process. Similar peaks were also observed at XRD for the raw and functional zeolites, including the standard sample. Dissimilarities were not found during the TGA analysis either. As such, it can be concluded that conditioning and functionalization processes did not change the structure

and behavior of the chabazites. This would help to use them as an antimicrobial additive for any industrial applications.

In the final powder formulations, 5% of the additives were used in this study, which was found to be the most appropriate composition. But due to the flow characteristics and charging capabilities of additives and the resin powder during spraying, it was evident that the percentage of additives in the coated surfaces remained as high as 85-87% when natural zeolite was used.

The reduction rate of silver during curing can be overcome by the addition of copper at different proportions in the additives, which can be determined from the color analysis of the coated surface after the curing. To understand the leaching rate of active agent and conformed the antimicrobial efficiency, the coated surfaces were exposed to microorganisms for different time intervals. It was found that the amount of silver leached out from the coating was in ppm level with the continuous contact of common cations available in the microorganisms. No trace of silver was found during the leaching test with only DI water, which also proved that silver did not leach out readily, but rather it needed some other cations for ion exchange.

The durability analysis of the prepared surfaces showed excellent performance against *E.coli* even after 15 trials. The study also showed that the conditioned chabazite containing surfaces had better efficiency than the unconditioned ones. Conditioning helped the chabazite to hold more active cations, which resulted in more durability and better performance.

The development of toxicity was determined by the formation of lactate dehydrogenate (LDH) during exposure to microorganisms on the coated surface. The percent of toxicity production with exposure to microorganisms increased with time. It should be noted that the same coated antimicrobial surface used for 15 times produced similar toxicity even after 24 hrs. of exposure with the microorganisms. Toxicity production proved the efficacy of the coated surface for a prolonged period. Production of LDH, from damaged or destroyed cells during exposure with the microorganism was considered as another evidence of the effective antibacterial properties of the coated surfaces.

Synthetic zeolite A, known as LTA, with sodium as its exchangeable cations was used as another carrier for silver and copper ions. It was found that the incorporation of copper into the additive was needed to minimize the reducing tendency of silver during the curing period of the powder coating process. Due to the reduction of silver, the surface became inactive against microorganisms and the color of the surface turned yellow. The amount of copper ions at particular concentration of silver ions was an important factor for a transparent coated surface, which was optimized by the ion exchange process with different combinations of silver and copper.

XPS analysis in this study proved that copper ions present in the additive was reduced before the silver ions and thereby were preventing the silver ions from reduction. Different characterization techniques (ICP, XRD and TGA) were used to identifying the physical changes after functionalization of synthetic zeolite A with silver and copper.

The leaching rate of silver ions from the coated surface into the microorganism can be correlated with the durability analysis. It was found that 100 % reduction of

microorganism can be achieved by exposing the surface with the microorganisms within 2 hrs time period. The release rate of the active agents is reported to have slowed down by encapsulation of the additives with 2% PVA. This polymeric encapsulation helped to reduce the release rate of active agent as well as increased the durability of the formulated antimicrobial surface.

Additional coating was applied underneath the active coating to avoid cracking in the film, since cracking appeared due to the addition of 6% PVA encapsulation on the additives. However, the transfer efficiency of the additives during spraying was improved by increasing the aggregated particle size of the final powder, which also helped to reduce the production cost as well as the system loss. The curing process of the powder coated surface was carried out at 200^{o}C for 15 minutes. Silver ions were reduced to metallic silver during this curing process. Low curing additives were incorporated into the resin system, which helped to cure the surface at lower temperatures than 200^{o}C. The effect of low curing additives on the reduction rate of silver ions was analyzed by checking the antimicrobial efficiency analysis, which was found not very satisfactory. The mechanical and chemical properties of low curing additives containing surfaces in this study were also checked following the ASTM standards.

The effect of autoclave on the coated surface color and antimicrobial efficiency was checked to find the applications of these coatings on those products that require a sterilization process. The additives containing silver and copper can be used in combination with different hydrophilic polymers, and this combination has huge potential in biomedical applications.

A novel antimicrobial surface coating containing silver nanoparticles was developed. This coating was successfully and efficiently able to inhibit the growth of *Escherichia coli*. Thus this novel antimicrobial coating can be an effective alternative in inhibiting microbial growth and thereby the toxic ecological effect from direct release of nanoparticles into the environment can be avoided.

Nano silver acts exactly in the same way as a drug delivery system, where the nanoparticles provide a concentrated storage of an active component. The ion delivery pathways follow the same route and nano-silver acts as its reservoir. Due to the highly reactive large surface areas available, nanoparticles have potential for rapid dissolution and oxidative production. The main source of ion is through oxidation. Release of silver ions from the surface depends on the hydrophilic polymer compositions, concentration of cations and the valences.

Natural polymers plays more important role than synthetic polymers in generating silver ions. At the beginning of the antimicrobial efficiency analysis, silver ion release from the coated surface of the specimen were found to dominate the process and achieved the antimicrobial efficiency in a short time. The silver ion movement from the bulk to the surface became more significant after a certain no of trials or cycles. So a sufficient amount of silver ions must be produced and stored for longer antimicrobial durability, with control release. It is also possible to minimize the toxicity effect through this controlled release of silver ions as well as increase the durability of the product.

Uniform distribution of silver nanoparticles on the zeolite surfaces enhances the efficiency of the oxidation of nanoparticles in the presence of moisture. Different

hydrophilic encapsulations were used in this study to provide a better insight for this purpose. Cross-linking between polymers and the cations present within the additives plays an important role in holding the polymers, as does the hydrophilic environment. The additives containing only the silver nanoparticles did not show such as holding capacity. Copper ions present within the additive helped to hold the polymer as well as preventing the silver ion already available from reduction during the curing process. The more cations present in the formulations, the stronger is the holding capacity of the polymer as well as the durability against microorganisms. Although the addition of external nanoparticles within the formulations was found to be effective, on the contrary, after several trials some black nanoparticles were found to leach out from the encapsulation and appeared on the surface.

The use of nano-particles for novel applications is opening the door for some critical toxicological and environmental issues to be resolved. Hydrophilic polymer blends are a promising encapsulation formulation for nanoparticles to produce their respective ions. Graft polymerization with synthetic and natural polymer combinations followed by physical cross-linking with cations between these polymers and additives are the best encapsulation combinations for antimicrobial surface preparation. This hydrophilic encapsulation helps to provide moisture for the nanoparticles in which to oxidize, and as such, this oxidation process can help to produce the Ag^{+} ions. Cross-linking helps to prepare hydrophilic three dimensional polymeric structures. The external cross-linker, like glutaldehyde, can join the different molecular chains by covalent bonds to make the polymer more stable. For this particular combination of polymers, a chemical cross-linker (GA) did not show any difference in respect to the reduction of microorganisms.

With an increased proportion of natural polymers, encapsulation of additives seems to be more stable and capable of holding more moisture within the polymer matrix by interpenetrating cross-linking. Physical cross-linking with natural and synthetic polymers make the polymer relaxation slower so that the release of silver ions also follows the same trend. Extra polymer encapsulation can also help to protect the color of the surface to some extent during the auto clave treatment.

The release rate of silver ions to the microorganisms from different formulated coated surfaces was observed. It was found that more silver was released from the surface that contained only the silver ions in comparison to the coated surface formulated with silver nano particles. It was also observed that the PVA encapsulation of the additives helped to control the release rate of silver even more. All microorganisms died within 2 hrs of exposure on the coated surface containing silver ions and the amount of silver leached out after 2 hrs was 0.14 ppm. It was found that the amount of silver after 24 hrs from the same coated surface was 0.22 ppm. So the excessive leached silver was not used for the reduction of microorganisms. The PVA encapsulation of additives helped to reduce the excess leaching from the surface, which increased the durability of that surface. The controlled silver release capability of the formulated surface with high concentration of silver enhanced the durability and efficiency, and this is promising for use in different food industry and in medical facilities.

Recommendations

Additives were mixed with the resin by dry blending. The uniform distribution of additives into the coated surface is a challenging task to achieve during spraying especially when polymer coated silver nano-particles were used as an additive. And also an additional clear coating was applied underneath the final coating, to avoid cracking of the coated surface after several time uses. All these problems can be avoided by the incorporation of the additive with the resin through extrusion process. The extrusion process may improve products performance and durability.

From the molar ratio calculation, it was found that excess carboxylate source can be added to the formulation, which can easily bound the available copper ions in the system to enrich the insolubility of the polymer followed by the enhancement of hydrophilicity. This could be a better option to get higher durability of the coated surface.

When durability was checked against microorganisms, it was found that the time needed for complete reduction of microorganisms increased as the trials number increased further. It seemed to be the availability of additives on the upper surface of the coating. To avoid cracking in the coated surface additional clear coat was applied underneath the active coating containing additives. Thickness of those coating was around 40-50 μm. To make the additives more accessible the thickness of the second coating can reduce which will also help to reduce the total thickness of the coating. In this approach, a higher concentration of antimicrobial additives can also be applied in the second coat while retaining the chemical and mechanical strength of the total film. The thinner second coat enrich with highly hydrophilic antimicrobial additives on a thicker first coat with no

antimicrobial additives, not only protects the underlying metal substrate which is the priority at the first place, but also maximizes the readily availability of Ag^{+} ions towards antimicrobial activity on the coating surface where it is necessary the most.

Nano particles remained on the zeolite surface by adsorption, so there is likely a chance to leach out the nanoparticles from the surface. These nano particles can be immobilized into the resin system by joining the thiol containing compound, such as Poly(ethylene glycol) 2-mercaptoethyl ether acetic acid. This compound contains thiol group at one end, where silver nano particles can bind and the other end contains carboxyl group, which is compatible with the polyester resin system. This compound will also provide hydrophilicity to the additive.

The formulated surfaces were checked against *E.coli only*, which was a gram negative bacteria. Further efficiency of the coated surfaces is needed to check against other gram negative and gram positive bacteria, including some in-vitro and in-vivo analysis to find the broadest area of application. The results of this study are expected to provide a promising future for nanoparticles in powder coating application as an antimicrobial surface and are likely to open the door for further research.

APPENDIX : (Chapter 4)

Table 1: Elemental analysis (milli eq.) of natural zeolites (LBC, LBN) before and after the ion- exchange with 0.05M $AgNO_3$ and 0.05M $Cu(NO_3)_2$ according to ICP-OES analysis (Table 2 shown in chapter 4)

Samples	**Ag**	**Na**	**Ca**	**Fe**	**K**	**Mg**	**Pb**	**Cu**
a) Raw LBC	0	1.833	0.4187	1.852	0.211	0.98	0.1146	0.0098
	0	2.16	0.4254	1.605	0.175	0.91	0.113	0.0010
	0	1.97	0.3557	1.97	0.179	0.86	0.0113	0.0009
Mean	**0.00**	**1.988**	**0.40**	**1.809**	**0.188**	**0.916**	**0.0113**	**0.001**
b) Ion exchange of LBC with 0.05M $AgNO_3$ for 24 hrs	0.79	0.690	0.31	1.89	0.193	0.63	0.00033	0.00067
	0.81	0.515	0.21	1.8	0.179	0.67	0.00030	0.0007
	0.86	0.570	0.36	1.71	0.187	0.76	0.00027	0.00078
Mean	**0.82**	**0.591**	**0.293**	**1.8**	**0.186**	**0.69**	**0.0003**	**0.0007**
c)Ion exchange of LBC with 0.05M $AgNO_3$ for 24 hrs,then 0.05M $Cu(NO_3)_2$for 24 hrs	0.78	0.351	0.232	1.71	0.174	0.51	0.00014	0.69
	0.84	0.32	0.191	1.769	0.178	0.49	0.00009	0.613
	0.76	0.331	0.22	1.83	0.185	0.53	0.00007	0.74
Mean	**0.79**	**0.334**	**0.21**	**1.77**	**0.179**	**0.51**	**0.0001**	**0.681**
d).Raw LBN	0	2.91	0.211	1.56	0.201	0.28	0.0134	0.00018
	0	2.77	0.207	1.49	0.209	0.23	0.012	0.00014

	0	2.81	0.197	1.44	0.206	0.263	0.009	0.00017
Mean	**0.00**	**2.83**	**0.205**	**1.50**	**0.205**	**0.26**	**0.011**	**0.00016**
e) Ion exchange of LBN with 0.05M $AgNO_3$ for 24 hrs	1.09	1.14	0.21	1.59	0.21	0.1	0.00032	0.00018
	1.05	1.09	0.18	1.41	0.195	0.084	0.00028	0.00015
	0.95	1.07	0.159	1.49	0.189	0.087	0.0003	0.00021
Mean	**1.03**	**1.10**	**0.183**	**1.50**	**0.198**	**0.09**	**0.0003**	**0.00018**
f)Ion exchange of LBN with 0.05M $AgNO_3$ for 24 hrs then 0.05M $Cu(NO_3)_2$ for 24 hrs	1.07	0.66	0.147	1.45	0.183	0.083	0.0004	0.757
	0.91	0.6	0.129	1.38	0.179	0.078	0.00034	0.715
	0.93	0.61	0.119	1.36	0.165	0.087	0.0003	0.729
Mean	**0.97**	**0.62**	**0.132**	**1.40**	**0.176**	**0.08**	**0.0003**	**0.733**

Table 2: Elemental analysis (milli eq) of LBC during pre-treatment and conditioning process with different orders of addition of silver (Ag) and copper (Cu) (Table 4 shown in chapter 4)

Samples	**Ag**	**Na**	**Ca**	**Fe**	**K**	**Mg**	**Pb**	**Cu**
a) Raw LBC	0	1.833	0.4187	1.852	0.211	0.98	0.1146	0.0098
	0	2.16	0.4254	1.605	0.175	0.91	0.113	0.0010
	0	1.97	0.3557	1.97	0.179	0.86	0.0113	0.0009
Mean	**0.00**	**1.988**	**0.40**	**1.809**	**0.188**	**0.916**	**0.011**	**0.001**
b) Water washed LBC	0.00	2.16	0.5	2.24	0.29	1.12	0.014	0.0023
	0.00	2.1	0.43	2.18	0.24	1.17	0.009	0.0019
	0.00	2.07	0.46	2.15	0.2	0.99	0.012	0.0016
Mean	**0.00**	**2.11**	**0.46**	**2.19**	**0.24**	**1.09**	**0.012**	**0.002**
c) LBC Conditioned with $NaNO_3$	0.00	3.21	0.08	1.59	0.14	0.761	0.00038	0.0009
	0.00	3.16	0.11	1.55	0.12	0.725	0.00034	0.0013
	0.00	3.09	0.096	1.52	0.109	0.759	0.0003	0.0016
Mean	**0.00**	**3.15**	**0.09**	**1.55**	**0.12**	**0.75**	**0.003**	**0.001**
d) Functionalized conditioned LBC with $AgNO_3$, for 24 hrs	0.00	1.45	0.09	1.45	0.12	0.66	0.0037	0.0009
	0.00	1.36	0.11	1.37	0.1	0.63	0.0032	0.0014
	0.00	1.28	0.081	1.34	0.109	0.676	0.0029	0.0017
Mean	**1.14**	**1.36**	**0.09**	**1.39**	**0.11**	**0.65**	**0.003**	**0.001**

e)Functionalized conditioned LBC with $AgNO_3$, 24 hrs $Cu(NO_3)_2$ for another 24 hrs	1.16	0.94	0.07	1.45	0.12	0.49	0.0024	0.89
	1.11	0.83	0.058	1.4	0.09	0.53	0.0027	0.95
	1.09	0.9	0.066	1.32	0.102	0.46	0.0021	1.02
Mean	**1.12**	**0.89**	**0.06**	**1.39**	**0.10**	**0.49**	**0.002**	**0.95**
f) Functionalized conditioned LBC with $AgNO_3$, $Cu(NO_3)_2$ together, for 24 hrs	0.89	0.81	0.1	1.45	0.11	0.57	0.0024	0.98
	0.9	0.79	0.09	1.39	0.13	0.53	0.0026	1.01
	1	0.85	0.087	1.46	0.102	0.49	0.0021	1.05
Mean	**0.93**	**0.82**	**0.09**	**1.43**	**0.11**	**0.53**	**0.002**	**1.01**
g) Functionalized conditioned LBC with $AgNO_3$, $Cu(NO_3)_2$ together, for 48 hrs	1.11	0.74	0.08	1.36	0.11	0.53	0.0025	1.21
	1.03	0.71	0.07	1.29	0.09	0.45	0.0025	1.17
	1.06	0.69	0.068	1.26	0.102	0.49	0.0021	1.16
Mean	**1.07**	**0.71**	**0.07**	**1.30**	**0.10**	**0.49**	**0.002**	**1.180**

Table 3: Elemental analysis (milli eq) of LBN during pre-treatment and conditioning process with different orders of addition of silver (Ag) and copper (Cu) (Table 5 in chapter 4)

Samples	**Ag**	**Na**	**Ca**	**Fe**	**K**	**Mg**	**Pb**	**Cu**
a) Raw LBN	0	2.91	0.211	1.56	0.201	0.28	0.0134	0.00018
	0	2.77	0.207	1.49	0.209	0.23	0.012	0.00014
	0	2.81	0.197	1.44	0.206	0.263	0.009	0.00017
Mean	**0.00**	**2.83**	**0.205**	**1.50**	**0.205**	**0.26**	**0.011**	**0.00016**
b) Water washed LBN	0.00	3.12	0.32	1.57	0.27	0.33	0.014	0.00023
	0.00	2.99	0.28	1.49	0.24	0.28	0.011	0.00017
	0.00	3.17	0.3	1.53	0.25	0.29	0.012	0.00019
Mean	**0.00**	**3.09**	**0.30**	**1.53**	**0.25**	**0.3**	**0.012**	**0.0002**
c) LBN Conditioned with $NaNO_3$	0.00	3.87	0.13	1.93	0.14	0.32	0.008	0.00059
	0.00	3.74	0.096	1.88	0.12	0.28	0.0068	0.00063
	0.00	3.83	0.09	1.86	0.11	0.275	0.0072	0.0006
Mean	**0.00**	**3.81**	**0.1**	**1.89**	**0.12**	**0.29**	**0.007**	**0.0006**
d)Functionalized conditioned LBN with $AgNO_3$, for 24 hrs	1.15	1.93	0.074	1.59	.105	0.31	0.0039	0.00049
	1.17	1.87	0.071	1.51	.1	0.24	0.0042	0.00053
	1.113	1.79	0.068	1.54	.095	0.26	0.0038	0.0006
Mean	**1.144**	**1.86**	**0.07**	**1.55**	**0.10**	**0.27**	**0.004**	**0.0005**

e) Functionalized conditioned LBN with $AgNO_3$, 24 hrs $Cu(NO_3)_2$ for another 24 hrs	1.15	1.04	0.045	1.07	0.1	0.29	0.0031	0.98
	1.131	1	0.038	0.93	0.092	0.24	0.0028	1.17
	1.11	0.94	0.039	0.99	0.088	0.26	0.0038	1.12
Mean	**1.130**	**0.99**	**0.04**	**1.00**	**0.09**	**0.26**	**0.003**	**1.090**
f) Functionalized conditioned LBN with $AgNO_3$, $Cu(NO_3)_2$ together, for 24 hrs	1.14	1.43	0.041	1.12	0.015	0.27	0.0028	1.08
	1.11	1.46	0.044	1.07	0.01	0.23	0.0033	0.95
	1.1	1.38	0.036	1.08	0.012	0.3	0.0038	0.9
Mean	**1.116**	**1.42**	**0.04**	**1.09**	**0.01**	**0.27**	**0.003**	**0.98**
g)Functionalized conditioned LBN with $AgNO_3$, $Cu(NO_3)_2$ together, for 48 hrs	1.1	1.05	0.039	1.012	0.103	0.26	0.0029	1.32
	1.06	1.039	0.032	1.004	0.091	0.23	0.0033	1.26
	1.13	1.03	0.034	0.989	0.088	0.3	0.0037	1.27
Mean	**1.097**	**1.04**	**0.035**	**1.002**	**0.09**	**0.26**	**0.003**	**1.28**

Table 4: Molar ratio, Na/Al

Treatment	% Alumina	Moles of Alumina	% sodium	Moles of Sodium	Molar ratio Na/AL	Mean	Std. Dev.	T-Test, p value 95% Confidence label
Waterwashed LBC	12.19	0.451481	4.92	0.213913	0.473802	0.474743	0.007451	0.000215
	12.02	0.445185	4.79	0.208261	0.467807			
	11.87	0.43963	4.88	0.212174	0.48262			
Conditioned LBC with 1M NaNO3	12.11	0.448519	7.37	0.320435	0.714429	0.713436	0.001316	
	11.79	0.436667	7.1703	0.311752	0.713936			
	11.9	0.440741	7.217	0.313783	0.711944			
Water washed LBN	12.94	0.479259	7.24	0.314783	0.656811	0.643032	0.01237	0.000981
	12.78	0.473333	6.961	0.302652	0.639406			
	13.19	0.488519	7.111	0.309174	0.632881			
Conditioned LBN with 1 M NaNO3	13.03	0.482593	8.89	0.386522	0.800928	0.798906	0.003509	
	12.75	0.472222	8.633	0.375348	0.794854			
	12.81	0.474444	8.74	0.38	0.800937			

Table 5: Standard value indication for the color analysis (Data color Tools 650 User Guide)

Red-Green Difference	(+Da) surface is redder than control (-Da) surface is greener than control
Yellow-Blue Difference	(+Db) surface is yellower than control (-Db) surface is bluer than control
Lightness-Darkness Difference	(+DL) surface is lighter than control (-DL) surface is darker than control
CIE DE	Overall Color Difference

Table 6: Color analysis of the panel made with LBC containing additive (Table 7 in Chapter 4)

Parameters	Ion exchange of Raw LBC with 0.05M $AgNO_3$	Ion exchange of Raw LBC with 0.05M $AgNO_3$ and 0.05M $Cu(NO_3)_2$	Ion exchange of conditioned LBC with 0.05M $AgNO_3$	Ion exchange of conditioned LBC with 0.05M$AgNO_3$, 0.05M$Cu(NO_3)_2$
CIE DL	-3.61	-1.12	-8.63	-5.31
	-3.52	-1.08	-8.72	-5.24
	-3.49	-1.08	-8.53	-5.33
Mean	**-3.54**	**-1.09**	**-8.63**	**-5.29**
CIE Da	-0.6	-0.32	-2.4	-2.09
	-0.52	-0.29	-2.1	-1.92
	-0.55	-0.25	-1.9	-1.84
Mean	**-0.56**	**-0.29**	**-2.1**	**-1.95**
CIE Db	6.34	4.07	10.51	6.18
	6.27	3.94	10.43	6.07
	6.21	4.13	10.39	6.11
Mean	**6.27**	**4.05**	**10.44**	**6.12**
CIE DE	7.27	3.56	11.36	9.17
	7.21	3.49	11.27	9.13
	7.17	3.47	11.22	9.07

Mean	**7.22**	**3.51**	**11.28**	**9.12**

Table 7: Color analysis of the panel made with LBN containing additive (Table 8 in Chapter 4)

Parameters	Ion exchange of Raw LBC with 0.05M $AgNO_3$	Ion exchange of Raw LBC with 0.05M $AgNO_3$ and 0.05M $Cu(NO_3)_2$	Ion exchange of conditioned LBC with 0.05M $AgNO_3$	Ion exchange of conditioned LBC with 0.05M$AgNO_3$, 0.05M$Cu(NO_3)_2$
CIE DL	-4.47	-1.31	-10.87	-6.34
	-4.38	-1.28	-10.83	-6.29
	-4.42	-1.22	-10.77	-6.4
Mean	**-4.42**	**-1.27**	**-10.82**	**-6.34**
CIE Da	-0.42	-0.29	-1.27	-0.11
	-0.37	-0.2	-1.24	-0.08
	-0.38	-0.19	-1.32	-0.09
Mean	**-0.39**	**-0.23**	**-1.28**	**-0.09**
CIE Db	8.01	4.94	10.49	5.39
	7.79	5.06	10.32	5.15
	7.6	4.79	10.37	5.30
Mean	**7.80**	**4.93**	**10.39**	**5.28**

CIE DE	7.72	3.14	10.77	8.07
	7.64	3.05	10.81	8.15
	7.48	3.09	10.65	8.03
Mean	**7.61**	**3.09**	**10.74**	**8.08**

Table 8: Antimicrobial efficiency before and after the leaching test (Figure 9 in chapter 4

Time of Exposure to microorganism	Before the leaching Test, no of microrganism, 10^9cfu/ml		After the leaching Test, no of microorganism, 10^9cfu/ml	
hrs	Values	Mean	Values	Mean
0	0.27, 0.21, 0.25	0.24	0.20, 0.23, 0.18	0.2
1	0	0	0.12. 0.09, 0.13	0.11
2	0	0	0.028, 0.023, 0.027	0.026
3	0	0	0.0020, 0.0016, 0.0018	0.0018
4	0	0	0.0001, 0.0002, 0	0.0001
24	0	0	0	0

Table 9: Consecutive use of antimicrobial surfaces prepared with 5% additives (Raw LBC ion-exchanged with 0.05M $AgNO_3$ and 0.05M $Cu(NO_3)_2$) (Figure 10 in chapter 4)

Change of microorganism, 10^9cfu/ml with different trials

Time, hr	Trial 1	Trial 3	Trial 5	Trial 9	Trial 12	Trial 15	Control
0	0.25	0.22	0.27	0.3	0.29	0.24	0.25
2	0.09	0.07	0.001	0.02	0.03	0.05	2.3
4	0	0	0	0.0024	0.0017	0.0021	2.9
8	0	0	0	0	0	0	2.4
24	0	0	0	0	0	0	21.00

Table10: Consecutive use of antimicrobial surfaces prepared with 5% additives (Conditioned LBC ion-exchanged with 0.05M $AgNO_3$ and 0.05M $Cu(NO_3)_2$)) (Figure 11 in chapter 4)

No of Microorganism, present at particular time, 10^9cfu/ml

Time , hr	Trial 1	Trial 3	Trial 5	Trial 9	Trial 12	Trial 15	Control
0	0.21	0.24	0.27	0.3	0.24	0.25	0.22
2	0	0	0	0.004	0.003	0.002	1.9
4	0	0	0	0.0002	0.0001	0.0003	2.3
8	0	0	0	0	0	0	2.9
24	0	0	0	0	0	0	23.00

APPENDIX for Chapter 5

Table 1: Elemental analysis (milli eq) of functionalized zeolite by ICP-OES (Table 2 in Chap.5)

Sample Labels	Ag	Mean	Cu	Mean	Na	Mean	Total cations
Raw Synthetic	0		0		7.02		
	0	0	0	0	7.05	6.98	6.98
	0		0		6.87		
Synthetic Ag 24 hrs	1.65		0		5.61		
	1.52	1.66	0	0	4.98	5.26	6.92
	1.82		0		5.19		
Synthetic, Ag, then Cu 48hrs	1.64		4.02		1.58		
	1.45	1.53	3.88	3.89	1.32	1.46	6.88
	1.51		3.76		1.48		
Synthetic Cu then Ag 48 hrs	1.4		3.45		2.51		
	1.28	1.30	3.29	3.32	2.32	2.35	6.97
	1.22		3.23		2.21		
Synthetic Ag, Cu together 24 hrs	1.57		3.49		2.3		
	1.36	1.41	3.36	3.38	2.09	2.20	6.99
	1.31		3.29		2.2		
Synthetic, Ag, Cu together 48hrs	1.62		3.58		2.26		
	1.33	1.45	3.27	3.43	2.04	2.14	7.02
	1.4		3.44		2.13		

Table 2: Additive concentration before and after pressing at different combination of additive and polyester resin (Table 5 in Chap.5)

Size of additive, µ	Size of polyester resin, µ	Additive in powder before spraying, %	Additive on surface after spraying, %	Mean	Additive after pressing (%), particle size, 30µ	Mean	Additive after pressing (%), particle size, 55µ	Mean
20	35	3.75	1.13	1.10	1.57	1.53	1.69	1.67
			1.09		1.49		1.72	
			1.1		1.52		1.6	
20	20	3.75	0.98	0.94	1.84	1.77	2.07	1.98
			0.91		1.68		1.87	
			0.94		1.79		1.99	
20	35	5.00	1.22	1.25	1.79	1.68	2.02	1.81
			1.39		1.65		1.79	
			1.13		1.59		1.63	
20	20	5.00	1.2	1.10	1.88	2.00	2.31	2.24
			1.13		2.1		2.22	
			0.97		2.04		2.19	

Table 3 : Physical and Chemical properties of panel with different low curing agent.

SAMPLE	IMPACT Resistance	Pencil scratch hardness	MEK (ASTM D 4752)	Color
0.05 M $AgNO_3$ With 5% promoter	30 lb/inch	2H	5, Resistance rating, No effect on surface after 50 rubs	DL, -8.01,Db, 11.48, DE 14.01
0.05M $AgNO_3$ and 0.05M $Cu(NO3)_2$ With 5% promoter	30 lb/inch	2H	5, Resistance rating, No effect on surface after 50 rubs	DL, -6.73, Db, 5.56, DE 8.75
0.05M $AgNO_3$ and 0.05M $Cu(NO3)_2$ With 5% promoter and 0.3% TP	30 lb/inch	2H	5, Resistance rating, No effect on surface after 50 rubs	DL, -0.62, Db, 3.77, DE 3.85

Antimicrobial analysis (No of microorganism present at every exposure, 10^9cfu/ml

Table 4: Synthetic Zeolite (ionexchanged with 0.05M $AgNO_3$) cured at 200^OC for 15 mines.

Time, hr	Trial 1	Trial 2	Trial 3	Trial 4	Trial 5	Trial 6	Control
0	0.24	0.21	0.2	0.25	0.24	0.25	0.24
2	0.000005	0.00011	0.06	0.12	0.2	0.21	1.9
4	0	0	0.0004	1.9	2.0	1.9	2.7
24	0	0	0	21	22	27	24

Table 5: Synthetic Zeolite (ionexchanged with 0.05 M $AgNO_3$) + 0.5% Promoter 1 cured at 150^oC for 1 hr

Time, hr	Trial 1	Trial 2	Trial 3	Trial 4	Trial 5	Trial 6	Control
0	0.24	0.21	0.2	0.25	0.24	0.25	0.25
2	0.04	0.19	0.3	0.18	0.22	0.28	1.8
4	0.00003	0.000001	0.00011	0.02	0.029	0.19	2.3
24	0	0	0.00001	0.0014	0.0014	0.0022	21

Table 6: Synthetic Zeolite (ionexchanged with 0.05M $AgNO_3$ and 0.5M $Cu(NO3)_2$) cured at 200^OC for 15 mins

Time, hr	Trial 1	Trial 2	Trial 3	Trial 4	Trial 5	Trial 6	Control
0	0.24	0.2100	0.2000	0.25	0.24	0.25	0.25
2	0.016	0.06	0.05	0.06	0.04	0.07	2.1
4	0	0	0	0	0	0	2.5
24	0	0	0	0	0	0	21.00

Table 7: Synthetic Zeolite (ionexchanged with 0.05M $AgNO_3$ and 0.05M $Cu(NO3)_2$) + 0.5% Promoter 1 cured at $150^{O}C$ for 1 hr.

Time, hr	Trial 1	Trial 2	Trial 3	Trial 4	Trial 5	Trial 6	Control
0	0.24	0.2100	0.2000	0.25	0.24	0.25	0.25
2	0.12	0.18	0.21	0.27	1.1	1.2	2.1
4	0.0002	0.0002	0.00019	0.0011	0.0012	0.0002	2.4
24	0	0	0	0	0	0	21.0

Table 8: Synthetic Zeolite (ionexchanged with 0.05M $AgNO_3$ and 0.05M $Cu(NO3)_2$) + 0.5% Promoter 1 + 0.3% TP, cured at $150^{O}C$ for 1 hr.

Time, hr	Trial 1	Trial 2	Trial 3	Trial 4	Trial 5	Trial 6	Control
0	0.24	0.2100	0.2000	0.25	0.24	0.25	0.25
2	0.15	0.17	0.15	0.15	1.8	1.9	1.8
4	0	0.00009	0.00001	0.00013	0.0001	0.0019	2.3
24	0	0	0	0	0	0	20.0

Appendix for (Chapter 6)

Table 1: Elemental analysis (milli eq) of additives containing silver nanoparticle (0.05M $AgNO_3$) synthesized with different amount of borohydride with additional silver and copper ions

Additive formulation	**Ag**	**Mean Ag**	**Cu**	**Mean Cu**	**Na**	**Mean Na**
Zeolite + 0.05M $AgNO_3$	1.67	1.66	0.00	0.00	5.39	5.26
	1.75		0.00		5.21	
	1.55		0.00		5.19	
Zeolite + 0.05M $AgNO_3$+ 0.1M $Cu(NO_3)_2$	1.62	1.53	3.71	3.89	1.49	1.46
	1.43		3.89		1.53	
	1.54		4.07		1.36	
Zeolite + 0.05M $AgNO_3$+ 2 times $NaBH_4$+previous silver soln + 0.1M $Cu(NO_3)_2$	1.78	1.65	3.6	3.47	1.14	1.07
	1.53		3.46		1.08	
	1.63		3.35		1	
Zeolite + 0.05M $AgNO_3$+ 1.5 times $NaBH_4$+previous silver soln + 0.1M $Cu(NO_3)_2$	1.85	1.69	3.62	3.51	1.05	1.07
	1.52		3.39		1.01	
	1.7		3.52		1.14	
Zeolite + 0.05M $AgNO_3$+ 1 times $NaBH_4$+previous silver soln + 0.1M $Cu(NO_3)_2$	1.72	1.59	3.94	3.78	1.08	1.08
	1.49		3.62		1.02	
	1.55		3.77		1.14	

Zeolite + 0.05M $AgNO_3$+ 0.5 times $NaBH_4$+previous silver soln + 0.1M $Cu(NO_3)_2$	1.66	1.61	3.97	3.86	1.02	1.09
	1.51		3.79		1.11	
	1.67		3.83		1.15	

Table 2: Elemental analysis (milli eq) of additives containing silver nanoparticle (0.05M $AgNO_3$) synthesized with 1.5 times borohydride with additional silver and copper ions

Additive formulation	**Ag**	**Mean Ag**	**Cu**	**Mean Cu**	**Na**	**Mean Na**
Zeolite + 0.05M $AgNO_3$	1.67	1.66	0.00	0.00	5.39	5.26
	1.75		0.00		5.21	
	1.55		0.00		5.19	
Zeolite + 0.05M $AgNO_3$+ 0.1M $Cu(NO_3)_2$	1.62	1.53	3.71	3.89	1.49	1.46
	1.43		3.89		1.53	
	1.54		4.07		1.36	
Zeolite + 0.05M $AgNO_3$+ 1.5 time $NaBH_4$	1.69	1.64	0.00	0.00	4.93	4.89
	1.73		0.00		5.02	
	1.51		0.00		4.72	
Zeolite + 0.05M $AgNO_3$+ 1.5 time $NaBH_4$ + 0.1M $Cu(NO_3)_2$	1.67	1.62	3.38	3.29	1.19	1.11
	1.49		3.28		1.03	
	1.71		3.22		1.12	

Zeolite + 0.05M $AgNO_3$+ 1.5 time $NaBH_4$ + 0.05M $AgNO_3$ (fresh) +0.1M $Cu(NO_3)_2$	1.78	1.87	3.43	3.31	0.98	1.09
	1.99		3.21		1.13	
	1.83		3.29		1.17	
Zeolite + 0.05 $AgNO_3$+ 1 time $NaBH_4$ + 0.05M $AgNO_3$ (fresh) +0.1M $Cu(NO_3)_2$	1.85	1.73	3.41	3.51	1.14	1.09
	1.61		3.49		0.95	
	1.74		3.63		1.19	

Table 3: Elemental analysis (milli eq) of additives containing silver nanoparticle (0.03M $AgNO_3$) synthesized with 1.5 times borohydride with additional silver and copper ions

Additive formulation	**Ag**	**Mean Ag**	**Cu**	**Mean Cu**	**Na**	**Mean Na**
Zeolite + 0.03M $AgNO_3$	1.11	1.19	0.00	0.00	5.19	5.06
	1.17		0.00		5.05	
	1.28		0.00		4.93	
Zeolite + 0.03M $AgNO_3$+ 0.06M $Cu(NO_3)_2$	0.98	0.92	3.37	3.37	2.31	2.20
	0.86		3.49		2.19	
	0.91		3.26		2.1	
Zeolite + 0.03M $AgNO_3$+ 1.5 time $NaBH_4$	1.29	1.21	0.00	0.00	5.07	5.00
	1.13		0.00		4.89	
	1.22		0.00		5.01	

Zeolite + 0.03M $AgNO_3$+ 1.5 time $NaBH_4$ + 0.06M $Cu(NO_3)_2$	1.19	1.09	3.52	3.43	2.29	2.19
	0.98		3.44		2.18	
	1.09		3.32		2.09	
Zeolite + 0.03M $AgNO_3$+ 1.5 time $NaBH_4$ +0.05M $AgNO_3$ (fresh) +0.1M $Cu(NO_3)_2$	1.57	1.46	2.91	2.82	2.33	2.21
	1.38		2.74		2.13	
	1.44		2.81		2.17	
Zeolite + 0. 03M $AgNO_3$+ 1.5 time $NaBH_4$+ previous silver soln +0.1M $Cu(NO_3)_2$	1.25	1.19	3.44	3.33	2.26	2.19
	1.11		3.35		2.12	
	1.2		3.21		2.18	

Table 4: Elemental analysis (milli eq) of additives containing silver nanoparticle (0.01M $AgNO_3$) synthesized with 1.5 times borohydride with additional silver and copper ions

Additive formulation	**Ag**	**Mean Ag**	**Cu**	**Mean Cu**	**Na**	**Mean Na**
Zeolite + 0.01M $AgNO_3$	0.49	0.51	0.00	0.00	6.21	6.14
	0.62		0.00		6.13	
	0.43		0.00		6.08	
Zeolite + 0.01M $AgNO_3$+ 0.02M $Cu(NO_3)_2$	0.51	0.48	1.56	1.43	4.83	4.72
	0.46		1.41		4.62	
	0.47		1.32		4.7	
Zeolite + 0.01M $AgNO_3$+ 1.5 time $NaBH_4$	0.61	0.52	0.00	0.00	5.81	5.91
	0.43		0.00		6.03	
	0.51		0.00		5.88	

Zeolite + 0.01M $AgNO_3$+ 1.5 time $NaBH_4$ + 0.02M $Cu(NO_3)_2$	0.52	0.49	1.52	1.44	4.57	4.59
	0.48		1.48		4.81	
	0.46		1.32		4.38	
Zeolite + 0.01M $AgNO_3$+ 1.5 time $NaBH_4$ +0.01M $AgNO_3$ (fresh) +0.02M $Cu(NO_3)_2$	0.82	0.73	1.46	1.38	4.12	4.08
	0.73		1.29		4.03	
	0.65		1.39		4.1	
Zeolite + 0.01M $AgNO_3$+ 1.5 time $NaBH_4$ +0.03M $AgNO_3$ (fresh) +0.06M $Cu(NO_3)_2$	1	0.90	3.11	3.21	2.68	2.54
	0.87		3.21		2.53	
	0.84		3.32		2.41	
Zeolite + 0. 01M $AgNO_3$+ 1.5 time $NaBH_4$+ previous silver soln +0.02M $Cu(NO_3)_2$	0.74	0.68	1.54	1.43	4.35	4.26
	0.67		1.42		4.17	
	0.62		1.33		4.25	

Table 5: Antimicrobial efficiency of ultrafine powder coated surface (Additive coated with 6% PVA) (Flow sheet 2)

Additive	Antimicrobial efficiency, checked	No of microorganism cfu /ml	Antimicrobial efficiency, checked	No of microorganism cfu /ml
Synthetic Zeolite+ Synthesized Nano Particles	At 1st trial	0 at 16 hrs 0 at 16 hrs 0 at 16 hrs	At 2 trials	0 at 24 hrs 0 at 24 hrs 0 at 24 hrs
Synthetic Zeolite+ Nano Particles Powder + Cu^{2+}	At 1st trial	0 at 8 hrs 0 at 8 hrs 0 at 8 hrs	At 3 trials	0 at 24 hrs 0 at 24 hrs 0 at 24 hrs
Synthetic Zeolite+ Synthesized Nano Particles+ Ag^{+} + Cu^{2+}	At 1st trial	0 at 8 hrs 0 at 8 hrs 0 at 8 hrs	At 8 trials	0 at 24 hrs 0 at 24 hrs 0 at 24 hrs
Synthetic Zeolite+ nano particle Powder	At 1st trial	0 at 18 hrs 0 at 18 hrs 0 at 18 hrs	At 2 trials	0 at 24 hrs 0 at 24 hrs 0 at 24 hrs
Synthetic Zeolite+ Synthesized Nano Particles + Cu^{2+}	At 1st trial	0 at 8 hrs 0 at 8 hrs 0 at 8 hrs	At 3 trials	0 at 24 hrs 0 at 24 hrs 0 at 24 hrs
Initial coating+ Synthetic Zeolite+ Synthesized Nano Particles+ Cu^{2+}	At 1st trial	0 at 8 hrs 0 at 8 hrs 0 at 8 hrs	At 5 trials	0 at 24 hrs 0 at 24 hrs 0 at 24 hrs
Synthetic Zeolite+ Powder Nano Particles+ Ag^{+} + Cu^{2+}	At 1st trial	0 at 8 hrs 0 at 8 hrs 0 at 8 hrs	At 8 trials	0 at 24 hrs 0 at 24 hrs 0 at 24 hrs

Table 6: Antimicrobial efficiency of ultrafine powder coated surface (Flow sheet 3)

Encapsulation Composition	**Additive**	**Antimicrobial efficiency, checked**	**No of microorganism cfu /ml**	**Antimicrobial efficiency, checked**	**No of microorganism cfu /ml**
1 % PVA	Synthetic Zeolite+ Synthesized Nano Particles+ Ag+ + Cu2+ (0.05M)	At 1st trial	0 at 8 hrs 0 at 8 hrs 0 at 8 hrs	At 6 trials	0 at 24 hrs 0 at 24 hrs 0 at 24 hrs
2 % PVA	Synthetic Zeolite+ Synthesized Nano Particles+ Ag^{+} + Cu^{2+} (0.05M)	At 1st trial	0 at 8 hrs 0 at 8 hrs 0 at 8 hrs	At 8 trials	0 at 24 hrs 0 at 24 hrs 0 at 24 hrs
2 % PVA	Synthetic zeolite + Cu^{2+}(0.05M)	At 1st trial	No antimicrobial activity, No crack	At 8 trials	No antimicrobial activity, No crack
2 % PVA	Synthetic Zeolite+ Synthesized Nano Particles + Cu^{2+}(0.1M)	At 1st trial	0 at 8 hrs 0 at 8 hrs 0 at 8 hrs	At 8 trials	0 at 24 hrs 0 at 24 hrs 0 at 24 hrs
2 % PVA	Synthetic Zeolite+ Synthesized Nano Particles + Cu^{2+}(0.05M)	At 1st trial	0 at 8 hrs 0 at 8 hrs 0 at 8 hrs	At 4 trials	0 at 24 hrs 0 at 24 hrs 0 at 24 hrs
2 % PVA	Initial coating+ Synthetic Zeolite+ Synthesized Nano Particles+ Cu^{2+}(0.05M)	At 1st trial	0 at 8 hrs 0 at 8 hrs 0 at 8 hrs	At 7 trials	0 at 24 hrs 0 at 24 hrs 0 at 24 hrs
1 % PVA	Synthetic Zeolite+ Synthesized Nano Particles+ Ag^{+} (0.1M)+ Cu^{2+} (0.05M)	At 1st trial	0 at 8 hrs 0 at 8 hrs 0 at 8 hrs	At 8 trials	0 at 24 hrs 0 at 24 hrs 0 at 24 hrs

Table 7: Antimicrobial efficiency of ultrafine powder coated surface (Flow sheet 4)

Encapsulation Composition	Additive	Antimicrobial efficiency, checked	No of microorganism cfu /ml	Antimicrobial efficiency, checked	No of microorganism cfu /ml
6 % PEO	Synthetic Zeolite+ Synthesized Nano Particles+ Cu^{2+} (0.05M)	At 1st trial	0 at 8 hrs 0 at 8 hrs 0 at 8 hrs	At 5 trials	0 at 24 hrs 0 at 24 hrs 0 at 24 hrs
6 % PEO	Synthetic Zeolite+ Synthesized Nano Particles+ Ag^{+} + Cu^{2+} (0.05M)	At 1st trial	0 at 8 hrs 0 at 8 hrs 0 at 8 hrs	At 8 trials	0 at 24 hrs 0 at 24 hrs 0 at 24 hrs
6 % PEO	Synthetic Zeolite+ Nano Particles Powder+ Ag^{+} + Cu^{2+} (0.05M)	At 1st trial	0 at 8 hrs 0 at 8 hrs 0 at 8 hrs	At 7 trials	0 at 24 hrs 0 at 24 hrs 0 at 24 hrs
4% PEO +8 % Na-Alginate	Synthetic Zeolite+ Synthesized Nano Particles + Cu^{2+} (0.1M)	At 1st trial	0 at 8 hrs 0 at 8 hrs 0 at 8 hrs	At 6 trials	0 at 24 hrs 0 at 24 hrs 0 at 24 hrs
4% PEO + 6% Na-CMC	Synthetic Zeolite+ Synthesized Nano Particles + Cu^{2+} (0.1M)	At 1st trial	0 at 8 hrs 0 at 8 hrs 0 at 8 hrs	At 6 trials	0 at 24 hrs 0 at 24 hrs 0 at 24 hrs
1 % PEO + 3% Na Alginate + 7 % Na-CMC	Synthetic Zeolite+ Synthesized Nano Particles+ Cu^{2+} (0.05M)	At 1st trial	0 at 8 hrs 0 at 8 hrs 0 at 8 hrs	At 7 trials	0 at 24 hrs 0 at 24 hrs 0 at 24 hrs
1 % PEO + 3% Na Alginate + 7 % Na-CMC	Initial coating+ Synthetic Zeolite+ Synthesized Nano Particles+ Cu^{2+} (0.05M)	At 1st trial	0 at 8 hrs 0 at 8 hrs 0 at 8 hrs	At 12 trials	0 at 24 hrs 0 at 24 hrs 0 at 24 hrs

Table 8: Antimicrobial efficiency of ultrafine powder coated surface (Flow sheet 5)

Encapsulation Composition	Additive	Antimicrobial efficiency, checked	No of micro organism cfu /ml	Antimicrobial efficiency, checked	No of micro organism cfu /ml
6 % PAM	Synthetic Zeolite+ Synthesized Nano Particles+ Cu^{2+} (0.05M)	At 1st trial	0 at 8 hrs 0 at 8 hrs 0 at 8 hrs	At 6 trials	0 at 24 hrs 0 at 24 hrs 0 at 24 hrs
6 % PAM	Synthetic Zeolite+ Synthesized Nano Particles+ Ag^{+} + Cu^{2+} (0.05M)	At 1st trial	0 at 8 hrs 0 at 8 hrs 0 at 8 hrs	At 8 trials	0 at 24 hrs 0 at 24 hrs 0 at 24 hrs
6 % PAM	Synthetic Zeolite+ Nano ParticlesPowder+ Ag^{+} + Cu^{2+} (0.05M)	At 1st trial	0 at 8 hrs 0 at 8 hrs 0 at 8 hrs	At 6 trials	0 at 24 hrs 0 at 24 hrs 0 at 24 hrs
4% PAM +6 % Na-Alginate	Synthetic Zeolite+ Synthesized Nano Particles + Cu^{2+}(0.1M)	At 1st trial	0 at 8 hrs 0 at 8 hrs 0 at 8 hrs	At 8 trials	0 at 24 hrs 0 at 24 hrs 0 at 24 hrs
4% PAM + 6% Na-CMC	Synthetic Zeolite+ Synthesized Nano Particles + Cu^{2+}(0.1M)	At 1st trial	0 at 8 hrs 0 at 8 hrs 0 at 8 hrs	At 8 trials	0 at 24 hrs 0 at 24 hrs 0 at 24 hrs

Table 9: Antimicrobial efficiency of ultrafine powder coated surface

Encapsulation Composition	Additive	Antimicrobial efficiency, checked	No of microorganism cfu /ml	Antimicrobial efficiency, checked	No of microorganism cfu /ml
6 % Na-CMC	Synthetic Zeolite+ Synthesized Nano Particles+ Cu^{2+} (0.05M)	At 1st trial	0 at 8 hrs 0 at 8 hrs 0 at 8 hrs	At 12 trials	0 at 24 hrs 0 at 24 hrs 0 at 24 hrs
6 % Na-Alginate	Synthetic Zeolite+ Synthesized Nano Particles+ Cu^{2+} (0.05M)	At 1st trial	0 at 8 hrs 0 at 8 hrs 0 at 8 hrs	At 12 trials	0 at 24 hrs 0 at 24 hrs 0 at 24 hrs
6 % Polyester	Synthetic Zeolite+ Synthesized Nano Particles+ Cu^{2+} (0.05M)	At 1st trial	0 at 8 hrs 0 at 8 hrs 0 at 8 hrs	At 6 trials	0 at 24 hrs 0 at 24 hrs 0 at 24 hrs
$Ca(PO_4)_2$	Synthetic Zeolite+ Synthesized Nano Particles+ Cu^{2+} (0.05M)	At 1st trial	0 at 8 hrs 0 at 8 hrs 0 at 8 hrs	At 8 trials	0 at 24 hrs 0 at 24 hrs 0 at 24 hrs

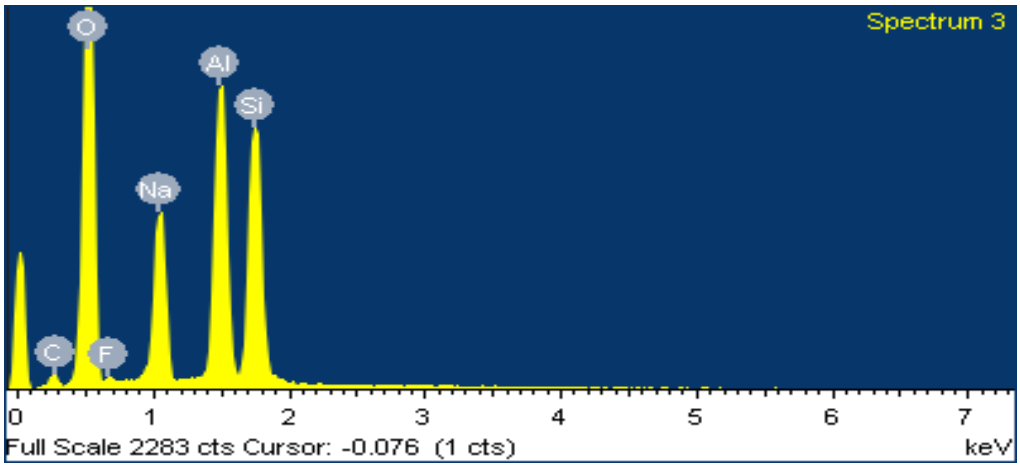

EDX of Synthetic zeolite contains silver nanoparticles prepared by using 0.01M silver nitrate

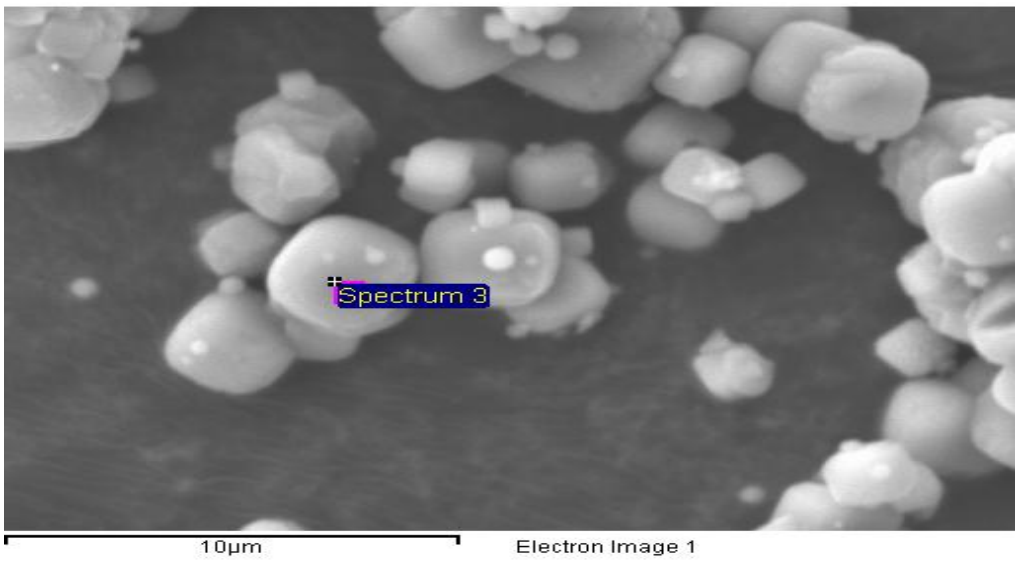

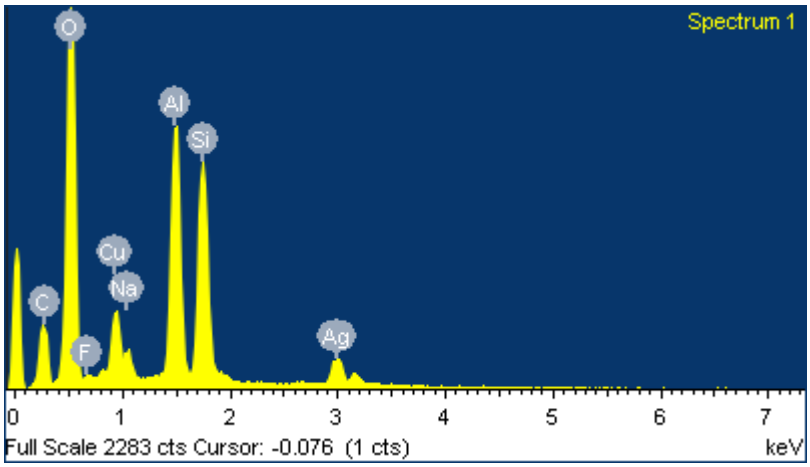

EDX of Synthetic zeolite contains silver nanoparticles prepared by using 0.03M silver nitrate

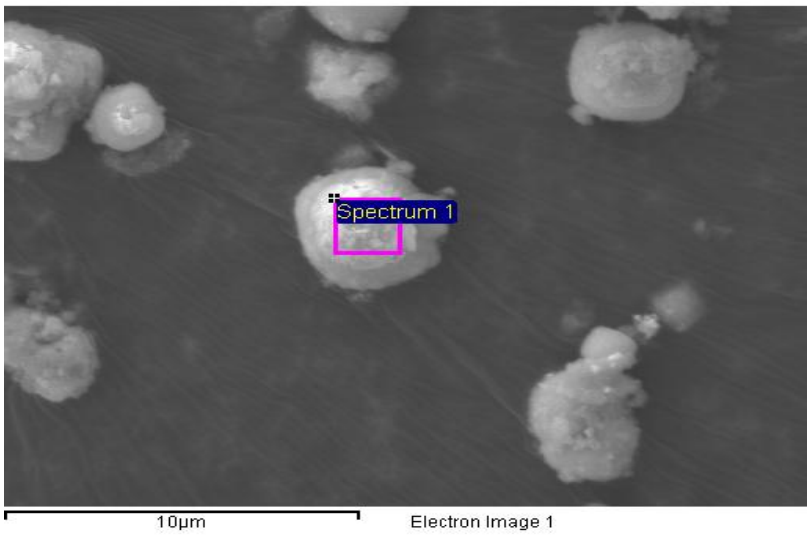

CURRICULUM VITAE

Name: REZWANA YEASMIN

Education:

MESc, Chemical and Biochemical Engineering
Western university, 2011

MSc. Food Engineering and Bioprocess Technology of
Asian Institute Technology, Thailand, 2004

BSc, Applied Chemistry
University of Dhaka, 1993

Work Experience:

Teaching Assistant
University of Western Ontario

Research Assistant
University of Western Ontario

Senior Scientific Officer
Bangladesh Council of Scientific and Industrial Research

Publications:

Articles published:

Rezwana Yeasmin and A.I.Mustafa (1996) Spectrophotometric determination of Vanadium (V) with Cinnamyl Hydroxamic acid (CHA). Bangladesh J. Sci. Ind. Res., XXXI. No. 2.

Rezwana Yeasmin and A.I.Mustafa (2001) Spectrophotometric determination of Vanadium (V) with Benzhydroxamic & Salicylic Hydroxamic acid. Bangladesh J. Sci. &Tech.3 (1), 67-77.

Articles submitted:

Rezwana Yeasmin, Hui Zhang, Jingxu Zhu, Hossein Kazemian (2015), Pre-treatment and conditioning of chabazites followed by functionalization for making suitable additives used in antimicrobial ultra-fine powder coated surface, *Journal of Hazardous Materials*

Rezwana Yeasmin, S. Rakshit, Md. Nazim Uddin (2015), Antioxidant activity, inhibition of DNA damage and anti-microbial activity of Black cumin oil and its effect on ready-to-eat food preservation, *Journal of Food Science*